INFORMATION TO USERS

This manuscript has been reproduced from the microfilm master. UMI films the text directly from the original or copy submitted. Thus, some thesis and dissertation copies are in typewriter face, while others may be from any type of computer printer.

The quality of this reproduction is dependent upon the quality of the copy submitted. Broken or indistinct print, colored or poor quality illustrations and photographs, print bleedthrough, substandard margins, and improper alignment can adversely affect reproduction.

In the unlikely event that the author did not send UMI a complete manuscript and there are missing pages, these will be noted. Also, if unauthorized copyright material had to be removed, a note will indicate the deletion.

Oversize materials (e.g., maps, drawings, charts) are reproduced by sectioning the original, beginning at the upper left-hand corner and continuing from left to right in equal sections with small overlaps.

ProQuest Information and Learning
300 North Zeeb Road, Ann Arbor, MI 48106-1346 USA
800-521-0600

Université d'Ottawa · University of Ottawa

NEOARCHEAN EVOLUTION OF THE WESTERN-CENTRAL WABIGOON BOUNDARY ZONE, BRIGHTSAND FOREST AREA, ONTARIO

by

Julie Louise Brown

A thesis submitted to the School of Graduate Studies and Research

in partial fulfilment of the requirements for the

degree of M.Sc. in

Earth Sciences

Ottawa-Carleton Geoscience Centre

University of Ottawa

Ottawa, Canada

The undersigned hereby recommend to the School of Graduate Studies and Research, acceptance of the thesis,

NEOARCHEAN EVOLUTION OF THE WESTERN-CENTRAL WABIGOON BOUNDARY ZONE, BRIGHTSAND FOREST AREA, ONTARIO

submitted by

Julie Louise Brown

in partial fulfillment of the requirements for the degree of

Master of Science

_____
Chair, department of Earth Sciences

_____
Thesis Supervisor

ABSTRACT

The boundary between the western and central domains of the Wabigoon subprovince has been considered to represent a ca. 2.7 Ga suture between juvenile Neoarchean volcanic rocks in the west and granitoid rocks with Mesoarchean ancestry in the central Wabigoon. The nature and timing of interaction between these two terranes was examined southeast of the Sturgeon Lake greenstone belt within the central Wabigoon, where amphibolite-facies supracrustal remnants are dismembered by Neoarchean plutonic rocks and shear zones.

Of the 4 preserved ductile deformation fabrics, D1 and D2 are bracketed by a 2718 +/- 7 Ma tonalite gneiss and crosscutting 2715 Ma tonalite dyke. The main penetrative S3 foliation affects most units, including quartz-rich sandstone deposited after 2701 Ma. A 2697 Ma granodiorite dyke cutting S3 in mafic and metasedimentary rocks provides a lower bracket on D3. Peak metamorphic conditions (M1) of 5.1 kbar, 640^{o}C were obtained through TWEEQU calculations on mineral compositions in the S3-defining equilibrium assemblage sil-crd-grt-bt-plag-qtz-ilm. Rapid burial and heating are required to accommodate age constraints on M1 (< 2701>2697 Ma), with a maximum ca. 4 m.y. time window in which sediments were deposited at the surface of the earth, buried to depths of ca. 15 km and heated to upper amphibolite-facies conditions.

North-south D4 shortening overprinted earlier structures with open E-W trending folds, developed axial planar biotite cleavage in metasedimentary units, and S4 grain – scale biotite cleavage in post-D3 granitoids (M2). Cooling between M1 and M2 is indicated by D4 biotite growth in the D3 cataclastic, chlorite-grade Hilltop Creek Fault zone. Regional, ductile, sinistral shear zones cut S3 and F4. The latest movement along these structures is constrained by post-tectonic 2678 Ma titanite from the Brightsand River shear zone.

Regional implications can be drawn from the observation of 2725-2715 Ma D1 and D2 deformation events in the central Wabigoon. These constraints overlap with an early deformation event in the Pipestone Lake area of the western Wabigoon (2727-2712 Ma; Edwards and Stauffer, 1999), implying that the western and central domains of the Wabigoon may have experienced common deformation prior to the putative D3 suturing event at ca. 2.7 Ga. Regional evidence from detrital zircon and inheritance studies in the western Wabigoon provide support for juxtaposition by ca. 2710 Ma with ancient crust of the Winnipeg River subprovince.

RÉSUMÉ

La limite entre les roches volcaniques juvéniles néoarchéennes de la partie occidentale de la sous-province de Wabigoon et les roches granitoïdes avec une ascendance mésoarchéenne de la partie centrale de cette sous-province est considérée comme ayant préservé une événement de collision entre ces deux terranes à environ 2,7 Ga. L'interface entre ces deux terranes a été examiné le long de la marge sud-est de la ceinture de roches vertes de Sturgeon Lake, là où des lambeaux de roches supracrustales du faciès des amphibolites sont démembrées par des roches plutoniques et des zones de cisaillement ductiles néoarchéennes.

Des quatres événements de déformation ductile, D1 et D2 sont délimités par un gneiss tonalitique daté à 2718 +/- 7 Ma et par un dyke de tonalite qui recoupe le gneiss et daté à 2715 Ma. La plupart des roches ont été affectées par la foliation pénétrative S3, incluant un grès quartzitique déposé après 2701 Ma. S3 et les roches mafiques et métasédimentaires sont recoupées par un dyke granodioritique daté à 2697 Ma. Des conditions métamorphiques (M1) de 5.1 kbar, 640°C ont été obtenues à partir de calculs TWEEQU sur l'assemblage minéralogique sil-crd-grt-bt-plag-qtz-ilm définissant la foliation S3. Pour accommoder la chronologie des événements de déformation et de métamorphisme associée à M1 (<2701>2697 Ma), il est nécéssaire d'invoquer un mécanisme permettant l'enfouissement (jusqu'à 15 km) et le réchauffement rapides des roches sédimentaires.

Le développement de plis ouverts (F4) à plongement faible vers l'est durant la déformation D4 est accompagné par un clivage de plan axial (biotite) dans les roches métasédimentaires et par un clivage de biotite S4 dans des roches granitoïdes post-D3 (M2) datées à <2697 Ma. Une période de refroidissement entre M1 et M2 est indiquée par la croissance de biotite D4 dans la faille cataclastique D3 de Hilltop Creek au grade de chlorite. Les zones de cisaillements ductiles à décrochement sénestre de Wapikaimaski Lake et de Brightsand River recoupent les structures S3 et F4. Des titanites post-tectoniques provenant de la zone de cisaillement de Brightsand River permettent de fixer l'âge minimum des fabriques tardives développées le long de ces structures à 2678 Ma.

Les observations faites sur les événements de déformation D1 et D2 datés de 2725-2715 Ma dans la partie centrale de la sous-province de Wabigoon permettent d'établir une histoire de déformation commune avec la partie occidentale de la sous-province, comme en témoigne l'événement de déformation précoce dans la région de Pipestone Lake (2727-2712 Ma; Edwards et Stauffer, 1999). Par conséquent, les terranes occidental et centrale de la sous-province de Wabigoon étaient accolés avant l'événement de collision putatif remontant à environ 2,7 Ga. Des études de zircon détritique et d'héritage dans la partie occidentale de la sous-province de Wabigoon appuient la juxtaposition de ce terrane avec la croûte ancienne de la sous-province de Winnipeg River vers 2710 Ma.

ACKNOWLEDGMENTS

This project was carried out at the Geological Survey of Canada and at the University of Ottawa under the supervision of John Percival. This research results from 14 weeks of field work and considerable laboratory work that was funded by the Geological Survey of Canada. The project was partially funded by a Lithoprobe-Natural Sciences and Engineering Research Council of Canada (NSERC) grant to John Percival. I would like to thank John Percival for his keen interest, support and assistance at every stage of this study. Our discussions over the course of this work have been invaluable to the formulation of the ideas presented in this work. His constructive criticism while writing has led to significant improvements in the manuscript. Vicki McNicoll instructed me in geochronological aspects of this thesis, and provided helpful advice and support over the course of study. I am grateful to Mary Sanborn-Barrie, Kirsty Tomlinson, and Tom Skulski for interesting discussions about western Superior geology, and much appreciated advice and encouragement over the years. Tom Skulski and Kirsty Tomlinson have generously shared geochemical data, and made themselves available for help with the interpretation. I thank Don White for providing the seismic data, and for telling me what I could, and could not do with it. I gratefully acknowledge Katherine Venance for ensuring the quality of the microprobe data, Julie Peressini for her assistance with geochronological aspects, Deborah Lemkow for drafting advice, and Joanne Dohar for time spent producing the Open File map. Kate Maclachlan is thanked for her thoughtful review of the Open File map contained in the back pocket of this thesis. Portions of the manuscript were initially prepared as a GSC Current Research Paper, which benefited from a thorough and critical review by Mary Sanborn-Barrie. In the field, Miriam Campbell provided capable assistance and appreciated companionship. My participation in the western Superior NATMAP field trips was a fantastic introduction to the regional geology, and I would like to thank all of the participants. Dr. Miller from Carleton University is thanked for his professional advice, offered from his unique non-geological vantage point, which continues though I have changed fields (for the better, as I continue to assure him). Many thanks to my sedimentologist friends Kelli Powis and Simone Dumas for stimulating discussions, some of which were even geological (most notably during the après ski of course). Stefan Kruse, thank you, for reading my structural geology chapter: I will try to remember about the shear zones (for next time). There are of course many other colleagues and friends that I would like to mention, but time is running short, and I must finish up these acknowledgments. Let us see... ah yes. How could I leave out the excellent Dr. Carson? Thanks, Chris.

Finally, I would like to extend my gratitude to my family for their love, support and encouragement over the years, and especially my grandparents Ken and Ena Rowsell.

This thesis is dedicated to my grandfather Ken Rowsell, who passed away shortly before I could finish writing these acknowledgments. I will always remember him for his home made red wine which he drank on the porch in the summer, his bottomless collection of red sweaters, his sense of humour, and his remarkable ability to build anything.

ORIGINAL CONTRIBUTION

This research focuses on understanding the interface of the western and central Wabigoon subprovince of the Superior Province through multi-disciplinary study of the geological, structural, and metamorphic history of the Brightsand Forest area. Mapping was carried out over 2 field seasons, in 1998 and 1999. In 1998, I was part of a GSC field crew supervised by John Percival, which produced a 1: 100 000 scale map which includes the thesis study area (Percival et al., 1999a,b). Over 11 weeks in 1999, I upgraded the mapping begun in 1998 to 1:25 000 scale in the thesis area. The map in the back pocket of this thesis is being prepared to ISO 9001 standards by the GSC Cartographic Section as Geological Survey of Canada Open File map #4286, with John Percival as co-author (Brown and Percival, 2002). I prepared AutoCAD drawing files showing point-source data and depicting the geology based on field mapping and aeromagnetic data interpretation. Detailed proprietary aeromagnetic data for the area was acquired from Noranda Ltd. and processed as part of a B.Sc. thesis by Miriam Campbell, whom I co-supervised during the 1999 field season.

The geochemical character of amphibolite units was assessed by analyzing selected samples. Major and trace element analyses were done at the Geological Survey of Canada. Treatment of the geochemical data was facilitated by consultation with Kirsty Tomlinson, who also provided Nd-Sm isotopic data on 8 samples. Technicians at the Geological Survey of Canada performed crushing, grinding and zircon separation of geochronology samples, under the supervision of Vicki McNicoll. I picked, abraded and photographed zircon separates, in consultation with Vicki McNicoll. Don White provided available seismic data acquired through Lithoprobe, and was consulted on the interpretation. The estimates of P-T conditions were calculated using TWEEQU software based on analyses of mineral assemblages I selected in consultation with John Percival. Microprobe analyses were done at the Geological Survey of Canada by Katherine Venance.

I wrote and compiled each chapter of this thesis and received comments regarding content, style, and format from John Percival and Vicki McNicoll (geochronology). Natasha Wodicka helped translate the abstract. A preliminary version of Chapter 2, also including some structural analysis and seismic data, was originally prepared as a contribution to the Geological Survey of Canada's Current Research volume, with myself as first author and with John Percival, Don White, Kirsty Tomlinson, and Vicki McNicoll as co-authors (Brown et al., 2000). This paper was reviewed by the co-authors, and internally refereed by Mary Sanborn-Barrie.

TABLE OF CONTENTS

Acceptance sheet ii

Abstract iii

Resume iv

Acknowledgments v

Original Contribution vi

Table of Contents vii

List of Tables xi

List of Figures xii

CHAPTER 1 Introduction 1

Accretionary tectonics in the Archean 1

Western Superior Lithoprobe (WSL) and NATMAP (WSN) projects 5

Terminology 5

The Brightsand Forest area 6

Contributions of this thesis to research and understanding of the Western Superior Province 8

CHAPTER 2 Geological Setting 9

REGIONAL GEOLOGICAL SETTING 9

Sturgeon Lake – Savant Lake greenstone belt (western Wabigoon) 10

Sturgeon Lake – Obonga Lake granitoid corridor (central Wabigoon) 12

Obonga Lake greenstone belt (central Wabigoon) 13

Onaman – Tashota greenstone belt (eastern Wabigoon) 14

GEOLOGY OF THE BRIGHTSAND FOREST AREA 15

Southern panel 15

Supracrustal rocks 16

Plutonic rocks 17

Cataclastic rocks 18

Central panel 18

Supracrustal Rocks 18

Rude Lake tonalite gneiss (unit "G", figure 2-11) 21

Other plutonic units 21

Northern panel 22

The Robert Lake high strain zone 22

Supracrustal Rocks 23

Plutonic units 23

ECONOMIC INTEREST 24

CHAPTER 3 Geochemistry 61
INTRODUCTION 61
REGIONAL GEOCHEMICAL AFFINITIES 61
Sturgeon Lake – Savant Lake greenstone belt 61
Obonga Lake greenstone belt 62
Central Wabigoon granitoids 63
METHODOLOGY 64
Analytical techniques 64
Sample collection and data treatment 65
MAJOR ELEMENT CHEMISTRY 65
TRACE ELEMENT GEOCHEMISTRY 66
Multi-element primitive mantle normalized diagrams 66
Southern panel 67
Central panel 67
Northern panel 6xiii
Nd Isotopes 68
DISCUSSION 69

CHAPTER 4 U-Pb Geochronology 84
INTRODUCTION 84
Regional Character and Constraints 84
U – Pb Analytical Techniques and Data Treatment 84
SAMPLE DESCRIPTIONS AND RESULTS 86
(A) Fine-grained felsic sill (J-737) 86
(B) Tonalite orthogneiss (J-551 Rude Lake tonalite gneiss) 87
(C) Quartz-rich metasandstone (p872) 88
(D) Granodiorite dyke (J-446b) 89
TIMING OF METAMORPHISM 90
(E) Annealed mylonite (p864b) 90
(F) Semipelite (J-446a) 91

CHAPTER 5 Structural Geology 115
INTRODUCTION 115
REGIONAL STRUCTURAL CHARACTER AND CONSTRAINTS 115

Sturgeon Lake – Obonga Lake granitoid – gneiss domain (central Wabigoon) 115
Sturgeon Lake – Savant Lake greenstone belt (western Wabigoon) 117
The Obonga Lake greenstone belt (central Wabigoon) 117
Correlation between Plutonic and Volcanic domains 119
STRUCTURAL GEOLOGY 120
Primary structures 120
D1 and D2 structures 120
D3 structures 122
I) S3 foliation 122
II) D3a structures 122
III) D3b structures 124
D4 structures 125
Fold Interference Patterns 126
D4a structures 126
The Robert Lake zone 128
Conclusions on D4 130
Absolute age constrains on deformation chronology 130
LITHOPROBE Seismic Line 1D 131
Cross – section 133
DISCUSSION 135
Nature of D1 135
Nature of D2 137
Nature of D3 137
Nature of D4 139
SUMMARY 140

CHAPTER 6 Metamorphism and Deformation 162
INTRODUCTION 162
PETROGRAPHY AND MINERAL COMPOSITIONS 163
South Sturgeon basalt 163
Southern Panel 163
Amphibolite 163
Metasedimentary rocks 164
Plutonic rocks 164
Central Panel 164
Amphibolite 164
Metasedimentary rocks 165

Plutonic rocks 166
Cataclasite 166
Northern Panel 167
Amphibolite 167
Plutonic rocks 167
STRUCTURAL – METAMORPHIC RELATIONSHIPS 168
METAMORPHIC CONDITIONS 169
METHODOLOGY 169
Part 1: TWEEQU 170
Part 2: Hornblende – plagioclase thermometry 172
Calculations (Holland and Blundy, 1994): 172
RESULTS 173
Part 1: TWEEQU 173
Part 2: Hornblende – plagioclase thermometry 175
DISCUSSION 176
CONCLUSIONS 180

CHAPTER 7: Summary and Conclusions 211
CORRELATION OF MAP UNITS: SUMMARY OF INTERPRETATIONS 211
Southern Panel 211
Central Panel 212
Northern Panel 213
Significance of the Hilltop Creek fault zone 213
REGIONAL CORRELATION OF DEFORMATION 214
TECTONIC EVOLUTION OF THE BRIGHTSAND FOREST AREA 214
CONCLUSIONS 219

REFERENCES 224

APPENDICES
Geochemical data 235
Mineral chemical data 238

GSC Open File Map # 4286 : is included in the back pocket of this thesis.

LIST OF TABLES

Table 3-1: Nd values from selected amphibolites from the Brightsand Forest area. K.Y. Tomlinson's unpublished data, 1999. 77

Table 4-1: U-Pb geochronology for the Wabigoon subprovince and the Kenora area of the Winnipeg River subprovince. 93

Table 4-2: U-Pb analytical data. 94

Table 5-1: Summary of deformation and intrusion chronology. 161

Table 6-1: Mineral assemblages and approximate modes for amphibolite and metasedimentary rock units. 181

Table 6-2: Molar fractions of garnet end members for pelite and amphibolite. 188

Table 6-3: Mineral analyses for pelite. 201

Table 6-4: Thermobarometry results for pelite. 201

Table 6-5: Mineral analyses for amphibolite. 202

Table 6-6: Thermobarometry results for amphibolite. 202

Table 6-7: Mineral analyses for hornblende-plagioclase thermometry. 205

Table 6-8: Results from hornblende-plagioclase thermometry. 206

LIST OF FIGURES

Figure 2-1: Map of the western Superior Province showing subprovincial structure. 27

Figure 2-2: A: Location map for the study area. B: Geology map of the Sturgeon-Savant greenstone belt. 29

Figure 2-3: Aeromagnetic map of the western-central Wabigoon subprovince. 31

Figure 2-4: Simplified geology map of the Brightsand Forest area. 33
With legend. 34

Figure 2-5: Metavolcanic rock units in the southern panel. 36

Figure 2-6: Metasedimentary rock units in the southern panel. 38

Figure 2-7: The Hilltop Creek fault. 40

Figure 2-8: Central panel rocks within the Rude Lake package. 42

Figure 2-9: Quartz-rich metasandstone within the central panel. 44

Figure 2-10: Conglomerate within the central panel. 46

Figure 2-11: The Robert Lake amphibolite and associated supracrustal rocks. 48

Figure 2-12: The Rude Lake tonalite gneiss. 50

Figure 2-13: The Robert Lake zone. 52

Figure 2-14: Mafic dykes cutting hornblende tonalite on Robert Lake. 54

Figure 2-15: Xenolithic amphibolite dykes on Robert Lake. 56

Figure 2-16: Northern panel mafic units. 58

Figure 2-17: Cross-cutting relationships. 60

Figure 3-1: Major element geochemistry diagrams. 72

Figure 3-2: Spider diagrams superimposed on the map area. 74

Figure 3-3: Spider diagrams for the southern, central, and northern panels. 76

Figure 3-4: εNd vs time for 8 samples from the study area. Regional data is also shown. 79

Figure 3-5: Spider diagrams comparing amphibolite in the study area to basalt in greenstone belts. 81

Figure 3-6: Spider diagram for comparison of felsic rocks. 83

Figure 4-1: Simplified geology map of the study area with U-Pb sample locations plotted. 96

Figure 4-2: Concordia diagram for sample A. 98

Figure 4-3: Concordia diagram for sample B. 100

Figure 4-4: Concordia diagram for sample C. 102

Figure 4-5: Granodiorite dykes cutting S3. 104

Figure 4-6: Concordia diagram for sample D. 106

Figure 4-7: Mylonitic tonalite along the edge of the Brightsand River shear zone. 108

Figure 4-8: Concordia diagram for sample E. 110

Figure 4-9: A: S3 with concordant migmatitic layering in semipelite crenulated by F4. B: The same relationships in thin section. 112

Figure: 4-10: Concordia diagram for sample F. 114

Figure 5-1: Lower hemisphere equal area stereographic projections of poles to planes of early fabrics including S1 layering and F2 axial planes. 142

Figure 5-2: S1 foliated tonalite gneiss (A) and S1 foliated hornblende tonalite (B). 144

Figure 5-3: D3 planar and linear structures. 146

Figure 5-4: A: Sketch map of the area west of Rude Lake. B: Form surface map of the same area. 148

Figure 5-5: D4 linear and planar structures. 150

Figure 5-6: The Brightsand River and Wapikaimaski Lake shear zones. 152

Figure 5-7: The Robert Lake straight zone. 154

Figure 5-8: Seismic profile along Lithoprobe line 1d. 156

Figure 5-9: Location map for the seismic profile, with station locations. Also shown are the profile lines for Figure 5-10. 158

Figure 5-10: Cross-section beneath the study area. 160

Figure 6-1: Fine-grained amphibolite from the Sturgeon belt and the southern panel. 183

Figure 6-2: The southern sedimentary group. 185

Figure 6-3: Coarse-grained amphibolite from the central panel. 187

Figure 6-4: A: Sillimanite-biotite-cordierite-garnet S3 fabric crenulated by F4. B: Garent in pelite with faint inclusion trails. 190

Figure 6-5: Felsic rocks in the study area. 192

Figure 6-6: The Hilltop Creek fault zone. 194

Figure 6-7: Coarse-grained amphibolite from the northern panel. 196

Figure 6-8: TWEEQU results for pelite. 198

Figure 6-9: TWEEQU results for amphibolite 200

Figure 6-10: Garnet with resorbed appearance in amphibolite. 204

Figure 6-11: Histogram of temperatures determined with using hornblende-plagioclase thermometry. 208

Figure 6-12: Pressure-temperature-time path from ca. 2700 to 2670 Ma. 210

Figure 7-1: Geology map of the western-central Wabigoon subprovince, superimposed by the ages of deformation events and ca. 2.7 Ga sedimentary rocks keyed to their location. 221

Figure 7-2: Tectonic model for the evolution of the western-central Wabigoon boundary zone. 223

CHAPTER 1: INTRODUCTION

The Canadian Shield is made up of Archean cratons stitched together by Proterozoic orogenic belts (Hoffman, 1989). The largest of these cratons is the Superior Province which has been divided into litho-tectonic domains (subprovinces) on the basis of lithology, structural trends, metamorphic grade, geophysical characteristics, cross-cutting relationships and absolute ages of rock units. Four subprovince types were recognized by Card & Ciesielski (1986): granite - greenstone (volcano - plutonic), metasedimentary - migmatite, high - grade gneiss and plutonic. The final stages of subprovince assembly occurred during the Kenoran orogeny, between 2720 and 2690 Ma (Williams et al., 1992).

Accretionary tectonics in the Archean

It is a widely held view that the geological history of the Superior Province was dominated by horizontal accretion of allochthonous terranes, resulting in alternating linear subprovinces in a manner analogous to processes of crustal accretion. For example, Card (1990), Williams (1990), and Williams et al. (1991) considered the tectonic evolution of the Superior Province to be directly comparable to that of younger orogens. Present plate configurations of the western Pacific region (vicinity of Japan and Philippines) provide a setting that could explain juxtaposition of oceanic assemblages with continental blocks such as those seen in the Superior Province subprovinces.

With the advent of plate tectonic theory came a debate about its relevance to crustal evolution in the Archean (pre 2.5 Ga). Prior to the early 1970s, greenstone belts were widely thought to be the product of volcanic rocks erupted into curvilinear rift

basins. The rise of buoyant gneiss domes caused wedging of greenstone belts into synforms (Jensen, 1985). Anhaeusser et al. (1969) suggested that the linear nature of greenstone belts was related to rift magmatism, in which volcanism occurred in linear basins along weakened zones in the thinned upper (continental) crust. Fixist models such as these assumed continuous ("layer cake") volcanic stratigraphy, and evolved initially without recognizing fault contacts and/or major unconformities between volcanic assemblages. In the absence of large-scale horizontal tectonic transport, volcanism would have to have occurred in situ (Ayres and Thurston, 1985). With the advent of modern U-Pb geochronology, significant time gaps have been recognized between volcanic assemblages in greenstone belts. Likewise, more recent mapping has recognized faults and shear zones that could have accommodated significant horizontal transport of allochthonous terrains.

The question of whether or not plate tectonics operated in the Archean has received much attention since mobilist interpretations for greenstone belts were suggested in the early 1970s (Krogh and Davis, 1971; Talbot, 1973; Langford and Morin, 1976). Skepticism about whether or not plate tectonics operated before about 2.0 Ga is based on the lack of certain geological features considered diagnostic of modern plate tectonics and which are preserved in many Phanerozoic and some Proterozoic orogens. Hamilton (1998) systematically reviewed components of convergent and divergent plate systems of Phanerozoic orogens and listed many differences between modern plate settings and their proposed Archean analogues. The lack of sedimentary sequences with characteristics of modern accretionary wedges speaks to process differences or lack of preservation of accretionary prisms at Archean and Proterozoic convergent margins. Significantly,

chaotic melanges, in which stratigraphic layering has been tectonically disrupted by intense shearing and fracturing into isolated inclusions within sheared matrix (Miall, 1990) have no recognized Archean or Proterozoic equivalents. Another characteristic of modern convergent margins is the presence of paired metamorphic belts (low P high T with high P low T, Miyashiro et al., 1982). High P low T metamorphic mineral assemblages (blueschist-facies) have not been recognized in rocks older than Neoproterozoic. Ophiolite complexes representing oceanic crust occur in many modern orogens as klippen thrust onto the upper plate. The oldest documented ophiolite complex with associated harzburgites is Paleoproterozoic in age (2.0 Ga Purtuniq ophiolite; Scott et al., 1992).

As an alternative to plate motion, Hamilton (1998) elaborated a plume – like model for Archean tectonics based on elevated temperatures in the mantle. The abundance of komatiitic (and other ultramafic lavas, possibly contaminated komatiite) requires temperatures of approximately 1600°C for generation of partial melts (200°C hotter than the present upper mantle temperatures, assuming the upper mantle was 'dry' (Arndt et al. 1998, Nisbet et al. 1993, Herzberg 1992). Conversely, if komatiites resulted from melting by mantle hot spots (e.g. Tomlinson and Condie, 2001), they would not reflect the ambient temperature of the rest of the mantle during the Archean. Higher mantle temperatures resulted from higher abundances of radiogenic elements in the Archean. In Hamilton's model, mafic and ultramafic lavas were erupted, creating a thick volcanic crust beneath which radiogenic heat accumulated (in the lower crust and mantle). Heat accumulation beneath the new volcanic crust outpaced the rate at which it was lost by conduction. Partial melting produced tonalite within the deep crust during

prolonged cyclical periods of heat accumulation (ca. 100 Ma) until crustal overturning by the rise of diapiric batholiths (partially driven by crustal delamination?) moved radioisotopes upward, permitting cooling and cratonization.

As the early Earth was undoubtedly richer in radioactive elements, the question of whether or not temperatures in the upper mantle were much greater than at present, are centered around komatiites (plumes vs 'normal' mantle) and whether they were generated in a dry or hydrous mantle (de Wit, 1998). If komatiites were produced from hydrous mantle, liquidus temperatures were lower than those cited above (Arndt et al., 1998; Pollack, 1997), and so Archean mantle geotherms may not have been greatly elevated with respect to the modern.

If indeed the mantle was hydrated, mantle dynamics would have operated in a different manner than at present. Different styles of plate subduction, and different (oceanic) crustal thicknesses (Pollack, 1997) may have been in play during Earth's early tectonic history. For example, shallow subduction (Condie, 1995) and possible thicker (hotter) oceanic crust would result in a much faster moving spreading system. De Wit (1998) proposed a thrust overstacking model for formation of early (>3.5 Ga) Archean continents. With shallow subduction of thicker, more buoyant (due to compositional differences) oceanic crust, large amounts of the incompletely subducting plate would be scraped off and thrust stacked on top of the accumulating craton, building a continent from the top down. This constrasts with models for Archean continent formation involving subduction-related underplating of oceanic slabs (e.g. Helmstaedt and Schulze 1989). In either case (thrust-overstacking or subduction-underplating), the driving

mechanism for heat loss is the same (convection), in contrast with Hamilton's model, where heat is lost through conduction.

Western Superior Lithoprobe (WSL) and NATMAP (WSN) projects

The main objective of the Western Superior LITHOPROBE transect is to test the accretionary model proposed for the Western Superior Province (see Stott, 1997; Chapter 2 this thesis) through seismic reflection/refraction profiles and detailed geological studies of important boundary zones. The Western Superior NATMAP was designed to complement Lithoprobe studies by examining the role of old (>2.8 Ga) continental blocks in the assembly of the Western Superior Province crust. Specifically, it is important to determine whether felsic crust acted as basement to greenstone belts, or was tectonically juxtaposed with the younger volcanic rocks.

The present project addresses objectives of both NATMAP and LITHOPROBE projects in examining the structure and chronology of the Brightsand Forest area, which straddles the boundary between the oceanic western Wabigoon and continental central Wabigoon subprovince (Blackburn, et al. 1991; Sanborn-Barrie and Skulski, 1999; see Figure 1 on attached full size map). Lithoprobe seismic reflection line 1d crosses the area, providing an image of the crust to 45 km depth.

Terminology

For the purpose of this work the following definitions apply, based primarily on those outlined in the Geology of Ontario (Williams et al., 1992) and Stott (1997).
An **assemblage** is defined as a package of supracrustal rocks which share a common volcanic and/or depositional history and may be bounded from other assemblages by unconformities, disconformities, or shear zones. Greenstone **belts** are made up of

supracrustal rocks belonging to one or more assemblage. A **subprovince** consists of rocks of broadly similar origin (e.g. volcano-plutonic; metasedimentary).

A **terrane** is a fault-bounded package. Within Phanerozoic orogens, terranes are allochthonous relative to rocks of continental affinity (Condie, 1995). Within the Superior Province, the term superterrane has been used to describe a group of subprovinces that had been amalgamated prior to the onset of the Kenoran orogeny (Stott 1997). The North Caribou terrane (Thurston et al. 1991) is considered to be a cratonic nucleus.

Subprovince boundaries are commonly linear structural features (see Fig. 2-1). For example, fault zones mark the southern boundary of the Wabigoon with the Quetico metasedimentary subprovince. The Seine fault exhibits features consistent with an early component of dip-slip movement (Fumerton, 1982; Davis et al., 1989), and is cut by the dextral-transcurrent Quetico fault (Devaney and Williams, 1989) both of which form part of the boundary. However, in many areas the concept of a boundary zone is more appropriate. For example, Beakhouse (1988) described the interface between the Winnipeg River and Wabigoon suprovinces as a boundary terrane, as the boundary is not a discrete feature.

The Brightsand Forest area

The Brightsand Forest area is located approximately 120 km southeast of Sioux Lookout (coordinates: 49°47' to 49°57'latitude, 90°05' to 90°26' longitude) covering approximately 100 square kilometers. Rogers (1964) first mapped the area as part of a larger reconnaissance survey at a scale of 1in to 1 mile (= 1 : 69 992.13). He noted the transition from metavolcanic rocks and associated sedimentary units at the southeastern

margin of the Sturgeon Lake greenstone belt to greenstone lenses to the east, dismembered by granitoid intrusions.

Lakes and rivers drain to the north and northeast. Relief is variable, depending on the nature of bedrock. Granites in southern Mountairy Lake, northern Rude Lake, parts of Harmon Lake and various other locations form hills and ridges up to 10s of meters above lake-levels. Sporadic sand deposits cover southern parts of the map area, and much of the topography here is attributed to the presence of moraine ridges.

Field work commenced in 1998 (3 weeks) when the author was a senior assistant with a GSC field party mapping the Sturgeon Lake – Obonga Lake area (Percival et al., 1999b), and was completed during the summer of 1999 (11 weeks). Logging roads allow access to the geographical centre of the map area where the 1999 camp was located. Mapping at the 1: 20 000 scale was accomplished through a combination of truck, ATV, canoe and foot traverses. The Brightsand River forms part of an extensive lake and river network accessible by canoe and portage routes. Most of the forest has been decimated by clear cut logging in the 1990s, although a border of trees was maintained along the river network. Limited replanting during the past 10 years has established sporadic Jack pine woods along remnant logging roads.

Contributions of this thesis to research and understanding of the Western Superior Province

1) Detailed geological map at the scale of 1: 20 000, of the BSF area, subdivisions into 3 structural panels (GSC Open File #4286).
2) Detailed geochemical analyses of metavolcanic rock units, as a basis for correlation with adjacent greenstone belts (Chapter 3).
3) Precise U – Pb geochronology of major rock types providing absolute age constraints on the geological history of the area (Chapter 4,5).
4) Elucidation of the metamorphic history of the region based on petrographic and thermobarometric analysis (Chapter 6).
5) Integrated thermotectonic model of the region, incorporating structural, metamorphic, geochronological, and seismic data (Chapter 6).
6) Regional tectonic model of the interface between the western and central Wabigoon subprovince (Chapter 7).

CHAPTER 2: GEOLOGICAL SETTING

REGIONAL GEOLOGICAL SETTING

The western Superior Province consists of ca. 3.0 - 2.7 Ga greenstone belts and granitoid rocks. In the north, the North Caribou terrane (Thurston et al., 1991) is considered to represent a ca. 3.0 Ga cratonic nucleus. The southern margin of this older region is generally thought to have been a continental margin to which the central subprovinces were accreted. Subprovinces of this central region are linear, east - trending belts of volcano - plutonic rocks (Wabigoon, Wawa), alternating with metasedimentary (Quetico, English River), and plutonic (Winnipeg River) domains (Fig. 2-1). The Minnesota River Valley gneiss terrane makes up the southernmost component of the Superior Province and contains rocks as old as 3.6 Ga (Card, 1990; Stott, 1997). Evidence for pre - Kenoran events comes from 3.0 Ga platformal sequences of the North Caribou terrane and from 2.99 - 2.80 Ga continental margin sequences of the Uchi subprovince. At North Caribou Lake, there is evidence for 2.87 Ga tectonism (Thurston et al., 1991). Amalgamation of the central subprovinces during the Kenoran orogeny proceeded from north to south during the interval 2.71 - 2.69 Ga and metasedimentary subprovinces, interpreted as trench fill sequences (e.g. Fralick et al., 1992) were transformed into linear east - trending belts during final collision (Stott, 1997).

Three distinct regions are recognized as subdivisions of the volcano-plutonic Wabigoon subprovince (Blackburn et al., 1991). The western Wabigoon subprovince consists predominantly of anastomosing greenstone belts of Neoarchean age and coeval or younger plutons. Neoarchean plutonic and gneissic rocks with Mesoarchean ancestry

make up most of the central Wabigoon subprovince (Percival et al., 1999a; Whalen et al., in press). The eastern Wabigoon subprovince consists of Mesoarchean and Neoarchean volcanic and plutonic rocks, with greenstone belts geometrically similar to those of the western Wabigoon, but bearing isotopic evidence of Mesoarchean ancestry (Tomlinson et al., 1999). The Brightsand Forest map area, the subject of this thesis, straddles the boundary between the western and central Wabigoon subprovinces, specifically at the southeastern margin of the Sturgeon Lake greenstone belt (Figs. 2-2, 2-3).

Sturgeon Lake – Savant Lake greenstone belt (western Wabigoon)

The Sturgeon Lake-Savant Lake greenstone belt (Fig. 2-2b) lies approximately 10 km west of the map area. The belt consists of three distinct tectono-stratigraphic packages: a continental margin sequence (Jutten group), a diverse oceanic terrane (Fourbay, Beckington, Central and South Sturgeon assemblages), and a polymictic conglomerate-turbidite succession (Savant sedimentary group) that marks the interface between the two. The Savant group appears to be conformably intercalated with the rocks of oceanic affinity, whereas their contact with the continental margin assemblage is unconformable (Sanborn-Barrie and Skulski, 1999).

Detrital zircons from quartz-rich clastic rocks basal to the continental margin sequence, termed the Jutten sedimentary sequence (Sanborn-Barrie, 1989), yield concordant U/Pb ages of 2948 +/- 3 Ma and 3199 +/- 3 Ma (Sanborn-Barrie and Skulski, 1999) and discordant ages of 3258 +/- 3 Ma and 3297 +/-6 Ma (Davis and Moore, 1991) indicating a Mesoarchean source. Volcanic rocks of the 2750-2880 Ma Jutten group (Sanborn-Barrie et al., 2002), are pillowed to massive tholeiitic basalts overlying the Jutten sedimentary sequence. Oceanic rocks were formed outboard from 2775 to 2718

Ma (Sanborn-Barrie and Skulski, 1999): the Fourbay assemblage (2775 Ma oceanic plateau), overlain by the Beckington, Handy Lake and South Sturgeon assemblages (2745-2730 Ma arc-like sequences) and the Central Sturgeon assemblage (2718 Ma arc-rift sequence). The turbiditic succession including the Savant sedimentary group is interpreted by Sanborn-Barrie and Skulski (1999) as a foredeep sequence, deposited during a ca. 2.7 Ga collisional event, and may conceal a suture zone between the continental margin sequence and the diverse oceanic terrane.

The southern portion of the greenstone belt, in the Sturgeon Lake greenstone belt is outlined here in detail: the metasedimentary Quest Lake assemblage; the volcanic Central Sturgeon assemblage; the Princess-Post Lake metasedimentary assemblage; and the volcanic South Sturgeon assemblage. The South Sturgeon assemblage (2735 Ma. Davis et al., 1985) associated with base-metal mineralization, and is interpreted as a submarine caldera complex (Morton et al., 1991). The westward younging Quest Lake sediments are a mixed package of siltstone, feldspathic wacke, chert and magnetite iron formation, the latter of which is restricted to the southeast (Sanborn-Barrie et al., 1998). SHRIMP (sensitive high resolution ion microprobe) II ages on detrital zircon from feldspathic layers within this unit indicate that it contains Mesoarchean and Neoarchean detritus and was deposited at ~2720 Ma (Skulski, Sanborn-Barrie and Stern, unpublished data 1999; Sanborn-Barrie et al., 2002). The Central Sturgeon Lake assemblage (2718 Ma, Davis and Trowell, 1982) includes mixed tholeiitic and calc-alkaline basalts. Basal units are pillowed to massive flows, with pillow and flow breccias, and hyaloclastite (Sanborn-Barrie et al., 1998). Near Quest Lake, intermediate volcanic breccia and iron-rich metasedimentary rocks overlie mafic rocks (Trowell, 1983). The Princess-Post Lake

metasedimentary rocks comprise clast-supported conglomerate and cross-bedded wackes (<2720 Ma, Skulski, Sanborn-Barrie and Stern, unpublished data 1999). Grading in certain beds indicates eastward younging in the Princess-Post Lake assemblage, interpreted to overlie the Central Sturgeon Lake assemblage (from which the sediments are derived; Sanborn-Barrie et al., 1998).

Sturgeon Lake – Obonga Lake granitoid corridor (central Wabigoon)

The granitoid-gneiss complex of the central Wabigoon subprovince to the east is made up of several generations of plutonic rocks and gneisses (Percival et al., 1999a). Interpreted previously as a zone of diapiric upwelling (Edwards and Sutcliffe, 1980), the central Wabigoon subprovince was also inferred to represent basement to some supracrustal sequences of the western Wabigoon subprovince (Blackburn et al., 1991; Thurston and Davis, 1985). The main components of this largely felsic granitoid domain include grey gneissic tonalites, foliated tonalite to granodiorite, mafic dykes, megacrystic granodiorite and granite dykes and sills. Age relationships between these phases have been determined in the field and by subsequent geochronological, and co-genesis by geochemical analyses.

The oldest components (foliated and gneissic tonalites) that have been dated include lithologically and structurally complex gneisses of the Harmon Lake area. A 2774 Ma tonalite from this vicinity occurs as a sheet in gneissic rocks and contains metamorphic zircon of 2697 Ma (Davis, 1989). A tonalite gneiss from near Harmon Lake yielded zircon ages of ca. 2.89 Ga, as well as zircon of 2693 Ma that may be metamorphic in origin (V. McNicoll, unpublished data 1998). Fabrics (S1 gneissosity and F2 upright folds) within the gneiss are cut by a tonalite dyke dated at 2715 Ma

(Percival et al. 1999b). This dyke is thought to be part of a suite of tonalitic and granodioritic rocks emplaced between 2723 and 2709 Ma.

D3 and D4 structures within homogeneous granitoid rocks include a regional S3 foliation, inferred to have been subhorizontal prior to development of F4 folds. The D3 and D4 structures may correlate with D1 and D2 fabric elements within the Sturgeon – Savant belt (Percival et al., 1999a, Sanborn-Barrie and Skulski, 1999), although S1 fabrics are steep in the greenstone belt and shallowly dipping in the gneisses.

Younger granitoid units consist mainly of granite and granodiorite dykes and sills in addition to large plutons of K-feldspar megacrystic granodiorite in the areas of Siess, Vista, and Wapikaimaski Lakes (Percival et al., 1999a, Whalen et al., in press).

Obonga Lake greenstone belt (central Wabigoon)

The Obonga belt is located 25 km along strike to the east of the map area. The belt is divided into southern and northern assemblages separated by a gabbroic core zone. The southern assemblage includes deformed mafic and felsic metavolcanic rocks dated between 2734 and 2726 Ma (Tomlinson et al., 2002). Their relationship with the core zone is ambiguous, although geochronology of a pegmatitic gabbro from the core zone yielded an age of 2733 Ma, suggesting some relationship to the southern assemblage (Tomlinson et al., 2002). The younger northern assemblage is composed partly of the Awkward Lake sedimentary package, a complexly deformed package of argillite, sandstone and pelite. Percival and Stott (2000) suggested that this unit may be correlative with turbidites of the Savant sedimentary group in the Sturgeon - Savant greenstone belt. A dacite from the northern assemblage yielded an age of 2703 Ma

(Tomlinson et al., 2002), coeval with the <2704 Ma turbidites of the Savant sedimentary group (Sanborn-Barrie and Skulski, 1999).

Onaman - Tashota greenstone belt (eastern Wabigoon)

The Onaman-Tashota greenstone belt, located to the east of Lake Nipigon, is the central feature of the eastern Wabigoon subprovince, and has been the subject of recent detailed remapping (Stott and Morrison, 1995; Stott and Parker, 1996 and 1997; Stott and Straub, 1999; Stott et al., 2002). The belt consists mainly of 2.75 – 2.72 Ga Neoarchean volcanic assemblages. Mesoarchean (pre-2.8 Ga) volcanic and intrusive units occur in the northwestern portions of the belt (Stott and Straub, 1999). The northern half of the belt shows extensive interaction with an older crustal component on the basis of Nd model ages on felsic rocks of 3.28 to 3.19 Ga, suggesting that volcanic rocks erupted through and digested Mesoarchean crust (Tomlinson et al., 2002). An igneous age of 3.056 Ga was obtained from one felsic rock (Stott, 2001). An apparent N-S symmetry is created by the presence of large felsic volcanic centres (2.735-2.74 Ma, Stott et al., 2002) along the northern and southern margins of the belt. Ages of calc-alkaline to intermediate volcanism appear to decrease southward from 2.739 Ga at Marshall Lake to <2.707 Ga dacitic rocks on Humboldt Bay (Stott, 2001). The <2707 Ma dacite could correlate with the 2703 Ma dacite (Tomlinson et al., 2002) of the Obonga belt.

GEOLOGY OF THE BRIGHTSAND FOREST AREA

At the southeastern margin of the Sturgeon Lake greenstone belt, volcanic units continue into the central Wabigoon granitoid domain as dismembered screens. The map area is divided into 3 panels on the basis of lithology, structural trends, mineral assemblages, and the location of brittle-ductile deformation zones. From south to north, the size and volume of supracrustal units decrease, whereas the volume of granitic intrusions increases. Units of supracrustal origin rarely preserve primary structures and carry two generations of deformation fabrics: a penetrative regional (S3) foliation subsequently openly folded (F4) about gently east plunging axes.

The lithotectonic map units are discussed in sections from south to north. Bounding structures (faults, shear zones, high strains zones) are discussed likewise where they separate panels, beginning with the Brightsand River shear zone. Figure 2-4 is a geological map with legend (2 pages), keyed to the text. Map unit nomenclature corresponds to a 1:25 000 geological map (Brown and Percival, 2002) located in the back pocket of the thesis, which includes more detail on rock types and structural information.

Southern panel

The ENE-trending Brightsand River shear zone bounds the southern panel in the southeastern corner of the map area. Mylonitic granodiorite and L>S syntectonic granite with subhorizontal stretching lineations characterize this deformation zone (Percival et al., 1999a). Amphibolite units appear to be deflected into this shear zone and cannot be traced east of the structure. The predominant rock type bounding the shear zone is homogeneous medium-grained biotite granodiorite. Strain partitioning becomes apparent in the northern margin of the shear zone, with the local development of (tonalitic)

mylonite. Geochronology and field relationships constrain the age of deformation and metamorphism within this structure (Chapters 4 and 5).

Supracrustal rocks

The Mountairy Lake and Hilltop Lake supracrustal units ("As" ***(1)*** and ***(2)***, Fig. 2-4) consist of amphibolite, interpreted as metamorphosed basalt and andesite based on fine grain size and local heterogeneities. Within the Mountairy Lake unit, dykes and sills of gabbro are common, and sporadic greywacke layers occur within the metavolcanic rocks of this package. Rare layers of garnet-bearing felsic volcanic rock, up to 2.5 m thick, are present within amphibolite in the hinge of a map-scale fold in northern Mountairy Lake (Fig. 2-5b). Common mineral assemblages in metavolcanic rocks are hornblende-plagioclase ± chlorite with minor clinopyroxene.

The Hilltop Lake unit is bound to the south and north by sedimentary rocks ("Sa" and "Sb", Fig. 2-4). The southern sedimentary package consists of metamorphosed sandstones and greywackes, and is interlayered with metavolcanic rocks of the Hilltop Lake unit. The northern sedimentary unit is a diverse panel that contains greywacke, quartz-rich sandstone, slate, granitoid-clast conglomerate, and oxide-facies iron-formation (Fig. 2-6). Sandstone units can be traced up to 7.5 km along strike. Graded and laminar bedding are preserved locally, and generally transposed into the dominant S3 foliation. Based on the continuity of these units along strike to the west of the study area (Rogers, 1964; Trowell, 1983) and similar rock associations, the southern and northern sedimentary units are correlated with the Princess-Post and Quest Lake groups respectively, associated with the Central Sturgeon Lake volcanic assemblage in the Sturgeon Lake greenstone belt (Sanborn-Barrie and Skulski, 1999). Primary features

(graded bedding, channel scours) within the Princess-Post Lake sediments west of the map area young to the north. Subsequent to the formation of graded bedding and chanel scours, folding may be responsible for different younging directions found within the greenstone belt and along its margin.

The meta-conglomerate in the northern sedimentary package is poorly exposed north of Mountairy Lake. Angular, pink, leucocratic, biotite granitoid clasts (Fig. 2-6b), are set in a very fine-grained mafic matrix, accompanied by an intense near vertically-plunging stretching lineation. Clasts do not appear to carry an internal deformation fabric. Along strike to the east, clasts are well foliated, and the unit becomes mylonitic near the Hilltop Creek fault.

The relationship between this unit and the structurally overlying magnetite iron formation to the north is not known, as the contact is not exposed. Iron formation is finely laminated south of Hilltop Lake, but occurs as iron formation intrusive breccia on Hilltop Lake, with a leucocratic monzogranite matrix. The unit is spatially associated with exhalative sedimentary rocks.

Plutonic rocks

Sheets of homogeneous, foliated granodiorite cut the supracrustal units. In the south, fine-grained foliated biotite granodiorite underlies a large area. In the north, medium- to coarse-grained, commonly K-feldspar porphyritic, hornblende-biotite granodiorite is present in the vicinity of Scruffy Lake. All units are cut by garnet-muscovite pegmatite, which is massive to weakly foliated and contains abundant supracrustal enclaves.

Cataclastic rocks

The southern panel is separated from the central panel by cataclastic rocks of the the northwest-trending Hilltop Creek fault (Fig. 2-7). A ~350 m-wide, steeply- to moderately-dipping zone of cataclastic rock is exposed east of Mountairy Lake and along Hilltop Creek on the eastern limb of a north-trending fold. The cataclasite contains angular fragments up to 10 cm in length of granite, amphibolite, and exhalative sedimentary rocks, set in a granular, fine-grained matrix made up of chlorite, epidote, and hematite. Fragments of iron formation within the fault zone may be as large as entire outcrops, but cannot be followed along strike. Dykes of granite are the youngest component of the zone, and also are brecciated. Finely disseminated sulphides occur throughout rocks of various origins within this unit. In thin section, rutile porphyroblasts are boudinaged parallel to the foliation (Chapters 5 and 6). Chlorite grains and rare biotite define a second, overprinting fabric.

Central panel

Supracrustal Rocks

Three main supracrustal units are present in the central panel. In the south, the Scruffy Lake unit ("Ac" ***(3)***) is dominated by fine- to medium-grained, mafic gneiss. It may be continuous with the fine-grained layered to gneissic amphibolites of the Brightsand River unit ("Ac" ***(5)***), on opposing limbs of a southeast trending synform, although the structure is disrupted by intrusive units (Chapter 5). Gabbroic dykes with pitted weathering surfaces cut the main foliation, and carry a northeast-trending mineral lineation. A narrow, <25-m-wide, splay from the Hilltop Creek fault (Fig. 2-7g) consists of a breccia of fine-grained amphibolite fragments within a fine-grained, granular mafic

matrix. This structure separates the Scruffy Lake supracrustal unit from the Rude Lake assemblage ("Ac" *(4)*) to the north.

Mafic rocks of the Rude Lake unit are distinct from adjacent amphibolite bodies (Fig. 2-8). The belt is up to 1.5 km thick and lacks primary volcanic features. Sills of plagioclase porphyritic gabbro commonly contain garnet, rimmed or pseudomorphed by plagioclase. Patches of randomly oriented, acicular amphibole crystals in a plagioclase-rich matrix are sporadically developed through the Rude Lake amphibolites. Amphibolite is cut by locally hornblende porphyritic felsic porphyritic dykes. Porphyritic dykes cross-cut structural layering in amphibolite, but are subsequently foliated and folded along their margins. The northern margin of the unit consists of metre-scale layering of mafic rocks and quartz-rich metasandstone and quartz-wacke (Fig. 2-9).

A 500 m-thick felsic sill (map unit "Fs") occurs in the southwest corner of the Rude Lake unit, where its contact with mafic units is transposed, layered, and sheared. The felsic unit is homogeneous, fine-grained, biotite – muscovite – quartz – plagioclase rock interlayered with pyritic and muscovite-rich schist. The muscovite schist preserves tight, N-trending, chevron-type crenulations of an earlier fabric. Fine to coarse disseminated sulphides occur throughout the felsic unit. Textures characteristic of volcanic origin were not observed, even in the least deformed parts of the body.

South of the felsic unit, a narrow conglomeratic ("Sc") unit contains rounded clasts up to 10 cm in length of granodiorite and volcanic rock types, as well as beds of quartz-rich sandstone (Fig. 2-10). The matrix varies compositionally from quartz-rich meta-sandstone to meta-greywacke. Mafic dykes locally intrude along layering, and

appear to replace the matrix in some places. Strain varies considerably within this unit judging by clast elongation ratios; near the Hilltop Creek fault, clasts attain ratios greater than 10:1.

The Robert Lake unit ("Ac" ***(6)***) consists of mafic and sedimentary units exposed for a strike length of 15 km (Fig. 2-11). Mafic rocks are fine-grained hornblende – plagioclase – clinopyroxene – garnet – epidote amphibolite with a well developed foliation. They are interlayered with sporadic plagioclase porphyritic gabbro, and rare coarse-grained ultramafic rock. Mafic rocks are associated along their entire strike length with psammitic to pelitic metasedimentary rocks. Pelites contain garnet – cordierite – sillimanite – biotite – muscovite – plagioclase – quartz assemblages and are locally migmatitic. Together with the mafic rocks, assemblages indicate metamorphism to upper amphibolite facies. Compositional layering in units of sedimentary origin is interpreted to represent relict bedding, which is now parallel to the penetrative foliation. Later crenulation of this fabric is accompanied by a weak axial planar biotite foliation in fold hinges. Sulphide-rich zones (pyrite, pyrrhotite, chalcopyrite) are localized along the sedimentary schist-amphibolite contact. Within the amphibolite, a 10 m thick unit of silicate-facies iron formation can be traced for 1 km in the Robert Lake area. Proprietary aeromagnetic data provided by Noranda Ltd. indicates that iron-formation within the Robert Lake unit extends from Hilltop Lake for 4 km eastward, through Robert Lake.

The Rude Lake supracrustal package ("Ac" ***(4)***) forms a broad map-scale "S" fold. Located on the eastern limb of the Mountairy Lake fold, this structure could be a F3 parasitic fold (see Chapter 5). These units are also located on the southern limb of a map-

scale synform which links the Scruffy Lake and Brightsand River units. The fold is open and upright in the west, becoming overturned and isoclinal toward the east.

Rude Lake tonalite gneiss (unit "G", figure 2-12:)

This complexly folded tonalite gneiss is a distinctive unit within the area, first described by Percival (1998, see Fig. 3 in Percival 1998). It contains 2 sets of structures which appear to predate fabrics preserved within the supracrustal units, which includes complex donut-shaped fold interference patterns not present in other rock units. Mafic dykes cross-cut most of the gneissic layering, but are boudinaged and folded. Several generations of tonalite, granodiorite and pegmatite are variably deformed. For the most part, grey, medium to fine-grained biotite tonalite constitutes the earliest phase. Gneissic layering is imparted by mm to cm-scale layers of leucotonalite. Subsequent intrusions include several generations of granodiorite and granite.

Other plutonic units

Additional plutonic units of the central panel include sheets of tonalite, granodiorite, tonalite gneiss, and granite. Most of these units have a penetrative, steeply dipping, grain-scale S3 foliation folded into open, east-trending F4 folds. Tonalite gneiss is similar in structural style to amphibolite bands. A massive, coarse-grained, 500 m-wide body of gabbro is exposed west of the Brightsand River within tonalite gneiss ("Gb"). Xenolithic amphibolite units are present within tonalite gneiss and younger plutons. Fine- to medium-grained biotite tonalite carries an S3 foliation and local quartz rodding lineation in the hinges of F4 folds. Sills and dykes of tonalite occur within tonalite gneiss, commonly cutting the layering at a low angle. Tonalite dykes also cut

foliated coarse-grained K-feldspar-porphyritic granodiorite. Granite and granodiorite dykes throughout this panel commonly carry a weak foliation oriented parallel to axial traces of F4 folds. Dykes of muscovite granodiorite cut the S3 fabric parallel to F4 axial planes. One such dyke was sampled to provide an age bracket between D3 and D4 events (see Chapter 4). Late, massive, garnet-, muscovite-bearing granites occur as small plugs and dykes which cut all previously described units.

Northern panel

The Robert Lake high strain zone

The Robert Lake amphibolite is bound along its northern flank by the WNW-trending ductilte Robert Lake high strain zone (Fig. 2-13), which also separates the central and northern structural panels. Steep to moderate, north-dipping structures are prominent along the strike length of the Robert Lake supracrustal belt. In several locations near Harmon Lake, this unit is in tectonic contact with granitoid units to the north. Such zones are characterized by steeply plunging folds, extensive epidote alteration, and local brecciation. Along the length of the Robert Lake supracrustal belt are ENE-trending, consistently moderately plunging mineral lineations (Chapter 5). The southern margin of the northern structural panel is dominated by tonalite gneiss in a 1.5-km-wide straight zone, part of the Robert Lake fault zone, well exposed on the southern portions of Robert Lake. Mafic dykes are transposed into parallelism with the dominant foliation (Fig. 2-14). Moderately east-plunging mineral lineations trend consistently at 070°. A xenolithic unit ("Md", Fig. 2-15) within this straight gneiss consists of dismembered mafic dykes which can be seen to cut the main fabric near the northern

edge of the straight zone. One generation of tonalite cuts mafic dykes, which is in turn cut by syn-D4 granodiorite and unfoliated pegmatite. "S" folds, sinistral offsets along late fractures and sinistral shear zones are all features of this unit. The structural style resembles that of the ductile, sinistral D4 Wapikamaiski and Brightsand River shear zones (Percival et al., 1999a) although the lineation is steeper, possibly indicating a component of dip-slip shear.

Supracrustal Rocks

The northernmost panel is characterized by sparse, discontinuous amphibolite screens, which appear to be the result of dismemberment by several generations of plutons. In some areas dominated by pegmatite, amphibolite units are traceable only as enclave-rich zones. The most prominent and continuous amphibolite is the 5-km-long Stinson Lake unit ("An" ***(7)***) of medium-grained, foliated to gneissic hornblende – plagioclase rocks (Fig. 2-16a). This unit contains pods and layers of a distinctive coarse-grained pyroxenite ("Um", Fig. 2-16b,c) with individual crystals up to 10 cm in size, associated with gabbroic layers containing nodular plagioclase phenocrysts. The northern amphibolite ("An" ***(8)***) is a homogeneous, medium-grained, mafic rock. Amphibolites consist of mineral assemblages of hornblende – plagioclase, with accessory epidote, and plagioclase pseudomorphs of garnet textures.

Plutonic units

Toward the north is a body of coarse-grained, commonly hornblende-porphyritic, hornblende – biotite tonalite ("Th", Fig. 2-14c). Tonalite carries an S1 foliation which is folded into isoclinal F2 folds (large wavelength, Chapter 5), whose limbs are crenulated by closed style, chevron-like, F3 folds. In higher strain areas, axial planar S3 foliation is

dominant. Mafic dykes cross-cut the "Th" tonalite unit. In some areas, xenolithic mafic dykes ("Md") form an intrusive breccia, enclosing fragments of "Th". The margins of these dykes are folded, although axial planar fabrics are not developed (Fig. 2-15c). The above "Th" tonalite may correlate with the Harmon Lake gneiss (Percival et al. 1999a) exposed further to the northeast on the basis of similar structural chronology, although mineralogy and grain size is quite different: Harmon Lake gneisses are finer grained and lack hornblende.

Homogeneous, foliated, medium- to coarse-grained, K-feldspar porphyritic granodiorite and sheets of fine-grained biotite granodiorite cut tonalite gneiss. Dykes of fine- to medium-grained, massive to weakly foliated tonalite cut all previously described units. Granite and pegmatite bodies are massive to weakly foliated, and cut all units within this block. Figure 2-17 illustrates cross-cutting relationships among intrusive units.

The ENE-trending, sinistral Wapikamaiski Lake shear zone (WLSZ) is a ductile D4 feature (Percival et al. 1999a) which transects the northwestern corner of the map area. Mylonitic tonalite gneisses characterize this ca. 1-km-wide zone.

ECONOMIC INTEREST

Within the study area, iron formation extends from Robert Lake to Hilltop Lake, and is spatially associated with sporadic sulphide-rich sedimentary rocks (herein referred to as exhalite). Disseminated sulphide occurrences were noted within the Hilltop Creek fault and the fine-grained felsic sill west of Rude Lake, dominated by the presence of pyrite, less common chalcopyrite, and rare pyrrhotite on southern Hilltop Lake.

Magnetite iron formation on Robert Lake is associated with grunerite-cummingtonite garnetite, but along strike to the northwest occurs with exhalitive metasedimentary schist and evolves to oxide-facies. Blocks of banded iron formation occur within the Hilltop Creek fault, and iron formation breccia is present along the south shore of Hilltop Lake. The latter unit can be traced to the west where it becomes finely laminated and is likely comformable with the northern sedimentary package within the southern panel of the map area. Detailed aeromagnetic maps (Campbell, 2000) helped to trace magnetite iron formation through cover and suggest that the Robert Lake iron formation extends for approximately 10 km continuously along strike. Most past economic interest has focused on possible eastward continuations of volcanogenic massive sulphide-bearing strata from the Sturgeon Lake greenstone belt.

Figure 2-1: Map of the Western Superior Province showing subprovinces. The southern margin of the North Caribou terrane is generally thought to be an ancient continental margin to which the central subprovinces (Uchi, English River, Winnipeg River, Wabigoon, Quetico, Wawa) were accreted. Central region subprovinces are linear, east-trending belts, with granite-greenstone subprovinces alternating with metasedimentary and plutonic subprovinces (see text). Box shows the location of the thesis area. Also shown are the locations of Sturgeon – Savant, Obonga, and Onaman-Tashota greenstone belts in the Wabigoon subprovince. The western Wabigoon extends west from the Sturgeon-Savant greenstone belt (most of which is part of the western Wabigoon), the central Wabigoon extends from the eastern margin of the Sturgeon-Savant belt to the western margin of the Onaman-Tashota greenstone belt, and the eastern Wabigoon extends east from (and including) the Onaman-Tashota greenstone belt.

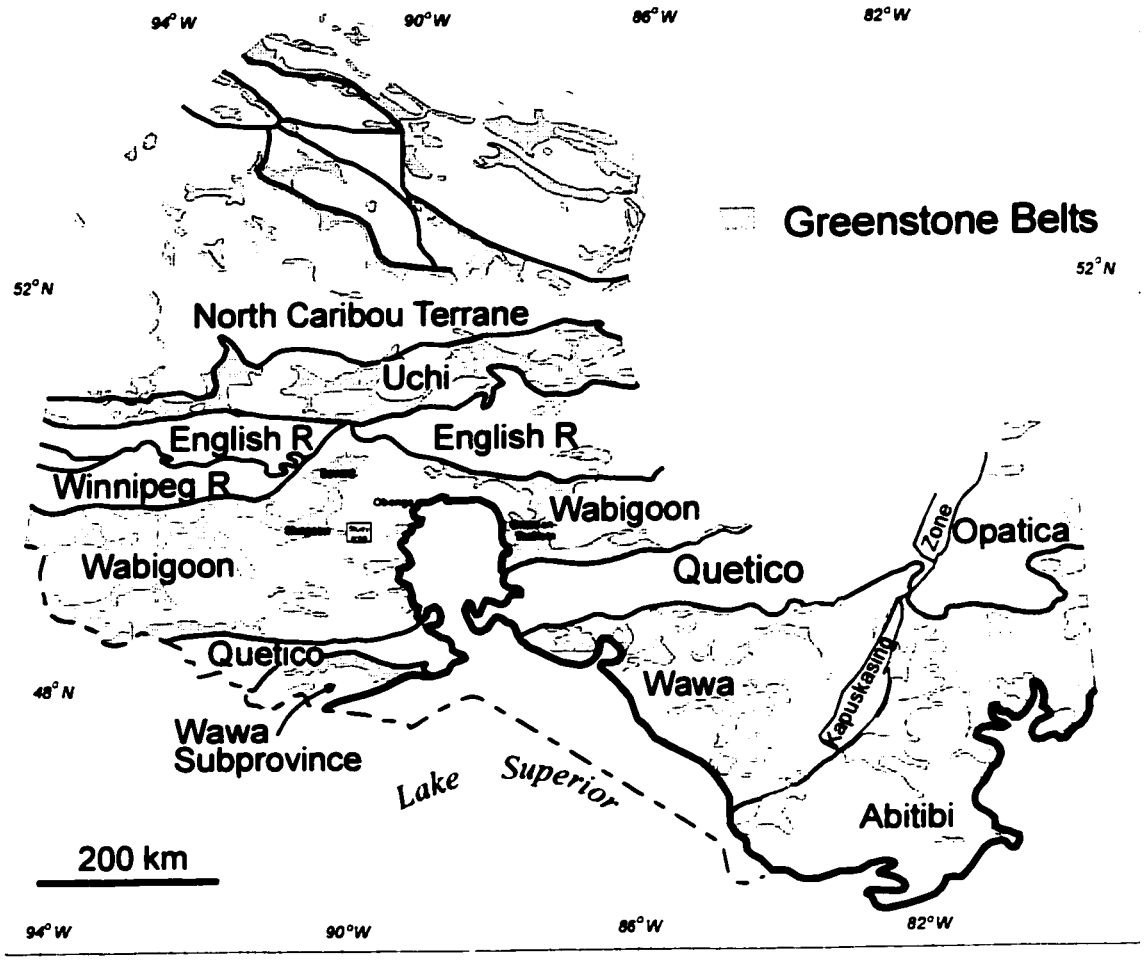
94°W
90°W
86°W
82°W
52°N
48°N
Greenstone Belts
North Caribou Terrane
Uchi
English R
English R
Winnipeg R
Wabigoon
Wabigoon
Quetico
Zone
Opatica
Quetico
Wawa
Kapuskasing
Wawa
Subprovince
Lake Superior
Abitibi
200 km

Figure 2-2: A: Location of the Brightsand Forest area at the southeastern margin of the Sturgeon Lake - Savant Lake greenstone belt. B: Geology map of the Sturgeon-Savant greenstone belt, after Sanborn-Barrie and Skulski (1999). Following the stratigraphy of Sanborn-Barrie and Skulski (1999) the Sturgeon-Savant greenstone belt is divided into 3 distinct packages: a continental margin sequence (the Jutten group), a diverse oceanic package (including Fourbay, Handy Lake, Beckington, Central Sturgeon and South Sturgeon assemblages), and a conglomerate-turbiditic succession (Savant Sedimentary group) that marks the interface between the two. The Jutten group comprises various sequences that have been deposited directly onto the continental margin that is now distinguished as part of the central Wabigoon subprovince. In contrast, the oceanic volcanic packages were erupted outboard and subsequently accreted to the margin of the central Wabigoon.

A: Location map

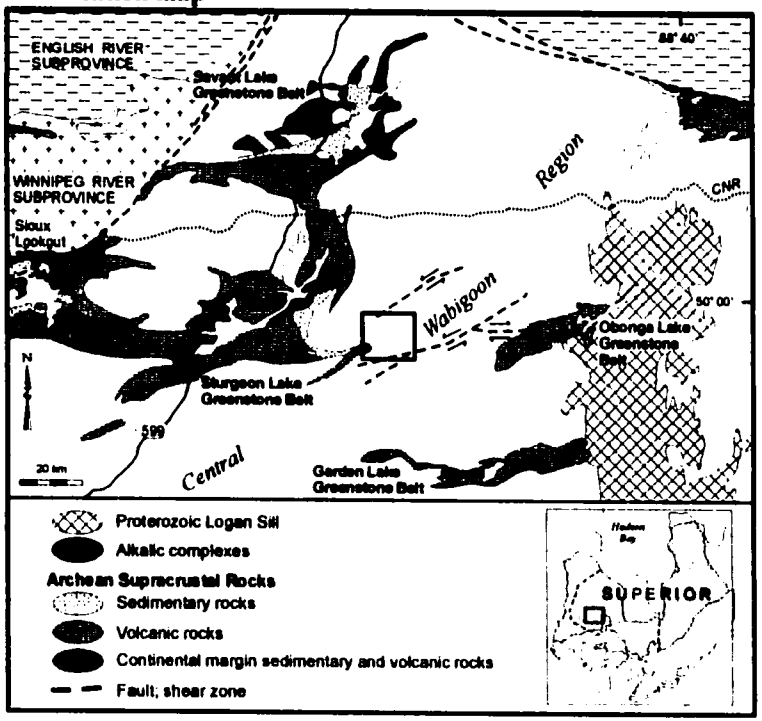

B: *Modified from Sanborn-Barrie and Skulski, 1999*

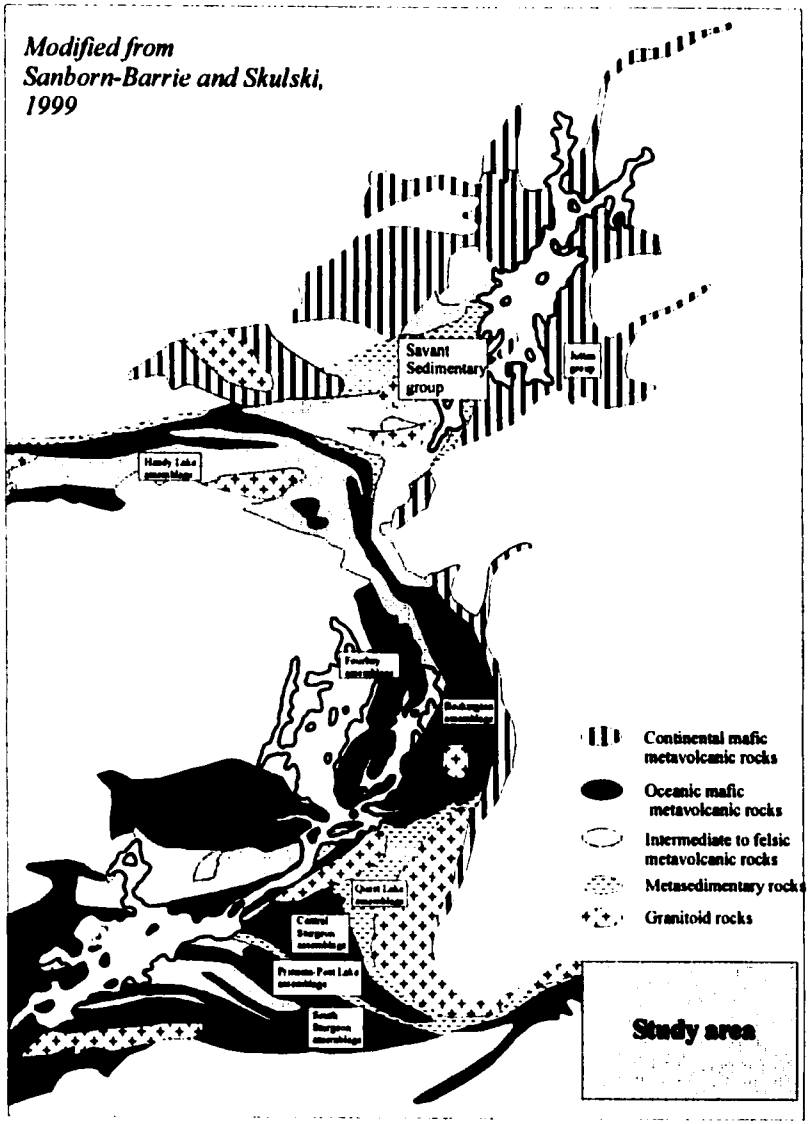

Scale 1:750 000

kilometres 50 0 50

Figure 2-3: Aeromagnetic map of the boundary zone between the western and central Wabigoon subprovince. The western Wabigoon is dominantly blue in colour with portions of the Sturgeon belt highlighted in red. The central Wabigoon including the study area is dominantly red and yellow in colour. The box shows the location of the study area.

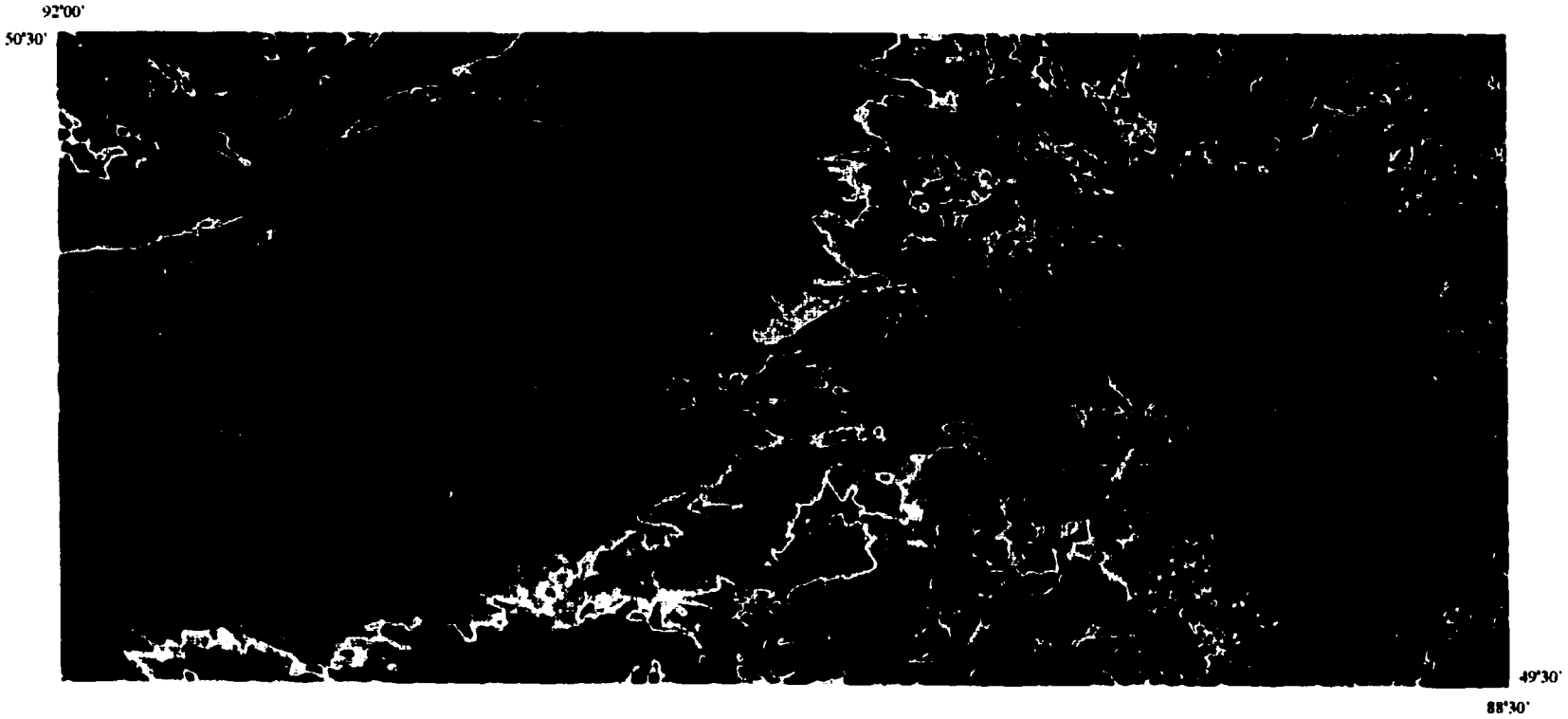
92°00'
50°30'
49°30'
88°30'

Figure 2-4: Geological map of the Brightsand Forest area, with legend (2p.). Bracketed numbers refer to specific supracrustal units in the legend. See map (GSC Open File #4286) in back pocket of this thesis for structural information and more detailed lithological information.

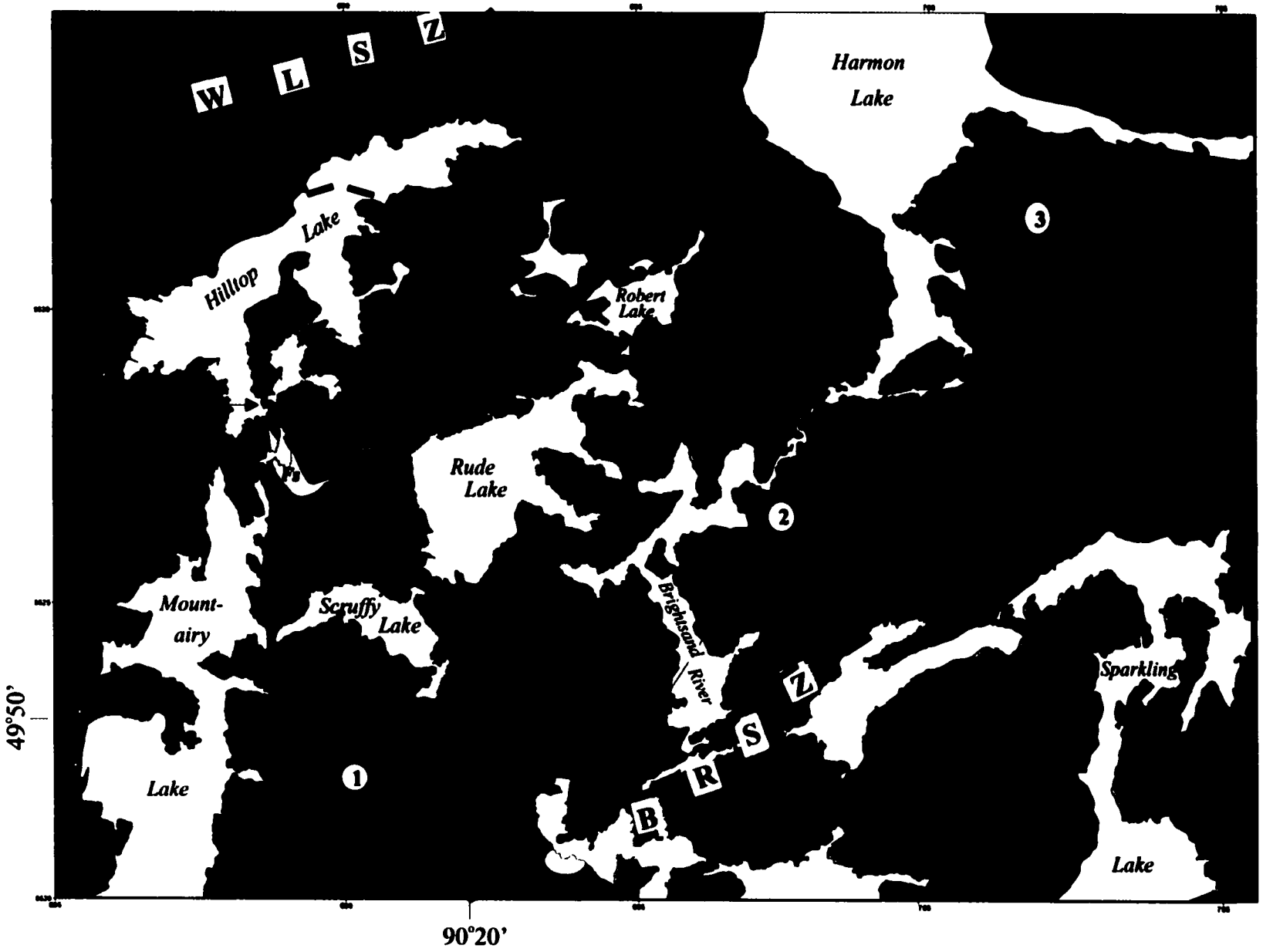
WLSZ
Harmon Lake
Hilltop Lake
Robert Lake
Rude Lake
Mount-airy
Scruffy Lake
Brightsand River
Sparkling Lake
Lake
BRSZ
1
2
3
49°50'
90°20'

LEGEND

FAULT RELATED ROCKS

C Cataclasite

INTRUSIVE ROCKS

Gg Garnet granite and pegmatite
G Granite and pegmatite
D Diorite
Gdp Porphyritic granodiorite
Fs Felsic sill
Gd Granodiorite
Md Mafic dyke
Gb Gabbro
Th Hornblende tonalite
T Tonalite
Tg Tonalite gneiss
TgR Rude Lake tonalite gneiss

SUPRACRUSTAL ROCKS

Southern Panel

S Unsubdivided metasedimentary rocks
Sa Northern sedimentary group
Sb Southern sedimentary group
As Southern panel amphibolite
(1) Mountairy Lake amphibolite
(2) Hilltop Lake amphibolite

Central Panel

Sp Pelitic metasedimenatry rocks
Sc Conglomerate
Sq Quartzite
Ac Central panel amphibolite
(3) Scruffy Lake amphibolite
(4) Rude Lake amphibolite
(5) Brightsand River amphibolite
(6) Robert Lake amphibolite

Northern Panel

Um Pyroxenite
An Northern panel amphibolite
(7) Stinson Lake amphibolite
(8) Northern amphibolite

Unsubdivided

A Amphibolite

SYMBOLS

Road
① Southern panel
② Central panel
③ Northern panel
Fault/Shear zone
HCF Hilltop Creek Fault
RLF Robert Lake Fault
BRSZ Brightsand River Shear Zone
WLSZ Wapikaimaski Lake Shear Zone

Figure 2-5: Meta-igneous units in the Southern panel. A: Felsic volcanic with Mountairy Lake amphibolite. B: Garnetiferous layer in felsic volcanic. C: Fine-grained Hilltop Lake amphibolite. D: Highly strained gabbroic amphibolite in the Mountairy Lake unit, with (F3?) z-folds.

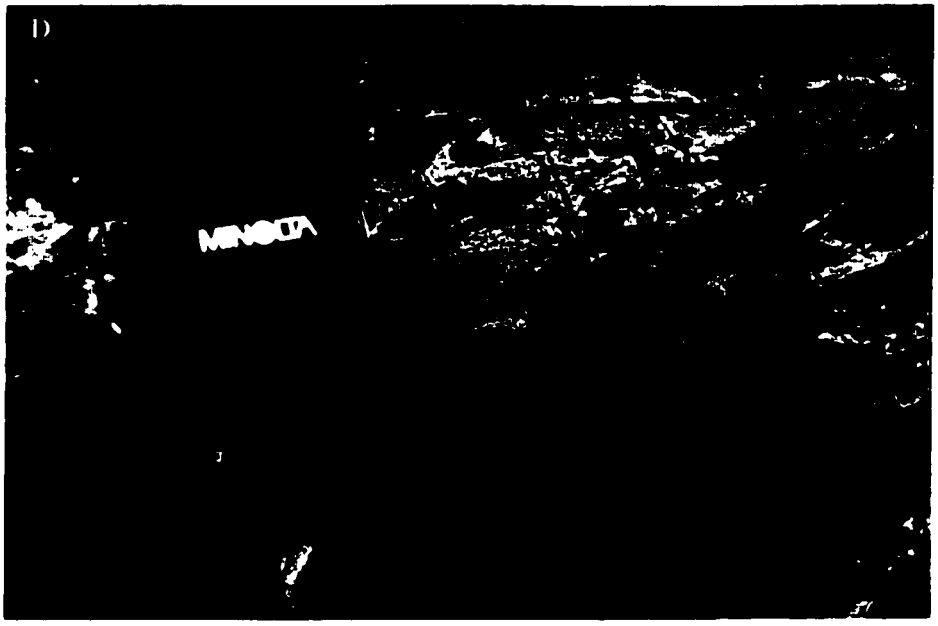
D
MINOLTA

Figure 2-6: Metasedimentary rocks in the Southern panel. A: Iron formation, northern sedimentary package. Brecciated by granodioritic injection (in white). B: Northern sedimentary group conglomerate (located in map scale F3b fold hinge, chapter 5), with angular granitoid clasts and fine-grained matrix. C: Southern sedimentary greywacke, with boudinaged garnet – rich bed(?).

Figure 2-7: Hilltop Creek Fault ("HCF"). A-C: Hematite – epidote rich layers, crenulated (a,b). D: Pyrite – rich zone E: Iron formation fragment F: Granitic dykes which intruded, and were subsequently dismbembered and deformed. G: Mafic breccia, in a splay from the HCF.

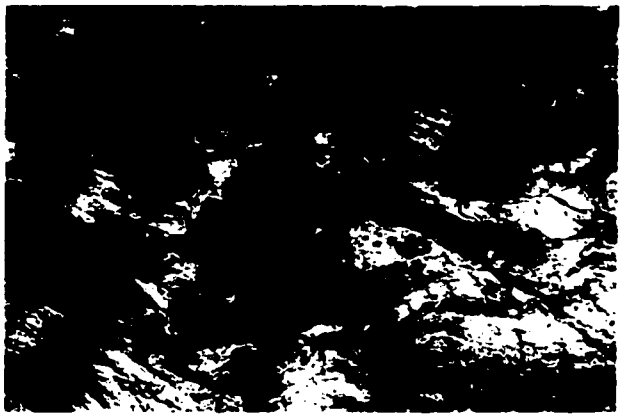

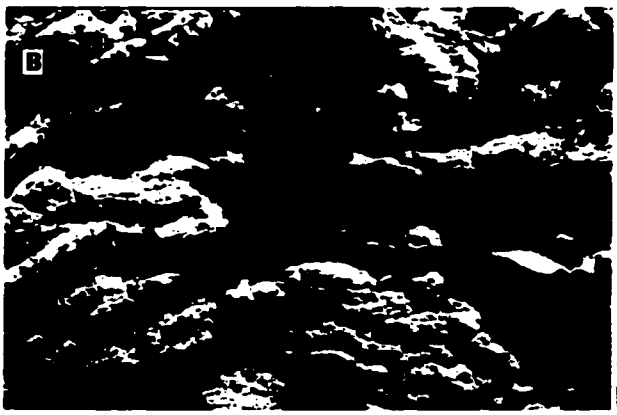
B

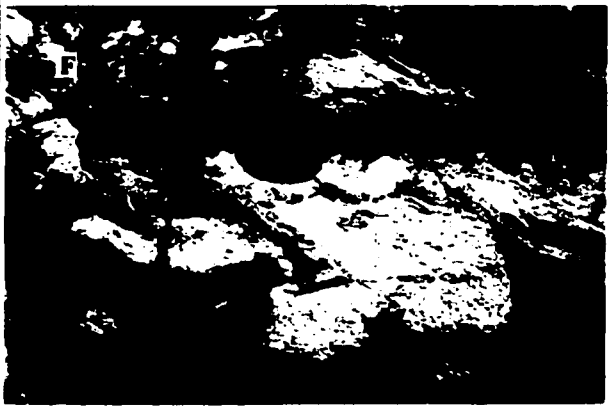
F


D

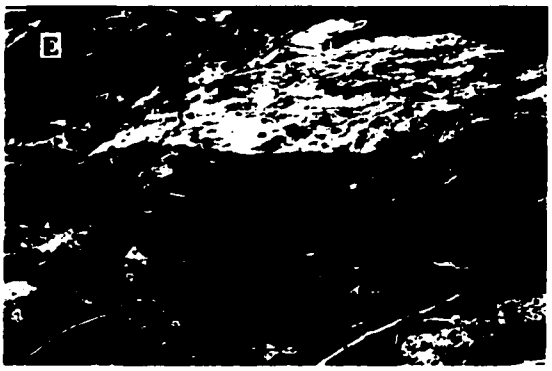
E

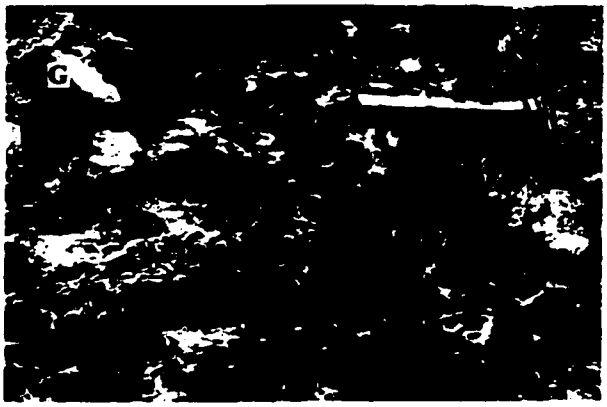
G

Figure 2-8: A: Rude Lake amphibolite (map unit "Ac *(4)*") with garnet (similar to Jutten group basalt in the Sturgeon-Savant greenstone belt). B: Boudinaged coarse-grained garnet-rich layer in Rude Lake amphibolite. C: Hornblende porphyritic feldspar porphry, which intrudes amphibolite. The margins of the porphyry are folded. D: Acicular random hornblende crystals in plagioclase – rich matrix.

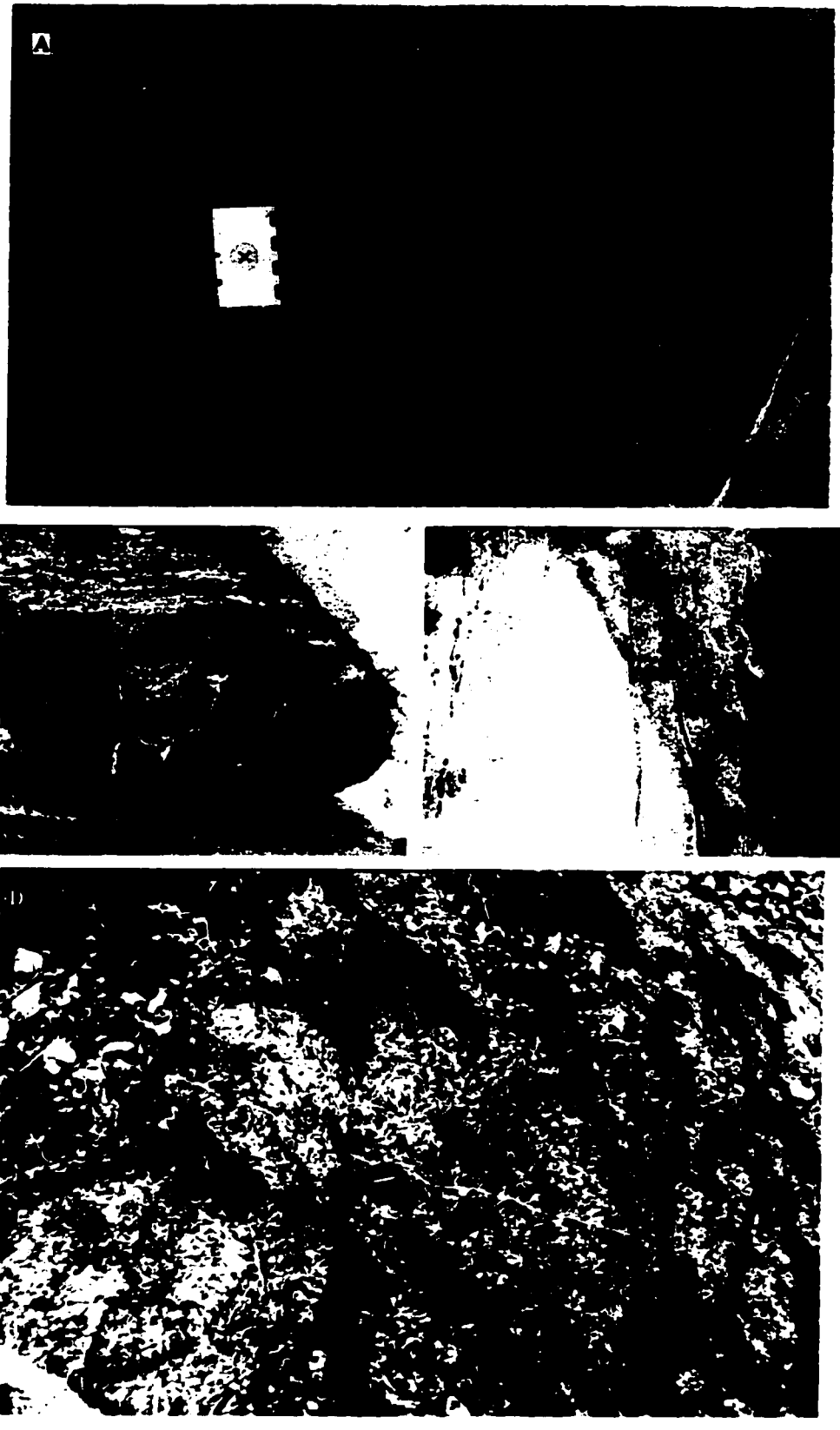
A

Figure 2-9: Quartz-rich metasandstone p865 (A) of central panel (map unit "Sq") in contact with quartzofeldspathic-metagreywacke (B). Detrital zircon of p865 were analysed and reported in Chapter 4 (sample C).

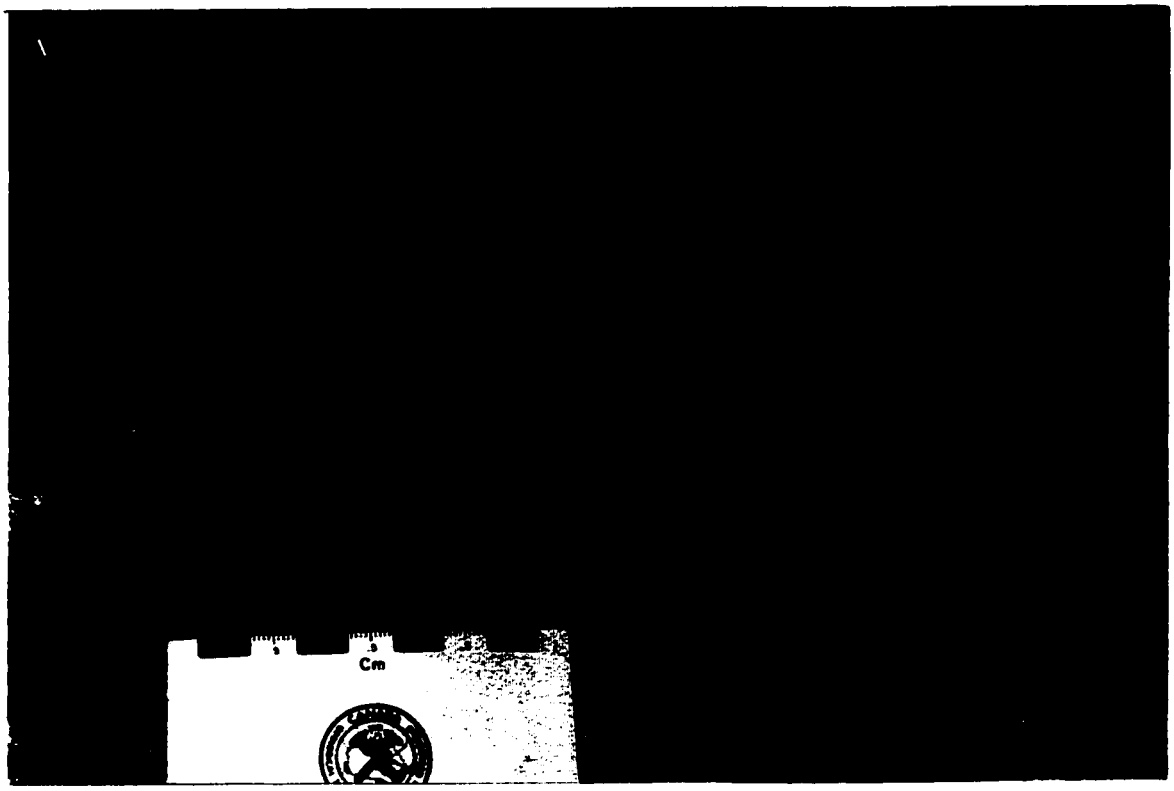
A
Cm


B

Figure 2-10: A: Low strain metaconglomerate, map unit "Sc" cut by mafic dyke (shown in B). This metaconglomerate is located within an F3b fold hinge (Chapter 5). It is also an L>>S tectonite (B). C: Highly deformed equivalent <1 km to the west.

Figure 2-11: Robert Lake amphibolite, map unit "Ac *(6)*" (A) and associated metasedimentary rocks including iron formation (B) and garnetite (C) with cummingtonite and grunerite.

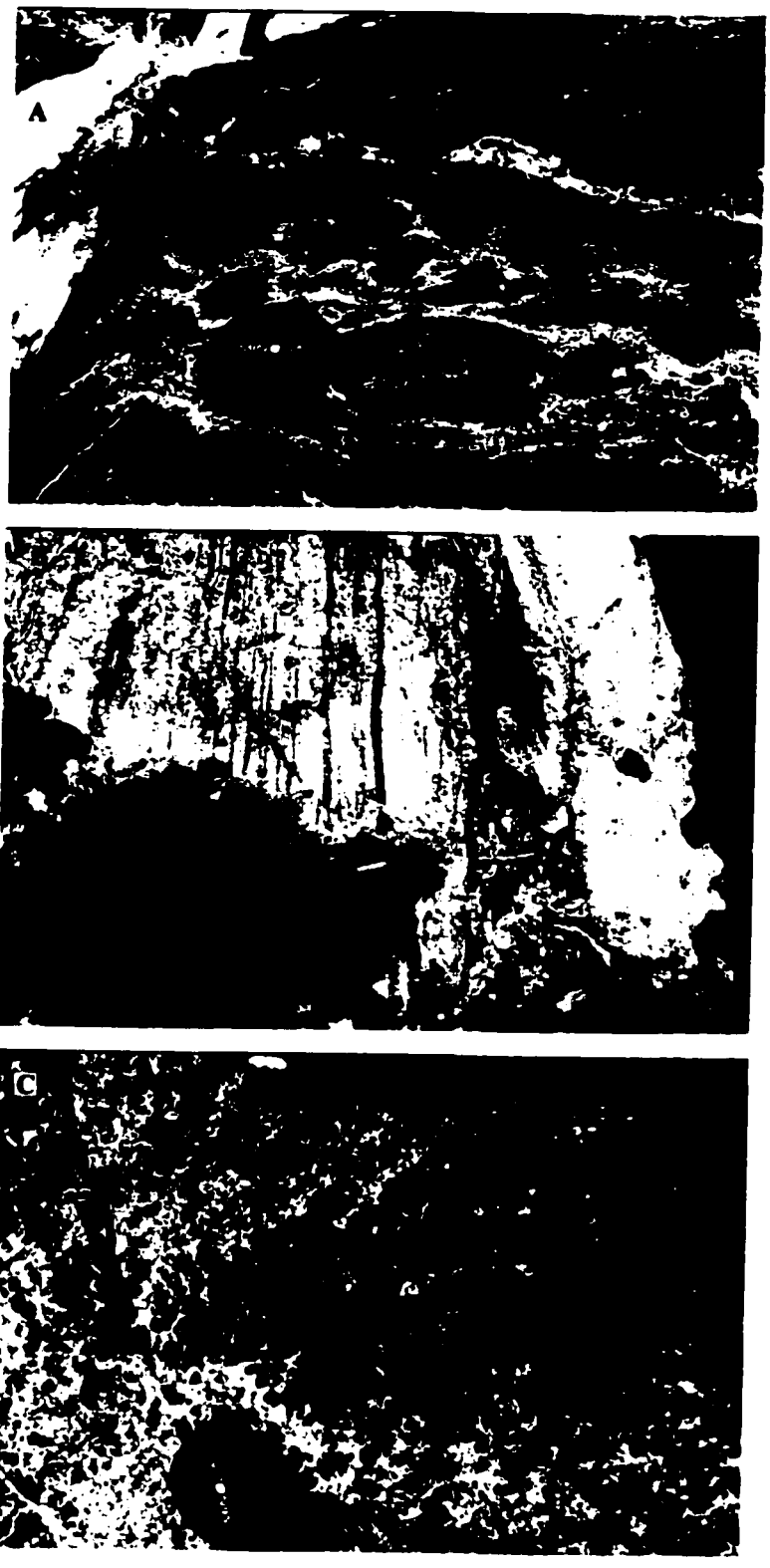
A
C

Figure 2-12: Rude Lake tonalite gneiss, map unit "TgR". A: Dome and basin (doughnut) shaped fold interference patterns. B: Tonalite gneiss with sheared and foliated mafic enclaves, cut by granite and pegmatite dykes.

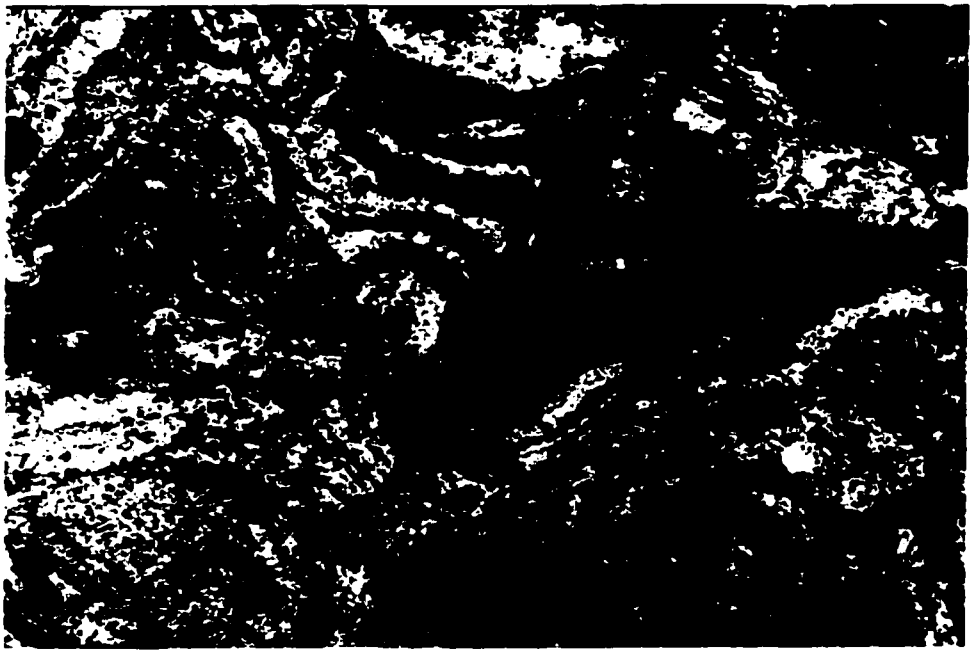


B

Figure 2-13: Robert Lake zone ("RLF"). These pictures were chosen to depict the variable nature of the Robert Lake high strain zone. A,B: chaotic folds along the northern edge of the Robert Lake amphibolite. Different fold styles occur in the same outcrop which include recumbent isoclinal folds, upright isoclinal folds (A), open and steeply plunging folds (B,1), and tight moderately plunging folds (B,2). Highly strained tonalite and granodiorite are cut by sheared pegmatite in the straight zone (C). Extensive epidotization of mafic rocks occurs along the northern edge of the Robert Lake amphibolite ("Ac *(6)*") (D).

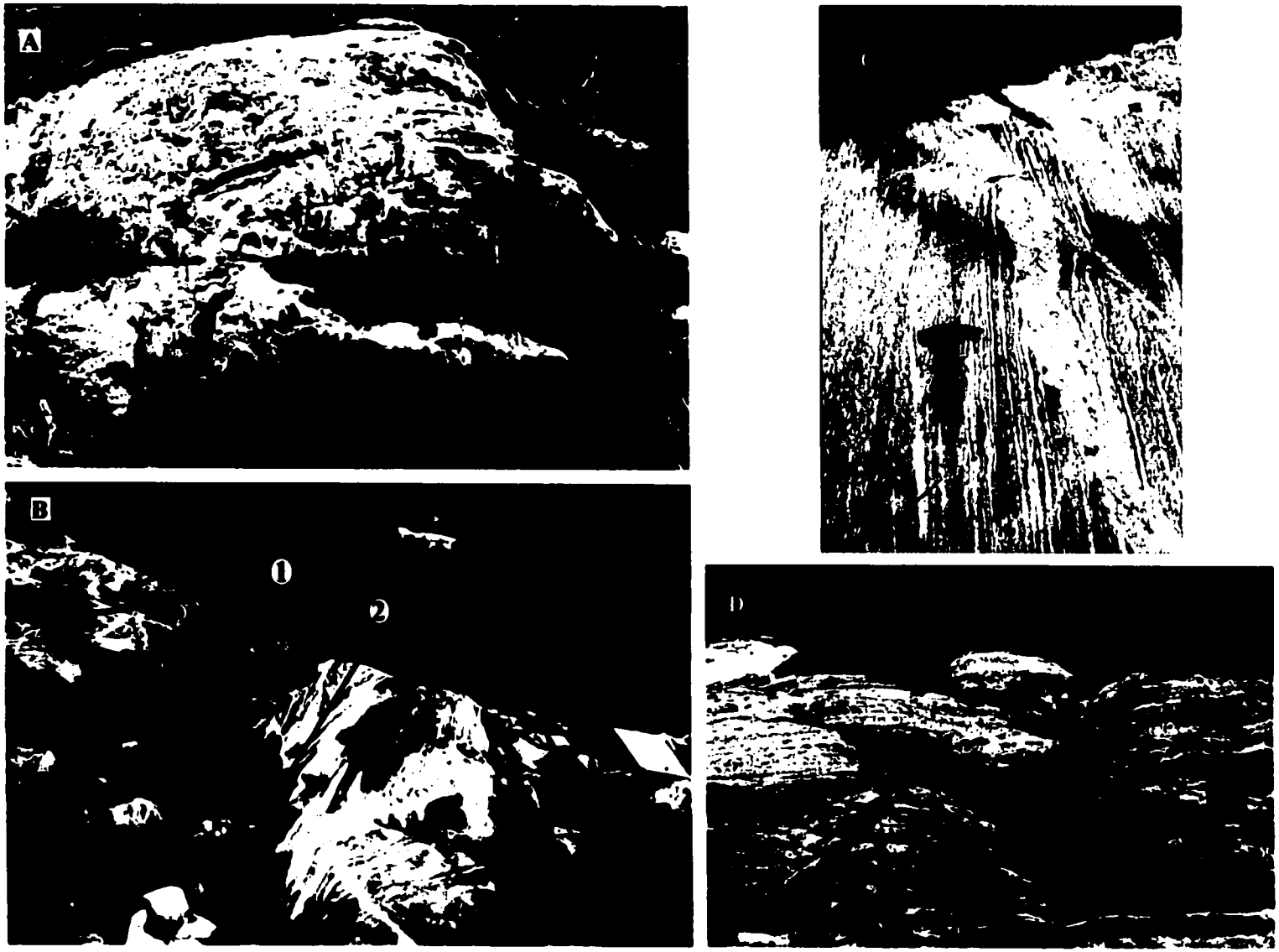
A
B
1
2
D

Figure 2-14: Mafic dykes cross- cut tonalite ("Th") on northern Robert Lake (A). On southern Robert Lake, within the straight zone ("RLF"), mafic dykes are rotated into parallelism with strain fabric (B). C: Hornblende tonalite ("Th") outside of straight zone.

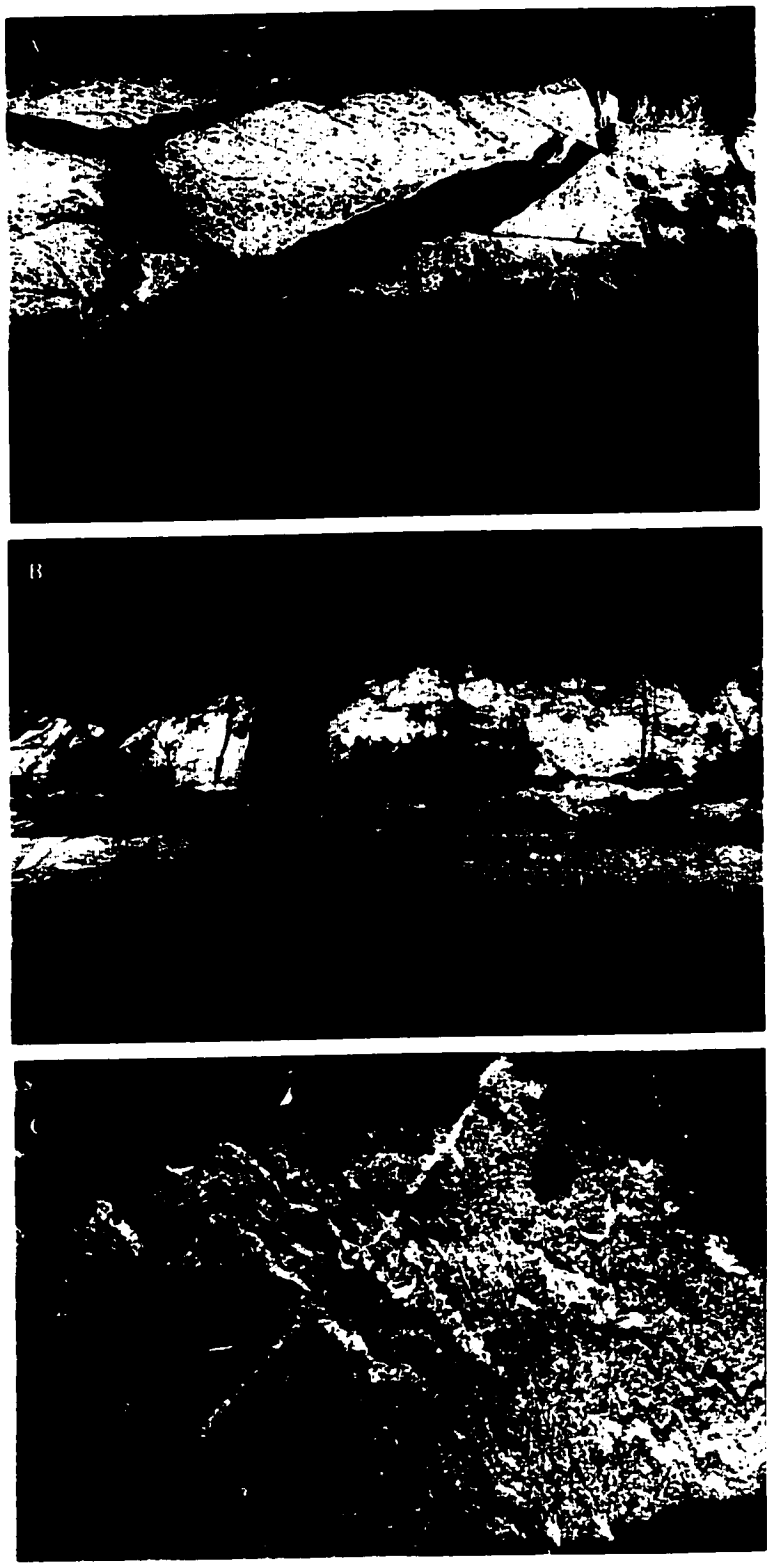

Figure 2-15: Xenolithic amphibolite dykes (map unit "Md") on Robert Lake (A), north of the straight zone. Mafic dykes intrude hornblende – tonalite (B,C) to create intrusive breccias. The contact between mafic dyke breccias and tonalite (Th) is folded (C).

Figure 2-16: Northern panel mafic units ("An"). A: Coarse grained amphibolite. B: Nodular gabbro associated with pyroxenite. C: Extremely coarse – grained pyroxenite.

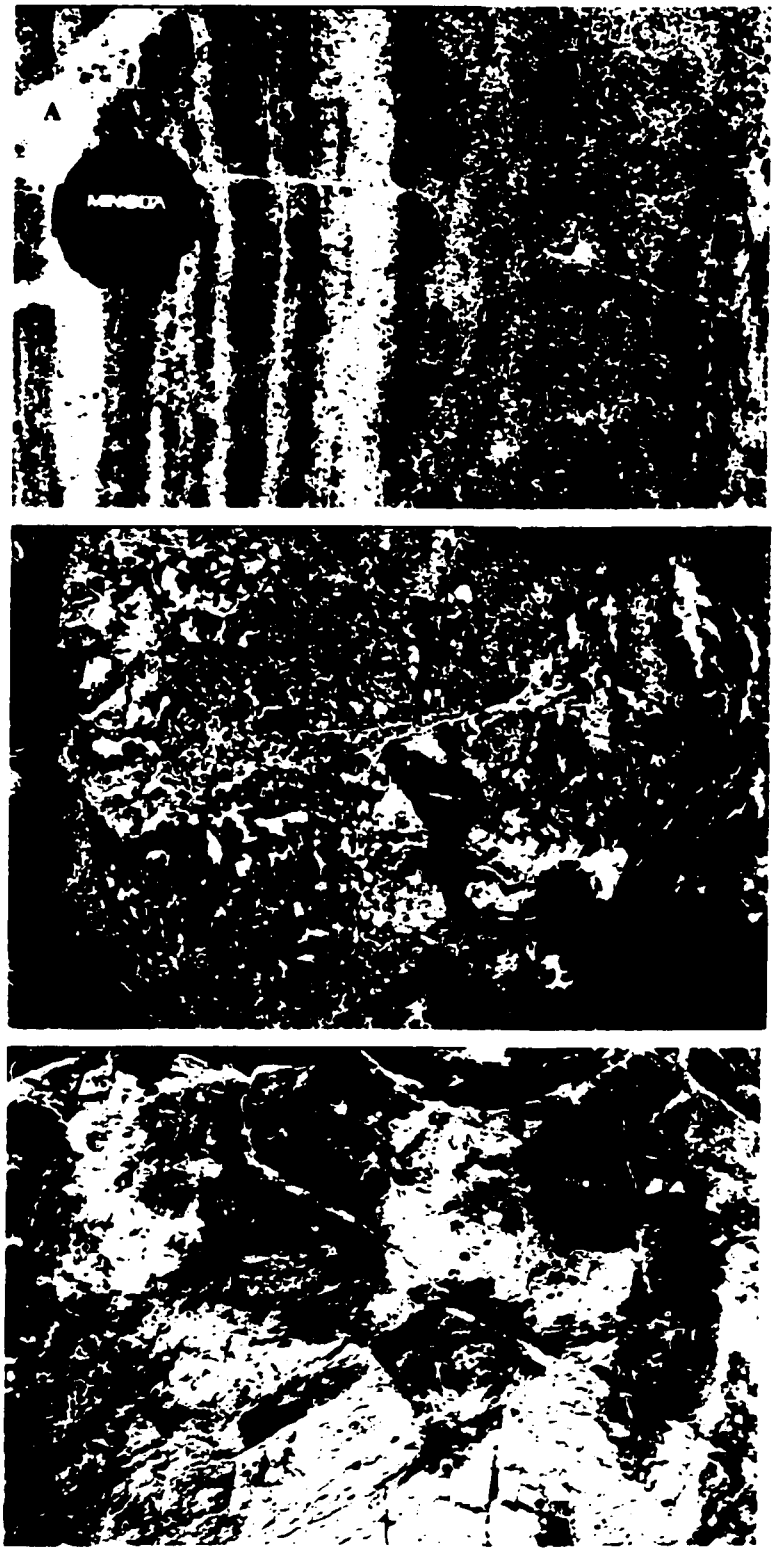
A

Figure 2-17: A: Near concordant layering in the Rude Lake tonalite gneiss "TgR" (which includes homogenous tonalite component and earlier gneissic layering) and amphibolite enclave likely part of the Rude Lake unit. Also parallel to the gneissic fabric are pegmatitic gabbro and homogenous tonalite. Granitic pegmatite cuts older units at a high angle. B: Tonalite and amphibolite are cut by medium-grained granite to granodiorite, which is in turn cut by pegmatite. C: Mafic dyke cuts coarse-grained tonalite, cross-cut by fine- to medium-grained biotite tonalite. C: Mafic enclave in hornblende tonalite is cut by biotite granodiorite.

CHAPTER 3: GEOCHEMISTRY

INTRODUCTION

Amphibolite units in the Brightsand Forest area are thought to be the metamorphosed, altered, and possibly dismembered equivalents of mafic volcanic rocks in adjacent greenstone belts. To the west and east, mafic volcanic assemblages within the Sturgeon - Savant Lake and Obonga Lake greenstone belts respectively are relatively well preserved, having experienced greenschist to amphibolite facies metamorphism. A geochemical study of the amphibolites was undertaken in order to correlate units of the study area with mafic metavolcanic assemblages in nearby greenstone belts.

REGIONAL GEOCHEMICAL AFFINITIES

The tectonostratigraphic framework of greenstone belts (Chapter 2) is partly constrained by geochemical studies of volcanic rocks. In particular, geochemical data from the Sturgeon - Savant and Obonga belts provide a basis for correlation with units in the map area. A brief description of trace element data available from the literature is provided for both greenstone belts and the central Wabigoon granitoid rocks.

Sturgeon Lake - Savant Lake greenstone belt

Sanborn-Barrie and Skulski (1999; see Fig. 2 in particular) summarized much of the geochemical data available for this belt. The Jutten group tholeiitic basalts (2750 - 2880 Ma, Sanborn-Barrie et al., 2002) are thought represent a rift sequence which erupted through continental crust. These rocks have flat rare earth element (REE) profiles, only slightly depleted in light rare earth elements (LREE), with Th and La enriched relative to

Nb. Samples that are depleted in Th may represent magmas that did not interact with continental crust. ε_{Nd} values of +0.6 and +1.7 using a possible crystallization age of 2.85 Ga, allow for some interaction with continental crust.

The Fourbay oceanic plateau (2775 Ma; Sanborn-Barrie and Skulski, 1999), Handy Lake volcanic arc (2745 Ma; Sanborn-Barrie and Skulski, 1999), Central Sturgeon arc rift sequence (2718 Ma; Davis and Trowell, 1982), and South Sturgeon (2735 Ma; Davis et al., 1985) submarine caldera complex (Morton et al., 1991) comprise an oceanic terrane. The Fourbay assemblage at the base of the pile consists of tholeiitic basalt. REE profiles are similar to those of the Jutten group: profiles are flat with slight LREE depletion, and variable enrichment in Th and La relative to Nb. However, ε_{Nd} values of +2.2 and +2.6 indicate a depleted mantle source. The lack of terrigenous sedimentary rocks supports an oceanic setting (Sanborn-Barrie and Skulski, 1999). Handy Lake (- Six Mile Lake) calc-alkaline basalts have LREE enriched profiles with marked Nb depletions. ε_{Nd} values are between +1.0 and +1.7. Enrichment in large ion lithophile elements (LILE) with respect to LREE and high field strength elements (HFSE) suggest arc-type magma generation processes. The Central Sturgeon assemblage is mixed calc-alkaline and tholeiitic mafic volcanic rock. The lower part of the assemblage is high Ti (0.58-2.47% TiO_2) basalt with flat REE profiles, some enrichment in LREE, and negative Nb anomalies. One ε_{Nd} value of +1.9 was obtained from tholeiitic basalt.

Obonga Lake greenstone belt

Tomlinson et al. (1999, 2002) present the geochemical data available for this belt. Northern assemblage mafic rocks (< 2.724 Ga) have been divided into two groups, using trace element profiles (Fig. 8 in Tomlinson et al., 2002). Group 1 rocks are enriched in

LREEs and HFSE, and depleted in heavy rare earth elements (HREE). Group 2 profiles show less fractionation than Group 1 rocks. ε_{Nd} values range from +0.7 to +2.4 for mafic rocks in the northern assemblage. 2703 Ma dacite from the northern assemblage is strongly enriched in LREE and depleted in HREE, with an intense negative Nb anomaly. Tomlinson et al. (2002) interpret this rock as a mantle-modified slab melt (the equivalent of Cenozoic arc adakites). Group 1 and 2 basalts associated with the dacite are the product of either: 1) adakitic metasomatization of the mantle wedge to produce a source that was subsequently melted to produce basalt (Group 1), or 2) direct melting of a deep asthenospheric source (mantle plume).

The southern assemblage (2.73 Ga) is dominantly tholeiitic basalt, basaltic andesite and calc-alkaline intermediate and felsic volcanic rocks. Trace element characteristics of these rocks show enrichment in LREE and negative Nb anomalies. Tomlinson et al. (2002) cite 3.16 Ga Nd model ages (from 2930 Ma granitoid rocks) and negative ε_{Nd} values from volcanic rocks (as low as –0.9) as evidence that southern assemblage basaltic rocks interacted with Mesoarchean continental crust. They suggest that the southern assemblage formed in a continental arc, or continental back arc system.

The two assemblages are separated by a 2733 Ma gabbroic core zone, which is likely related to the southern assemblage (Percival and Stott, 2000).

Central Wabigoon granitoid rocks

Whalen et al. (in press, 2002) used geochemical data and Nd isotopes of granitoid rocks to establish that the central Wabigoon subprovince contains vestiges of 2.93 – 3.07 Ga crust. Crystallization ages of granitoid rocks indicate magmatic episodes (Whalen et al., in press): <2.89 to 2.72 Ga for tonalitic gneisses (V. McNicoll, unpublished data,

1998); ca. 2.77 to 2.71 Ga for tonalite and granodiorite; ca. 2.77 to 2.69 Ga for mafic intrusions; ca. 2.69 Ga for granite and granodiorite; and 2.69 Ga for K-feldspar megacrystic granodiorite. Widespread low-K felsic (TTG) magmatism is documented between 2722 and 2709 Ma (including granodiorite ca. 20 km north of the study area on Seseganaga Lake) with ε_{Nd} values between –3.1 and +3.3. Whalen et al. (in press) suggest that 2709 Ma granodiorite intruded during the final stages of widespread felsic magmatism in a continental arc setting, to explain variable input from older (Mesoarchean), LREE-enriched, crust.

METHODOLOGY

Analytical techniques

Whole rocks were crushed and ground in steel media and major elements analyzed by XRF on fused glass discs at the Geological Survey of Canada (GSC) in Ottawa. FeO was measured by dichromate titration and F contents by ion electrode at the GSC. Trace elements were analyzed through a combination of ICP and ICP-MS techniques at the GSC. Separation of REE was done by standard cation exchange chromatography. Analyses are reported in Appendix 1.

Eight amphibolite samples were analyzed for Nd isotopes by K.Y. Tomlinson at the GSC, Ottawa. Mapping was incomplete at the time samples were chosen for analysis, and data is concentrated in the central panel. Results are listed in Table 3-1. εNd values are calculated to express deviations from CHUR (chondritic uniform reservoir) where

$$\varepsilon Nd = [\{^{143}Nd/^{144}Nd\}_{sample}(t)\ 4\ \{^{143}Nd/^{144}Nd\}_{CHUR}(t) - 1] * 10^4$$

and

$^{143}Nd/^{144}Nd = [\{^{143}Nd/^{144}Nd\}i + \{^{147}Sm/^{144}Nd\}*(e^{\lambda t-1})]$ (*source:* Dickin, 1995)

CHUR reflects primordial nuclide abundances. Positive εNd values reflect a depleted mantle source, while values close to zero or below reflect interaction with isotopically evolved crust, which is generally continental igneous rock (DePaolo and Wasserburg, 1976).

Sample collection and data treatment

Samples were collected for geochemistry from all metavolcanic units, and many were resampled along strike. In each case, approximately 2-3 kg of rock chips were collected for analysis, along with a hand specimen for thin section study (and for P-T study where appropriate). To minimize the problem of element mobility, alteration zones and shear zones were avoided where possible. However, the entire study area has experienced lower to upper amphibolite-facies metamorphism, with evidence of injection of granitoid layers and local intense retrograde metamorphism (particularly in the northern panel). Rare earth elements (REE) are the least mobile of the relatively immobile trace elements, and generally remain unaffected by metamorphism and hydrothermal alteration (Rollinson, 1993). Major elements are more susceptible to loss or gain during metamorphism.

MAJOR ELEMENT GEOCHEMISTRY

Major element data were plotted on a Jensen diagram (1976) for the classification of subalkaline volcanic rocks (Fig. 3-1a). The diagram uses cation proportions (Fe^{2+} + Fe^{3+} + Ti), Al, and Mg recalculated to 100%, plotted on a ternary diagram. Most of the amphibolites plot between high Fe and high Mg tholeiitic basalt. The intrusive felsic sill

from the central panel plots as a calc – alkaline rhyolite. Samples j807 and j810 from the Sturgeon Lake belt plot between high Mg tholeiitic basalt and komatiitic basalt (10.33 and 11.02% MgO). Komatiites have not been reported from the Sturgeon belt, although rocks with greater than 11% MgO have been reported from the Jutten group (13.6% MgO) and from the Central Sturgeon assemblage (Sanborn-Barrie and Skulski, 1999). The Hilltop Lake amphibolite (j510) is a high Ti (2.25% TiO_2) tholeiitic basalt (Fig. 3-1b). By comparison, other amphibolite units have much lower Ti: the South Sturgeon amphibolite has 0.71-1.06% TiO_2, the Mountairy Lake amphibolites have 0.82 – 1.13% TiO_2, central panel amphibolites have 0.43 – 1.13% TiO_2, and northern panel amphibolites have 0.54 – 0.98% TiO_2.

TRACE ELEMENT GEOCHEMISTRY

Amphibolite samples were grouped according to their location within the BSF area (Fig. 3-2). Samples from the southern, central, and northern panels are treated separately, and the characteristics of individual rock units (and some individual samples) are emphasized where necessary.

Multi-element primitive mantle normalized diagrams

Coryell et al. (1963) suggested plotting REE abundance in rocks as a ratio of their abundance in chondritic meteorites. Diagrams herein are constructed similarly, except that trace element data are presented on multi-element diagrams normalized to primitive mantle values. Elements are plotted in order of increasing incompatibility from left to right. Normalization factors used are those of Sun and McDonough (1989).

Southern panel

Amphibolites from the southern panel (Figs. 3-2 and 3-3) have primitive mantle-normalized profiles showing enrichment of light REEs with respect to the weakly fractionated heavy REE profile. Most samples have pronounced negative Nb and Ti anomalies. Analyses of two basalts from the Sturgeon belt along strike to the west of the field area show more pronounced fractionation between light and heavy REE, sloping HREE profiles as well as negative Nb, Ti, Zr and Hf anomalies (Fig. 3-3). The Hilltop Lake amphibolite has a flat profile, but is enriched (10x primitive mantle) relative to other rocks in the area.

Central panel

Based on multi-element profiles (Fig. 3-3), amphibolites have been divided into two groups. The first group (Rude Lake and Robert Lake units) have very flat patterns with abundances between 2 and 7 times primitive mantle. Th-Nb relationships vary: rocks with slightly higher Nb values have negative Th anomalies, while other samples have slight negative Nb anomalies.

The second group includes the Brightsand River and Scruffy Lake units. Multi - element profiles show slight enrichment in highly incompatible trace elements, with negative Nb and Ti anomalies. Sample j682 (Fig. 3-3) shows significant enrichment in incompatible trace elements, along with pronounced negative Nb, Hf and Zr anomalies.

The fine-grained felsic rock from the Rude Lake unit (Fig. 3-3) has a steeply fractionated pattern with a pronounced negative Nb anomaly, and positive Hf and Zr anomalies. It also is the only rock that has a significant (positive) Eu anomaly. Eu anomalies ($Eu/Eu^* = Eu/(Sm^*Gd)^{1/2}$) were calculated for all samples (Appendix A).

When divalent, Eu is highly compatible in plagioclase and K-feldspar. Positive Eu may be attributed to feldspar phenocrysts which crystallized initially as cumulates within a magma. The felsic rock is also enriched in light REE relative to heavy REE. HREE are significantly more depleted than in mafic rocks, with a Tm concentration of 0.6x primitive mantle values. The presence of garnet in the source may account for the enrichment of LREE and depletion of HREE, as the range of partition coeffiecients for garnet from light to heavy REE increases by 2 orders of magnitude (Fig. 4.10, Rollinson 1993) in felsic melts. A similar effect may be caused by residual hornblende. Trace element characteristics of this 71% SiO_2 rock may also be the product of fractionation of accessory minerals such as zircon, allanite, monazite and titanite.

Northern panel

The multi-element diagram in Figure 3-3 for northern panel amphibolites shows relatively flat patterns, with values from 3 - 10x primitive mantle. Patterns show negative Nb and Ti anomalies. Amphibolites from the northern unit exhibit slight negative Zr and Hf anomalies as well and are slightly more enriched in LREE than the Stinson Lake unit. One of the Stinson Lake amphibolites has a moderately fractionated REE profile.

Nd Isotopes

εNd calculations and results are present in Table 3-1. εNd values, calculated at 2.73 Ga, range from +0.86 to +2.69. Neodymium isotopic data from amphibolite of the Scruffy Lake unit yelded ε_{Nd} values of +0.8, +1.8, and +2.1; Brightsand River amphibolites have values of +1.5, +1.8, and +2.7; and a sample of Rude Lake amphibolite gave a value of +2.4 (K.Y. Tomlinson, unpublished data 1999). The high positive ε_{Nd} values indicate predominantly depleted mantle sources, although the lowest

values suggest the possibility of minor assimilation of older crust (Fig. 3-4). Neodymium data from the northern unit yielded an ε_{Nd} value of +2.1 (K.Y. Tomlinson, unpublished data 1999) indicating a relatively depleted mantle source.

DISCUSSION

The most likely correlative units of the Mountairy Lake amphibolite are the 2735 Ma (Davis et al., 1985) basalts of the along - strike South Sturgeon assemblage to the west. Trace element patterns are qualitatively similar, although LILE (large ion lithophile element) enrichments and HFSE (high field strength element) depletions are less pronounced in the Mountairy Lake amphibolite. One sample from the Brightsand River (j682) has a profile that resembles ca. 2735 Ma South Sturgeon basalts (Fig. 3-5). The sample was taken from an isolated sliver of unaltered amphibolite located east of the Brightsand River and appears to have no physical connection to the South Sturgeon assemblage (Fig. 3-2). The Hilltop Lake sample has a very similar geochemical profile to some basalts of the ca. 2718 Ma Central Sturgeon assemblage within the Sturgeon belt in the vicinity of Quest Lake. Furthermore, the lower Central Sturgeon assemblage consist of high Ti basalt, and the Hilltop Lake unit is a high titanium amphibolite. The trace element characteristics are also somewhat similar to group 1 amphibolites from the northern assemblage of the Obonga belt (Fig. 3-5).

The multi - element diagrams for northern panel amphibolite units resemble the Brightsand River and Scruffy Lake amphibolites in their slight incompatible element enrichment. The Rude and Robert Lake amphibolites have similar trace - element characteristics to some basalts of the Jutten group in the Savant Lake belt at

Kashaweogama Lake (Fig. 3-5). ε_{Nd} values of +0.6 and +1.76, calculated at 2.85 Ga for the Jutten group (Sanborn-Barrie and Skulski, 1999), compare to ε_{Nd} values of +2.28 for Rude Lake alone, and ε_{Nd} values of +1.00 to 3.07 Ga for the entire central panel when data are recalculated using an assumed age of 2.85 Ga for consistency.

Figure 3-6 compares the fine-grained felsic sill (2707 Ma, Chapter 4) to geochemical profiles available for similar rock types with similar ages, in the region. Felsic volcanic rocks from the Handy Lake group (northeast Savant Lake belt) also have similar geochemical profiles, including HREE depletion. The Handy arc is thought to have formed between 2745 and 2704 Ma (Sanborn-Barrie and Skulski, 1999; Davis. 1995). 2703 Ma dacite from the northern assemblage in the Obonga belt is less depleted in HREE, with a pronounced negative Ti anomaly (Tomlinson et al., 2002 Fig. 9), not present in the Rude Lake rock. The profile also resembles that of granodioritic plutons (2709 Ma) in the region (Fig. 7 in Whalen et al., in press), which are both spatially and temporally related. The sill could represent a high level equivalent of these continental arc plutons (Chapter 7).

Figure 3-1: Major element diagrams
(a) Jensen ternary diagram for the classification of subalkaline volcanic rocks.
(b) TiO_2 vs MgO diagram. Hilltop Lake amphibolite is Ti rich.

(a)

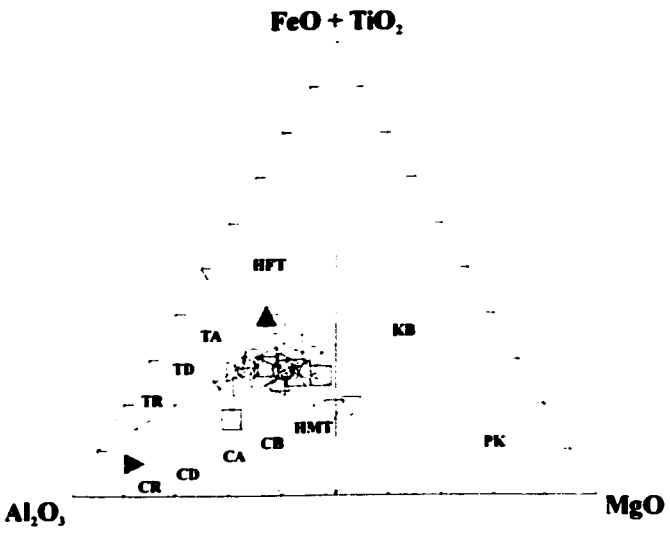

(b)

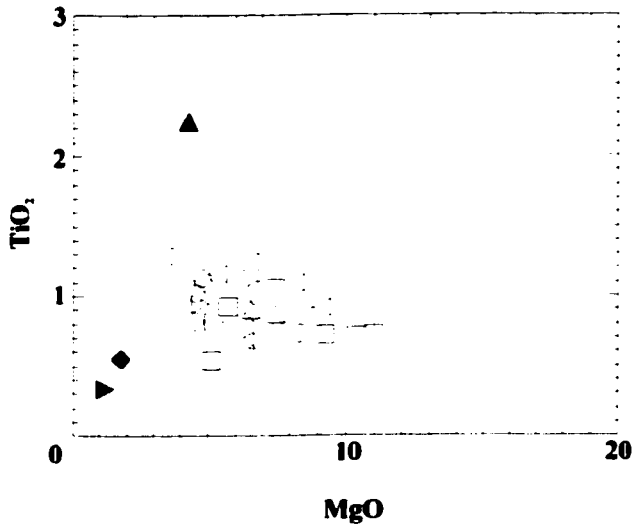

- Felsic sill
- South Sturgeon basalt
- Mountairy Lake
- Hilltop Lake
- Scruffy Lake
- Rude Lake
- Robert Lake
- Brightsand River
- Stinson Lake
- Northern

Figure 3-2: Primitive mantle normalized extended element profiles superimposed on the map area. Samples are grouped together within amphibolite units.

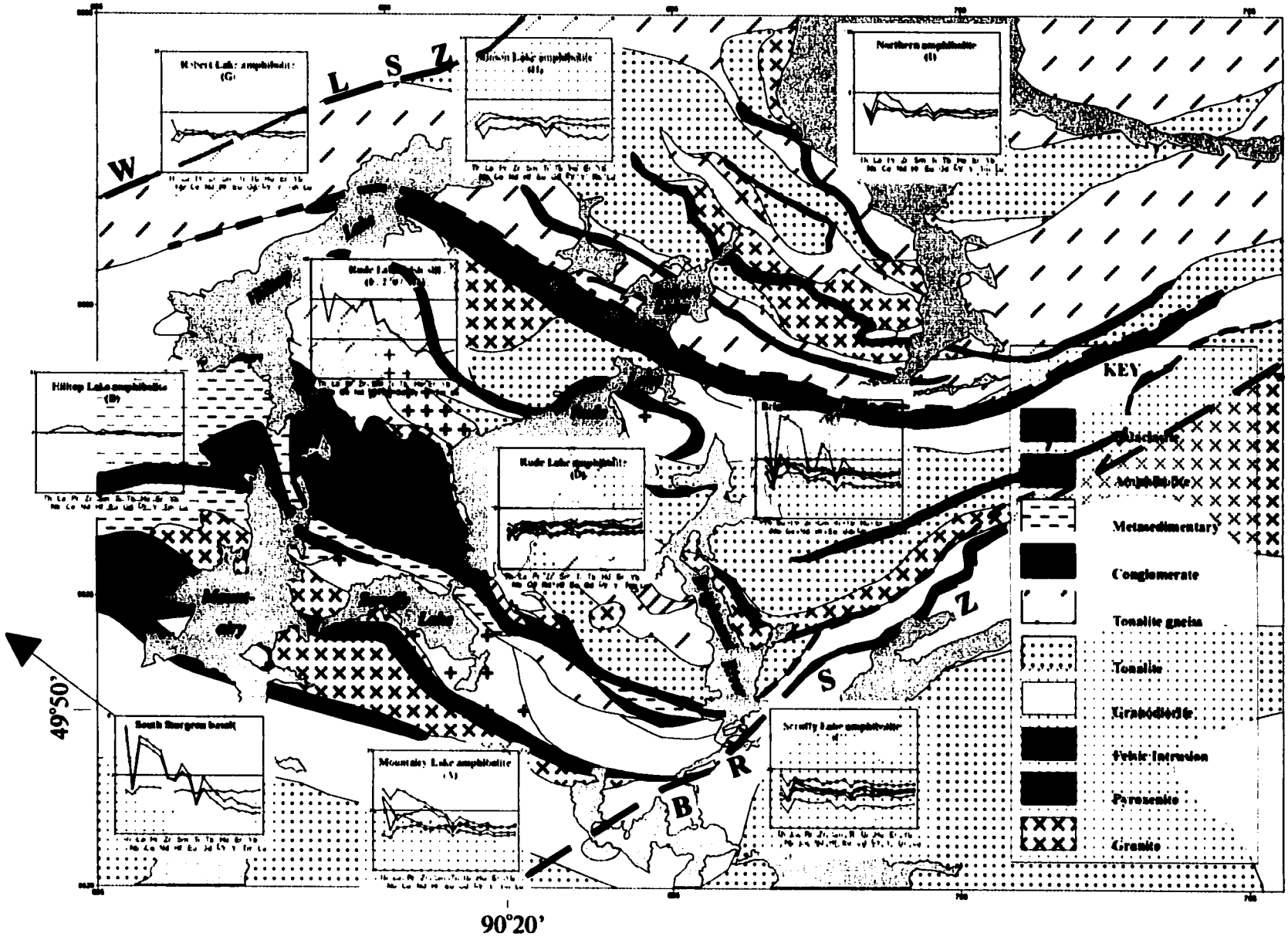
W
L
S
Z
Hilltop Lake amphibolite
(B)
Rude Lake amphibolite
(D)
Northern amphibolite
(I)
Mountain Lake amphibolite
(A)
KEY
Metasedimentary
Conglomerate
Tonalite gneiss
Tonalite
Granodiorite
Felsic intrusion
Peraluminite
Granite
S
Z
R
B
49°50'
90°20'

Figure 3-3: Primitive mantle normalized extended element profiles for the southern, central, and northern panels.

Southern panel

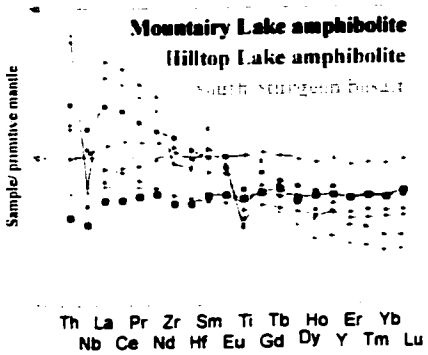

Central panel

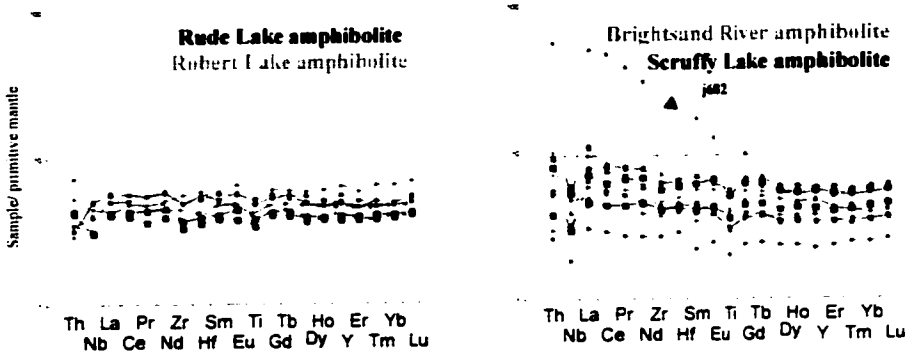

Rude Lake felsic volcanic

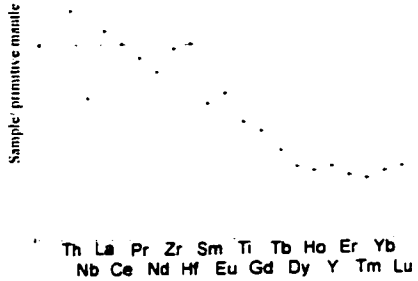

Northern panel

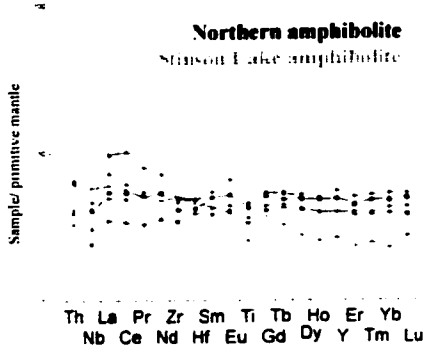

Table 3-1: Nd values from selected amphibolites from the Brightsand Forest area. K.Y. Tomlinson's unpublished data, 1999.

		Measured	measured											Recalculated
Sample #		143Nd/144Nd	147Sm/144Nd	143Nd/144Nd CHUR T	age	εNd (0)	εNd (T)	T(CHUR)	Sm ppm	Nd ppm	1/Nd	f(Sm/Nd)	Q*f(Sm/Nd)	εNd (2.65)
Northern panel	Unit													
J136	Stinson	0.512392	0.177067	0.509201869	2.73E+09	-4.60	2.11	1.91E+09	1.66	6.66	0.150	-0.0997	-2.6957	2.48
Central panel														
P374	Brightsand	0.511725	0.141739	0.509171637	2.73E+09	-17.81	1.51	2.52E+09	1.8	7.69	0.130	-0.2794	-7.0217	2.38
J120	Brightsand	0.512340	0.172566	0.509231303	2.73E+09	-5.81	2.69	1.88E+09	2.89	10.12	0.099	-0.1227	-3.0833	3.07
J121	Brightsand	0.512411	0.176869	0.509200307	2.73E+09	-4.43	1.84	1.94E+09	3.09	10.45	0.096	-0.0905	-2.2755	2.12
[redacted]														
J115	Scully	[redacted]												
J141	Scully	[redacted]												
[redacted]	Scully	[redacted]												

Figure 3-4: εNd vs time, for seven samples within the central panel and one sample from the northern panel (Stinson Lake). CHUR (chondritic uniform reservoir) is shown for comparison. Also shown are data from: the Obonga Lake greenstone belt (Tomlinson et al., 2002); the Sturgeon Lake – Savant Lake greenstone belt (Sanborn-Barrie and Skulski, 1999); and granitoid rocks from the central Wabigoon (Whalen et al., in press).

Neodymium evolution vs time

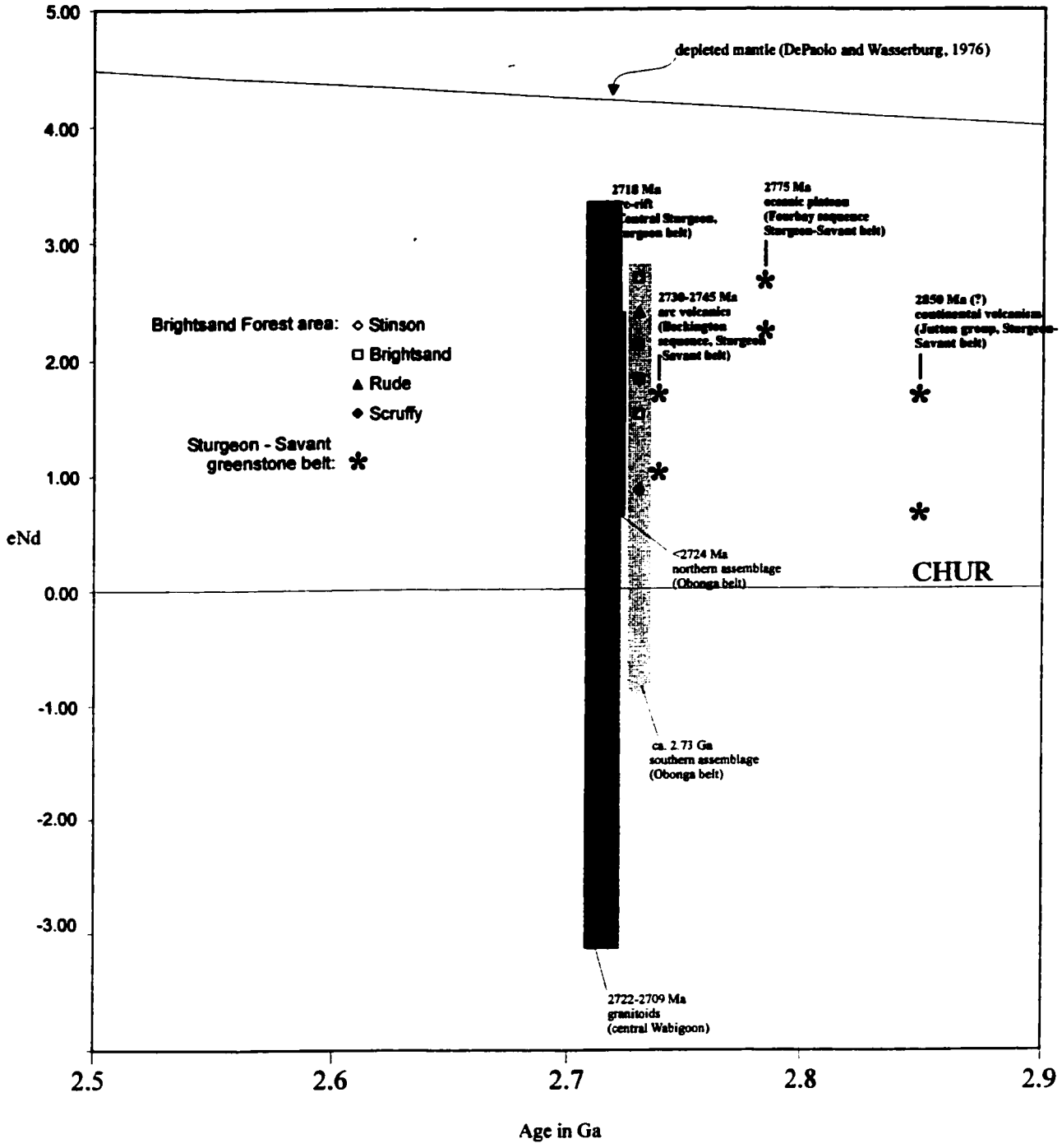

Figure 3-5: REE diagrams to compare amphibolite in the map area to basalt in greenstone belts. Amphibolite samples are black lines and greenstone belt samples are grey lines. Tom Skulski and Kirsty Tomlinson provided data from the Sturgeon - Savant Lake greenstone belts (Sanborn-Barrie and Skulski, 1999) and the Obonga Lake greenstone belts respectively (Tomlinson et al., 2002).

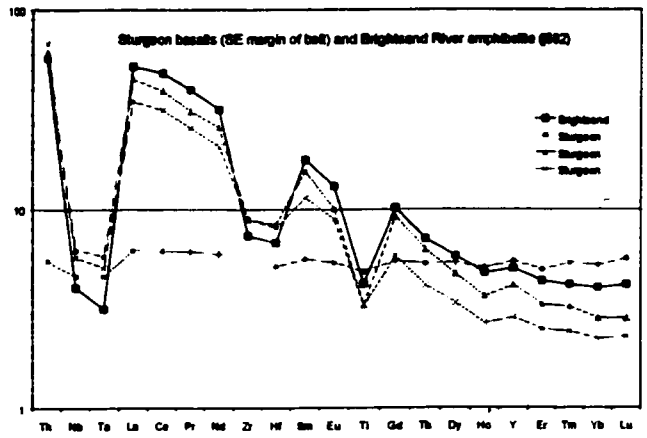

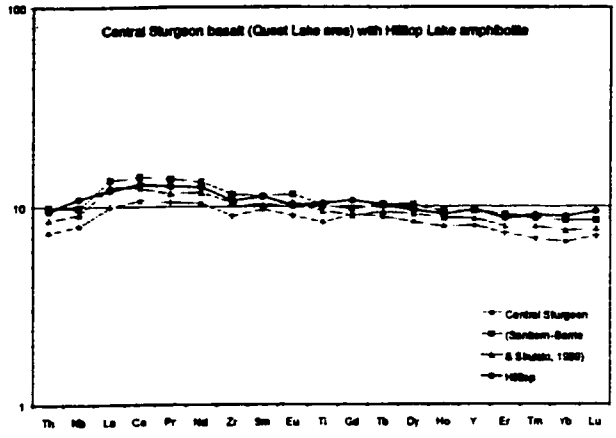

Jutten group basalt with Rude Lake and Robert Lake amphibolites

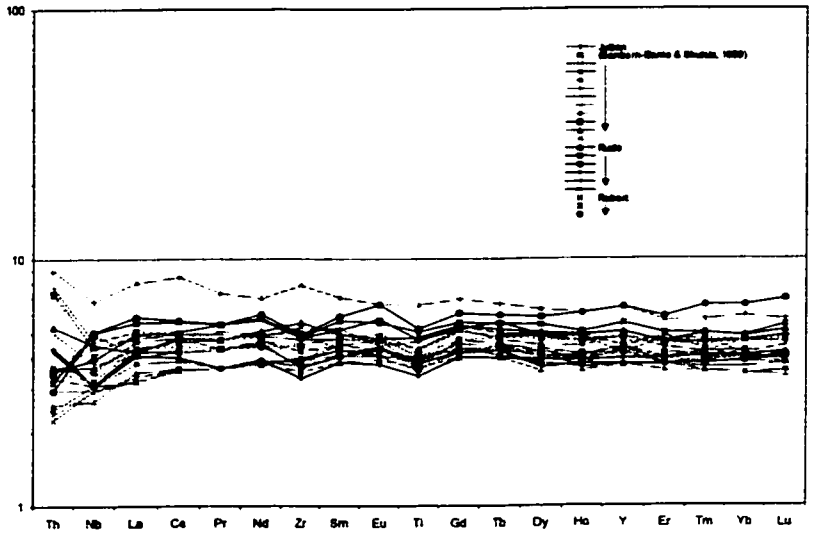

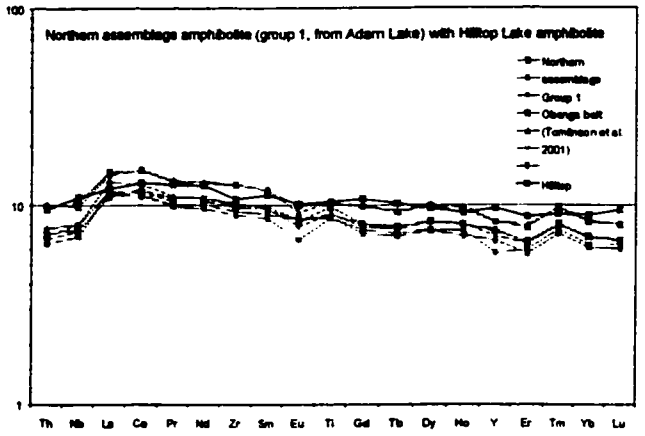

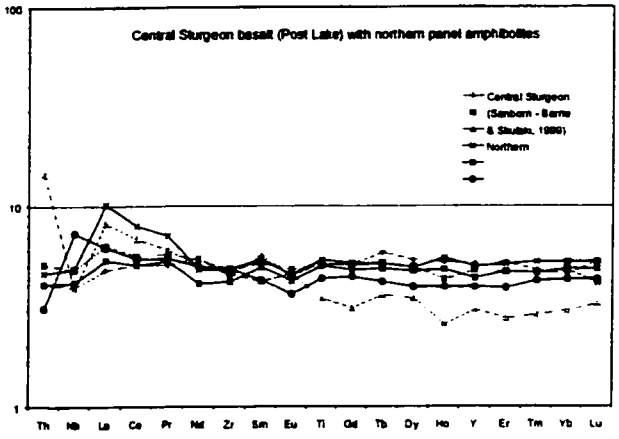

Figure 3-6: Primitive mantle normalized extended element profile for comparison of felsic sill ("Fs") with granitoid rocks in the north-central Wabigoon of similar age (2709 Ma; Whalen et al., in press), and with dacite from the northern assemblage of the Obonga belt (Tomlinson et al., 2002).

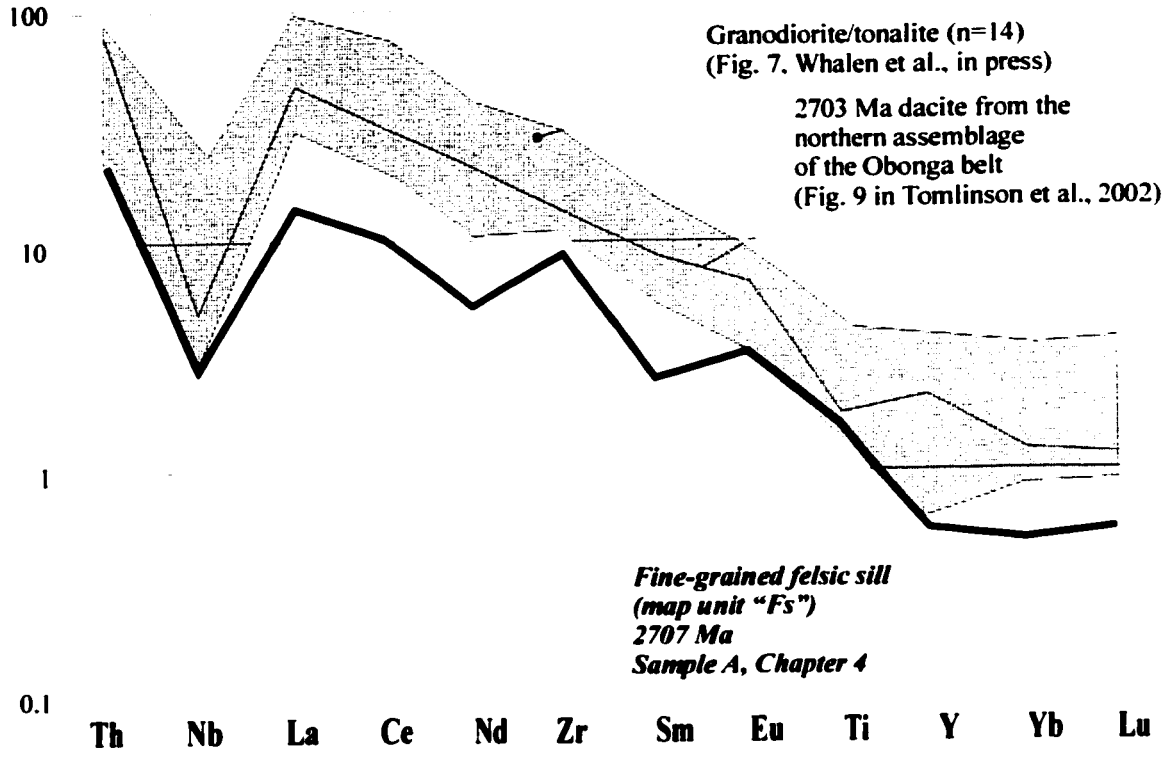
100
10
1
0.1
Granodiorite/tonalite (n=14)
(Fig. 7, Whalen et al., in press)
2703 Ma dacite from the
northern assemblage
of the Obonga belt
(Fig. 9 in Tomlinson et al., 2002)
Fine-grained felsic sill
(map unit "Fs")
2707 Ma
Sample A, Chapter 4
Th
Nb
La
Ce
Nd
Zr
Sm
Eu
Ti
Y
Yb
Lu

CHAPTER 4: U-Pb GEOCHRONOLOGY

INTRODUCTION

U-Pb geochronology studies were undertaken to address several important issues in the geology of the Brightsand Forest area. The first goal was to establish the chronostratigraphy of the gneisses and supracrustal rocks in the Rude Lake assemblage and thereby test the hypothesis of a basement - cover relationship. A second objective was to provide constraints on the timing of deformation and metamorphic events in the Brightsand Forest area, in order to correlate these with tectonic events in adjacent greenstone belts. Determining the ages of depositional, intrusive, deformation and metamorphic events in the Brightsand Forest area will allow correlation with those established regionally in the eastern and western Wabigoon and Winnipeg River subprovinces.

Regional Character and Constraints

Table 4-1 is a compilation of geochronological data from the Lake of the Woods area to the Onaman-Tashota greenstone belt. Included are the Kenora gneisses along the southern margin of the Winnipeg River subprovince: the Lake of the Woods, Pipestone Lake, Kakagi Lakes, Sturgeon Lake, Savant Lake, Obonga Lake and Onaman-Tashota greenstone belts; and the central Wabigoon granitoids. U-Pb geochronology constraints on deformation for the areas in Table 4-1 are discussed in Chapter 7 (see Fig. 7-1).

U – Pb Analytical Techniques and Data Treatment

Analyses were carried out at the Geochronology Laboratory at the Geological Survey of Canada in Ottawa, following the techniques detailed in Parrish et al. (1987)

and outlined below. Standard crushing and grinding techniques were carried out on samples. Minerals were separated on a Wilfley™ table, by heavy liquid (methylene iodide, MI), and by magnetic separation techniques using a Frantz™ isodynamic separator. Samples were then sieved into size fractions. Individual fractions were hand-picked in ethyl alcohol, using a binocular microscope, selecting in favour of clear, crack-free crystals lacking inclusions or cores. Fractions are differentiated on the basis of crystal size and morphology, the latter of which may be diagnostic of metamorphic vs. igneous origin in some cases (e.g. van Breemen et al., 1987, Roddick and Bevier, 1995). Zircon grains were air abraded (Krogh, 1982) with pyrite, for periods of 5 to 10 hours. Titanite grains were lightly air abraded without pyrite (Davis et al., 1997). The minerals analyzed were spiked with a mixed isotope tracer (^{205}Pb-^{233}U-^{235}U) (Parrish and Krogh, 1987). Zircon, monazite, and titanite were dissolved and U and Pb were separated using methods described in Parrish et al. (1987) and Davis et al. (1997). Isotopic compositions for U and Pb were measured on Finnigan-MAT261 variable multi-collector mass spectrometer (Roddick, 1987). The treatment of analytical errors is that outlined in Roddick (1987). Linear regression analysis follows York (1969). MSWD (mean square of weighted deviates) of greater than 1 reflects scatter in the data beyond that which can be accounted for by analytical error alone. Analytical results are presented in Table 4-2. Analytical uncertainties on the ages are reported at the 95% confidence (2 sigma) limit in the text and in error ellipses on concordia plots (Figs. 4-2 to 4-4, 4-6, 4-8, 4-10). Data points are marked with letters keyed to sample fractions in Table 4-2 and in the text. UTM coordinates of sample locations are shown in Table 4-2.

Sensitive High Resolution Ion MicroProbe (SHRIMP) II analyses were done on one sample (C) by V. McNicoll (unpublished results, 2001) at the Geological Survey of Canada. A detailed description of the analytical techniques followed can be found in Stern (1997).

SAMPLE DESCRIPTIONS AND RESULTS

Figure 4-1 is a simplified geology map of the Brightsand Forest area showing sample locationsthat are keyed to the text by sample letter.

(A) Fine-grained felsic sill (J-737, map unit "Fs")

A felsic sill east of Mountairy Lake (sample A. Fig. 4-1) is fine grained, with plagioclase (>50%) – quartz – muscovite – biotite – pyrite, with or without garnet and hornblende. This unit is interlayered with schistose muscovite – biotite – rich layers, and contains boudinaged remnants of mafic layers or xenoliths. Sulphides are finely disseminated throughout the felsic unit. To the south, the contact with quartz-rich clastic conglomerate is not exposed. To the west, the unit is truncated by the Hilltop Creek fault zone. Structurally overlying mafic volcanic rock to the north (Rude Lake amphibolite), is in sheeted contact with the felsic unit, contacts between layers are sheared and may have been transposed during deformation.

The least magnetic zircon was obtained during separation at 1.8A and 1 degree side slope. Zircons were sieved into 3 size fractions: < 74μm; 74-105μm; >105μm. The few zircons from the largest size fraction were a discolored yellow-brown, with prominent cracks, and a high probability of lead loss by diffusion or leaching. Therefore, the largest grains were not selected for analysis. From the 74-105μm size fractions, well-

faceted equant crystals (B1,B3) and prismatic crystals (A1) were analyzed. In addition, elongate well-faceted zircons from the smallest size fraction (D) were selected. The small size of good-quality zircon was problematic when selecting for analysis, and so multi-grain fractions were analyzed from population D, while A1, B1, and B3 were single grain analyses. All of the analyses are discordant (ranging between 1.0 and 8.3% discordant). A linear regression (MSWD = 1.6) including all four analyses has an upper intercept of 2707 $\pm$ 2 Ma, which is taken to be the crystallization age of the rock (Fig. 4-2, Table 4-2). The lower intercept of this line intersects concordia close to zero, suggesting that discordance of the zircons analyzed may be explained by recent lead loss.

Other morphologies of zircon that were not analyzed include those with likely metamorphic overgrowths from all size fractions, although these are less common in the smallest (<74μm) grains. Zircon twins are present in the smallest size fraction (Fig. 4-2).

(B) Tonalite orthogneiss (J-551 Rude Lake tonalite gneiss "TgR")

Tonalite west of Hilltop Lake (called the Rude Lake tonalite gneiss, sample B, Fig. 4-1) has a well-developed, pervasive gneissosity defined by compositional layering (S1) of mafic (biotite – rich) and felsic (plagioclase –quartz) rock components. In many areas, it is an injection gneiss consisting of several generations of tonalitic material, from dark grey, finer grained tonalite to coarser, more leucocratic layers. The distinguising characterisitic of this unit is the presence of complex donut - shaped fold structures, the result of F2-F3 fold interference, which are present in most locations (Fig. 2-12), including the sample location (B, Figure 4-1). To the south, the relationship of the polydeformed gneiss to quartz-rich metasandstone in the northern Rude Lake package is obscured by numerous granite and pegmatite intrusions.

Zircon grains from this unit include several different morphologies. Those selected for analysis were picked from the least magnetic fraction at 1.8 A and 1 degree side slope. Fractions A and H1 are elongate prismatic zircon grains, the largest of which is 300μm in length. Crystals are fairly clear although the largest grains have some fractures and surface discoloration (within fraction A in particular), which was reduced after abrasion. Fractions C and I2 are clear, equant, well-faceted crystals and are the highest quality zircons in the sample. Fraction D crystals are smaller, stubbier prismatic zircon with fractures and resulted in the most discordant analysis. All fractions analyzed were multigrained. Linear regression analysis (MSWD = 3) of all five data points fits a line whose upper intercept intersects concordia at 2718 +/- 7 Ma (Fig. 4-3, Table 4-2). This intercept is interpreted as the crystallization age of the rock. The lower intercept intersects concordia close to zero, suggesting that discordant results are related to recent lead loss

(C) Quartz-rich metasandstone (p865, "Sq")

At the northern margin of the Rude Lake amphibolite, quartz-rich metasedimentary rocks and interlayered metagreywacke are interleaved with amphibolitic rocks to the south. A quartz-rich metasandstone (sample C, Fig. 4-1; field photo: Fig. 2-9) was collected for analysis. The metasandstone is composed of >50% quartz, with up to 40% plagioclase and 10% biotite. Sub-centimetric granitoid veins, problematic during sampling, were cut out prior to crushing and grinding to eliminate contamination.

Several morphologies of zircon are distinguished from this sample, separated from the least magnetic fraction at 1.8A and 5 degrees side slope. B3 and B2 are stubby prismatic crystals, clear with no inclusions or fractures. C1 and C2 crystals are acicular

elongate zircon, without fractures. D1, D2 and D3 are rounded clear grains, with few facets prior to abrasion. E1 and E2 are similar in morphology to D grains, but are multi-faceted. Analysis of single grains yielded 2 populations (Fig. 4-4, Table 4-2). C and D morphological types (5 grains) yield analyses with 2-8% discordance, with 207/206 ages that range between 2.84 and 2.89 Ga. The younger three zircons consist of two morphological types, B and E, and group close to concordia at about 2700 Ma, this includes a super-concordant grain (B2). Equant, multi-faceted grains are present in both morphological groups. Analyses of rounded, yet tabular, zircon grains Y and Z yielded very discordant results (Fig. 4-5, Table 4-2). The most concordant points come from young grains at ca. 2700 Ma.

Figure 4-4b shows elongate prismatic zircon with metamorphic tips. Spot analyses of zircon cores (SHRIMP II, V. McNicoll unpublished results) yield a range of ages: 3 analyses between 2985 – 2970 Ma; 2936 Ma; 2780 Ma; 5 analyses between 2730 – 2712 Ma; 2701 Ma. Although quite small in size (the largest metamorphic zircon tip is 10-15μm) two metamorphic tips were analyzed, yielding ages of 2707 and 2676 Ma. The large discordance for many of the fractions using conventional geochronology, especially with respect to fractions Y and Z, may be partially explained by recent lead loss. The youngest concordant (conventional) analysis is therefore taken to represent the youngest detrital zircon grain, giving a maximum depositional age for the sandstone of ~2701 Ma (Fig. 4-4, Table 4-2).

(D) Granodiorite dyke (J-446b)

A sample of granodiorite was collected west of Robert Lake (Fig. 4-1) where 80 cm wide dykes of granodiorite cut the main fabric (S3) in semi-pelite and amphibolite.

and are oriented parallel to the axial planes of later folds (F4) striking 080 (Fig. 4-5). Pale pink, leucocratic, and homogeneous granodiorite is medium- to fine - grained with assemblages of K-feldspar – quartz – plagioclase – muscovite – biotite and accessory amounts of titanite and zircon.

Zircon fractions were selected from the least magnetic fraction at 1.8A, 1 degree side slope. Small, clear, prismatic and acicular zircon (B1, B2 and A2) without fractures yielded discordant analyses (2.0-2.6% discordance, Fig. 4-6, Table 4-2). Equant, clear, multi-faceted crystals (C) yielded more concordant results. A linear regression through the four zircon analyses has an upper intercept of 2697 +/- 3 Ma (MSWD = 0.26), which is interpreted to be the crystallization age of granodiorite. The granodiorite provides a minimum age bracket for S3 development in the map area, and a maximum age for D4 development (possibly syn – D4). Two fractions of 15-20 titanite grains each were analyzed from this same sample. Titanite grains were anhedral fragments, pale yellow to gold in colour. The weighted average of the $^{207}Pb/^{206}Pb$ ages of the two slightly discordant titanite analyses is 2687 +/- 8 Ma (MSWD = 1.7).

TIMING OF METAMORPHISM

(E) Annealed mylonite (p864b)

North of the Brightsand River shear zone (sample E, Fig. 4-1), ultramylonite is developed locally within mm-scale banded biotite - tonalite orthogneiss. Feldspar porphyroclasts show dextral assymetric rotation tails (Fig. 4-7). Thin sections also show biotite randomly overgrowing high strain fabrics. Large euhedral titanite crystals overgrow microfolds and foliation (Fig. 4-7b,c), and appear to post-date the latest phase of deformation (D4).

Three fractions of 12-15 titanite crystals each were selected from this sample for analysis. Anhedral grain fragments with minor inclusions were selected from the separate at 0.5-0.75A, 10 degrees side slope. Grain fragments were free of cracks and pale gold-yellow in colour. Analyses of the three titanite fractions overlap with each other and cluster near concordia (Fig. 4-8). A weighted average of the $^{207}Pb/^{206}Pb$ ages of all three titanite analyses is 2678 +/- 2 Ma (MSWD = 0.65).

F: Semipelite (J-446a)

A garnet – sillimanite – cordierite – biotite – muscovite – plagioclase – quartz migmatitic semipelite from the northern part of the central panel (sample F, Fig. 4-1) carries a strong (S3) foliation that contains leucosome (Fig. 4-9). The S3 layering is refolded by F4 folds whose axial planes are parallel to granodiorite dykes such as J-446. In thin section, sillimanite and cordierite define the S3 which is crenulated (Fig. 4-9). Biotite defines an F4 axial planar cleavage (Fig. 4-9b). Rare monazite grains from the sample are small (<100μm) and yellow - gold in colour. Single grain analyses of four grains are less than 0.5% discordant and range in age from 2687 to 2692 Ma (Fig. 4-10, Table 4-2). Monazite grains in the semipelite are interpreted to have been formed either before, during, or after metamorphism related to D3. This is assumed because peak metamorphic conditions were attained during D3, defined by migmatitic layering formed at temperatures of up to 650°C (Chapter 6). Metamorphism during D4 attained only biotite - grade metamorphic conditions, insufficient to reset monazite grains. The range in ages for the monazite grains, and the cross-cutting granodiorite dyke at 2697 Ma (Fig.4-5, sample D described above) suggest that monazite grains formed subsequent to peak metamorphic conditions (prior to 2697 Ma, perhaps ca. 2.7 Ga), and were reset

along a cooling path. Alternatively, the discordant results, and different U-Pb ages obtained from monazite crystals may indicate a subsequent metasomatic or hydrothermal event, causing some new growth, and pulling the resultant age determinations further from their initial ages of crystallization.

Further implications of the geochronology in the regional context will be discussed in the remaining chapters (Chapters 5, 6, and 7).

Table 4-1: U-Pb zircon geochronology for the Wabigoon subprovince and the Kenora area of the Winnipeg River subprovince

Location	Rock Unit	Igneous age	Reference
	Mesoarchean crust		
Winnipeg River	Tonalite gneiss	<2.95 Ga	11
Obonga belt	Granitoid basement south of the Obonga belt	2931	7
Central Wabigoon	Tonalite gneiss east of Harmon Lake	2.89 Ga	12
Minniss River fault	Mylonite	3046	14
	Volcanic rocks		
Sturgeon-Savant	Jutten continental margin volcanic rocks	2750-2880	1
	Fourbay oceanic plateau	2775	2
	Volcanic arc (Handy, Six Mile, Beckington)	2745-2733	3, 2
	South Sturgeon submarine caldera complex	2735	4
	Volcanic rift (Central Sturgeon assemblage)	2718	3
Obonga belt	Southern assemblage volcanic rocks	2734-2726	5
	Gabbroic core zone	2733	5
	Northern assemblage volcanic rocks	2703-2724	5
	Dacite (northern assemblage)	2703	5
Onaman-Tashota	Neoarchean volcanic rocks	2.75-7.72	6
	Felsic centres	2735-2740	6
	Humboldt Bay dacite	<2707	
Lake of the Woods	Volcanic rocks	2712-2723	16, 17
Metasedimentary rocks			
Sturgeon-Savant	Jutten sedimentary group	<2.95	7
	Quest Lake assemblage	ca. 2720	8
	Princess-Post Lake assemblage	<2720	8
	Savant sedimentary group	<2704	9
Obonga	Awkward Lake metasedimentary rocks	< 2701	5
Onaman Tashota	Marshal Lake metasedimentary rocks	< 2706	6
Kakagi Lakes area	Warclub group	< 2716	9
Central Wabigoon	Seseganaga Lake wacke	< 2706	10
	Quartz-rich metsandstone	< 2701	Chapter 4
	Neoarchean granitoid rocks		
	Harmon Lake gneiss	2774, with 2697 (m)	18
	Marchington granite	2735	14
Western Wabigoon	Lewis Lake batholith	2733	12
Central Wabigoon	Tonalite	2723	12
Central Wabigoon	Seseganaga Lake granodiorite		
Central Wabigoon	(part of Central Wabigoon magmatic arc)	2709	13
Brightsand Forest	Rude Lake tonalite gneiss	2718 +/- 7	Chapter 4
Brightsand Forest	Tonalite dyke, cuts D1 and D2, folded by F3	2715	12
Brightsand Forest	Felsic sill	2707+/-2	Chapter 4
Winnipeg River	Widespread TTG magmatism		
Winnipeg River	(includes granodiorite below)	2710	11, 15
Winnipeg River	Dalles batholith	2709	11
Winnipeg River	Marginal granodiorite	2709	11
Onaman-Tashota	Scheff pluton	2698	6
Brighsand Forest	Granodiorite dyke	2697+/-3	Chapter 4
Sturgeon-Savant	Vista Lake complex	2690	
Central Wabigoon	Wapikaimaski Lake pluton	2688	10
Central Wabigoon	Syn-tectonic granite	2685	10
Miniss River Fault	L>>S granite dykes (syn-tectonic)	2681	14

1 *Sanborn-Barrie et al., 2002*
2 *Davis et al., 1988*
3 *Davis and Trowell, 1982*
4 *Davis et al., 1985*
5 *Tomlinson et al., 2002*
6 *Stott et al., 2002*
7 *Davis and Moore, 1991*
8 *Skulski, Sanborn-Barrie, and Stern, unpublished results*
9 *Davis, 1996*
10 *Percival et al., 1999b*
11 *Corfu, 1988*
12 *V. McNicoll, unpublished data*
13 *Whalen et al., in press*
14 *Bethune et al., 2000*
15 *Cruden et al., 1998*
16 *Davis and Edwards, 1986*
17 *Davis and Smith, 1991*
18 *Davis, 1989*

Table 4-2: U-Pb analytical data

Fraction	Wt. (µg)	U (ppm)	Pb[1] (ppm)	$^{206}Pb/^{204}Pb$[2]	Pb_c[3] (pg)	$^{206}Pb/^{208}Pb$	Isotopic Ratios[4] $^{206}Pb/^{238}U$	$^{207}Pb/^{235}U$	$^{207}Pb/^{206}Pb$	Ages[5] $^{206}Pb/^{238}U$	$^{207}Pb/^{235}U$	$^{207}Pb/^{206}Pb$
(A) J737 (UTM: zone 15, 689120E - 5527967N)												
A1	8	93	58	4288	5	0.227	0.5146±0.10	13.124±0.12	0.18496±0.05	2676 ± 4	2689 ± 2	2698 ± 2
B1	6	96	61	2785	6	0.255	0.5135±0.11	13.102±0.13	0.18505±0.06	2672 ± 5	2687 ± 2	2699 ± 2
B3	6	142	90	7635	4	0.262	0.5085±0.10	12.931±0.12	0.18442±0.04	2650 ± 4	2675 ± 2	2693 ± 1
D	3	281	147	3799	5	0.139	0.4631±0.10	11.378±0.12	0.17819±0.05	2453 ± 4	2555 ± 2	2636 ± 2
(B) J651 (UTM: zone 15, 691042E - 5517810N)												
A	3	176	91	334	40	0.141	0.4528±0.12	11.626±0.29	0.18624±0.23	2408 ± 5	2575 ± 6	2709 ± 8
C	6	63	33	2207	5	0.095	0.4666±0.12	12.029±0.14	0.18697±0.05	2469 ± 5	2607 ± 3	2716 ± 2
D	3	191	82	3179	4	0.105	0.3852±0.10	9.847±0.12	0.18539±0.05	2101 ± 4	2421 ± 2	2702 ± 2
H1	4	215	107	3074	7	0.084	0.4563±0.11	11.707±0.13	0.18607±0.06	2423 ± 5	2581 ± 3	2708 ± 2
I2	7	19	10	703	7	0.019	0.5109±0.30	13.125±0.28	0.18634±0.16	2660 ± 13	2689 ± 5	2710 ± 5
(C) PBA98-865 (UTM: zone 15, 690800E - 5527512N)												
B2	1	118	68	374	7	0.106	0.5205±0.24	13.342±0.29	0.18592±0.19	2701 ± 11	2704 ± 6	2706 ± 6
B3	1	89	50	292	7	0.118	0.5056±0.35	12.879±0.36	0.18474±0.22	2638 ± 15	2671 ± 7	2696 ± 7
C1	1	741	434	5327	6	0.071	0.5344±0.09	15.060±0.12	0.20439±0.04	2760 ± 4	2819 ± 2	2862 ± 1
C2	2	464	263	7092	3	0.099	0.5425±0.10	15.511±0.12	0.20735±0.04	2794 ± 4	2847 ± 2	2885 ± 1
D1	2	265	162	6170	2	0.087	0.5504±0.09	15.528±0.12	0.20462±0.05	2827 ± 4	2848 ± 2	2863 ± 2
D2	1	319	181	3872	3	0.097	0.5096±0.11	14.209±0.13	0.20223±0.05	2655 ± 5	2764 ± 2	2844 ± 2
D3	1	225	139	1444	5	0.107	0.5447±0.12	15.609±0.16	0.20782±0.08	2803 ± 6	2853 ± 3	2889 ± 3
E1	1	128	73	747	4	0.091	0.5106±0.23	14.284±0.30	0.20292±0.18	2659 ± 10	2769 ± 6	2850 ± 6
E2	1	201	114	714	6	0.073	0.5240±0.27	13.389±0.27	0.18530±0.13	2716 ± 12	2707 ± 5	2701 ± 4
Y	1	552	278	3118	6	0.118	0.4471±0.10	11.736±0.12	0.19037±0.05	2382 ± 4	2584 ± 2	2745 ± 2
Z	4	113	56	232	51	0.101	0.4467±0.14	11.694±0.39	0.18988±0.31	2381 ± 5	2580 ± 7	2741 ± 10
(D) J446B (UTM: zone 15, 692980E - 5530091N)												
A2	2	214	123	1980	7	0.134	0.5052±0.11	12.744±0.14	0.18296±0.06	2636 ± 5	2661 ± 3	2680 ± 2
B1	3	214	122	629	30	0.142	0.5007±0.10	12.581±0.18	0.18222±0.12	2617 ± 4	2649 ± 3	2673 ± 4
B2	2	219	128	779	20	0.172	0.5039±0.21	12.709±0.21	0.18292±0.11	2631 ± 9	2658 ±4	2680 ± 4
C	4	98	62	3784	3	0.243	0.5161±0.11	13.124±0.13	0.18443±0.05	2683 ± 5	2689 ± 2	2693 ± 2
T1	25	849	3530	12174	49	8.177	0.5125±0.10	12.709±0.21	0.18385±0.04	2667 ± 4	2679 ± 2	2688 ± 1
T2	154	959	4167	19417	214	8.561	0.5148±0.11	12.709±0.21	0.18371±0.04	2677 ± 5	2683 ± 3	2687 ± 1
(E) PBA98-846B (UTM: zone 15, 703122E - 5531358N)												
T1A	89	60	46	995	153	0.562	0.5146±0.09	12.962±0.13	0.18270±0.08	2676 ± 4	2677 ± 3	2678 ± 3
T1B	102	59	44	1387	124	0.504	0.5134±0.09	12.938±0.11	0.18277±0.06	2671 ± 4	2675 ± 2	2678 ± 2
T2B	56	34	26	511	112	0.506	0.5143±0.14	12.934±0.21	0.18241±0.15	2679 ± 5	2676 ± 4	2675 ± 5
(F) J446A (UTM: zone 15, 692980E - 5530091N)												
M1	5	922	2509	21677	6	4.899	0.5166±0.09	13.126±0.11	0.18426±0.04	2685 ± 4	2689 ± 2	2692 ± 1
M2	9	1664	3220	38553	11	3.159	0.5149±0.09	13.046±0.11	0.18375±0.04	2678 ± 4	2683 ± 2	2687 ± 1
M3	4	1983	3787	23664	10	3.101	0.5150±0.09	13.072±0.12	0.18408±0.04	2678 ± 4	2685 ± 2	2690 ± 1
M4	8	1291	1927	37092	8	2.160	0.5165±0.09	13.138±0.11	0.18449±0.04	2684 ± 4	2690 ± 1	2694 ± 1

Notes: [1]radiogenic Pb; [2]measured ratio, corrected for spike and fractionation; [3]total common Pb in picograms in analysis corrected for fractionation and spike; [4]corrected for blank Pb and U and common Pb, errors quoted are one sigma in percent; [5]corrected for blank and common Pb, errors quoted are two sigma.

Figure 4-1: Simplified geology map of the Brightsand Forest area with U-Pb sample locations plotted. Sample A: Felsic sill "Fs"; Sample B: Tonalite gneiss "TgR"; Sample C: Quartz-rich metasandstone "Sq"; Sample D: granodiorite dyke; Sample E: tonalitic mylonite; Sample F: Migmatitic semipelite.

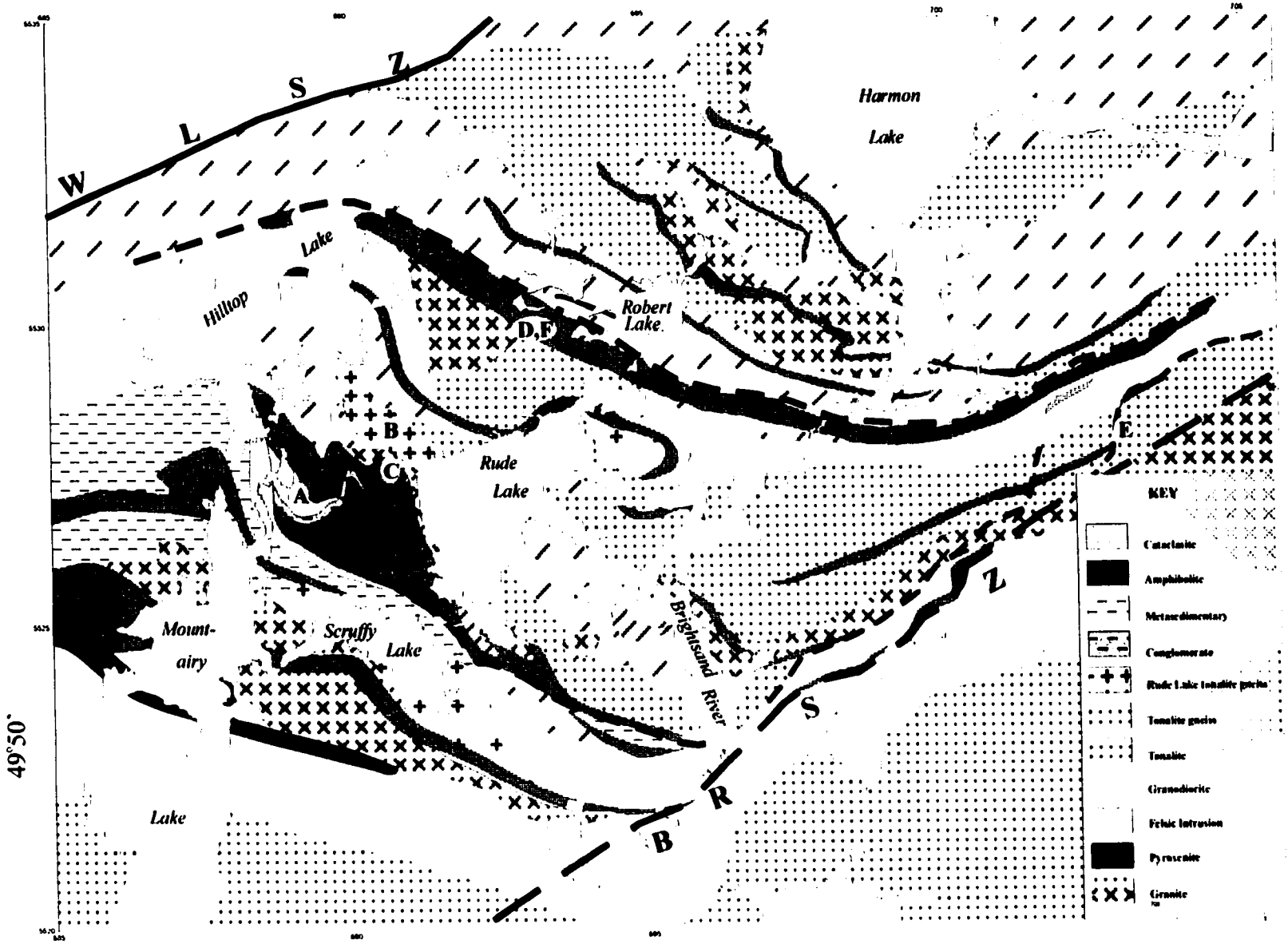
W L S Z
Harmon Lake
Hilltop Lake
Robert Lake
D,E
B
C
A
Rude Lake
E
Mount-airy
Scruffy Lake
Brightsand River
Z
S
R
B
Lake
KEY
Cataclasite
Amphibolite
Metasedimentary
Conglomerate
Rude Lake tonalite gneiss
Tonalite gneiss
Tonalite
Granodiorite
Felsic Intrusion
Pyroxenite
Granite
49°50'
90°20'

Figure 4-2: Concordia diagram for sample A, showing zircon morphologies, including zircon twins that were not analyzed. Photographs of zircon show different populations based on morphology. Single grains used for analysis were selected from the different populations for A1, B1 and B3. Analysis D was a multigrain analysis; the zircon from this fraction were selected from population D.

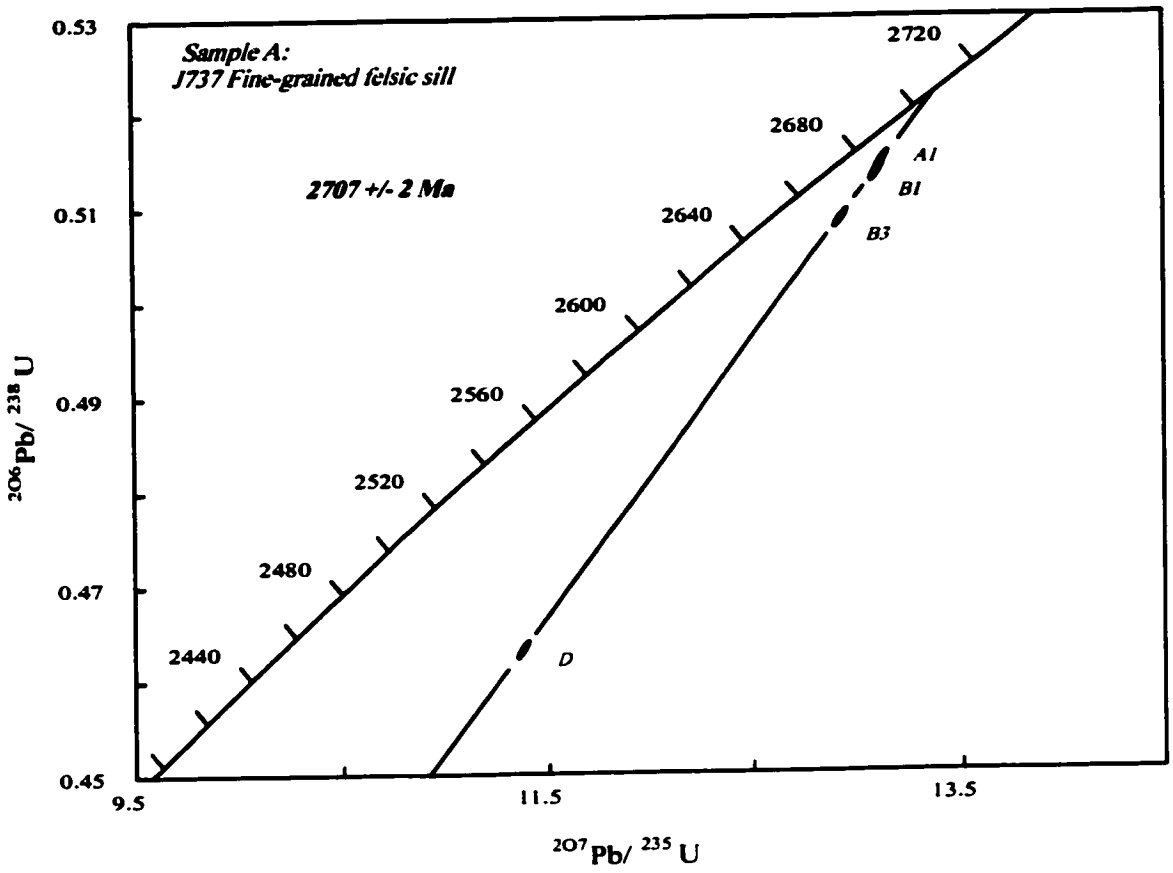
Sample A:
J737 Fine-grained felsic sill
2707 +/- 2 Ma
0.53
0.51
0.49
0.47
0.45
2720
2680
2640
2600
2560
2520
2480
2440
A1
B1
B3
D
9.5
11.5
13.5
206Pb/ 238U
207Pb/ 235U

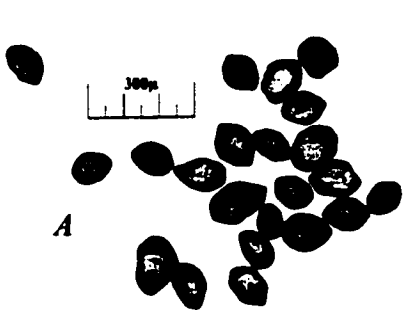
A


B

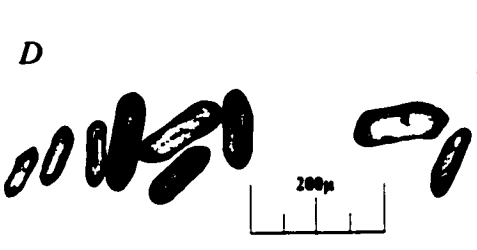
D
Small overgrowths


Twins

Figure 4-3: Concordia diagram for sample B, with analyzed zircon morphologies. Photographs of zircon show different populations of zircon based on morphology from which analyzed grain fractions were selected (described in the text).

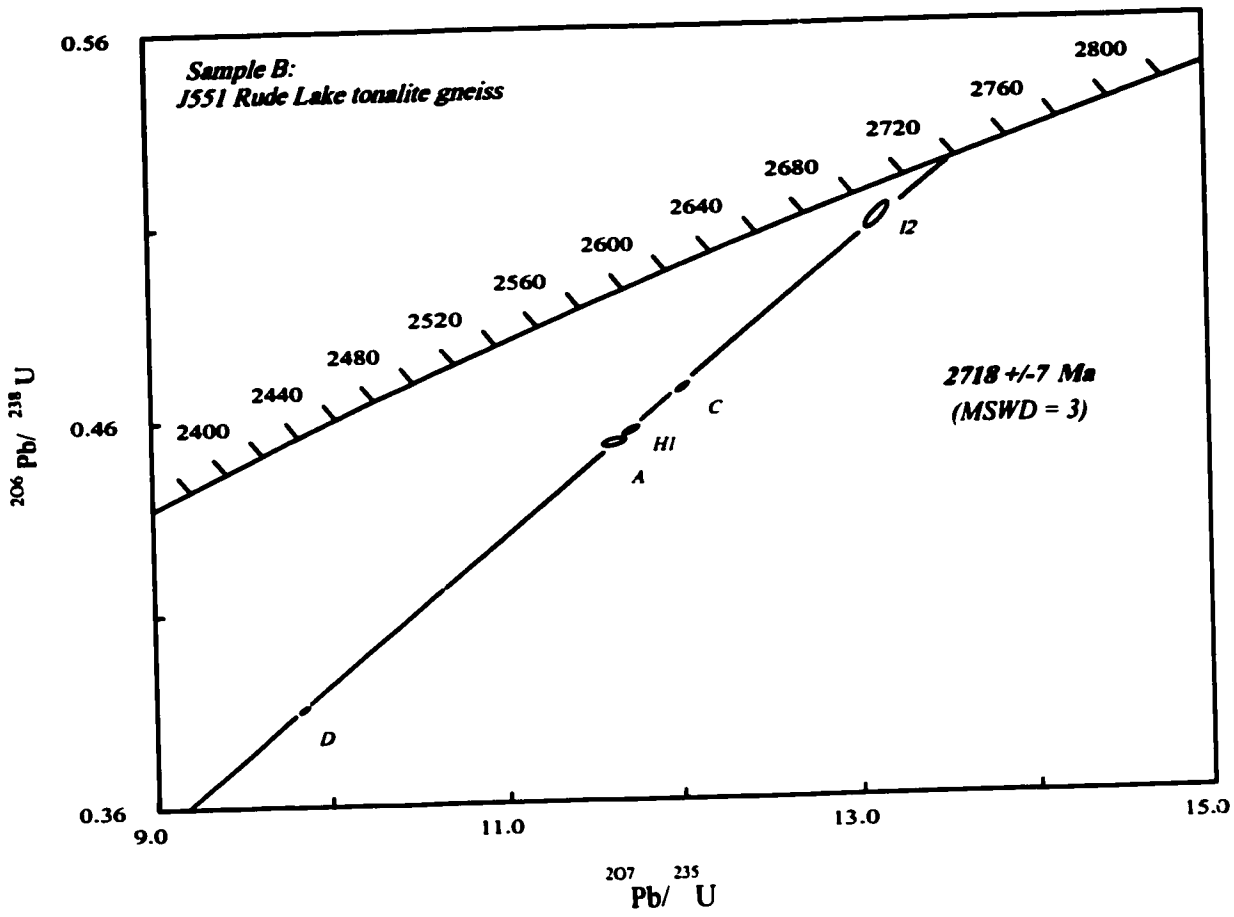
Sample B:
J551 Rude Lake tonalite gneiss
2718 +/-7 Ma
(MSWD = 3)
0.56
0.46
0.36
9.0
11.0
13.0
15.0
2400
2440
2480
2520
2560
2600
2640
2680
2720
2760
2800
I2
C
HI
A
D
206 Pb/ 238 U
207 235 Pb/ U

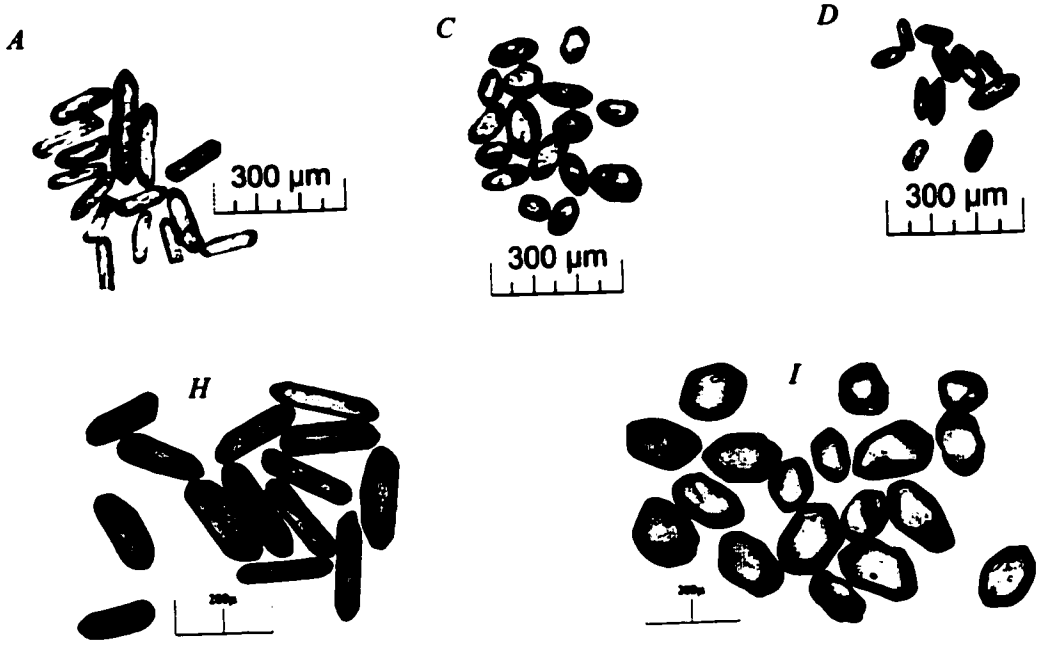
A
300 µm
C
300 µm
D
300 µm
H
I

Figure 4-4: Concordia diagram for sample C (zircon). Zircon on concordia diagram show populations based on morphology. All fractions analyzed were done on single grains. Also shown are the results from SHRIMP II ion microprobe study on elongate zircon with metamorphic tips. The zircon used in this study were selected from the population in the photo below the concordia diagram.

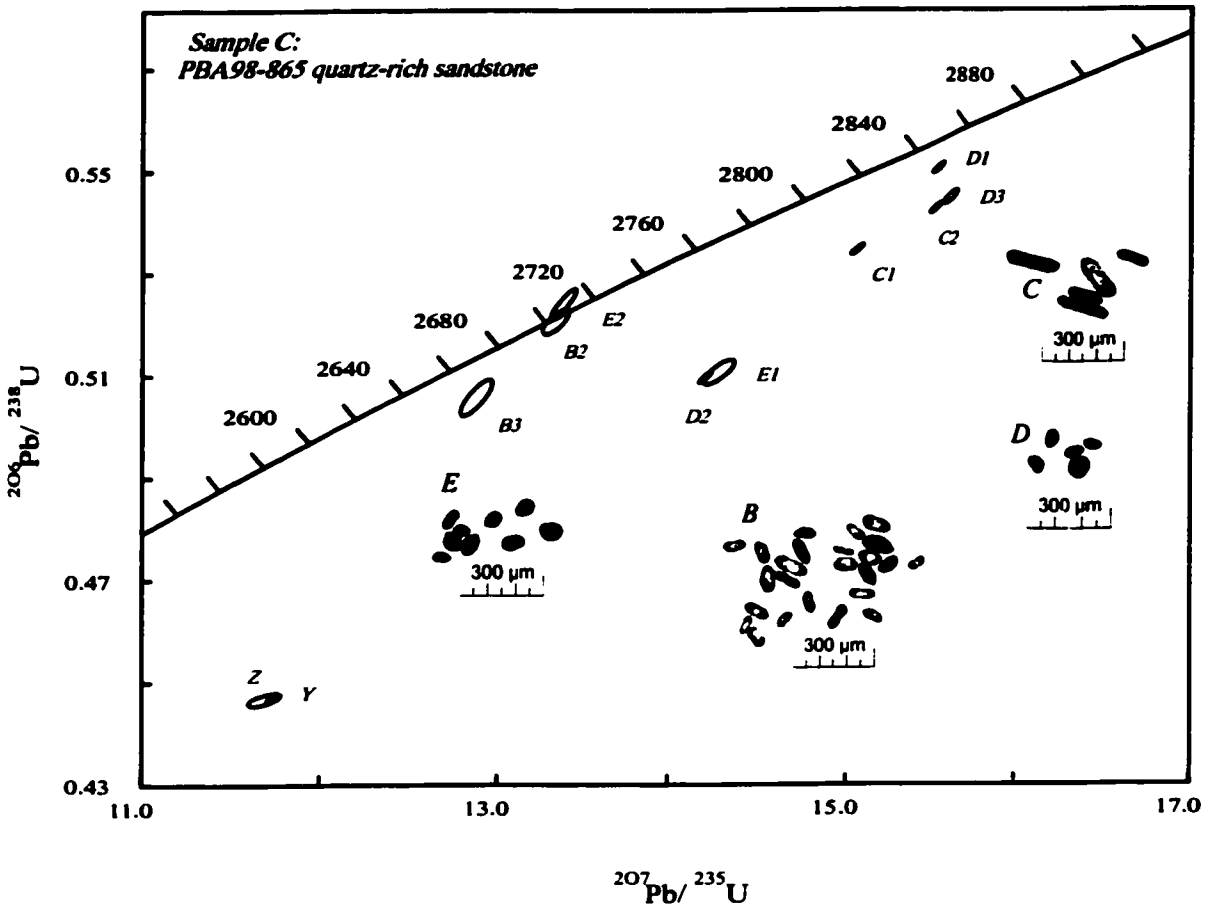

Shrimp ages:
detrital: three grains from 2985-2970 Ma
one grain at: 2936 Ma, 2780 Ma
five grains from 2730-2712 Ma
one grain at: 2701 Ma
metamorphic rim: 2707 and 2676 Ma
(V. McNicoll, unpublished data 2001)

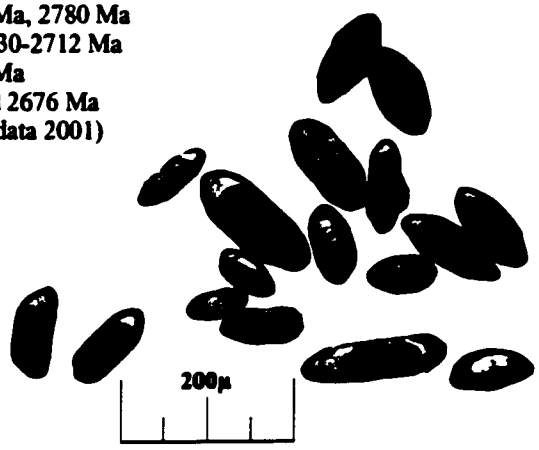

Figure 4-5: Granodiorite dykes (striking at 080°) cutting S3 in amphibolite (A) and semipelite (B.C). C shows a xenolith of semipelite in a granodiorite dyke.

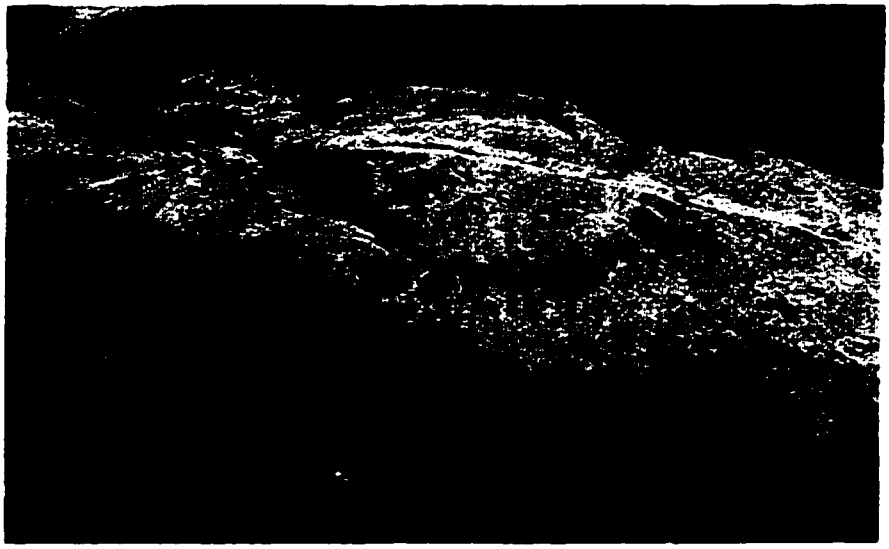

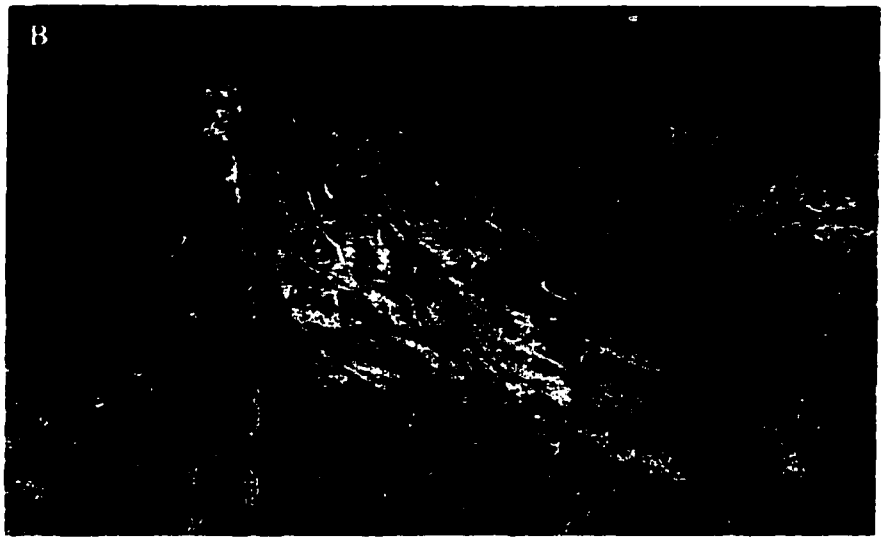
B

Figure 4-6: Concordia diagram for sample D including results from zircon and titanite analyses. A, B and C are zircon populations based on morphology. T1 and T2 are titanite grains.

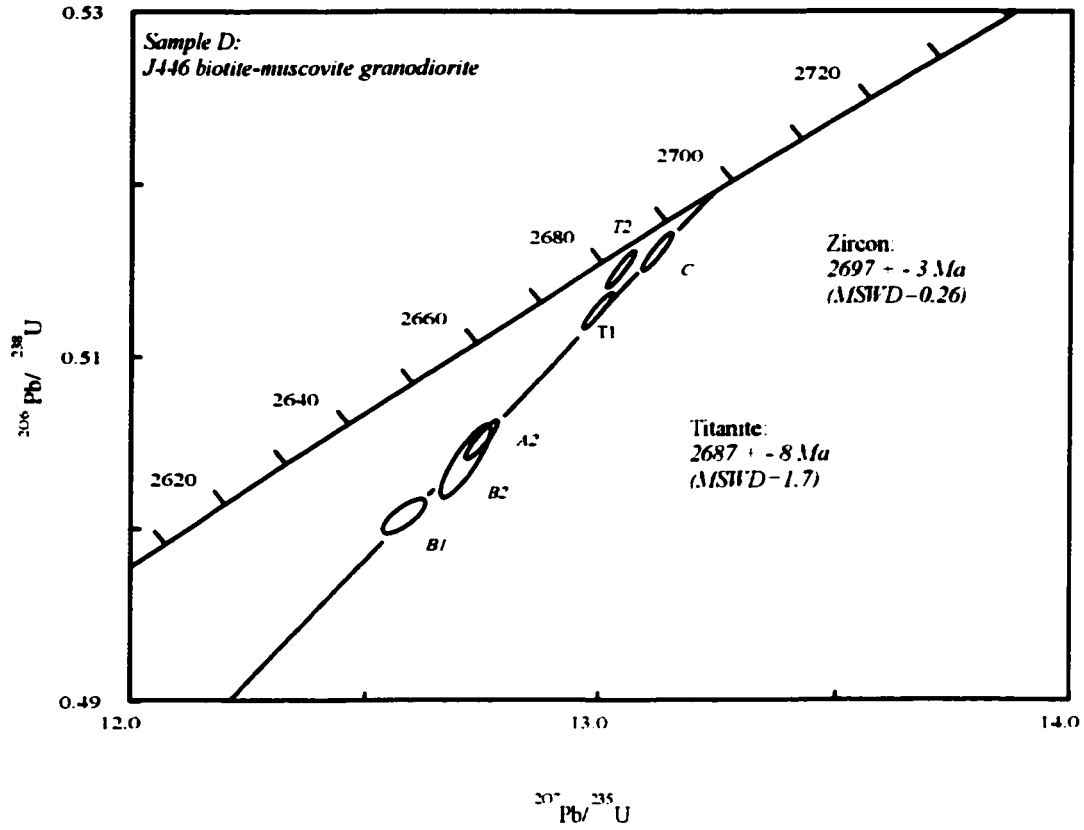
Sample D:
J446 biotite-muscovite granodiorite
Zircon:
2697 + - 3 Ma
(MSWD=0.26)
Titanite:
2687 + - 8 Ma
(MSWD=1.7)
2720
2700
2680
2660
2640
2620
T2
C
T1
A2
B2
B1
0.53
0.51
0.49
12.0
13.0
14.0
$^{206}Pb/^{238}U$
$^{207}Pb/^{235}U$

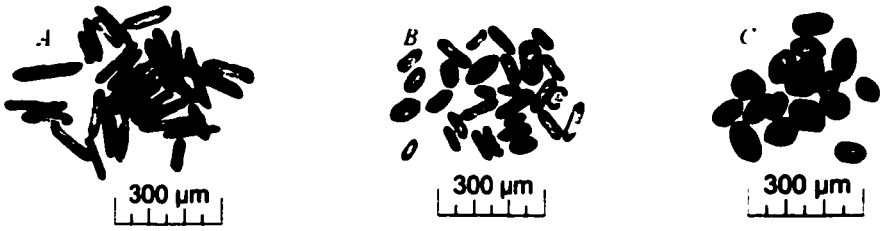
A
300 μm
B
300 μm
C
300 μm

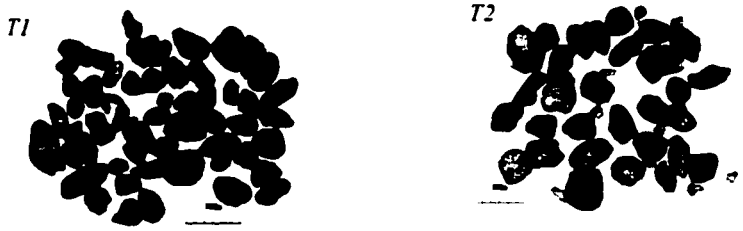
T1
T2

Figure 4-7: Mylonitic tonalite along the edge of the Brightsand River shear zone. Feldspar porphyroclasts have dextral shear sense (A); planar fabrics in the shear zone are steep (sub-vertical), photograph is taken on a horizontal surface. Titanite (in thin section) is overgrowing planar fabrics in B and C.

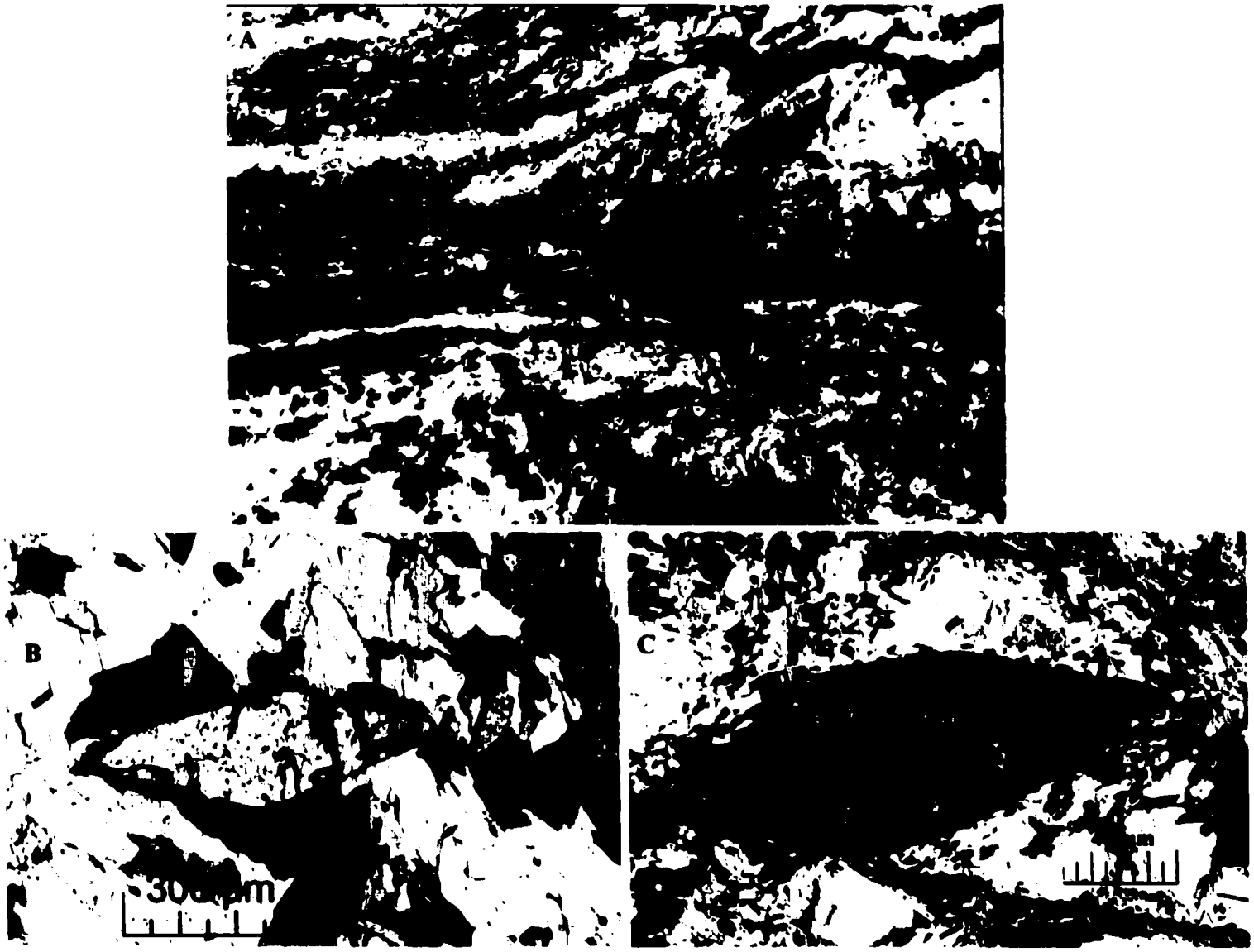
A
B
C

Figure 4-8: Concordia diagram for sample E (titanite).

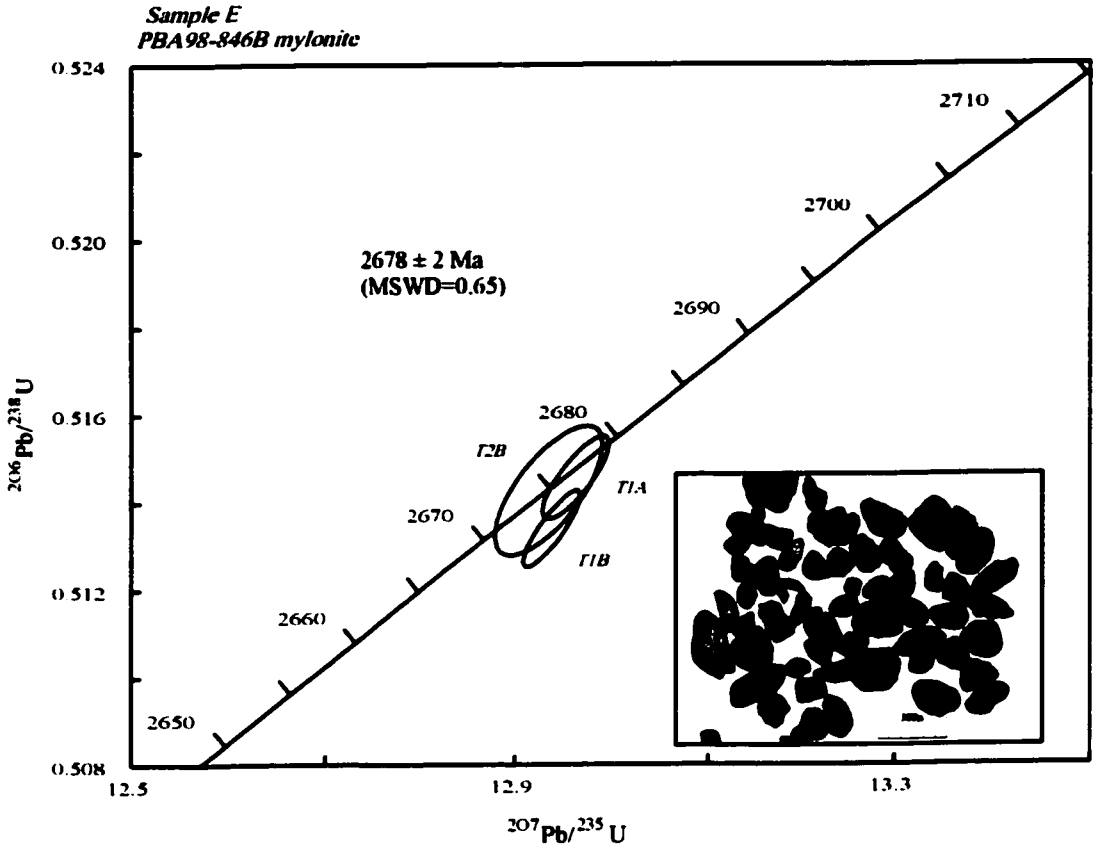
Sample E
PBA98-846B mylonite
0.524
0.520
0.516
0.512
0.508
12.5
12.9
13.3
2710
2700
2690
2680
2670
2660
2650
2678 ± 2 Ma
(MSWD=0.65)
T2B
T1A
T1B
206Pb/238U
207Pb/235U

Figure 4-9: A: S3 fabric in migmatitic semi-pelite, with concordant leucosome. Biotite cleavage is parallel to the axial planes of F4 folds that crenulate S3 and leucosome. B: In thin section, the same relationships are observed. S3 in this view is defined by cordierite (Crd), sillimanite (Sil), and biotite (bt-1). S4 biotite (Bt-2) has grown over this fabric at a high angle.

Figure 4-10: Concordia diagram for sample F (monazite).

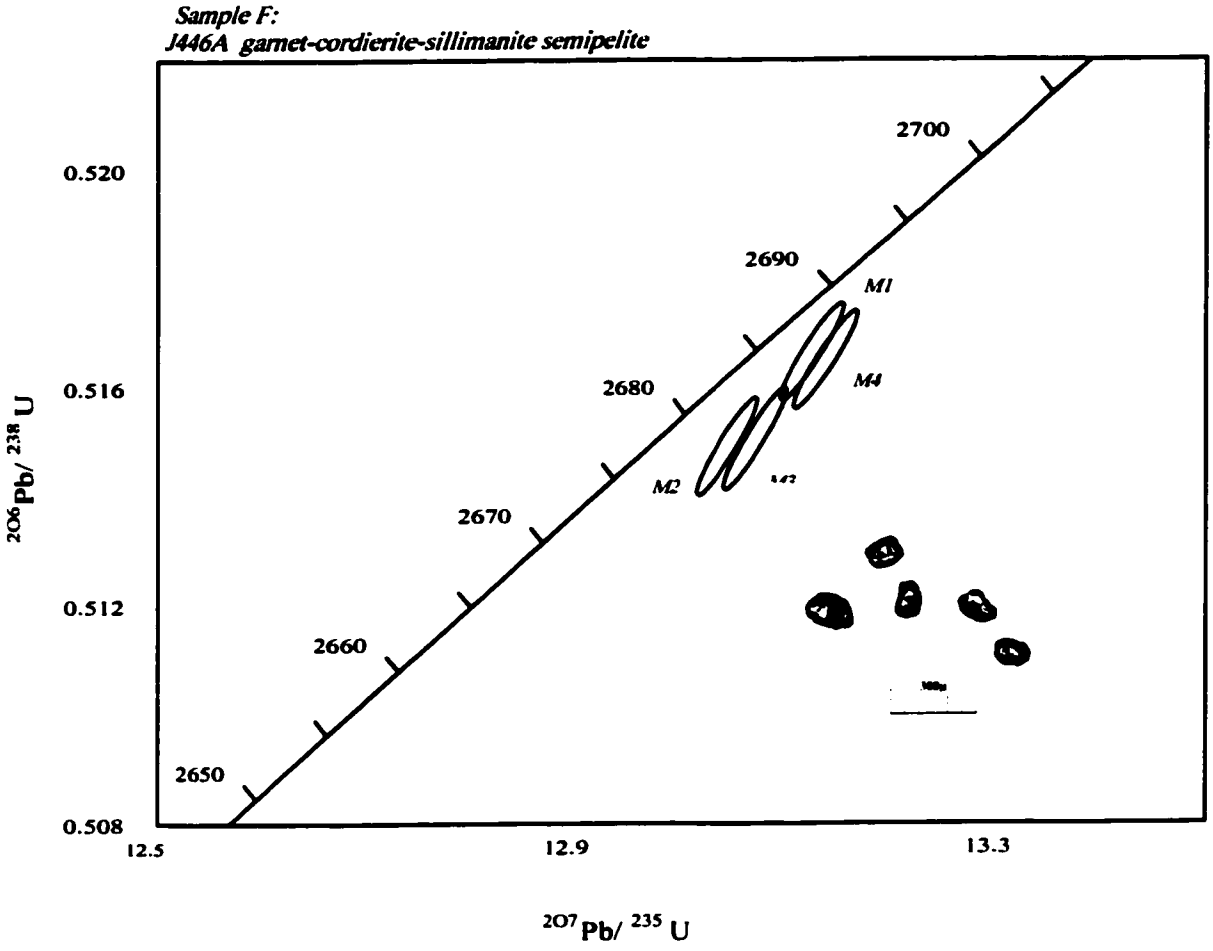
Sample F:
J446A garnet-cordierite-sillimanite semipelite
2700
2690
2680
2670
2660
2650
M1
M2
0.520
0.516
0.512
0.508
12.5
12.9
13.3
$^{206}Pb/^{238}U$
$^{207}Pb/^{235}U$

CHAPTER 5: STRUCTURAL GEOLOGY

INTRODUCTION

Rocks of the Brightsand Forest area preserve evidence for five distinct structural events, four of which resulted in penetrative foliations and/or mesoscale folds. The earliest structures are D1 and D2 fabrics, which occur only in tonalitic gneissic rocks. The main penetrative foliation, S3, affects all map units with the exception of late garnet - bearing granites and pegmatites.

A late D3 event, D3b, is inferred from a N-S oriented map-scale fold in the western part of the area. D4 resulted in upright folds of lithological layering and S3, and rare S4 foliation. Regional shear zones post - date D4 structures and are locally overgrown by post - tectonic titanite dated at 2678 Ma.

F3b folds characterize the south and west, and are responsible for the map pattern in this area. To the east, metavolcanic and plutonic units are warped by the Brightsand River shear zone.

REGIONAL STRUCTURAL CHARACTER AND CONSTRAINTS

Sturgeon Lake – Obonga Lake granitoid – gneiss domain (central Wabigoon)

Within the central Wabigoon subprovince between the Sturgeon Lake and Obonga Lake greenstone belts, the map pattern is dominated by ENE - striking lithological units with some oval plutonic bodies. All major map units carry a prominent S3 fabric. Some late granites, granodiorites, and pegmatites postdate the D3 event. S3 is axial planar to tight to isoclinal F3 folds rarely preserved in the hinges of F4 folds (Percival et al. 1999a, Fig. 6). L3 lineations are uncommon, though present in the

Seseganaga Lake area (Percival et al. 1999a) as well as in the Brightsand Forest area west of Rude Lake.

F4 folds are open, upright and plunge shallowly and almost uniformly to the east (Percival 1998, Fig. 3; Percival et al. 1999a, Fig. 7). Quartz rodding lineations (L4) are prominent in F4 fold hinges and other mineral and stretching lineations are developed sporadically. Mesoscale and map-scale F4 fold formation was followed by the development of ductile shear zones. The Wapikaimaski Lake and Brightsand River shear zones are late D4, regional, ductile, sinistrally transpressive, deformation zones, which transect the edges of the Brightsand Forest area. The Brightsand River Shear Zone extends from southeast of the Sturgeon Lake greenstone belt toward the Obonga belt, transecting the southeastern corner of the map area. It defines the boundary between elongate sheet – like plutonic bodies in the north and large homogeneous plutons in the south. Sporadic, narrow bands of ultramylonite mark the northern, left – stepping boundary of the shear zone, whereas most of the southern portion is occupied by subhorizontally lineated L>S tectonites. Toward the northeast the Brightsand River zone broadens to a width of >10 km where it has significantly reworked the dextral Gunter Lake shear zone (Percival et al., 1999a) of uncertain absolute age (D3 or earlier D4). The Wapikaimaski Lake shear zone, which transects the northwestern portion of the Brightsand Forest area, is similar in style and age to the Brightsand River shear zone. Zones of ultramylonite mark the southern boundary of the shear zone.

Earlier (pre - D3) structures in the central Wabigoon subprovince are preserved in tonalitic gneisses. The early events are recognized within complex fold interference

structures and by cross-cutting relationships. At one time, D1 and D2 were thought to be Mesoarchean structures formed prior to 2715 Ma (Percival et al. 1999a).

Sturgeon Lake - Savant Lake greenstone belt (western Wabigoon)

Two main episodes of ductile deformation (D1 and D2) have been documented within the Sturgeon Lake-Savant Lake greenstone belt (Sanborn-Barrie and Skulski, 1999). Within the Savant Lake area, S1 is an axial planar cleavage to F1 folds that are N and NW trending and shallow – plunging. F1 folds were overprinted by steeply plunging, NE trending F2 folds with an axial planar S2. In the Sturgeon Lake area, S1 is a north - striking, steeply dipping penetrative foliation, that is axial planar to tight, north-plunging F1 folds. D2 structures are similar to those observed in the Savant Lake area, although developed only locally (Sanborn-Barrie and Skulski 1999). Sanborn-Barrie et al. (1998) also described structural facing reversals in the central Sturgeon belt, in ca. 2720 Ma sedimentary rocks (Skulski, Sanborn-Barrie and Stern, unpublished data 1998) of the Quest Lake area, indicating the presence of pre - D1 folds. In the Savant Lake area, a non - penetrative, pre -D1 tilting event was recognized to predate the <2704 Ma (Davis, 1996) Savant sedimentary group (Sanborn-Barrie and Skulski, 1999). Foliated clasts within conglomerate at the base of the Jutten sedimentary group (< 2950 Ma, Davis and Moore, 1991) suggest a still older (Mesoarchean) deformation event affected the basement to the greenstone belt (Sanborn-Barrie and Skulski, 1999). D2 shear zones with east and northeasterly trends transect the belt.

The Obonga Lake greenstone belt (central Wabigoon)

A modern tectono - stratigraphy of the Obonga belt is presented in Percival and Stott (2000). The older (2734 - 2727 Ma; Tomlinson et al., 2002) southern assemblage is

a north - facing package of calc - alkaline volcanic rocks. A large body of gabbro (2733 Ma) separates these rocks from the younger (<2724 - 2703 Ma), south - facing northern assemblage. Numerous shear zones bound assemblages and older (ca. 2930 Ma) granitic rocks to the south.

Tectonic breaks are ENE - trending high strain zones along boundaries between supracrustal rocks and inferred basement, occurring also between assemblages. With respect to the northern assemblage, two fabrics are described within the Puddy Lake serpentinite: an early, N dipping (roughly east - trending) foliation which is cut by later 'bifurcating' shear zones (Percival and Stott, 2000). Early structures within this unit are parallel to structures at the northern margin (Percival et al., 1999b) while the younger shear zones are parallel to the sheared northern contact of the belt. Also within the northern assemblage, complex internal structures within the Awkward Lake sedimentary group include isoclinal, refolded, and disharmonic folds, dismembered beds, and strong transposition foliations. 2703 Ma dacite (Tomlinson et al., 2002) within sedimentary units east of and continuous with the Awkward Lake group is thought to reflect the age of these rocks. A package of < 2724 Ma pillowed volcanic rocks (Tomlinson et al., 2002) has consistent southward younging, and is in fault contact with structurally underlying sedimentary units. It is possible that complex structures within the Awkward Lake group are the result of early soft sediment deformation, although partitioning of strain into less competent sedimentary units is feasible (Percival and Stott, 2000). Pillow facing of the southern assemblage is generally obscured by high strain, although where younging is observed, it is consistently to the north. The southern volcanic contact is a northeast trending greenschist-facies high strain zone (Thurston, 1968a,b) which transects the belt

south of Silk Lake (Percival and Stott, 2000; Figure 2). The main fabric within the 2733 Ma gabbroic to ultramafic core zone (Tomlinson et al. 1999) consists of small - scale shear zones cut by later alteration zones (Percival et al. 1999a).

Correlation between Plutonic and Volcanic domains

It is possible to correlate structural fabrics in the granitoid gneiss domain with those in the Sturgeon Lake and Obonga Lake greenstone belts on the basis of geometric and chronological similarities. All major map units in the granitoid domain carry an S3 foliation that is in turn folded into upright, map - scale F4 folds. S1 in the supracrustal belts is parallel to S3 in granitoid rocks where observed along the steeply dipping eastern margin of the Sturgeon Lake - Savant Lake belt. Likewise, in the Obonga belt, the earlier high strain fabric (pervasive in the southern assemblage and described in the Puddy Lake serpentinite) is parallel to fabrics in plutonic rocks along the northern margin, and is correlated with S3. F2 folds observed in greenstones are correlated with F4 folds within the granitoid domain on the basis that F2/F4 are folds of the S1/S3 penetrative foliation with consistent easterly trends. Whereas F2 folds plunge steeply in the Savant belt, F4 folds plunge shallowly in the granitoids. This implies that prior to D4, S3 was subhorizontal within the granitoid terrane and S1 was steep in the greenstone belts. Correlation of D1 and D2 structures in the gneisses to pre - D1 structures of the Sturgeon - Savant belt is a possibility, and the implications of this common deformation chronology are explored further in the discussion below.

STRUCTURAL GEOLOGY

Primary structures

Depositional features within sedimentary units have been almost completely obliterated by deformation, prograde and retrograde metamorphism and alteration. However, compositional variation across strike within sedimentary units may reflect relict bedding. Locally, semipelite in the Robert Lake area exhibits alternating garnet-rich and garnet-poor layers, while meta-psammites in the Northern sedimentary group have alternating light and dark (biotite - rich) layers. Primary features have not been observed in volcanic units. Approximately 10 km west of the map area, deformed pillows with selvages are preserved in central Sturgeon basalt, and graded beds within the Princess-Post Lake assemblage indicate younging to the north.

D1 and D2 structures

D1 developed a foliation/gneissosity is prominent in certain tonalites and tonalite gneisses. Units characterized by S1 range from approximately 2.5 to 7 km long, and include the Rude Lake tonalite gneiss (TgR), gneisses on Harmon Lake (TgH) and hornblende - tonalite (Th) north of the Robert Lake zone. The S1 fabric is a compositional layering of alternating leucocratic and mafic mineral bands in the gneiss units (Fig. 5-1). Leucocratic layers are medium-grained, plagioclase-, quartz-rich tonalitic phases. Mafic layers are fine-grained biotite with some plagioclase and quartz. Compositional layers have variable thickness: leucocratic bands are commonly from 0.8 to 1.5 cm in width, while mafic layers can be narrower, from 1 - 2 mm in width. Diffuse, grey, biotite – plagioclase – quartz layers appear intermediate in composition, forming up to ~30% of the rock. Within unit Th, S1 is variably a foliation defined by grain-scale

alignment of hornblende +/- biotite, and a compositional layering defined by mafic- and felsic-rich zones. Where layering occurs, it is on the scale of 0.5 - 1 cm. Overprinting of D1 by subsequent deformation caused F2/F3 fold interference patterns (described below). Stereographic projection of poles to S1 (and S2) fabrics (Fig. 5-1) form a small circle around a point representing steeply plunging fold axes (of F2 folds).

The origin of D1 is subject to various interpretations. It is possible that gneissosity is primary, in which case S1 = S0 (primary gneissosity, Lucas and St. Onge 1995). However, some of the S1 compositional banding is discrete mm-scale layering attributed to metamorphic segregation or in situ melting of a tonalitic protolith, whereas cm – scale leucocratic tonalite layers appear to have been injected later.

D2 resulted in tight and isoclinal F2 folds of S1 layering. F2 folds are preserved in tonalite gneiss units: TgR and TgH (Fig. 5-2). Within these units, folds of primary gneissossity have been reoriented during D3 and D4 deformation. Figure 5-1d shows reoriented F2 axial planes are E-W trending, steeply dipping structures of close to vertical plunging folds. D3 low strain zones are present within hornblende tonalite (Th), in which F2 folds are preserved with uniquely larger wavelengths than F2 folds in TgR/TgH. Within the Th tonalite, possible F2 folds have wavelengths of ~0.4 - 0.8 m, and N - S trending axial planes and limbs transposed into S3 trends (Fig. 5-2a). Differences in fold styles between TgR/H and Th are attributed to the different compositions/competencies of these rock units. The relatively coarse-grained Th unit contains abundant hornblende and may have behaved more rigidly than more felsic, biotite-bearing units during deformation. F2 folds in low strain zones trend at a high angle to E-W D3 structures.

suggesting that F2 folds were originally shallow plunging, roughly N-S trending folds of S1.

D3 structures

I) S3 foliation

The trend of most major map units is parallel to S3. Regional fabric development during D3 is expressed mainly as a penetrative S3 foliation in most map units. S3 is a grain-scale foliation in homogeneous tonalite, granodiorite, granite, and metavolcanic and metasedimentary rocks. It is also defined by layering in migmatitic semi-pelites near Robert Lake and in some mafic gneiss units, mainly within the northern panel. Sillimanite and biotite define S3 in the peak metamorphic mineral assemblage sillimanite-garnet-cordierite-biotite-muscovite-plagioclase in migmatitic semi-pelites.

S3 fabrics (Fig. 5-3a) generally dip steeply and strike E-W. F3 folds have been observed within 3 tonalitic map units: Th, TgR and TgH. Where present, F3 folds are generally tight, with axial planar S3 foliation. Within Th, tight F3 folds locally overprint isoclinal F2 folds (Fig. 5-2a). F3 folds in biotite-tonalite gneisses refold smaller wavelength (>10 cm) F2 folds. Differences in fold style between units is attributed to variable internal competency contrasts between coarse-grained, homogenous hornblende-tonalite and layered biotite-tonalite gneiss. The F3 fold axis data show similar trends to those of L4/F4 (Fig. 5-3b), interpreted as the result of rotation and transposition during D4.

II) D3a structures

The Hilltop Creek Fault is a discrete zone of cataclasis preserving evidence of brittle deformation during D3. The ~ 350 m wide cataclastic unit (C) of brecciated rock

includes fragments of granite, amphibolite, exhalative sedimentary rocks, and iron formation, set in a granular, fine-grained matrix with abundant chlorite, epidote, and hematite. Partially dismembered dykes of granite are the youngest component of the zone, and show brecciation followed by ductile deformation (Fig. 2-7f). Finely disseminated sulphides occur throughout fragments of various origin within this unit.

The zone of cataclasis is discordant to the trend of units to the east and concordant with those to the west. In the east, the shape of clasts within conglomerate (Sc) records increasing D3 ductile strain with proximity to the HCF. With respect to western rock units, the HCF is concordant in that it contains fragments of distinctive rock units: psammites and iron formation.

A narrow zone (10-m-wide) of brecciated amphibolite separates the Scruffy Lake and Rude Lake amphibolite packages (Fig. 2-7g). Tabular bodies of amphibolite within a fine-grained mafic matrix characterize this area. Its similarity in structural style to the Hilltop Creek Fault, as well as its proximity, suggests this zone to be a splay from the Hilltop Creek fault. These rocks lack obvious D4 effects, likely as a result of the E-W trend of the splay.

Lineations in the area west of Rude Lake are not consistent with the geometry of local and regional linear fabrics formed during D4. Figure 5-3e is a plot of linear data from this area, showing differences in this area with respect to L3 data from the entire map area (Fig. 5-3b). It is apparent that structures in this area have not been affected (significantly) by F4 overprinting. Figure 5-4a is a sketch map of the major structural features in the southwest, and is accompanied by a form surface map of the southwestern corner of the map sheet (Fig. 5-4b). The Rude Lake amphibolite preserves L3 lineations,

which have been refolded about a NW trending axis consistent with map-scale "S" fold axes. The preservation of L3 lineations is unique in the map area. It is possible that the L3 lineations were formed during early D3 deformation, related to S3 development and/or thrusting along the Hilltop Creek Fault. They may be uniquely preserved in this location because late folding (F3b) resulted in a thickened package of mafic rocks, not as susceptible to overprinting during D4, and thus preserving L3 lineations (D4 strain shadow). Where the amphibolite unit narrows to the southeast, overprinting by F4 folds and L4 lineations is evident. In both areas with map scale D3a folds of S3 (Mountairy Lake and west of Rude Lake), the limbs of these folds are overprinted by open east-trending F4 folds, as well as by L4 mineral lineations with the same trend.

III) D3b structures

A north - trending open fold plunging steeply to the NNE is a prominent feature of the southwestern portion of the map (Mountairy Lake fold; Fig. 5-4a). It folds bedding and parallel S3 foliation, as well as the Hilltop Creek Fault. The penetrative fabric (S3) along its eastern limb is crenulated by E-W trending F4 folds. Steeply plunging map-scale "S" folds of S3 foliation and L3 lineation occur in the Rude Lake package occur east of the Hilltop Creek fault. Conglomerate in the northern sedimentary package located within the hinge zone of the Mountairy Lake fold is an L>>S tectonite with steep northerly plunge. Likewise, conglomerates (Sc) in the hinges of parasitic folds (~1.5 km east of the Hilltop Creek fault) are much more strongly lineated than foliated (Fig. 2-10b). In both areas the stretching lineation plunges steeply north parallel to fold axes. Mesoscale folds of F3a generation are not apparent. The orientation of the map scale "S" folds west of Rude Lake is such that they appear to be parasitic to the Mountairy Lake

fold. Fold asymmetries in strained conglomerate (Sc) in this area are consistent with map-scale fold geometry (Fig. 5-4).

D4 structures

Regionally, D4 is recognized to be a widespread folding and shearing event responsible for the general map pattern. D4 affected most of the map area by folding D3 planar features into open, upright east-plunging folds. The Rude Lake synform (Fig. 5-4a) is a map-scale feature cored by the Rude Lake tonalite gneiss. It is a broad open fold affecting granodiorite, tonalite gneiss and amphibolite units. In particular, the synform appears to have tightened and steepened D3b (S type) map-scale folds in amphibolite west of Rude Lake, which lie in its southern limb. Folds of tonalite gneiss and tonalite in the northern package are close to tight in style, and are possibly parasitic to the Rude Lake fold, on its northern limb (this will be discussed subsequently in conjunction with a cross-section).

Open F4 mesoscale folds are often accompanied by prominent quartz - rodding lineations which develop in shallow plunging fold hinges within granitoid lithologies. Limbs of these folds are generally not apparent on the outcrop. Where observed, tight to close parasitic folds occur on limbs. Sillimanite layering (peak metamorphic during D3) in semipelite is crenulated by F4 folds, which have axial planar biotite cleavage (Fig. 4-9b). Within supracrustal packages, crenulation of S3 by F4 resulted in an L4 intersection lineation. L4 mineral lineations defined by plagioclase phenocrysts or porphyroblasts within supracrustal rocks is common. Figure 5-5 shows the trend of D4 linear fabric elements. L4 stretching and mineral lineations, as well as F4 minor fold hinges plunge shallowly to moderately east (28° toward 090°). It is evident from the reorientation of

ESE to ENE trends of lineations and folds axes (see map in back pocket) that L4 structures have been affected by ENE striking shear zones such as the Brightsand River shear zone.

Less common is the development of an S4 planar fabric (Fig. 5-5d,e). Within the central and northern panels, dykes of granite and granodiorite which cut D3 features carry an internal foliation striking parallel to F4 fold axes. In some locales, the trend of granodiorite dykes is axial planar to F4 folds (e.g. geochronology sample D).

Fold Interference Patterns

The superposition of D3 and D4 fabric elements upon S1 and F2 structures within the Rude Lake tonalite gneiss results in outcrop-scale dome and basin fold interference patterns (Fig. 2-12a), reflected in the map pattern by the ovoid shape of this unit. F4 folds affect the map pattern west of Rude Lake where tonalite gneiss (TgR), cores an F4 synform. Fold interference between F3b (Mountairy Lake fold) and F4 are reflected in the map pattern by the ovoid shape of the TgR unit.

D4a structures

Ductile shear zones transect the study area, including the regionally extensive Brightsand River and Wapikaimaski Lake shear zones and the newly discovered Robert Lake zone. Shear zones are late, sinistral zones of deformation. Possessing these common traits, it is likely that they are related. Regionally (outside of the central Wabigoon), these shear zones are similar in orientation, style and age to the Miniss River fault at the boundary between the English River, Winnipeg River, and Western Wabigoon subprovinces (Fig. 2-2a). Other regionally significant shear zones are dextral

transpressive subprovince-bounding faults such as the Quetico, Seine River, and Pashkokogan faults.

The Brightsand River and Wapikaimaski Lake sinistral shear zones (Fig. 5-6) are interpreted as late D4 ductile structures (Percival et al., 1999a). They are regional structures extending through the southeastern and northwestern portions of the study area. The trend of major map units and parallel S3 foliation, swing from generally E-W into the NE – SW trending shear zones.

The 3-10 km wide Brightsand River shear zone extends through the map area and approximately 20 km beyond to the ENE. It is an anastomosing, left-stepping zone (Percival et al., 1999a) characterized by L > S fabrics including subhorizontal quartz stretching mineral lineations trending 080°. Dextrally rotated porphyroclasts in annealed ultramylonite (Fig. 4-7, geochronology sample E) from the northern margin of the Brightsand River shear zone suggest an earlier phase of deformation, overprinted by late sinistral shearing. Shear zones also affect the hinges and trends of map-scale folds (e.g. the Rude Lake synform) which are reoriented by the BRSZ from ESE to ENE.

The Wapikaimaski Lake shear zone is characterized by gneisses and local mylonite. It is a more discrete feature than the Brightsand River zone, less than 1 km in width for most of its strike length. Mylonitic rocks occur along the southern margin of the shear zone. It extends west of the study area for less than 10 km and to the northeast approximately 15 km. Both shear zones contain syn-tectonic granites with ENE-trending sub-horizontal lineations. They lack S3 foliation, and carry only a weak planar fabric with respect to the prominent stretching lineation.

The Robert Lake zone

The Robert Lake zone trends ESE and links the Brightsand River and Wapikaimaski Lake shear zones. It is characterized by strong planar fabrics with moderate to weak lineations defined by quartz and feldspar. The mode of mineral lineations within granitoid rock types trends 074°, plunging 47 degrees ENE (Fig. 5-7). which is slightly oblique to and generally steeper than L4 regionally (28° toward 090°). It defines the northern margin of the Robert Lake amphibolite, and varies in character along strike and within different units. On Robert Lake, it is characterized by a 500-m-wide straight zone of medium-grained gneissic tonalite whose low strain equivalent north of the straight zone is a coarse-grained hornblende tonalite, with local heterogeneous layering. North of the straight zone, mafic dykes cut tonalite at a high angle, striking roughly ENE with 30 - 40° dips to the north. Within the straight zone, mafic dykes have been transposed into parallelism (see Fig. 2-14a,b). Rotation of cross-cutting dykes by movement on the Robert Lake zone would be consistent with dextral kinematic sense.

The southern margin of the straight zone occurs along the Robert Lake amphibolite and is marked by extensive epidotization of mafic rocks (Fig. 2-13d), with boudinaged hornblenditic layers giving shear sense indicators (Fig. 5-7). Macroscopic folds and (normally) rotated mafic boudins show dextral kinematics. However, back - rotated boudins indicate sinistral sense of shear on the horizontal erosion surface where the foliation dips steeply north, and lineations plunge moderately with trends of 075°.

A pegmatitic granite dyke near Harmon Lake just north of the straight zone cuts mafic and plutonic gneissic units (Fig. 5-8c). Foliation (266/60) within the dyke is defined by alignment of biotite grains parallel to the foliation in country rock gneiss.

Shear planes (striking at ~055°; dipping steeply) cut the foliation which wraps into C planes locally. Weakly defined mineral lineations developed on the foliation plane plunge 32° toward 070°. Sinistral transcurrent shearing is implied by kinematic observations on the horizontal surface.

Near Harmon Lake, the Robert Lake amphibolite is in fault contact with granitoid rocks to the north, as indicated by extensive epidote alteration, local breccias and chaotic folds (Fig. 2-13). The straight zone which occurs along strike within gneisses at Robert Lake has not been traced to this point, as a result of poor exposure in this area.

The Robert Lake zone appears to merge with the Brightsand River and Wapikaimaski Lake shear zones, in a geometry congruous with sinistral transcurrent movement. Differences between the Robert Lake straight zone and the more regional shear zones include a dip slip component of shear in addition to transcurrent, dominant S>L tectonites, the absence of mylonites, and some variation in deformation style along strike. Stretching lineations plunge more steeply in this zone suggesting a dip slip shear component, yet the trend of the lineations parallels those within the master structures (BRSZ and WLSZ). The inconsistent shear sense indicators within the Robert Lake zone suggest a complex movement history, similar to that preserved within the Brightsand River shear zone, where earlier dextral transcurrent motion was overprinted by sinistral shear (Percival et al. 1999a). As such, the Robert Lake zone is interpreted as a zone of late D4 deformation genetically related to the BRSZ and WLSZ. Geometrically, the Hilltop Creek fault and Robert Lake straight zone divide the study area into sigmoidal z - shaped panels between the Wapikaimaski Lake and Brightsand River shear zones.

Disregarding temporal differences, this would be consistent with an overall sinistral sense of transcurrent movement along the master structures.

The Miniss River fault defines the boundary between the Winnipeg River and Wabigoon subprovinces and has been the topic of detailed structural and geochronological study. The fault is interpreted as a late Kenoran structure cutting across subprovince boundaries (Corfu et al., 1995) and appears to have accommodated approximately 30 km of sinistral oblique displacement. The age of a granite dyke cross-cutting the mylonitic fault fabric and offset by oblique sinistral shear bands constrains the main period of faulting as pre - 2681 Ma (Bethune et al., 2000). This age is similar to those of late syn - tectonic granites dating the ductile sinistral transcurrent Brightsand River and Wapikaimaski Lake shear zones in the central Wabigoon (2685, 2680 Ma; Percival et al., 1999a). The significance of the Robert Lake zone (and the BRSZ and WLSZ) of similar age and kinematics to the Miniss River fault, is examined subsequently (Chapter 7). The Robert Lake zone may coincide with the location of an earlier fault, reactivated late in D4 and masking previous deformation.

Conclusions pertaining to D4

D4 was a pervasive ductile event, resulting most commonly in the development of tight, east-trending, upright folds that dominate the map pattern. A penetrative S4 foliation is rare in granodiorite and granite. D4 can be related to a broadly N - S directed shortening event that was followed by sinistral shearing in discrete zones.

Absolute age constrains on deformation chronology

Absolute age constraints arise from TIMS (thermal ionization mass spectrometry) U/Pb geochronology on zircon and titanite (Chapter 4). Regionally, D1 marks the

earliest onset of ductile deformation in plutonic rocks of the central Wabigoon. Geochronology of S1 foliated tonalite gneiss (TgR) provides a maximum age for D1 of 2718 +/- 7 Ma (sample B, Chapter 4). On Harmon Lake, a 2715 Ma, S3-foliated tonalite dyke (Percival et al. 1999b) cross-cuts F2 folds of S1 gneissosity providing an upper limit on D2. 2697 Ma granodiorite cuts S3 providing a lower limit for D3 and an upper limit for D4 deformation (Sample D, Chapter 4). Quartz diorite dated at ~2690 Ma (Davis 1989) was strongly affected by deformation associated with the BRSZ event. L > S syn-tectonic granite associated with D4a shear zones have been dated at 2685 Ma and 2680 Ma (Percival et al., 1999b), providing a lower bracket for F4 folding and L4 lineation development. Titanite from annealed ultramylonite along the Brightsand River shear zone provides a lower limit of 2678 Ma (Sample E, Chapter 4) for late (D4) shearing.

LITHOPROBE Seismic Line 1D

The area was imaged as part of the 1997 phase of Western Superior LITHOPROBE seismic data acquisition. The profiles were acquired to test the accretionary model at a very regional scale. Locally, the data for the Brightsand Forest area has been used to correlate features mapped on the ground to imaged subsurface structures. Seismic records extend to 16s two - way travel time (ca. 48 km depth). However, as interpretations presented herein are for the shallow subsurface, only the upper four seconds (ca. 12 km) of migrated data for the northern end of line 1D are illustrated in Figure 5-8. This attempt at subsurface interpretation is made possible because of anomalous shallow reflectivity for this part of the profile. Seismic station

locations can be found on Figure 5-9. Figure 5-10 is a N - S cross-section beneath the study area along the Hilltop Lake logging road.

The upper 1 second of the profile (N of the BRSZ) is not reflective, which is consistent with 50° to >70° dips of lithological units at the surface. At greater depth, broad antiformal structures are apparent, and form discrete reflective packages with shallow north and south apparent dips. Discontinuities between these shallow dipping packages of reflectors have steeply north-dipping trajectories which seem to correspond to surface structures (the Hilltop Creek fault, the Robert Lake zone, and possibly the Brightsand River shear zone) with similar dips. Other (for example steeply S dipping) truncation trajectories are possible, but these would not project to known structures at the surface. At depths beneath the illustrated profile, reflectors are subhorizontal and continuous (Brown et al, 1999).

At the southern end of the profile, the truncation trajectories illustrated (zone A) correspond to the Brightsand River shear zone as a moderately north-dipping, bifurcating zone. Steeper (> 70°) northerly dips are possible, though discontinuous (B). To the north, several parallel, steeply north-dipping trajectories are evident (C, D, E, F), some of which correspond to surface structures. Truncation C separates two groups of reflectors with shallowly opposing dips, and projects to the surface near the Hilltop Creek fault, which is a steeply (>70°) north dipping structure where crossed by the seismic line. Truncation D does not project to an observed shear zone or fault at the surface, but corresponds to the southern contact of the Rude Lake tonalite gneiss (TgR), where quartz - rich sedimentary rocks (Sq, geochronology sample C) related to the Rude Lake package are located. Truncation E projects to the steeply north-dipping Robert Lake straight zone.

Truncations that define zone F correspond to surface expressions of mylonite zones of the Wapikaimaski Lake shear zone and separate the map area from relatively non-reflective crust to the north.

Steep dips prevent direct association of seismic features to lithological units. Therefore, only fault and shear zone orientations are constrained by the discontinuities imaged in the subsurface. The sense of displacement along faults cannot be determined on the basis of seismic data alone in the absence of obvious dip-slip deflections into faults, or offsets of seismic marker horizons. The subsurface geometry of the map area as constrained by seismic data alone, is that of a series of fault-bounded, north-dipping panels. Without taking into account metamorphic grade or lithological variations across panels, transcurrent, thrust, or normal displacements are possible.

Cross – section

Figure 5-10 is a cross-section incorporating the regional and local geochronology and seismic constraints. The Hilltop Creek and Robert Lake faults are steeply north-dipping features that may continue to depths of ca. 10 km. The section was constructed from different profile lines within each panel to show variations in structural style between map units and between panels (Fig. 5-9). Profile lines are perpendicular to strikes of lithological units, S3, and F4 fold axes. North-trending, steeply plunging F3b folds such as the Mountairy Lake fold are not represented in the projection.

The Brightsand River shear zone is dominated by subhorizontal ENE - trending stretching lineations (L4a). A northerly dip for this zone is based solely on the seismic image. Map units of the southern panel strike ESE.

Most units within the central panel also trend ESE, although a change in orientation toward ENE occurs with proximity to the BRSZ. This panel is dominated by the presence of the ESE trending F4 fold centered on the Rude Lake tonalite gneiss. The Rude Lake amphibolite is fault bounded to the south. Its relationship the the Rude Lake tonalite gneiss to the north is obscured by granite intrusions. This may be a basement - cover type relationship, based on geochronological constraints, or could be a fault as indicated by the seismic profile. The structure and geometry of the Rude Lake amphibolite and tonalite gneiss is largely the effect of a recumbent F3 fold, intermediate thickening of amphibolite units by F3a folding (steep north plunging folds with N - S striking axial planes not shown on the cross-section), overprinted by F4 folds. Recumbent (F3, possibly F2) folding, and subsequent F3a folding, of the tonalite gneiss unit is inferred from geometry of meso-scale refolded folds and doughnut-shaped fold interference patterns (Fig. 2-12). A close to flat-lying map-scale axial plane for the recumbent fold, with an EW - trending fold axis, is depicted in the cross-section as having been refolded about an upright F4 axial plane (also with an EW - trending hinge line).

The Robert Lake straight zone cuts through portions of the Robert Lake amphibolite and gneissic tonalite on its northern side. The presence of map scale F4 folds is interpreted based on flips in S3 dip direction (as well as opposing dips on reflectors in the shallow subsurface along the seismic profile north of the straight zone). Table 5-1 summarizes the deformation and intrusion chronology.

DISCUSSION

Nature of D1

Tonalitic gneisses preserve S1 gneissosity and F2 folds in the central Wabigoon region. The origin of this fabric is attributed to metamorphic segregation, implying an event which occurred some time between 2718 +/- 7 Ma (actual upper limit of 2725 in light of the large error) and 2715 Ma, the age of cross – cutting S3 foliated tonalite. Events during this time window have not been recognized widely in the western Wabigoon, although early deformation that predates regional ductile deformation has been recognized in the Sturgeon – Savant belt (Sanborn – Barrie and Skulski, 1999). Also in the western Wabigoon region, early deformation has been documented by Edwards and Stauffer (1999) in the Pipestone Lake area and bracketed between 2727 (Phinney – Dash Lakes rhyodacite; Davis and Edwards 1982) and 2712 Ma (Schistose Lake sedimentary and volcanic rocks). The inferred unconformity between these packages also separates an early D1 event from D2, which affects both assemblages. Possibly indicative of an accompanying thermal event around this time are ca. 2726 metamorphic zircons from the Marchington granite (igneous age of 2735 Ma, Bethune et al., 2000) in the footwall of the Miniss River fault.

Detrital zircon studies of sedimentary rocks in the western Wabigoon reveal the presence of Mesoarchean grains in Neoarchean sedimentary rocks deposited after 2716 Ma. Within the ca. 2716 Ma Warclub Group sediments south of the Winnipeg River – Wabigoon subprovince boundary, > 3 Ga old zircons indicate proximal continental material (Davis,1996). Similarly, > 3 Ga zircons are present within the ca. 2720 Ma Quest Lake sediments (Skulski, Sanborn-Barrie and Stern, unpublished; and >2.844 Ga

grains are present in the < 2701 Ma Rude Lake quartz-rich sandstone in the central Wabigoon, this study). Other evidence for older components in 'younger' rock units in the western Wabigoon derive from the Snowshoe Bay batholith in the Lake of the Woods area. The batholith has an igneous age of 2708 Ma, yet shows evidence of contamination, in the form of 2802 Ma xenocrystic grains (Davis and Smith, 1991) thought to be inherited from underlying Winnipeg River- type crust. Similarly, the Mesoarchean detritus in the Warclub Group was most likely derived from rocks of the Winnipeg River subprovince (Davis, 1990 and Davis, 1996).

Several pieces of evidence suggest that the Winnipeg River and north - central Wabigoon were a single terrane prior to accretion of the western Wabigoon. These include similar styles and ages of structural evolution along the boundary, as reported in several studies (for example: Cruden et al., 1998; Sanborn-Barrie and Skulski 1999; Brown et al., 2000; Melnyk et al., 2000). Furthermore, it appears that the western Wabigoon was sutured to the central Wabigoon prior to the onset of the earliest ductile deformation (D1) in greenstone belts. This is implied by structural evidence combined with detailed geochronology, on both sides of the interface. This event occurred between 2718 +/- 7 Ma and 2715 Ma, as recorded in pervasively affected gneissic rocks of the central Wabigoon, and early folding in the Pipestone Lake area of the western Wabigoon, which is bracketed within a similar time window (2727 – 2712 Ma). The presence of >3 Ga (Winnipeg River/central Wabigoon) detritus in ca. 2720 Quest Lake sediments and < 2716 Ma Warclub Group sedimentary rocks in different locations along the boundary also supports the interpretation that the two terranes were juxtaposed by the onset of D1 in the Sturgeon – Savant belt (D3 in the central Wabigoon).

This interpretation contrasts with that involving suturing of the western to the central Wabigoon at ca. 2700 Ma. In that model, the suture is marked by < 2704 Ma turbiditic sedimentary rocks (Savant Sedimentary group) which were deposited in a foredeep setting. In the Sturgeon-Savant greenstone belt, the sediments cover the suture between continental basalts of the Jutten group to the east and oceanic type volcanic rocks to the west (Sanborn-Barrie and Skulski, 1999). If the western and central Wabigoon regions were indeed together by ca. 2700 Ma (having collided by 2715 Ma at the latest), then the widespread presence of ca. 2700 Ma sedimentary rocks (the Savant Sedimentary group, Princess-Post Lake sediments, Rude Lake sediments, Awkward Lake sediments) remains to be explained. Their presence does, however, provide an upper limit for D3 deformation, as explained below.

Nature of D2

D2 deformation is constrained by the same factors and time frame as is D1. In order to explain fold interference structures, a second ductile event, D2 must have occurred at a high angle to D1 in order to explain fold geometries in gneisses on Harmon Lake and west of Rude Lake. In the absence of geochronological constraints, the tectonic significance of the D2 event is uncertain, although it may reflect the convergence direction of a later collisional stage, from N directed during D1 to eastward for D2.

Nature of D3

D3 deformation was common to both the western and central Wabigoon subprovinces. Deposition and consolidation of ca. 2700 Ma sedimentary units must have occurred prior to D3, as all supracrustal units carry a strong S3 foliation. An upper limit for S3 development is provided by the cross-cutting granodiorite dated at 2697 Ma. In

the present map area, a lower limit for sediment deposition of 2701 Ma comes from the youngest zircon analyzed in the quartz-rich sandstone (Sq, geochronology sample C). Peak metamorphic conditions attained in the area are coincident with the development of S3 (see details in Chapter 6). Therefore, between 2701 and 2697 Ma, sediment deposition and burial to depths consistent with sillimanite - grade metamorphism must have occurred.

Style differences between S1 in greenstone belts and correlative S3 in granitoid rocks are apparent. S1 foliations are steep in greenstone belts and S3 was shallow throughout much of the granitoid domain prior to steepening during D4. Original subhorizontal S3 orientations are preserved in northwestern Seseganaga Lake in a D4 strain shadow (Percival et al., 1999a,b). Instead of attributing S3 development to the collision between the west and central Wabigoon, which is ruled out if collision occurred prior to 2715 Ma, S3 may be related to dextral transpression most prominently developed along subprovince boundaries. The timing is similar to that documented by Stott et al. (2002) for the northern margin of the eastern Wabigoon subprovince, where transpression occurred prior to 2698 Ma, the age of the cross-cutting Sheff pluton, during the late stages of the Kenoran orogeny.

Late D3 folding (D3b) appears to be a local phenomenon. The F3b Mountairy Lake fold, and parasitic Rude Lake structures helped to create a thickened volcanic package (Rude Lake package) that resisted overprinting during D4. While being parasitic F3b type folds in plan view, this package of rocks resides in the southern limb of an F4 synform.

Nature of D4

In general, N-S oriented compression created upright, gently east – plunging folds. The age of deformation is constrained by the 2697 Ma granodiorite dykes that cut S3 layering at a high angle. The dykes were subsequently deformed, and, in addition to being oriented axial planar to the trend of regional F4 fold axes, also carry a weak S4 foliation.

At map scale (Fig 5-9), the Brightsand amphibolite shows E-trending folds that are dismembered by tonalite and granodiorite. On the basis of regional age relationships, it is likely that these folds represent a pre-D4 episode of map-scale fold generation.

Late sinistral shearing is regionally significant, and is similar in timing and style to that along the Miniss River fault at the juncture between the Winnipeg River and Wabigoon subprovinces. Sinistral mylonitization along the Miniss River fault occurred mainly prior to 2681 Ma (Bethune et al., 2000), and similar ages (2680 and 2685 Ma) were obtained for syn-tectonic granite within the Brightsand River shear zone (Percival et al., 1999a,b). 2678 Ma titanite marks late crystallization subsequent to ductile shearing. Regional cooling began shortly thereafter, as indicated by titanite cooling ages (ca. 550°C closure temperature) between 2685 and 2670 Ma (Percival et al., 1999b).

SUMMARY

1) All four phases of deformation recorded in gnessic tonalites in the map area are Neoarchean in age.
2) D1 and D2 occurred between 2718 +/- 7 Ma and 2715 Ma.
3) Collision between the Neoarchean greenstone - dominated western Wabigoon terrane and the granitoid Winnipeg River - Central Wabigoon is indicated by D1 deformation before 2715 Ma. This contrasts with models for ca. 2.7 Ga collision.
4) S3 is the main pervasive foliation affecting all major units. It is constrained by S3 foliated sediments (< 2701 Ma) and cross-cutting granodiorite > 2697 Ma.
5) Two unique D3 structures occur in the present area: the D3a HCF and D3b Mountairy Lake fold. The N - S trending F3b fold created a D4 strain shadow in the Rude Lake area, by thickening of competent amphibolite units. This stage of D3 indicates E - W directed compression.
6) North-south shortening produced upright F4 folds which post date 2697 Ma.
7) Fold interference between (F2 or F3) recumbent folds, steeply plunging F3b folds and F4 folds imposed on D1 (and possibly D2) structures within the Rude Lake tonalite gneiss produced fold interference structures, including dome and basin geometries. This is reflected by the map pattern in the southwestern portion of the map area.
8) Steep, WSW-ENE trending, late D4 shear zones overprint F4 folds. However, the timing is only loosely constrained between 2697 and 2685 Ma, the age of a syn - tectonic granodiorite dyke. The latest movement along ductile shear zones occurred prior to 2678 Ma.

Figure 5-1: S1 foliated tonalite gneiss (A). B-C: Lower hemisphere equal area stereographic projections of poles to planes of early fabrics including S1 layering and F2 axial planes. Poles to D1/D2 fabrics from areas which were not as strongly overprinted by later events form small circle with a steep fold axis (to F2 folds). Axial planes strike roughly E-W and are now close to vertical in orientation (Figure 5-2-AII). Early fold axes (F2) had steep to vertical plunges, where measurement was possible. Most early fabrics were transposed somewhat during D3.

A: S1 and S2

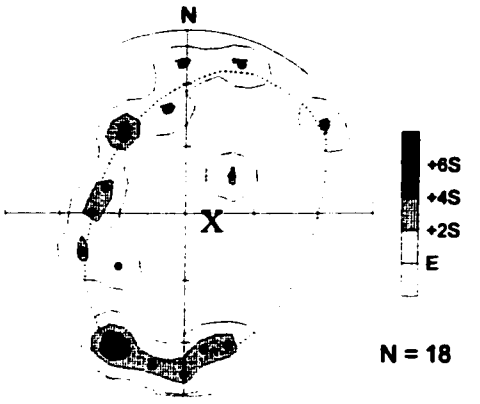

B: Transposition foliations (of S1 and S2 by S3)

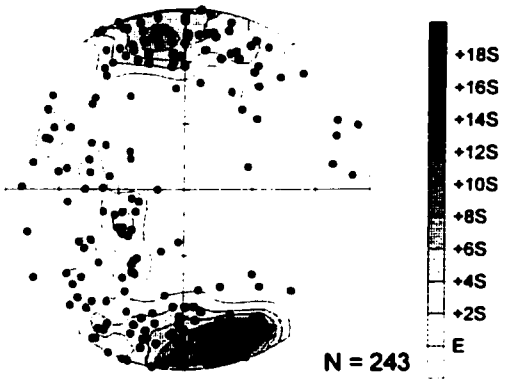

C: F2 axial planes

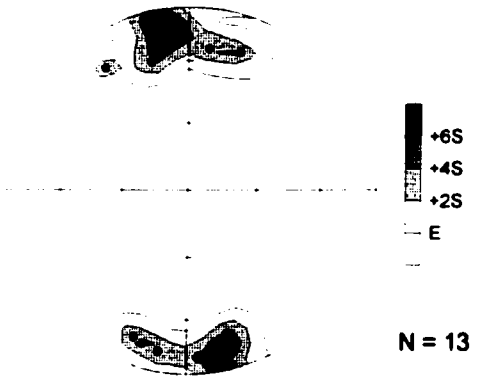

Figure 5-2: S1 foliated tonalitic rocks (TgR and Th). A: D1 and D2 fabrics overprinted by S3 and F4 in biotite tonalite gneiss. B: D1 and D2 fabrics overprinted by S3 and F4 in hornblende tonalite.

A: TgR

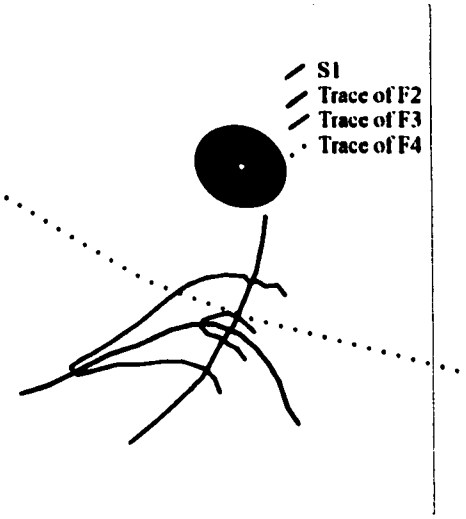

B: Th

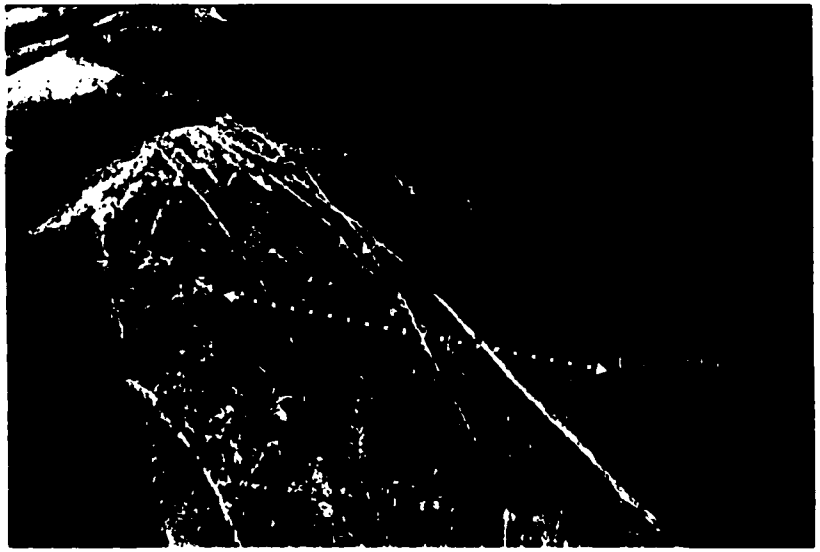

Figure 5-3: Lower hemisphere equal area projections of D3 structures. A: Poles to S3 foliation data for the entire map area, shows that foliations trend roughly east-west, and are steeply north or south plunging. B: L3 mineral lineations from the entire map area, showing that lineations trend predominantly to the east (reoriented by F4 folding, see Fig. 5-5). A granodiorite dyke is shown cutting S3 in metasedimentary rocks. This dyke carries a weak S3 'ghost' foliation.
C, D, and E refer to data west of Rude Lake (within the area shown in the sketch map on Fig. 5-4). C: Poles to S3 foliation data west of Rude Lake only. D: S3 foliation west of Rude Lake showing poles to planes as well as planes (great circles). E: L3 data west of Rude Lake. Note the difference in orientation with respect to B. This area may be part of a D4 strain shadow.

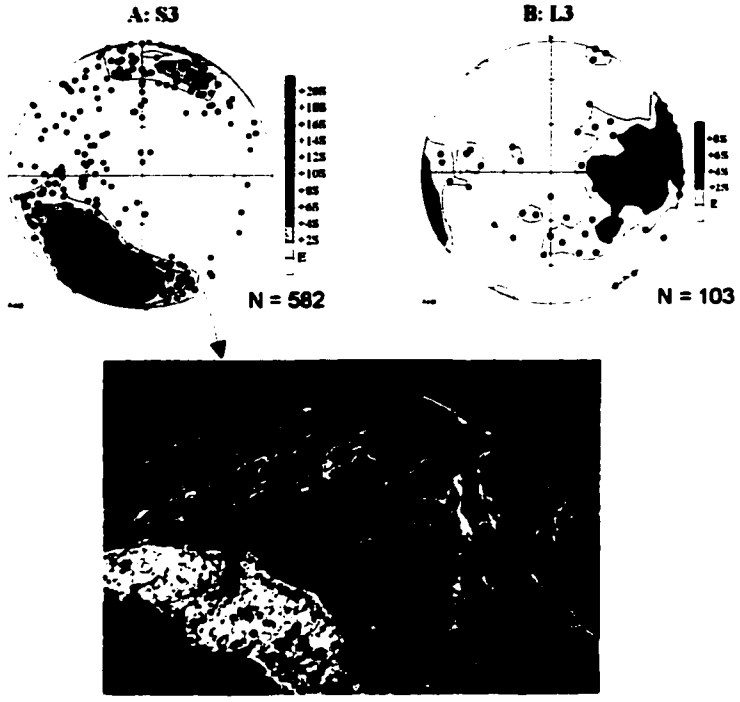

Late D3 Structures (west of Rude Lake)

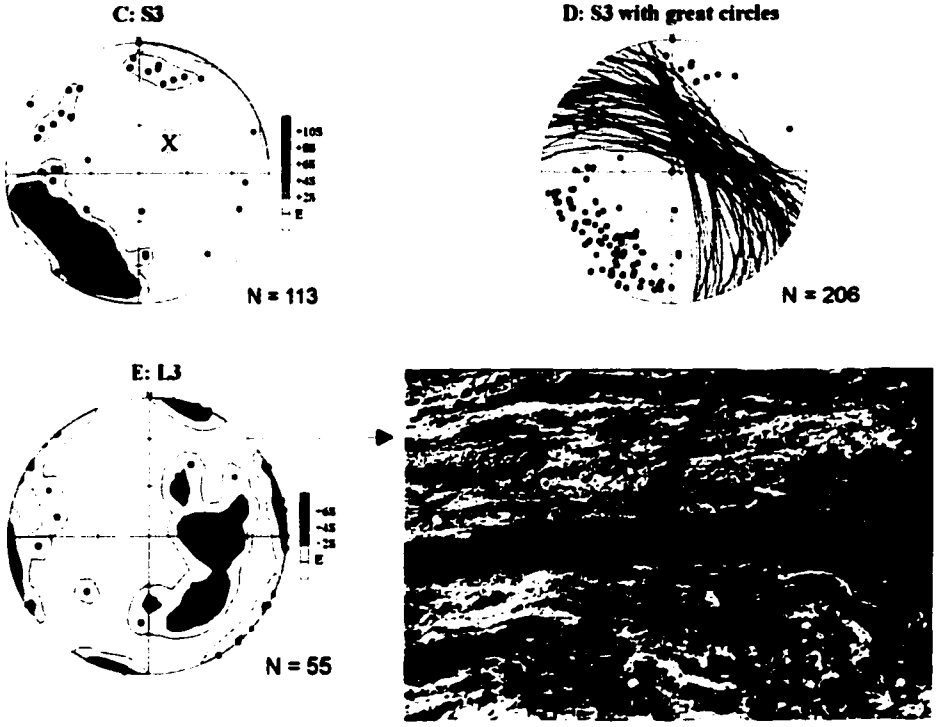

Figure 5-4: A: Sketch map of the area west of Rude Lake. B: Form surface map of the same area. Contacts are in black. Green lines show the trajectory of unusual lineations in this area, thought to be preserved L3 mineral lineations. Blue lines show the trajectory of mineral lineations related to L4, which carry the regional trend of D4 structures (fold axes and mineral lineations). The lineations which define the trend of the green lines may preserve L3 lineations because they are located within a D4 strain shadow. Red arrows are lineations imported from the geology map (GSC Open File #4286, included with the thesis).

A) Sketch map of major structural features (SW portion of the map area)

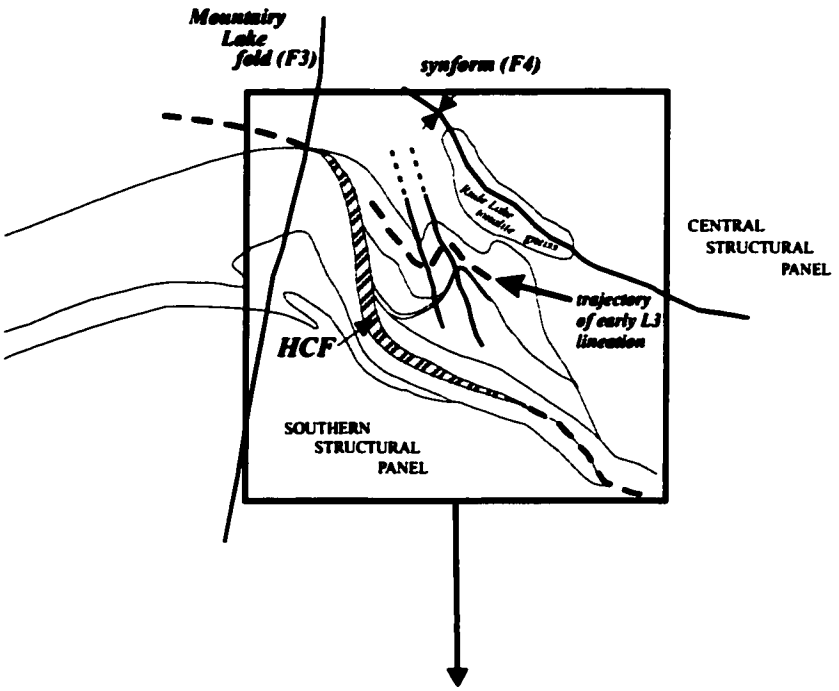

B) Form Surface Map

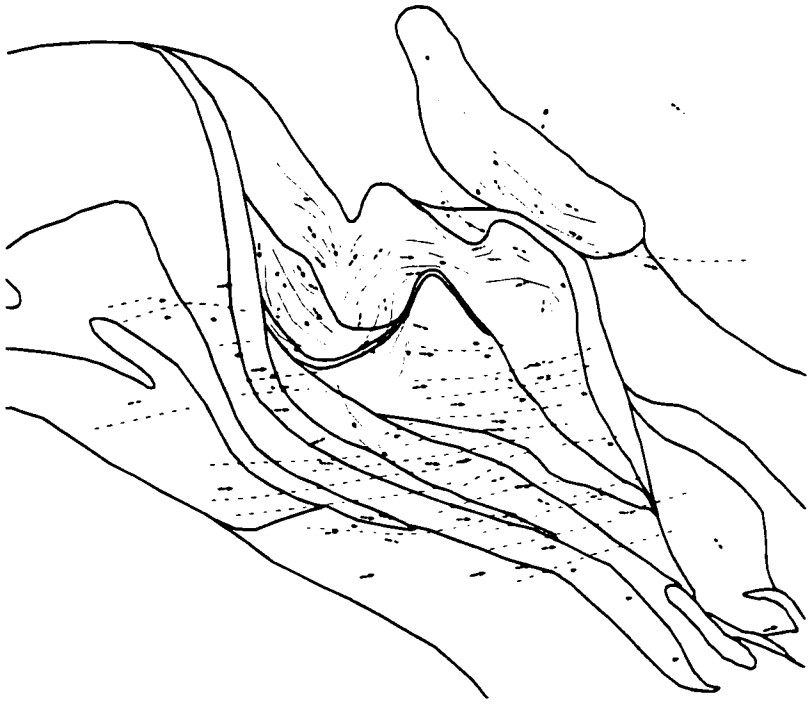

Figure 5-5: Lower hemisphere equal area stereographic projections of D4 planar and linear structures. A: L4 mineral lineations. B: Quartz rodding in the hinges of F4 folds. C: F4 fold axes. D: S4 foliation in granodiorite and granite dykes and sills which cut S3. E: Macroscopic shear planes which cut S3 are steeply dipping, east-west trending structures.

A: L4

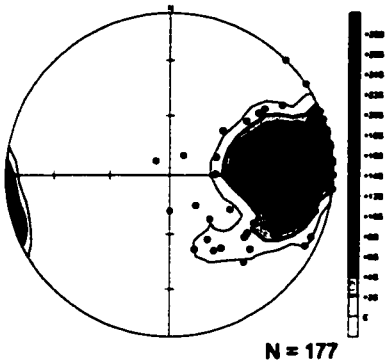

N = 177

C: F4 fold axes

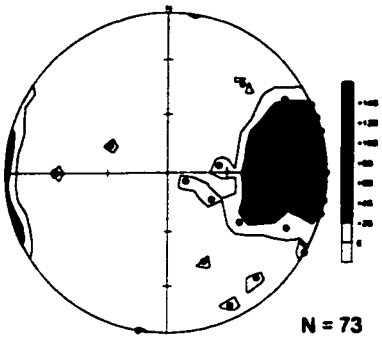

N = 73

B: quartz rodding

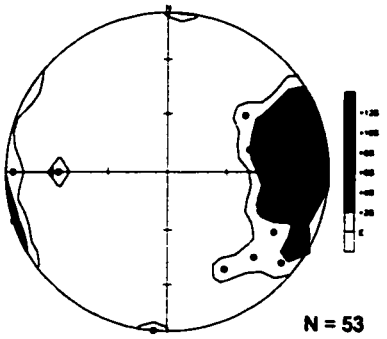

N = 53

D: S4

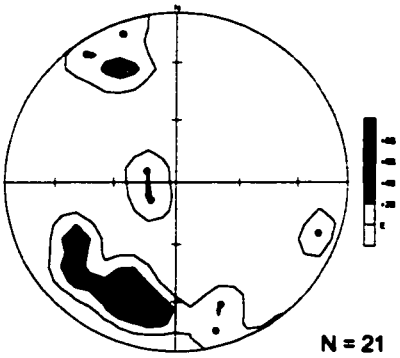

N = 21

E: Shear planes

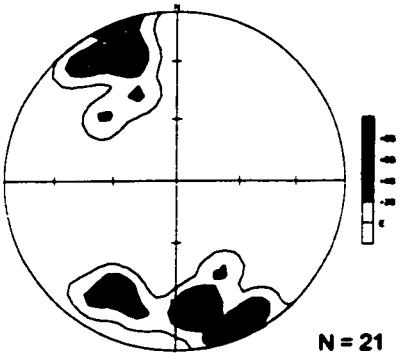

N = 21

Figure 5-6: The Brightsand River (A-C) and Wapikaimaski Lake (D,E) shear zones. All photos area taken on the horizontal erosion surface; fabrics depicted are all steeply dipping. A: Horizontal surface within the Brightsand River shear zone. High strain fabric is a steeply dipping, near vertical foliation striking WSW-ENE. B: Sheared and folded pegmatite, with sinsitral shear bands and sinistrally folded offshoot. C: Foliation in highly strained tonalite, with dismembered granodioritic fold hinges. D: Feldspar porphyroclastic mylonite in the Wapikaimaski Lake shear zone. E: Mylonitic tonalite gneiss.

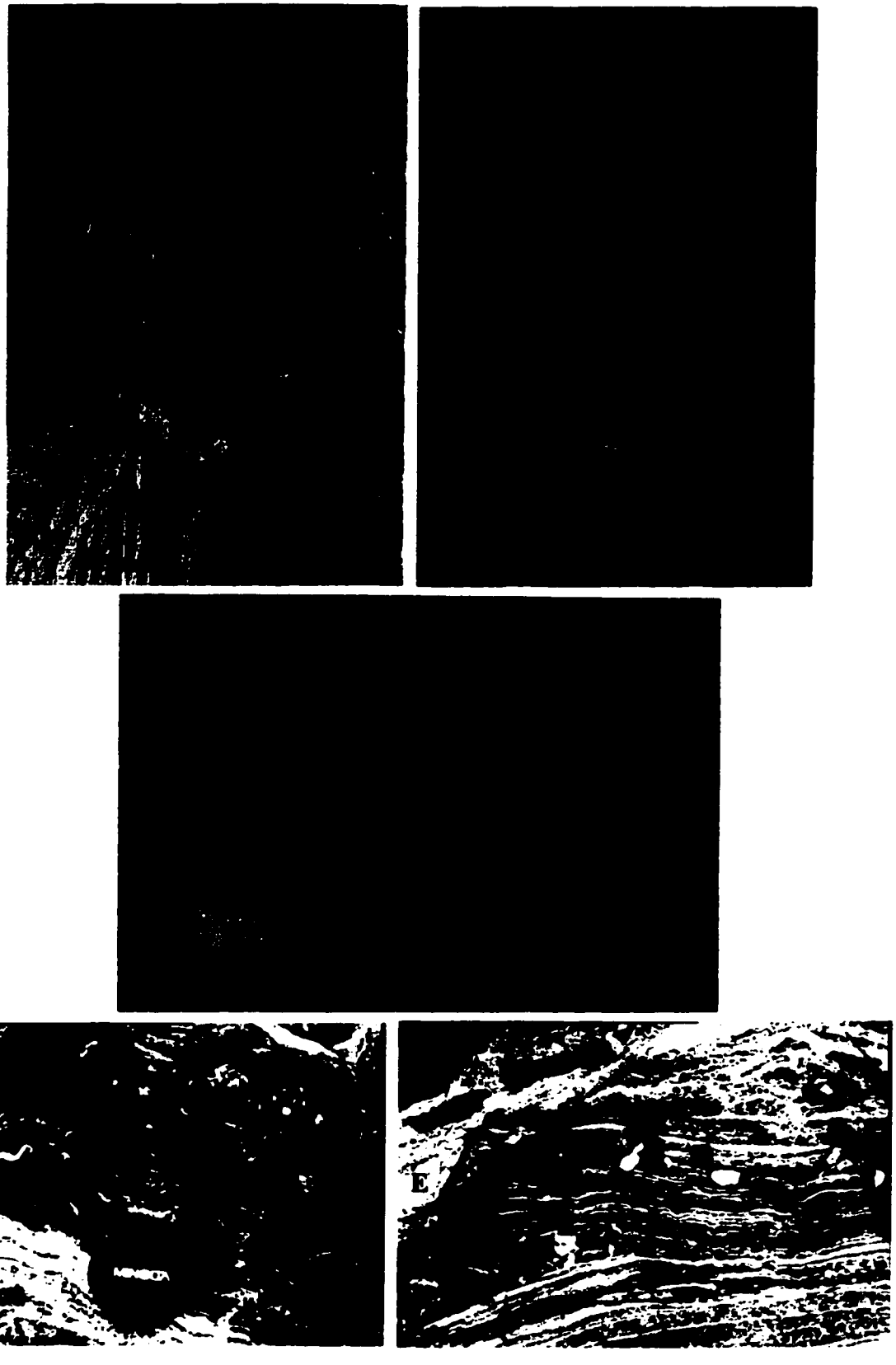
D
E

Figure 5-7: The Robert Lake straight zone. Stereographic projection of lineations within the straight zone on Robert Lake (see Fig. 2-14B). Photographs A to C depict fabrics along the southern margin of the 'straight zone'. A: dextral asymmetric fold. B: Back-rotated amphibolite boudin. C: C-S fabrics in granite.

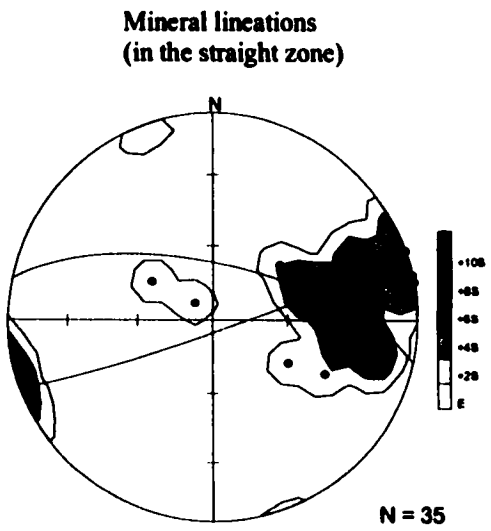
Mineral lineations
(in the straight zone)
N
N = 35


B

Figure 5-8: Seismic section along Lithoprobe line 1d showing migrated data (courtesy of D. White, G.S.C.). The dashed box on the seismic section shows the area below the Study area which corresponds to the cross-section in Figure 5-10. HCF and RLF are the Hilltop Creek fault and Robert Lake fault (straight zone) respectively.

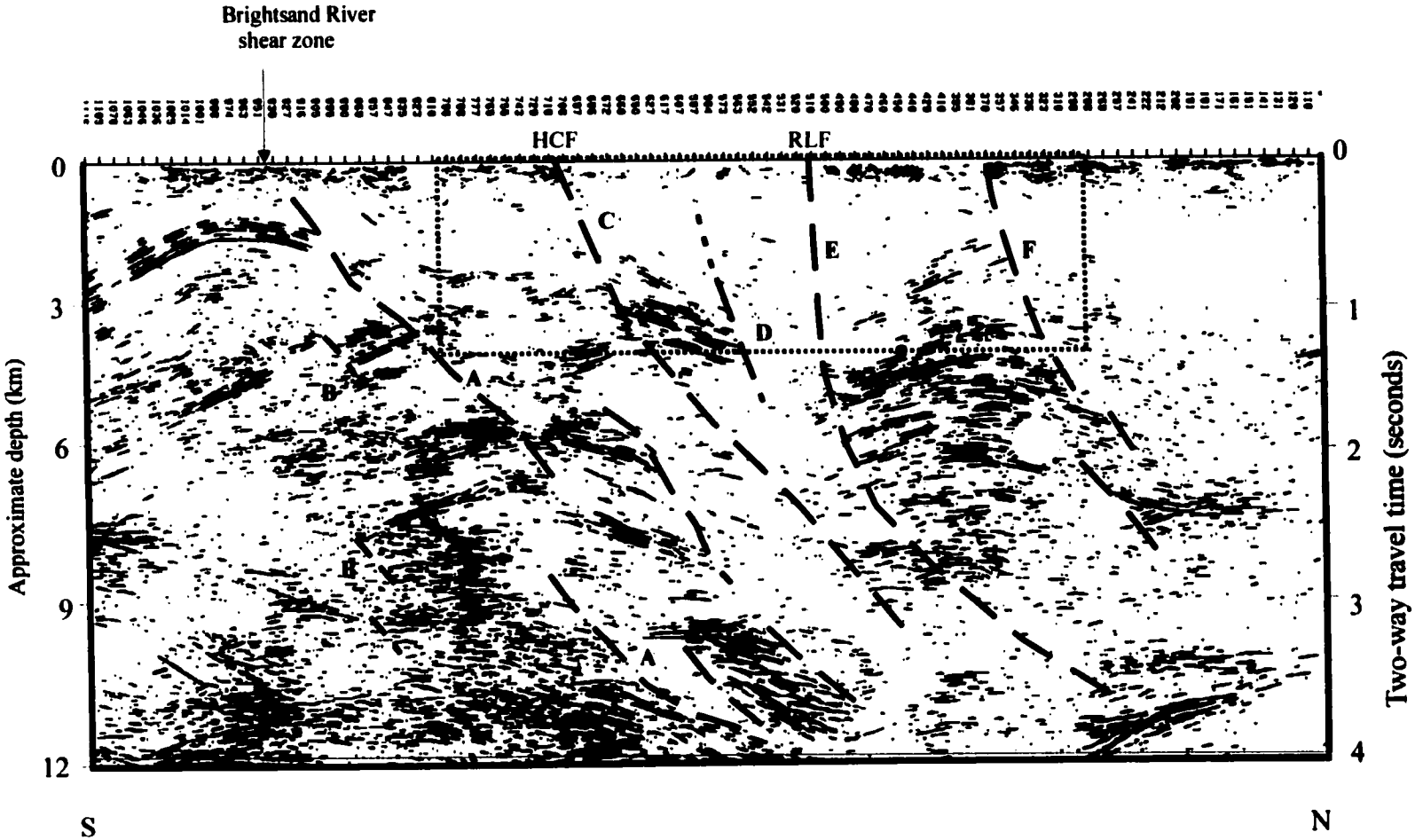
Brightsand River
shear zone
HCF
RLF
C
E
F
D
A
B
A
0
3
6
9
12
Approximate depth (km)
0
1
2
3
4
Two-way travel time (seconds)
S
N

Figure 5-9: Location map for seismic profile, with seismic station locations. Also shown are the profile lines for Figure 5-10. Line AB follows the portion of the profile in Figure 5-10 from the S to the HCF (the southern panel). Line CD extends from the HCF to the RLZ (the central panel). Line EF extends north from the HCF into the northern panel.

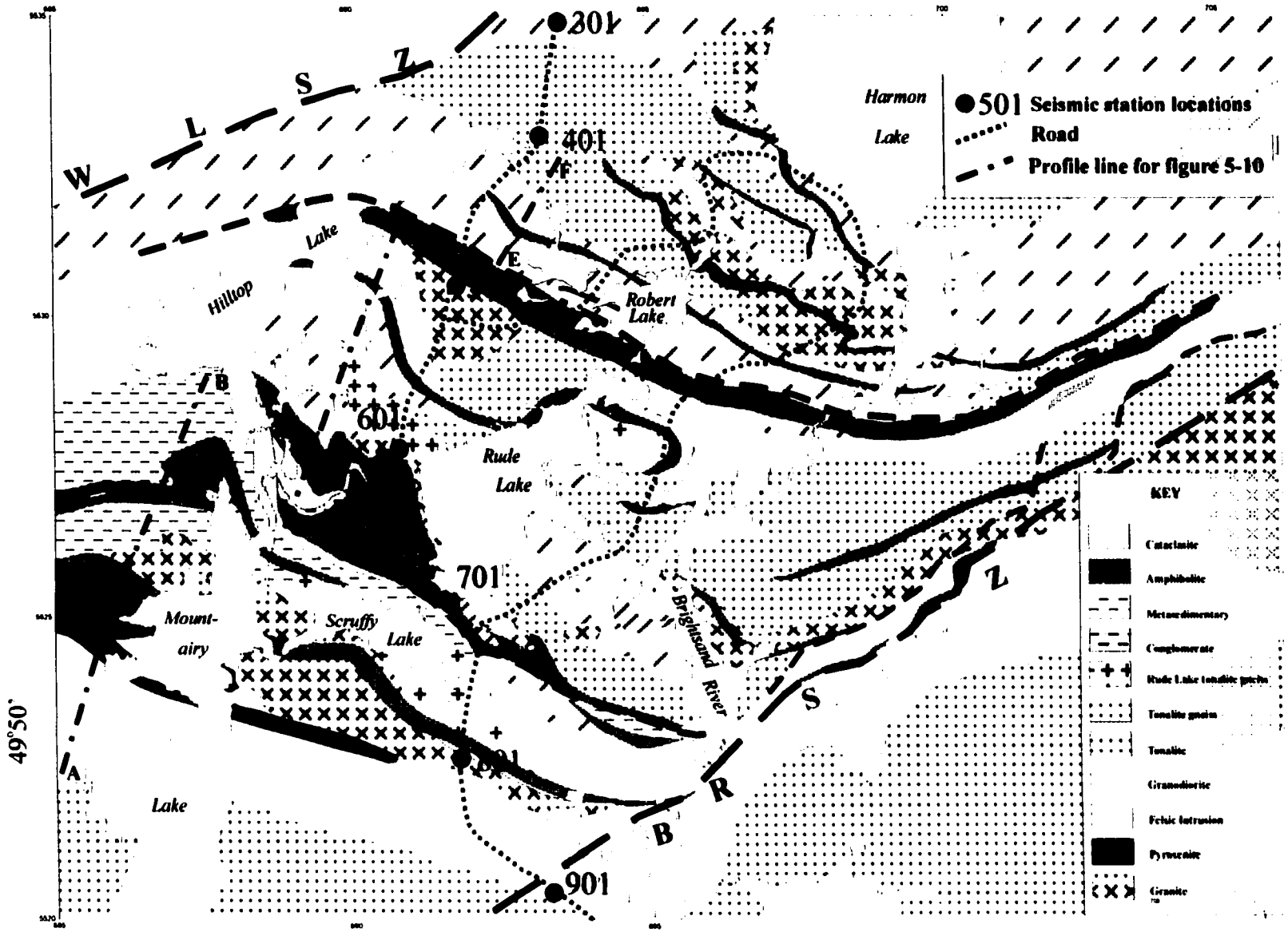
301
401
501 Seismic station locations
Road
Profile line for figure 5-10
Harmon Lake
Hilltop Lake
Robert Lake
Rude Lake
601
701
Mount-airy
Scruffy Lake
Brighsand River
Lake
901
KEY
Cataclasite
Amphibolite
Metasedimentary
Conglomerate
Rude Lake tonalitic gneiss
Tonalite gneiss
Tonalite
Granodiorite
Felsic intrusion
Pyroxenite
Granite
49°50'
90°20'

Figure 5-10: Composite cross-section of the Brightsand Forest area. Profile lines are given in Figure 5-9.

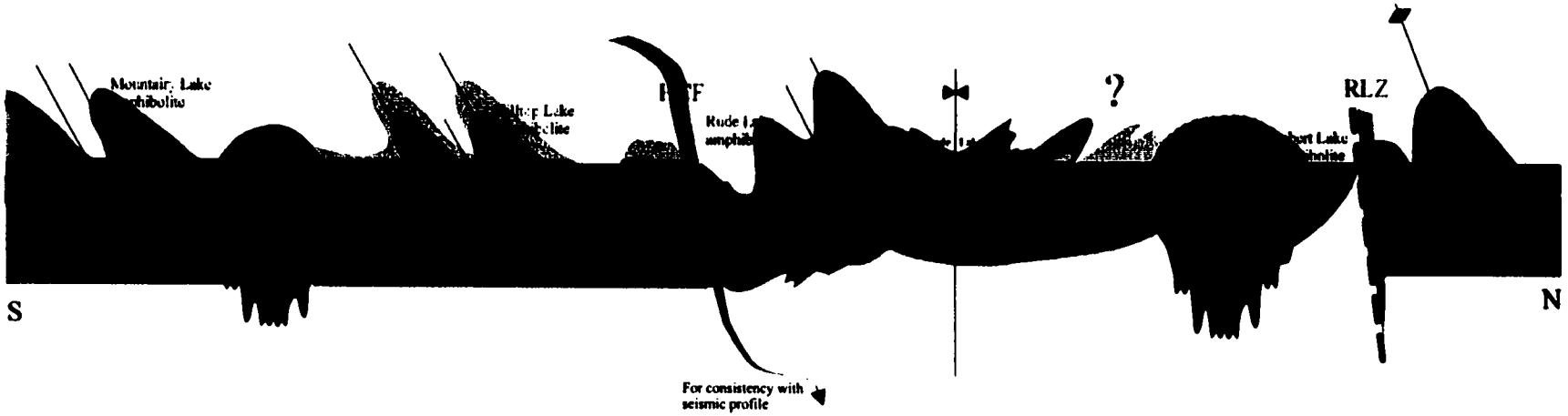

0 km 6

F4 Antiform

F4 synform

Possible F4

Cataclasite

Southern panel amphibolite

Metasedimentary

Gabbro

Central panel amphibolite

Mafic dyke

Rude Lake tonalite gneiss

Tonalite gneiss

Hornblende tonalite

Biotite tonalite

Felsic sill

Granodiorite

Granite

Table 5-1: Summary of deformation and intrusion chronology

Deformation Event	Litholigical unit/ main fabric	Age	Comment
	Tonalite gneiss (and Th?)	2774 Ma 2880 Ma	Davis, 1989
	Volcanic rocks?	~2740 – 2720 Ma?	
	Tonalite Tonalite gneiss (TgR)	2722 Ma 2718 +/- 7 Ma	South of BRSZ *Sample B, Chapter 4*
D1	S1 gneissosity		
D2	North trending F2 folds		
	Quest Lake wacke Post Lake wacke	ca. 2720 Ma < 2720 Ma	Skulski, Sanborn – Barrie and Stern, unpublished.
	Biotite tonalite (T)	2715 Ma	V. McNicoll, unpublished 1999
	Felsic sill (F)	2707 Ma	Age of continental arc magmatism. *Sample A, Chapter 4*
	Savant Sedimentary group	< 2704 Ma	Sanborn – Barrie and Skulski, 1999.
	Quartz-rich metasandstone	< 2701 Ma	*Sample C, Chapter 4*
D3	(I) S3 penetrative fabric, F3 (II) D3a= HCF, L3 (III) D3b= N-S folds		(I) coincides with peak metamorphism (during M1)
	Granodiorite (Gd)	2697 Ma	Dykes cross cut S3 in F4 axial planar orientation (080) *Sample D, Chapter 4*
D4	E trending folds, quartz rodding		Associated with M2 metamorphic event.
	Semipelite	2687 – 2694 Ma MONAZITE	Hydrothermal? From S3 foliated semipelite cut by 2697 Gd. *Sample F, Chapter 4*
	Quartz diorite	2690 Ma	High strain D4 rock
	Granodiorite (Gd)	2687 Ma TITANITE	From above Gd dyke (igneous age of 2697 Ma)
	Granite (G)	2686 Ma	Wapikaimaski Lake pluton (Percival et al., 1999a,b)
Shear zones	Late syn – D4 granites in shear zones	2685, 2680	
	Tonalite mylonite	2678 Ma TITANITE	*Sample E, Chapter 4*
	Granites (Gg)		Late unfoliated, including pegmatites

CHAPTER 6: METAMORPHISM AND DEFORMATION

INTRODUCTION

Greenstone belts of the Wabigoon subprovince have generally experienced low- to medium-grade metamorphic conditions (Blackburn et al., 1991). In many greenstone belts, metamorphic grade increases from central greenschist facies to marginal amphibolite facies (Ayres, 1978). Archean greenstone belts and gneiss terranes are generally characterized by low P/high T metamorphic conditions (e.g. Condie, 1984; Sandiford, 1989).

Metamorphic grade in the Sturgeon Lake greenstone belt is greenschist facies in the interior, increasing to amphibolite facies toward the study area in the east. Aluminosilicates in altered volcanic rocks of the Handy Lake assemblage (northeast Savant Lake greenstone belt) indicate triple point conditions (ca. 500°C, 3.8 kbar, Lefebvre et al., 1978). Within the study area, two metamorphic event, M1 and M2, are described. M1 corresponds to peak metamorphic conditions which developed with S3 foliation. M2 overprints M1, and is related to D4 deformation. Volcanic and sedimentary units have experienced middle to upper amphibolite facies conditions. Their textures, mineral assemblages, and mineral compositions provide insight into the orogenic history of the interface between the western and central Wabigoon subprovinces.

The chapter is organized in the following way. First, rock unit textures, mineral assemblages, and mineral compositions are described within the framework of the three structurally defined panels. This largely petrographic account is followed by a

description of structural-metamorphic relationships, and the nature of panel boundaries. The quantitative assessment of peak metamorphic conditions uses thermobarometric software (TWEEQU; Berman, 1991) and thermometric calculations (Holland and Blundy, 1994). Lastly, a discussion of metamorphic conditions is integrated with development of a P-T-t path for the Brightsand Forest area.

PETROGRAPHY AND MINERAL COMPOSITIONS

South Sturgeon basalt

Mineral assemblages for mafic metavolcanic units are presented in Table 6-1. Pillow basalt of the South Sturgeon assemblage, located 10 km to the east to the map area, and thought to correlate with the Mountairy Lake amphibolite unit, is fine-grained with hornblende-plagioclase assemblages (Fig. 6-1a). Following the nomenclature of Leake (1978) for the classification of amphiboles, central Sturgeon samples are uniformly magnesio-hornblende. Anorthite content in plagioclase varies between individual grains, within the range An_{58-78}.

Southern Panel

Amphibolite

Southern panel Mountairy Lake amphibolites are predominantly fine – grained rocks consisting of hornblende – plagioclase – quartz – titanite, with or without clinopyroxene (Table 6-1, Fig. 6-1b,c,d,e). Clinopyroxene occurs mainly in quartz-rich layers. Coarse clinopyroxene in sample p857b is partly altered to a very fine-grained, optically unidentifiable product, which may comprise epidote and chlorite, isochemical with clinopyroxene (+/- actinolite). Similar features are observed along strike, in a finer

grained rock (sample B1). The Hilltop Lake amphibolite screen is also fine-grained, with hornblende – plagioclase – quartz – ilmenite – titanite assemblages. Hornblende is deep emerald green and strongly pleochroic (Fig. 6-1f). Amphibole compositions within the southern panel vary from ferro – hornblende to magnesio – hornblende (Leake, 1978). This minor compositional variation occurs between mineral grains within rock samples. Anorthite content varies between mineral grains: from Mountairy Lake amphibolite, anorthite varies from An_{63-86} in contrast to An_{37-44} for the Hilltop Lake amphibolite (sample j510).

Metasedimentary rocks

Metasedimentary units within the southern sedimentary group are biotite – plagioclase – quartz schists (Fig. 6-2) with local cummingtonite – hornblende, or cummingtonite – hornblende – garnet – bearing assemblages (Table 6-1). Garnet and cordierite do not coexist within the same sedimentary layers. Bands of cummingtonite – rich and siliceous layers reflect compositional variations that may represent relict bedding.

Plutonic rocks

Granitoid rocks occur within all panels and are petrographically similar. Except for some plutonic gneisses, their simple mineral assemblages (quartz – plagioclase – K-feldspar – biotite +/- hornblende) present little insight into metamorphic conditions.

Central Panel

Amphibolite

Central panel amphibolites are predominantly medium to coarse – grained rocks with hornblende – clinopyroxene – plagioclase – quartz – titanite assemblages (Table 6-

1), with or without garnet, epidote, ilmenite, and hematite (Fig. 6-3). Garnet commonly occurs in quantities up to 15% within mafic rocks of this panel as ragged to rarely euhedral grains 1.5-2 mm in size. Garnet compositions (Table 6-2) are in the range XGr_{30-37}, XPy_{7-11}, $XAlm_{47-58}$, and XSp_{4-7}, with smaller variation within individual samples (e.g. XGr_{30-34} in sample j121; XGr_{35-37} in sample j734). No zoning trends are evident in garnet. Epidote and clinopyroxene co-exist in some samples (Table 6-1), where clinopyroxene is generally altered to a very fine-grained product (perhaps epidote and chlorite, with or without actinolite). Coarse epidote occurs along the edges of the alteration zones. Amphibole compositions vary between mineral grains and among different samples, from ferroan pargasitic hornblende to ferroan hornblende to ferroan tschermakitic hornblende. Variation in anorthite content of plagioclase occurs between samples, but also within samples to a lesser extent. For example, sample J121 (Brightsand River amphibolite) has An_{39-51} and sample J339 (Scruffy Lake amphibolite) has An_{55-68}. Overall, anorthite content in plagioclase varies within the range An_{39-68}.

Metasedimentary rocks

Central panel metasedimentary rocks are variable in composition. Quartz-rich metasandstone within the Rude Lake package contains ~50% quartz, with 40% plagioclase and up to 10% biotite. Leucosome within this rock may represent anatexis. Similarly, mm-scale leucosome veins in garnet – cordierite – sillimanite – quartz – plagioclase – biotite – muscovite – ilmenite pelite in the Robert Lake amphibolite may represent a granitic melt phase (Fig. 4-5). The occurrence of muscovite- and garnet-rich layers within pelite reflects compositional layering that may be relict bedding. In contrast to the texture of garnet in amphibolites, garnet in pelite forms subhedral to euhedral

porphyroblasts. A weak foliation is preserved within garnet, evident from felsic mineral inclusion trails (Fig. 6-5c). Garnet is almandine, with Alm_{79-82}, anorthite content in plagioclase is An_{34-41}, cordierite is predominantly magnesian, with $Cd_{[XMg]62-65}$ (where XMg = Mg/Mg:Fe) and Bt has [XMg] of ~0.3. Small variations in composition occur within and between grains, although no systematic zoning trends were noted.

Plutonic rocks

Tonalite gneisses (Tg) have quartz – plagioclase – biotite assemblages with or without epidote and titanite. Leucosome layers with biotite-rich selvages may be the product of in situ melting, although some compositional layering may have been produced by the injection of tonalite (Chapter 5). New mineral growth associated with D4 includes biotite (M2).

Tonalite gneiss (TgR) in the central panel exhibits mineral overgrowth relationships. Figure 6-5 shows euhedral epidote crystals overgrowing biotite, and titanite crystals that in turn overgrow epidote. The felsic sill (map unit Fs) in the Central panel has qtz – plag – bt – ms – ep – cht mineral assemblages (Table 6-1), with the main S3 foliation defined by biotite and muscovite.

Cataclasite

In thin section, the main fabric (S3) in cataclasite of the Hilltop Creek fault zone is defined by the alignment of matrix chlorite crystals. Rutile is boudinaged parallel to the foliation, and may be accompanied by quartz pressure shadows (Fig. 6-6a). Euhedral hematite grains overgrow the main S3 fabric defined by the assemblage chlorite – plagioclase – quartz – titanite – rutile – epidote. Titanite grains are elongate parallel to the foliation. A second generation of epidote crystals appear to overgrow chlorite, as well as

hematite in some areas. There may be several generations of epidote in this rock (Fig. 6-6b): 1) epidote which developed with the main fabric; 2) epidote that overgrows the main fabric but is overgrown by hematite; and 3) epidote which overgrows hematite.

Northern Panel

Amphibolite

Northern panel amphibolites are coarse – grained hornblende – epidote – actinolite – plagioclase – quartz rocks, with minor titanite (Fig. 6-7a,b,c,d). An amphibolite from the Stinson Lake unit has a quartz – hornblende intergrowth texture, overgrown by subhedral hornblende porphyroblasts (Fig. 6-7e). The northern amphibolite samples are more highly altered, with abundant epidote and actinolite overgrowths defining a retrograde assemblage. Retrograde epidote forms anhedral masses, but actinolite forms euhedral grains, 0.3-0.5 mm in length, clearly overgrowing hornblende grains and S3 fabrics (Fig. 6-7a,b,c). Garnet is not present in amphibolite from the northern assemblage, although textures suggest pseudomorphic replacement of garnet by retrograde plagioclase. Hornblende compositions are magnesio – hornblende and ferroan edenitic hornblende. Plagioclase grains from the sample with magnesio – hornblende have An_{48-62}, and plagioclase from the sample with ferroan – edenitic hornblende has An_{58}.

Plutonic rocks

Within the northern panel, aligned hornblende in coarse – grained tonalite (qtz – plag – hb – bt – ep) is overgrown by uniformly oriented biotite overgrowths.

STRUCTURAL – METAMORPHIC RELATIONSHIPS

The alignment of hornblende grains defines an S3 foliation in most amphibolite samples. Within the southern and central panel mafic rocks, a weak fabric oblique to S3 is also defined by hornblende in thin section and is taken to be S4 (Figs. 6-1, 6-3). Within the central panel the main foliation, S3, defined by coarse clinopyroxene and hornblende, is overgrown by hornblende defining an S4 fabric (Fig. 6-3c). In the northern panel, generations of structures are more difficult to discern, owing to coarse grain size, alteration, and retrograde mineral growth.

Southern panel metasedimentary rocks have S3 defined by the orientation of mafic mineral – rich layers and internal alignment of mineral grains. Randomly oriented cummingtonite overgrows biotite that defines S3, and is in turn overgrown by a second generation of biotite taken to define S4 (Fig. 6-2). In iron formation within the Hilltop Creek Fault, S3 is defined by aligned biotite and muscovite that are crenulated by cm-scale F4 folds (Fig. 6-2f). A prominent S3 foliation is defined by peak metamorphic biotite and sillimanite, along with concordant leucosome veins within metapelites associated with the Robert Lake unit. Both fibrolitic and prismatic sillimanite are crenulated by F4 microfolds (Fig. 6-4a). The crenulation folds have local axial planar biotite, defining an S4 foliation (Fig. 6-4b). Inclusion trails in garnet preserve early S3 fabric development (Fig. 6-4c).

Generally, plutonic rocks carry an S3 foliation that is defined by the pervasive alignment of mafic minerals. Recognition of secondary fabrics is difficult in thin section because of coarse grain sizes (Fig. 6-5b). In the central and northern panels, granodiorite and granite lacking S3 have developed an S4 biotite alignment (M2). The fine-grained

felsic sill (Fs) shows S3-S4 relationships, including S4 biotite and chlorite mineral growths axial planar to F4 crenulations (Fig. 6-5c).

The Hilltop Creek cataclastic zone exibits crenulations of S3 in the field that are not readily apparent in thin section, although a second generation of chlorite and some"M2" biotite define a weak, overprinting fabric interpreted here as S4 (Fig. 6-6).

METAMORPHIC CONDITIONS

In order to further constrain variations of metamorphic conditions within the map area, samples with appropriate assemblages for thermobarometry were collected from within each structural panel and from the eastern margin of the Sturgeon Lake greenstone belt. In only the central panel are assemblages sufficient for full thermobarometric analysis. These include a pelite from the Robert Lake assemblage and amphibolites from the Rude Lake and Brightsand River assemblages.

METHODOLOGY

All mineral spot analyses were done on the Cameca Camabax electron microprobe at the Geological Survey of Canada, carried out by K. Venance. The microprobe uses a wavelength dispersive analysis system, with a spot size of 3 μm, a beam current of 10 nA, with an accelerating potential of 15 kV. Counting time for all analyses was 10 – 20 s. A PAP (Pouchou and Pichoir, 1985) correction program was used to reduce the data.

Part 1: TWEEQU

Estimation of metamorphic conditions was carried out using the TWEEQU (Thermobarometry With Estimation of EQUilibrium state) software of Berman (1991). The program uses an internally consistent set of thermodynamic parameters for end member mineral compositions, with mixing properties selected by the user. It calculates the position of all possible equilibria among minerals for which analyses and thermochemical properties are available. An uncertainty of approximately +/- 50°C, +/- 1 kbar (1kbar = 10^5 Pa = 0.1 Gpa) can be assigned as a result of 1) uncertainties in experimental data on which the thermodynamic properties are based, and 2) the microprobe analytical uncertainty. Additional uncertainty relates to the assumption that all minerals last equilibrated at the same pressure and temperature conditions (Berman 1991).

Thermochemical properties used in the TWEEQU database are those of Berman (1988 and 1991). Mixing properties of garnet are defined by the non-ideal solution models of Berman (1990), and those for biotite and plagioclase by the equations of McMullin et al. (1991) and Fuhrman and Lindsley (1988) respectively. Ideal solution models were used for cordierite. End member compositions and mixing properties for amphiboles are those of Mader et al. (1994), and maintain consistency with version 1.02 of the thermodynamic database. Version 2.01 of TWEEQU was used to calculate metamorphic conditions from pelite. The uncertainty introduced as a result of this variation is thought to be negligible (e.g. Sanborn-Barrie, 1999). A test using version 1.02 of TWEEQU with pelite analyses was done for comparison.

The following equilibria yield the most consistent results in TWEEQU, and are generally considered to be reliable indicators of metamorphic conditons. For the pelites, equilibria were calculated by TWEEQU for the mineral assemblage: garnet – biotite – cordierite – sillimanite – quartz – plagioclase.

Equilibria:

1) 4 Sil + 5 Qtz + 2 Pyp = 3 Mg-Crd (P sensitive).

2) 6 An + 2 Pyp + 3 Qtz = 2 Grs + 3 Mg-Crd

3) Alm + Phl = Pyp + Ann (garnet – biotite thermometer, Kretz 1964)

4) 2 Sil + Qtz + Grs = 3 An (GASP equilibrium)

5) 4 Sil + 5 Qtz + 2 Phl + 2 Alm = 2 Ann + 3 Mg-Crd

Equilibria calculated for amphibolite for the assemblage garnet – hornblende – plagioclase – quartz are as follows:

6) 3 Ab + 2 Grs + Pyp + 3 Tsc = 3 Parg + 3 Qtz + 6 An

7) 3 Ab + 2 Grs + 4 FeTs = 3 FePa + Tsc + 6 Qtz + 6 An

8) 3 Parg + 4 Alm = 4 Pyp + 3 FePa

9) Alm + Tsc = FeTs + Pyp

10) 3 Ab + 2 Grs + 4 Pyp + 3 FeTs = 3 Parg + 6 Qtz + 6 An + 3 Alm

Mineral/end member abbreviations:

Sil = sillimanite	Phl = phlogopite
Qtz = quartz	Ann = annite
Mg-Crd = magnesian cordierite	Tsc = tschermakite
Pyp = pyrope	Parg = pargasite
Grs = grossular	FeTs = ferroan tschermakite
Alm = almandine	FePa = ferroan pargasite
Ab = albite	An = anorthite

Part 2: Hornblende – plagioclase thermometry

Estimates of metamorphic temperatures from amphibolite units including one sample within the Sturgeon Lake belt were made using the hornblende – plagioclase thermometer of Holland and Blundy (1994). The calibration for calcic amphiboles takes account of non – ideal interactions and is useful for a wide range of bulk compositions. The data set used for calibration is composed predominantly of natural metamorphic rock samples, augmented by some experimental data. For plagioclase mixing relations, a simplification of the Darken's Quadratic Formulation model of Holland and Powell (1992) is used. The thermometer functions well for temperatures between 400 and 1000 °C and pressures of 1 to 15 kbar with +/- 40 °C uncertainty.

The two thermometers used include a revised (from Blundy and Holland, 1990) edenite – tremolite thermometer:

T1: edenite + 4 qtz = tremolite + albite

and a new edenite – richterite thermometer:

T2: edenite + albite = richterite + anorthite.

A pressure estimate is required for calculations, and 4.5 kbar was assumed, based on the median value of TWEEQU results for pelite p872.

Calculations *(Holland and Blundy, 1994)*:

Edenite – tremolite (with quartz, requires silica saturation)

$$\text{Temperature (T1)} = \frac{-76.95 + 0.79P + Y_{ab} + 39.4X^{a}_{Na} + 22.4X^{a}_{K} + (41.5 - 2.89P)*X^{M2}_{Al}}{-0.0650 - R*\ln\left\{\frac{(27*X^{a}_{blank}*X^{T1}_{Si}*X_{ab})}{(256*X^{a}_{Na}*X^{T1}_{Al})}\right\}}$$

Edenite – richterite (with or without quartz)

$$\text{Temperature (T2)} = \frac{-78.44 + Y_{ab\text{-}an} - 33.6X^{M4}_{Na} - (66.8 - 2.92P)*X^{M2}_{Al} + 78.5X^{TI}_{Al} + 9.4^{Xa}_{Na}}{-0.0650 - R*\ln\{(27*X^{M4}_{Na}*X^{TI}_{Si}*X_{an})/(64*X^{M4}_{Ca}*X^{TI}_{Al}*X_{ab})\}}$$

Temperature is in Kelvin

X^{ϕ}_{i}: where X is the molar fraction of component i, and ϕ is the crystallographic site.

P (Pressure) = 4.5 kbar

R (gas constant) = 0.0083144

Y_{ab}: for $X_{ab} > 0.5$, $Y_{ab} = 0$
For $X_{ab} < 0.5$, $Y_{ab} = 12*(1 - X_{ab})^2 - 3$ kJ

Y_{ab-an}: for $X_{ab} > 0.5$, $Y_{ab-an} = 3$ kJ
For $X_{ab} < 0.5$, $Y_{ab-an} = 12*(2X_{ab} - 1) + 3$ kJ

For data tables and calculations see Appendix 2.

RESULTS

Part 1: TWEEQU

Figures 6-8 and 6-9 are examples of the graphical representation given by TWEEQU for possible equilibria within a given mineral assemblage. Tables 6-3 and 6-4 list compositions and P-T results respectively for pelite sample p872. Calculations were made on core, midpoint, and rim compositions from minerals (i.e. garnet core with biotite, plagioclase, and cordierite cores). Core compositions give metamorphic conditions based on the intersection of equilibria 1 to 5 between 4.1 and 6.1 kbar at 615 – 670 °C, midpoints between 3.8 – 4.8 kbar at 600 – 670 °C, while rims equilibrated at 3.3 – 5.1 kbar and 590 – 660 °C. Good convergence of the calculated equilibria suggests that these compositions reflect equilibrium conditions. Rim mineral compositions were tested

for consistency with TWEEQU version 1.02. Version 1.02 gave estimates of 3.5-5.3 kbar, and 620-700°C for rim conditions, overlapping but slightly higher than results obtained using version 2.01.

Results for amphibolite obtained using TWEEQU are based on mineral compositions presented in Table 6-5. Table 6-6 summarizes pressure and temperature results. Overall, pressure and temperature estimates from amphibolite are higher than those for the pelite, and some temperatures exceed amphibolite – facies conditions. The most extreme example of this occurs in sample j734(g1-4), which yields pressures greater than 11 kbar and temperatures close to 800°C. In this rock, disequilibrium may be a factor (Fig. 6-10).

The grossular content of garnet within amphibolite, with Grs_{30-37}, is much higher than that in pelitic garnet, with Grs_{4-5} (Table 6-2), corresponding to 10.6-13.5 wt% CaO within amphibolitic garnets and to 1.3-1.7 wt% CaO for pelitic garnets. One spot from sample j734(g8), from the Rude Lake amphibolite, yielded conditions of 5.1-5.9 kbar and 570-585 °C, comparable to pressures and temperatures obtained from pelite p872 interleaved with the Robert Lake amphibolite. Sample j121 (located between Rude and Robert Lakes, from the Brightsand River amphibolite), also yielded a range of values, from 7.4-8.2 kbar, and 615-630 °C to >10 kbar and temperatures of 690-705 °C. The garnet – hornblende barometer is less reliable than the GASP barometer in terms of defining pressure conditions because P-T slopes of phase equilibria are much steeper. The lowest pressure results coincide with results from the pelite, and may reflect an accurate measure of the equilibration of garnet with hornblende and plagioclase. However, the higher values are unsupported by independent evidence and may be

spurious. This could be a function of the steep dP/dT slopes in this system, and(or) disequilibrium among garnet, hornblende, and plagioclase.

Part 2: Hornblende – plagioclase thermometry

Mineral analyses are listed in Table 6-7 and results for both thermometers in Table 6-8. The edenite – tremolite thermometer (T1) yielded much higher temperatures (717-950°C) than did the edenite – richterite thermometer (T2) (565-776°C). T1 requires silica saturation, and when applied to quartz-free rocks, it is expected to yield anomalously high temperatures (Holland and Blundy, 1994). T2 is the more reliable thermometer for amphibolites sampled in this study, as it is not dependent upon the presence of quartz in the assemblage.

Temperatures calculated with T2 are lowest in the Sturgeon assemblage, giving temperatures from 565 to 588°C. In the southern panel, the Hilltop Lake amphibolite yielded temperatures between 611 and 647°C, showing little variability when compared to the Mountairy Lake amphibolite that yielded temperatures between 591 and 739°C. The central panel amphibolites give temperatures with a wide range of variation, from temperatures of 685-776°C for the Scruffy Lake unit, to 512-658°C for the Rude Lake unit, and 571-744°C for the Brightsand River unit. The two samples from the Northern amphibolite yield temperatures from 592 to 677°C.

Comparison of average temperatures between structurally defined panels in the study area and with a pillowed basalt in the South Sturgeon assemblage in the Sturgeon Lake greenstone belt (sample j804) are presented in Table 6-8 and Fig. 6-11. The lowest average temperature (579 +/- 12°C) is found from the greenstone belt sample, while

central panel amphibolites (n = 3) yielded the highest average temperature (660 +/- 81°C). The southern and northern panels have average temperatures of 648 +/- 58°C and 626 +/- 38°C respectively. The central panel amphibolites exhibits a large variability in temperature within and between samples overall, although sample p857b (clinopyroxene – bearing amphibolite) within the southern panel also exhibits a wide variation between spot analyses. These estimates overlap within analytical uncertainty. It is therefore concluded that the temperatures are statistically indistinguishable.

DISCUSSION

The most reliable constraint on peak metamorphic conditions comes from pelite within the Robert Lake assemblage. Structural - metamorphic relationships are well constrained from thin section study, and minerals used in pressure - temperature determinations form part of the assemblage grt – crd – sill – plag – bt – qtz – ilm. Estimates from garnet cores of 5.1 kbar (+/- 1 kbar), 642°C (+/- 27°C) are taken as peak metamorphic, wheras rim conditions of 3.7 kbar (+/- 0.4 kbar), 625°C (+/- 35 °C), suggest ~5 km of uplift with little cooling.

Retrograde plagioclase from garnet preserves textural evidence for garnet growth in the northern panel. Retrograde epidote and less common chlorite overgrows hornblende grains. Euhedral actinolite crystals overgrow retrograde epidote and early hornblende. These textures involving late actinolite and chlorite suggest that retrograde metamorphism from amphibolite to greenschist facies occurred within the northern panel. The localization of greenschist facies retrogression in the northern panel suggests that this

area remained subject to recrystallization during the cooling history subsequent to normal movement along the Robert Lake zone.

The youngest detrital zircon from metamorphosed quartzite of the central panel provides an upper limit of 2701 Ma for deposition of the rock, and for its metamorphism. Burial required to attain the ca. 5 kbar metamorphic peak must have occurred prior to 2697 Ma, the age of granodiorite dykes cutting peak - metamorphic S3 foliation (Chapter 4). These constraints suggest a ca. 4 m.y. time window in which sediments were deposited, buried to depths of ca. 15 km and heated to ca. 650°C. The rapidity of these events requires some form of tectonic burial, presumably by thrusting, accompanied by rapid heating.

A second generation of metamorphic minerals is associated with D4 structures. These include retrograde minerals in amphibolites, particularly in the northern panel, and overprinting minerals in the Hilltop Creek fault rocks as well as biotite in F4 axial planes of metasedimentary units; and S4 grain-scale biotite foliations in post-D3 granitoid rocks. Textural evidence from cataclastic rocks in the Hilltop Creek fault suggests interim cooling between M1 and M2. Biotite overgrowing chlorite - defined S3 fabrics in the fault zone suggests that re-heating (M2) occurred during the D4 deformation. Although biotite growth is associated with D4 regionally, cooling between M1 and M2 is recognized only within the Hilltop Creek fault because heating is required to produce biotite. Most rocks in the area do not show evidence of reheating because biotite is consistent with their peak metamorphic grade.

Geochronological constraints on the M2 event are similar to those developed for D4, because the M2 minerals can be related texturally to D4 deformation. To reiterate,

D4 is bracketed between 2697 and 2678 Ma, the latter referring to the age of titanite overgrowing sheared rocks of the Brightsand River zone.

Only minor differences in metamorphic temperature between panels is suggested by hornblende – plagioclase thermometry, and these are within the uncertainty of the measurement technique. Mineral assemblages including garnet occur only within the central panel. Garnet has retrogressed completely within the northern panel, and is not present within amphibolites in the southern panel.

High grossular content of garnet in amphibolite may reflect the high-CaO bulk composition of amphibolite, also indicated by the calcic minerals high An plagioclase, calcic hornblende, clinopyroxene, titanite, and epidote present in these rocks.

It is possible that the large mole fractions of grossular within amphibolitic garnets are vestigal from a higher-pressure state as indicated by the equilibria calculated for these rocks using TWEEQU. This may be consistent for pelites with the right bulk composition: Figure 17-10d in Spear (1990) shows the activity of grossular in garnet increasing with increasing pressure for the assemblage garnet – biotite – chlorite – plagioclase – muscovite – quartz. However, for mafic rocks, pyrope is taken to indicate high pressures rather than grossular (e.g. Cox and Indares 1999, looking at eclogites). In fact, the use of grossular as a barometer in garnet-bearing assemblages is problematic, owing to differences in the thermodynamics of high-Ca and low-Ca garnet (Guiraud and Powell, 1996).

Constraints on metamorphic pressure are scarce in the greenschist- to amphibolite-facies Sturgeon Lake greenstone belt. A single occurrence of coexisting sillimanite-andalusite-kyanite was reported from altered volcanic rocks of the north-

central Sturgeon-Savant Lake greenstone belt (Lefebvre et al., 1978), suggesting conditions of 3.8 kbar, 500 °C using Holdaway's (1971) aluminosilicate triple point. Assuming that peak metamorphism was coeval with that in the present area, this indicates that a ca. 5 km deeper structural level is exposed in the central panel of the map area than within the central Sturgeon-Savant Lake greenstone belt. Metamorphic temperature in the central panel was ~160°C higher than that in the interior of the greenstone belt.

Figure 6-12 is a pressure-temperature-time diagram which summarizes chronological and structural controls on metamorphism between 2701 and 2670 Ma. Details are described in the figure caption.

CONCLUSIONS

1) Peak metamorphic conditions of 5.1 kbar and 642°C were obtained using TWEEQU software. This was obtained from pelitic rocks with equilibrium assemblages and well - defined structural - metamorphic relationships.
2) The syn - D3 metamorphic peak M1 is bracketed between 2701 and 2697 Ma.
3) The area underwent rapid burial to depths of ~15 km between 2701 and 2697 Ma.
4) Cooling and reheating between M1 and M2 is indicated by new biotite growth during S4 in the Hilltop Creek Fault.
5) Syn - D4 M2 metamorphism is loosely bracketed between 2697 and 2678 Ma.
6) Metamorphic temperatures estimated from hornblende – plagioclase thermometry are statistically indistinguishable between panels, across the Hilltop Creek fault and the Robert Lake zone. The highest temperatures using Holland and Blundy (1994) calculations are within the central panel (660°C), consistent with TWEEQU data.
7) Garnets from central panel amphibolite have high grossular contents that yield a range of pressure between 5 and >11 kbar. These garnets are not in textural equilibrium with the matrix, and may relate to high-Ca bulk compositions or less likely, to an early higher pressure segment of the PT path.

Table 6-1: Mineral assemblages and approximate modes for amphibolite and metasedimentary rock units, where m=minor or accessory

Sturgeon belt	Sample	Ti	Grt	Cpx	Hb	Act	Ep	Sil	Bt	Ms	Pl	Qtz	Crd	Cm	Ilm	Cht	Hm	Rt	Opaque
South Sturgeon assemblage	j804	x			x						x	x-m			x				
Southern panel																			
Amphibolite																			
Mountary	j548	x			x				x		x	x							
	B1	x		x	x						x	x							x
	p857b	x		x	x						x	x							
Hilltop	j510	x			x						x	x							
Southern metasedimentary rocks																			
	j352		x						x		x	x		x					
	j351								x		x	x	x						
	j59				x				x		x	x		x					
	j57				x						x	x		x					
Hilltop Creek Fault	j732	x							x		x	x				x	x	x	x
Central panel																			
Amphibolite																			
Scruffy	j115	x			x		m				x	x							
	j316	x		x	x		m				x	x					x		
	j141			x	x		m				x	x							x
	j95	x			x						x	x							
Rude	j339	x		x	x						x	x							x
	j334	x		x	x		x				x	x					x		
	j734	x	x	m	x						x	x							
	j772	m		x	x						x	x							
	j1000	x			x				x		x	x			x				
	p857b	m		x	x						x	x							
	j142	x		x	x						x	x							
Brightsand	j121		x	m	x		x				x	x							x
	j111	x		x	x		x				x	x							
	j120	x		x	x		x				x	x							
Robert	p780	x		x	x		m				x	x							
	j446	m		m	x		m				x	x							
Central panel sempelite																			
	j446		x					x	x		x	x	x	x	x	m			
	p872		x					x	x	x	x	x	x		x				
Robert Lake zone	j128				x		x				x	x							
Northern panel																			
Amphibolite																			
Stinson	j132	m				m-x					x	x							
Northern	j135	m				x	x				x	x							m
	j135b					x	x				x	x							
	j536	m				m-x	x				x	x							

Figure 6-1: Fine-grained amphibolite from the margin of the Central Sturgeon greenstone belt (A) and the Southern panel (B,C (close up of B),D,E,F). Very fine – grained titanite overgrows hornblende-defined fabrics in all samples. Clinopyroxene in B,C and D is partly altered to fine – grained chlorite and epidote. S4 is defined by biotite in E, and weakly by hornblende in B,F. F: Emerald green hornblende from the Hilltop Lake amphibolite.

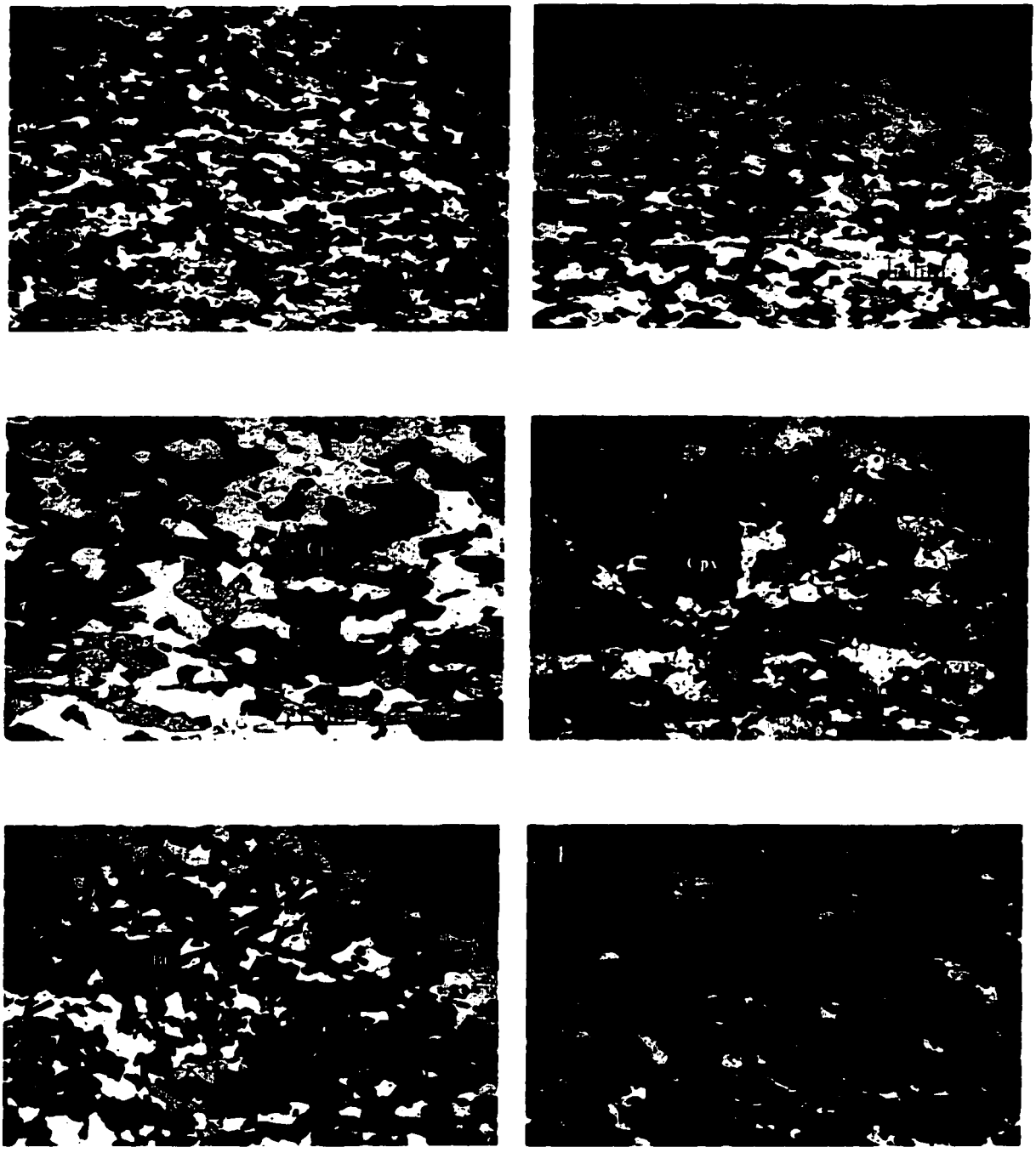

Figure 6-2: A,B,C,D,E: Southern sedimentary group. A: Garnet – biotite metasedimentary schist. B: Cordierite – biotite schist. C: Cummingtonite porphyroblast. D: Hornblende overgrowing biotite. E: Hornblende-rich and quartz-rich layering in metasedimentary layer. F: Pyrite and magnetite overgrowing cordierite – biotite – muscovite – quartz in iron formation from the northern sedimentary group near the Hilltop Creek Fault.

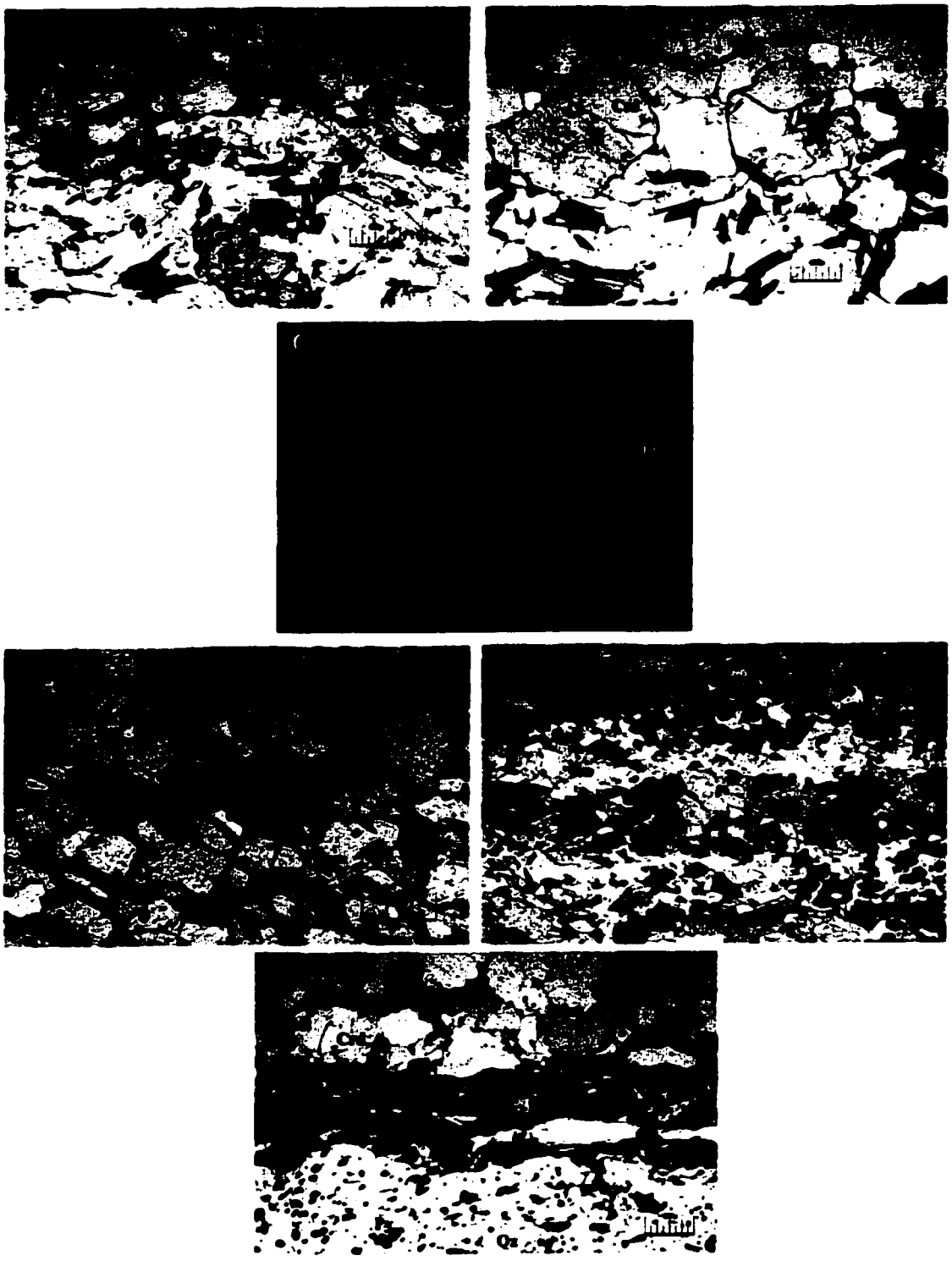

Figure 6-3: Coarse grained amphibolite from the central panel. A: Clinopyroxene and epidote amphibolite, Rude Lake package. B: Late hematite overgrowing biotite (S4). C: Aligned hornblende overgrown by clinopyroxene porphyroblast.

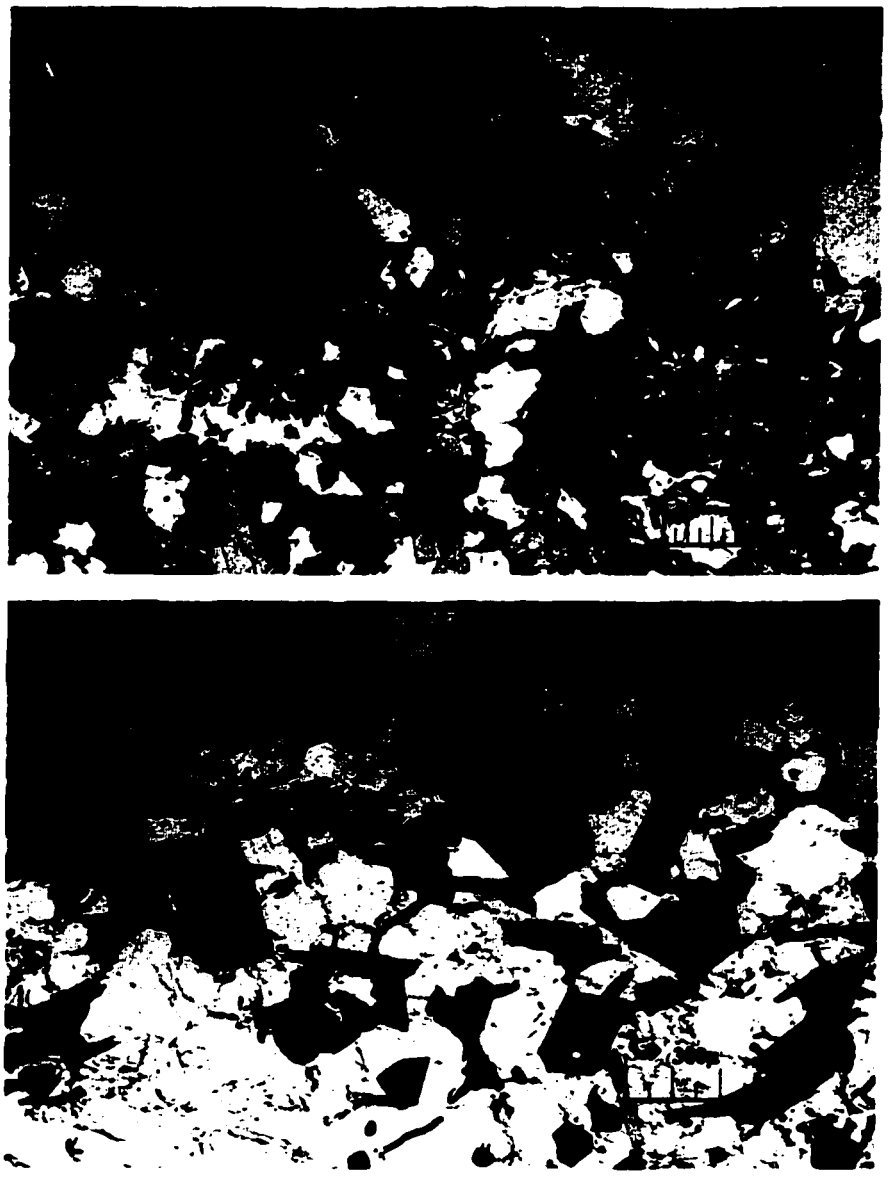

Table 6-2: Mole fractions (converted to mole %)

Pelite	Grs	Pyp	Alm	Sp
Rim	4	11	82	2
	4	14	79	3
	4	11	82	2
Midpoint	4	12	81	2
	5	12	81	2
	4	13	81	2
Core	5	13	80	2
	5	12	81	3
	5	13	80	2

Amphibolite	Grs	Pyp	Alm	Sp
J734	36	10	48	6
	36	10	48	6
	35	10	49	6
	35	10	48	6
	36	10	47	7
	37	9	48	6
J121	32	10	53	5
	32	10	53	5
	30	11	53	5
	34	7	55	4
	31	7	58	4
	33	7	56	5

Figure 6-4: A: Sillimanite – biotite – cordierite – garnet S3 fabric crenulated by F4. B: Garnet in pelite. Weak foliation from felsic mineral inclusion trails.

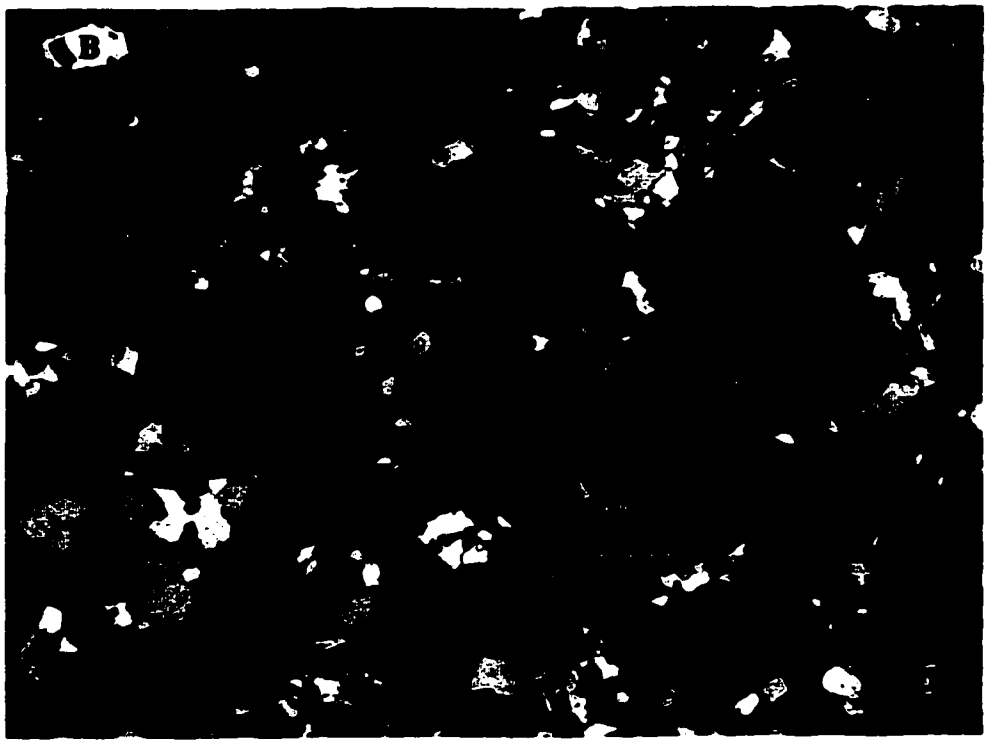
B

Figure 6-5: A: Titanite inclusion in epidote overgrowing biotite. B: Crenulations in granodiorite. C: S4 cleavage defined by biotite and chlorite in felsic sill, <25 m east of the Hilltop Creek Fault.


B

Figure 6-6: The Hilltop Creek Fault zone. A: Rutile boudinaged parallel to S3 in chlorite – sericite matrix. Weak S4 is defined by aligned chlorite and biotite. B: Late hematite porphyroblasts. Hematite overgrows and is overgrown by epidote. Also, note secondary overgrowths of chlorite defining S4.

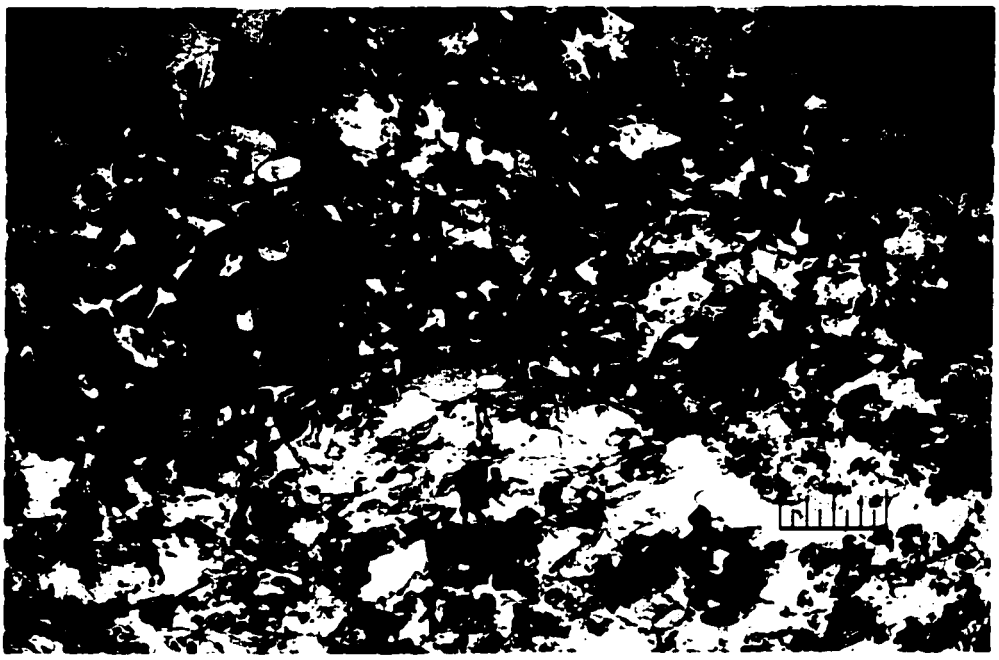


1 μm

Figure 6-7: Coarse - grained northern panel amphibolite. A,B,C: Actinolite overgrowths. B: Hornblende rims altered to actinolite. D: Abundant epidote in amphibolite. E: Hornblende – quartz intergrowth texture.

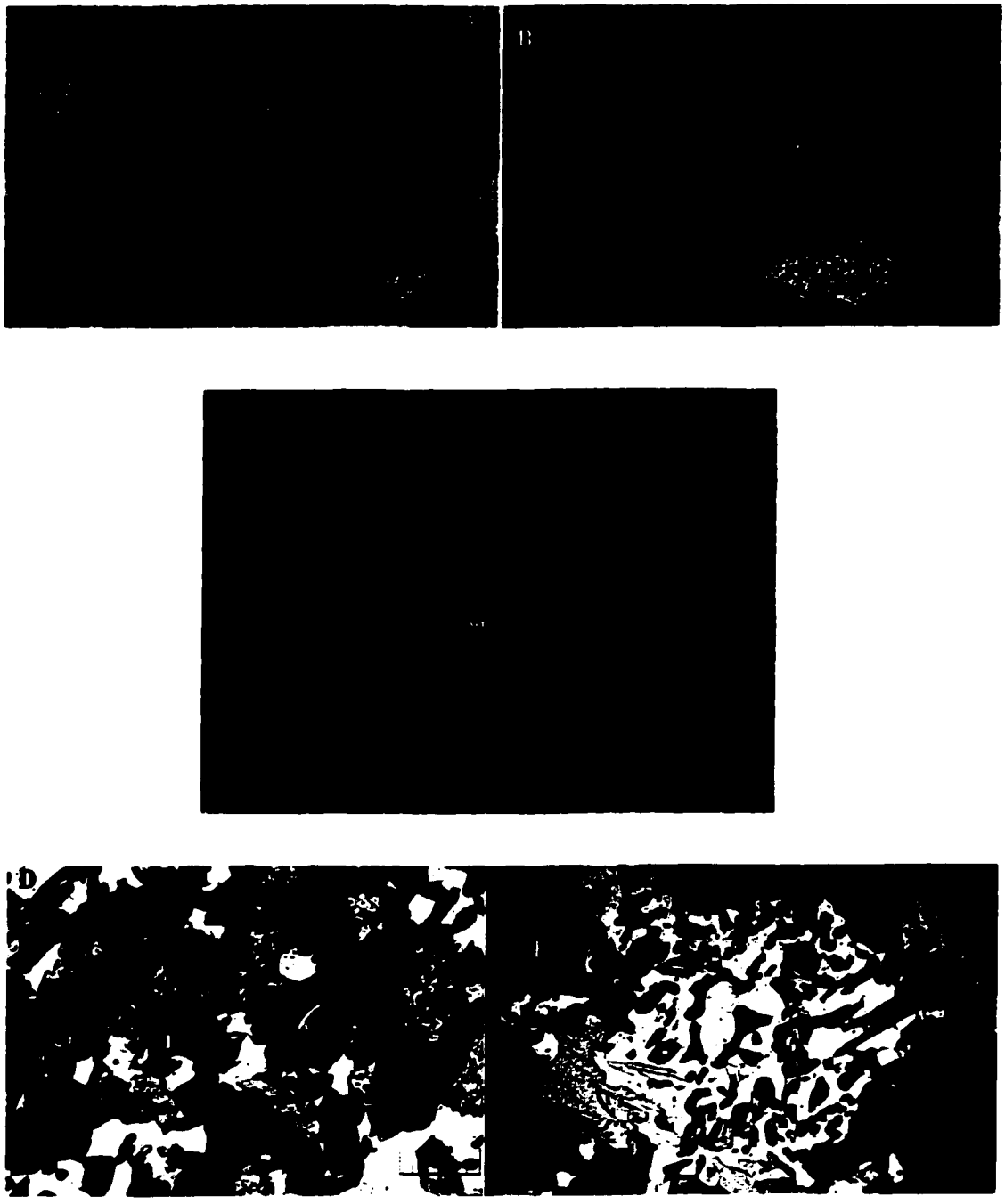

Figure 6-8: Graphical representation of garnet with rim sillimanite, bioite, plagioclase, cordierite and quartz using TWEEQU, version 2.01. The same run using version 1.02 yielded pressure between 3.5-5.3 kbar, and temperature between 620-700°C.

Garnet rim in pelite

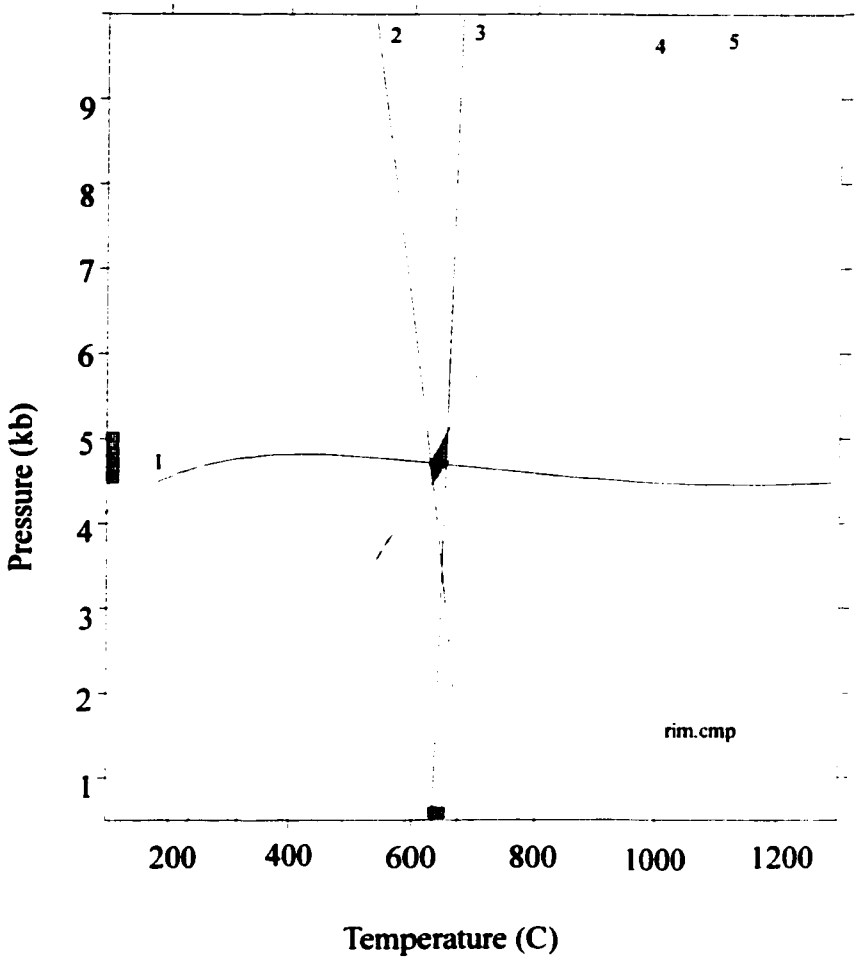

Equilibria used for PT estimation using TWEEQU v. 2.02 (Berman 1991).

1) 4 Si + 5 Qz + 2 Py = 3 Cd

2) 6 An + 2 Py + 3 Qz = 2 Gr + 3 Cd

3) Alm + Phl = Py + Ann

4) 2 Si + Qz + Gr = 3 An

5) 4 Si + 5 Qz + 2 Ph + 2 Alm = 2 Ann + 3 Cd

Figure 6-9: Graphical representation of PT conditions defined by garnet rim, hornblende, plagioclase and quartz in amphibolite, using TWEEQU version 1.02.

Garnet in amphibolite.

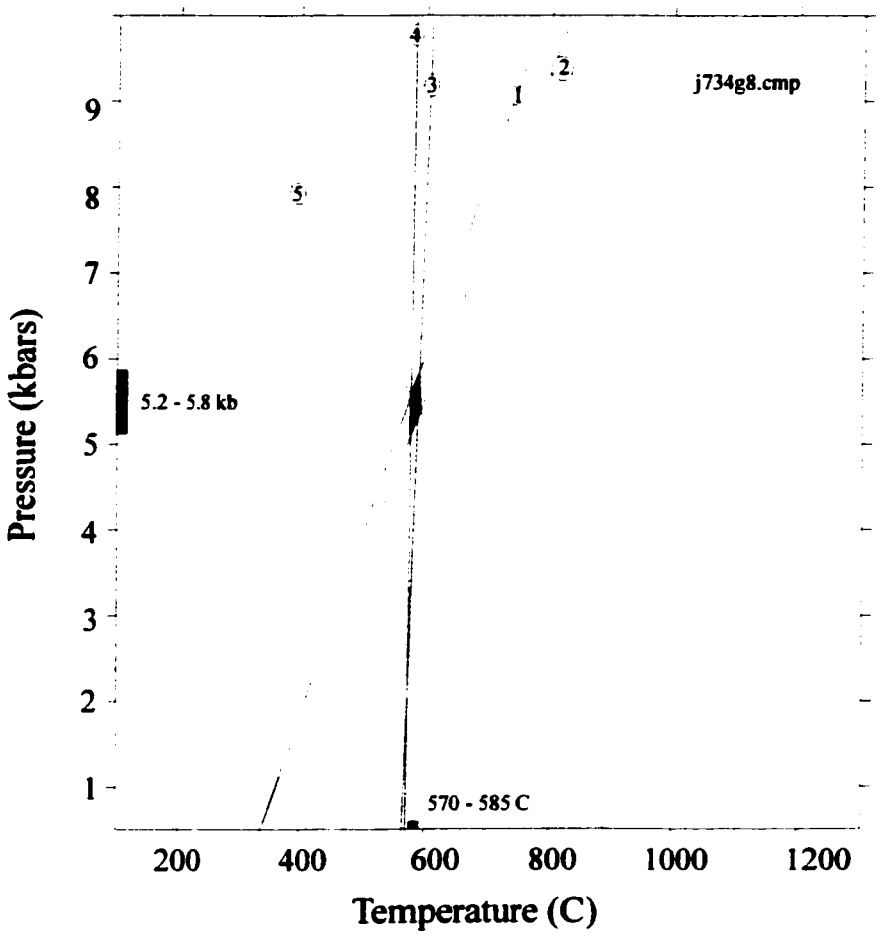

Equilibria used for pressure - temperature estimations in TWEEQU v.1.02 (Berman 1991).

1. 3 Ab + 2 Gr + Py + 3 Tsc = 3 Parg + 3 Qz + 6 An
2. 3 Ab + 2 Gr + Py + 4 FeTs = 3 FePa + Tsc + 6 Qz + 6 An
3. 3 Parg + 4 Alm = 4 Py + 3 FePa
4. Alm + Tsc + FeTs + Py
5. 3 Ab + 2 Gr + 4 Py + 3 FeTs = 3 Parg + 6 Qz + 6 An + 3 Alm

Table 6-3: Mineral analy ses for pelite

SAMPLE	Biotite	0872-S1IC1	"0872-S1IM2"	0872-S1IR3	"0872-S2IC1	0872-S2IM2	"0872-S2IR3"	Cordierite	"0872-S1IC1	"0872-S1IM2	"0872-S1IM3	"0872-S1IR4	"0872-S1IR5	"0872-S2IC1	"0872-S2IM2	"0872-S2IR3"
NA2O		0 37	0 28	0 24	0 29	0 29	0 29		0 59	0 59	0 57	0 56	0 63	0 70	0 65	0 64
K2O		9 33	9 07	9 30	8 77	8 98	8 84		0 03	0 02	0 03	0 01	0 02	0 02	0 03	0 03
FEO		19 15	19 71	18 90	20 01	20 72	20 24		8 06	8 11	8 02	7 86	7 93	7 76	8 29	8 08
MGO		9 43	9 66	9 59	9 41	9 33	9 85		7 81	7 56	7 91	7 42	7 83	8 08	7 50	7 69
MNO		0 06	0 03	0 00	0 02	0 07	0 01		0 03	0 07	0 00	0 03	0 01	0 00	0 08	0 04
AL2O3		19 40	19 48	19 60	18 11	18 07	18 21		32 99	32 68	32 79	32 30	32 59	32 68	32 50	32 36
SIO2		34 75	34 33	34 46	34 33	34 41	33 87		48 59	48 30	47 80	47 09	48 56	48 19	47 31	48 93
CAO		0 05	0 05	0 05	0 09	0 08	0 07		0 05	0 03	0 07	0 04	0 03	0 06	0 02	0 06
TIO2		1 46	1 46	1 55	1 37	1 59	1 64		0 01	0 00	0 00	0 00	0 02	0 06	0 00	0 08
CR2O3		0 35	0 41	0 46	0 45	0 48	0 41		0 01	0 00	0 01	0 00	0 01	0 00	0 07	0 03
CL		0 04	0 01	0 01	0 03	0 03	0 02		0 01	0 02	0 00	0 01	0 02	0 01	0 01	0 00
F		0 06	0 04	0 24	0 00	0 44	0 55		0 00	0 00	0 00	0 00	0 13	0 06	0 00	0 00
BAO		0 18	0 31	0 19	0 20	0 33	0 13		0 20	0 00	0 00	0 00	0 00	0 01	0 00	0 16
TOTAL		94 61	95 43	94 58	93 87	94 73	94 12		99 37	97 38	97 22	95 33	97 78	97 64	96 46	98 06

SAMPLE	Garnet	0872-S1IC5	"0872-S1IC6"	0872-S1IM3	0872-S1IM4	"0872-S1IM7	"0872-S1IM8	"0872-S1IR1	"0872-S1IR1	"0872-S1IR2	"0872-S1IR9	"0872-S2IC3	"0872-S2IR1	"0872-S2IR2	"0872-S2IR4	Ilmenite	"1872-S1IC1"	"1872-S2IC1"
NA2O		0 01	0 04	0 06	0 04	0 03	0 02	0 03	0 03	0 05	0 00	0 01	0 05	0 00	0 05		0 05	0 02
K2O		0 01	0 01	0 03	0 01	0 00	0 00	0 01	0 01	0 01	0 01	0 00	0 01	0 03	0 00		0 00	0 01
FEO		35 96	37 32	36 92	38 02	37 87	37 10	37 54	37 04	36 47	37 07	37 64	37 96	37 28	37 34		49 21	48 68
MGO		3 24	3 14	3 15	3 10	3 08	3 21	2 94	2 86	3 56	3 72	3 01	2 71	3 29	2 91		0 20	0 18
MNO		1 10	1 18	1 07	1 11	1 14	1 01	1 07	1 05	1 21	1 06	1 16	1 09	1 12	1 10		0 16	0 13
AL2O3		20 51	20 69	20 24	20 90	20 49	20 83	20 55	20 24	20 51	20 57	19 75	19 93	20 27	20 30		0 06	0 04
SIO2		36 47	36 54	36 03	36 75	36 50	36 84	36 82	36 70	37 20	36 99	36 43	36 97	36 56	36 72		0 00	0 00
CAO		1 71	1 64	1 46	1 68	1 66	1 44	1 35	1 38	1 49	1 38	1 65	1 38	1 36	1 53		0 03	0 01
TIO2		0 03	0 00	0 56	0 00	0 02	0 06	0 00	0 00	0 02	0 05	0 08	0 00	0 01	0 00		46 94	47 20
CR2O3		0 15	0 08	0 07	0 10	0 09	0 08	0 04	0 03	0 10	0 01	0 10	0 05	0 07	0 04		0 30	0 22
CL		0 02	0 01	0 00	0 00	0 00	0 00	0 02	0 01	0 01	0 03	0 00	0 03	0 02	0 00		0 01	0 00
F		0 00	0 00	0 00	0 08	0 36	0 05	0 21	0 00	0 00	0 31	0 00	0 18	0 44	0 00		0 03	0 19
BAO		0 08	0 03	0 14	0 07	0 00	0 09	0 16	0 00	0 12	0 01	0 12	0 01	0 09	0 10		0 24	0 27
TOTAL		99 30	100 68	99 74	101 86	101 23	100 73	100 72	99 33	100 44	101 21	99 94	100 33	100 54	100 08		97 21	96 98

Feldspar	SAMPLE	"0872-S1IC1	"0872-S1IM2"	0872-S1IR3	"0872-S2IC1	0872-S2IM2	"0872-S2IR3"	"0872-S22C1"	"0872-S22M2	"0872-S22R3"
	NA2O	6 76	2 95	7 73	6 82	7 11	7 36	6 72	7 02	6 79
	K2O	0 02	0 02	0 02	0 05	0 03	0 03	0 06	0 03	0 03
	FEO	0 10	0 26	0 15	0 02	0 04	0 01	0 06	0 05	0 09
	CAO	7 78	2 87	7 25	8 59	8 40	8 09	8 56	8 15	8 48
	SIO2	56 14	67 15	58 95	57 18	57 31	58 25	57 10	57 70	57 25
	AL2O3	27 58	48 92	25 88	26 86	26 57	26 27	26 82	26 30	26 76
	BAO	0 00	0 00	0 09	0 00	0 00	0 00	0 12	0 00	0 11
	SRO	0 00	0 00	0 03	0 00	0 08	0 00	0 06	0 18	0 12
	TOTAL	98 38	102 16	100 09	99 52	99 54	100 01	99 50	99 44	99 62

Table 6-4: Thermobarometry results for pelite

	Pressure (kbar)	Temperature (Celsius)
Cores	4.4-6.5	615-650
	4.29-4.32	626-628
	4.2-4.8	624-640
	4.1-6.1	610-670
Midpoint	4.2-4.8	625-640
	3.8-4.7	625-670
	4.2-4.8	600-615
	4.1-4.6	645-675
Rim	3.4-4.6	590-640
	4.5-5.1	640-665
	3.7-4.4	590-625
	3.3-4.6	509-650

Table 6-5: Mineral analyses for amphibolite

Garnet	SAMPLE	*J121-G1*	*J121-G2*	*J121-G3*	*J121-G4*	*J121-G5*	*J121-G6*	*J734-G1*	*J734-G2*	*J734-G3*	*J734-G4*	*J734-G5*	*J734-G6*	*J734-G7*	*J734-G8*
	NA2O	0 00	0 00	0 00	0 01	0 00	0 00	0 00	0 00	0 00	0 00	0 00	0 01	0 00	0 00
	K2O	0 00	0 02	0 01	0 00	0 00	0 01	0 00	0 00	0 00	0 00	0 00	0 02	0 01	0 02
	FEO	22 71	22 86	23 16	22 53	22 26	22 53	24 21	24 29	24 55	24 46	25 79	26 76	25 69	23 54
	MGO	2 52	2 45	2 78	2 83	2 54	2 47	2 53	2 61	2 55	2 79	1 77	1 75	1 72	1 21
	AL2O3	20 57	19 93	20 12	20 58	20 76	19 85	20 58	20 62	20 82	20 64	20 06	20 46	20 14	20 19
	SIO2	37 14	37 26	37 36	37 40	37 52	36 89	37 00	36 75	36 89	37 03	36 96	36 87	37 02	36 49
	CAO	13 02	13 37	13 14	12 75	13 37	13 53	11 63	11 58	11 47	11 03	12 38	11 35	11 71	10 58
	TIO2	0 08	0 20	0 43	0 12	0 12	0 42	1 19	0 24	0 24	0 24	0 15	0 11	0 14	0 10
	CR2O3	0 00	0 03	0 01	0 01	0 00	0 05	0 01	0 03	0 00	0 00	0 00	0 00	0 04	0 02
	MNO	2 95	2 81	2 72	2 70	3 10	2 84	2 13	2 32	2 33	2 39	1 88	2 01	2 08	4 87
	TOTAL	98 98	98 92	99 73	98 93	99 66	98 59	99 29	98 43	98 86	98 59	98 99	99 36	98 55	97 01

Amphibole	SAMPLE	*J121-A1*	*J121-A2*	*J121-A3*	*J121-A4*	*J734-A1*	*J734-A2*	*J734-A3*
	NA2O	1 29	1 37	1 18	1 47	0 97	1 17	1 14
	K2O	0 79	0 83	0 69	0 72	0 56	0 62	0 74
	FEO	18 06	17 61	18 23	17 46	21 26	21 98	20 74
	MGO	8 93	9 06	9 06	9 14	7 16	6 55	6 45
	AL2O3	11 45	11 74	10 86	11 52	10 79	11 21	12 48
	SIO2	40 99	41 17	41 44	42 17	42 56	42 07	40 40
	CAO	11 72	11 31	11 87	11 56	11 74	11 68	11 53
	TIO2	1 98	1 97	1 76	1 50	0 73	0 71	0 83
	CR2O3	0 04	0 00	0 00	0 00	0 07	0 00	0 09
	MNO	0 27	0 43	0 42	0 39	0 78	0 62	0 50
	NIO	0 03	0 03	0 00	0 02	0 04	0 04	0 02
	F	0 19	0 16	0 10	0 15	0 23	0 10	0 23
	CL	0 00	0 00	0 01	0 03	0 06	0 00	0 05
	RB2O	0 00	0 00	0 00	0 00	0 12	0 00	0 00
	SRO	0 00	0 00	0 00	0 00	0 00	0 00	0 00
	BAO	0 20	0 00	0 12	0 00	0 02	0 00	0 04
	ZNO	0 00	0 00	0 02	0 00	0 02	0 18	0 13
	V2O3	0 02	0 06	0 01	0 06	0 02	0 00	0 09
	P2O5	0 00	0 00	0 00	0 02	0 06	0 00	0 00
	TOTAL	95 97	95 74	95 77	96 22	97 19	96 92	95 45

Feldspar	SAMPLE	*J121-F1*	*J121-F2*	*J121-F3*	*J121-F4*	*J734-F1*	*J734-F2*	*J734-F3*
	NA2O	6 73	6 71	5 14	5 40	1 75	5 77	0 01
	K2O	0 03	0 07	0 03	0 05	0 04	0 05	0 00
	FEO	0 08	0 11	0 14	0 11	0 07	0 14	0 13
	CAO	7 76	8 14	10 70	10 15	13 33	9 54	0 02
	SIO2	58 17	57 35	54 22	55 32	51 60	55 68	101 27
	AL2O3	25 74	26 02	28 25	27 50	30 37	27 20	0 05
	BAO	0 33	0 21	0 01	0 00	0 14	0 03	0 00
	TOTAL	98 84	98 61	98 48	98 54	99 10	98 21	101 48

Table 6-6: Thermobarometry results for amphibolite

	Pressure (kbar)	Temperature (Celsius)
121g1	7 6-8 4	625-640
g2	7 4-8 2	615-630
g3	8 2-9 1	645-662
g4	9 6-10 8	680-710
g5	8 9-9 8	665-680
g6	8 8-9 0	630-635
734g1	11 2-14 4	810-875
g2	11 4-14 7	825-890
g3	11 0-14 2	810-870
g4	11 8-15 2	845-905
g5	8 2-9 7	655-680
g6	7 5-8 8	640-660
g7	7 8-9 2	645-670
g8	5 1-5 9	565-580

Figure 6-10: Garnet with resorbed appearance in amphibolite. Matrix consists of hornblende-plagioclase+/-quartz.

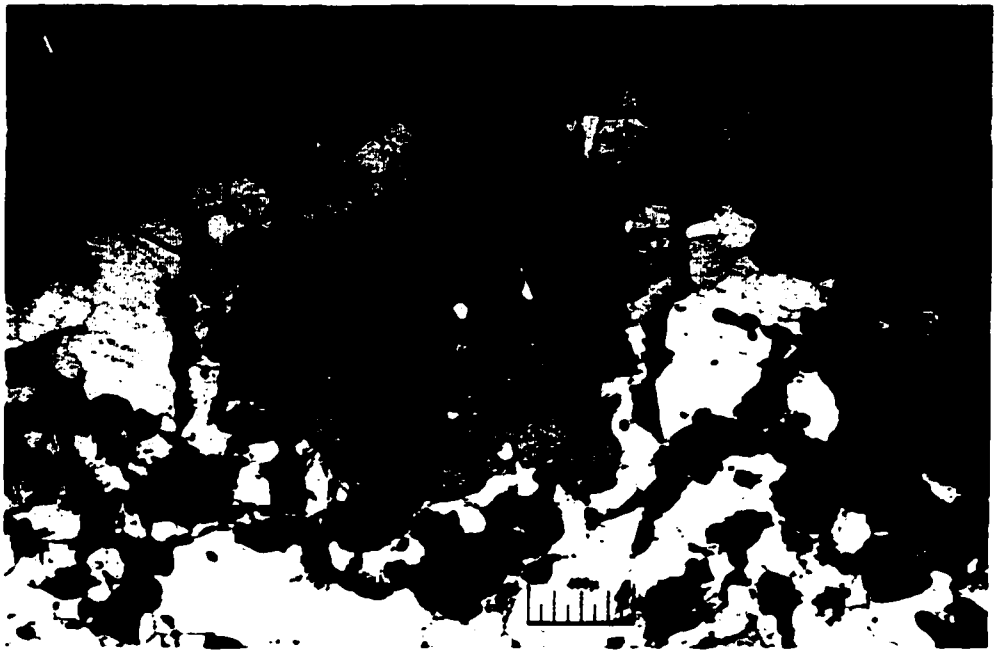
A

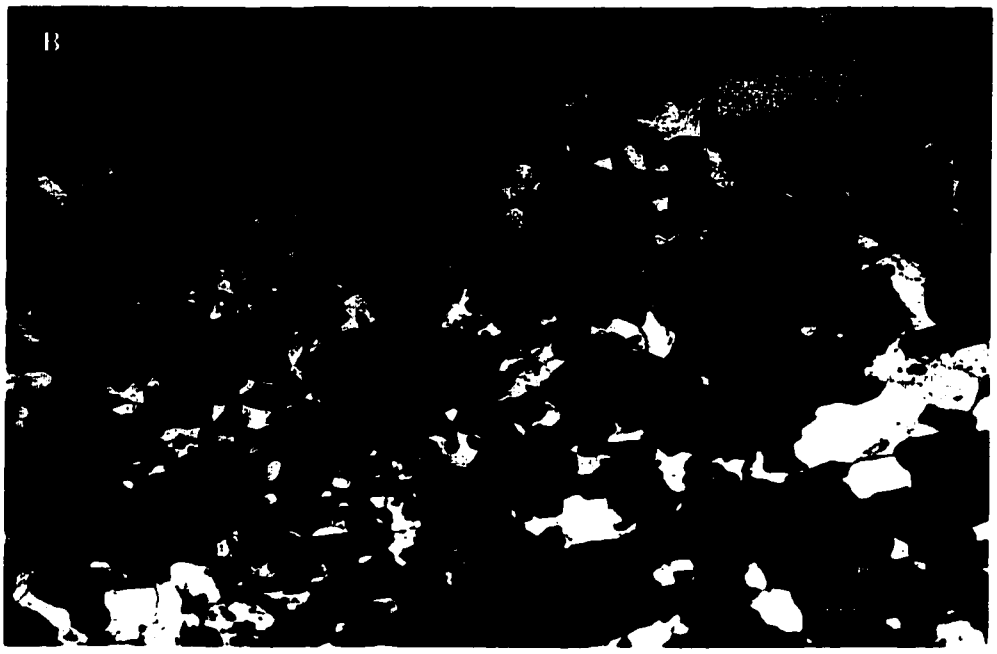
B

Table 6-7: Mineral analyses used for hornblende-plagioclase thermometry

Amphibole	SAMPLE	* J121-A1*	* J121-A2*	* J121-A3*	* J121-A4*	* J734-A1*	* J734-A2*	* J734-A3*	*P857B-A1*	*P857B-A2*	*P857B-A3*	*P857B-A4*	* J133-A1*	* J339-A1*	* J339-A2*	* J339-A3*
	NA2O	1.29	1.37	1.18	1.47	0.97	1.17	1.16	0.80	0.84	0.84	0.73	1.09	0.89	1.03	1.31
	K2O	0.79	0.83	0.69	0.72	0.36	0.62	0.76	0.18	0.18	0.16	0.22	0.92	0.80	1.00	0.71
	FEO	16.06	17.61	18.23	17.66	21.36	21.98	20.76	17.29	18.37	16.28	18.50	17.96	20.75	21.31	21.32
	MGO	8.93	9.06	9.06	9.14	7.16	6.91	6.45	10.69	9.54	11.62	9.31	9.66	7.67	7.41	7.30
	AL2O3	11.45	11.74	10.86	11.52	10.79	11.21	12.48	7.73	8.54	8.60	8.52	10.09	10.06	10.05	11.12
	SIO2	40.99	41.13	41.44	42.17	42.36	42.07	40.60	46.66	45.19	47.51	44.74	42.97	41.81	41.27	41.01
	CAO	11.72	11.31	11.87	11.56	11.74	11.66	11.93	11.99	12.21	11.93	11.99	11.76	11.76	11.85	11.95
	TIO2	1.86	1.97	1.76	1.90	0.73	0.71	0.85	0.78	0.99	0.37	0.61	0.95	0.58	0.99	1.01
	CR2O3	0.04	0.00	0.00	0.00	0.07	0.00	0.09	0.05	0.00	0.00	0.10	0.07	0.13	0.08	0.12
	MNO	0.27	0.43	0.42	0.39	0.78	0.82	0.50	0.22	0.36	0.30	0.25	0.38	0.29	0.41	0.46
	NIO	0.03	0.03	0.00	0.02	0.04	0.04	0.02	0.01	0.01	0.01	0.04	0.00	0.00	0.06	0.02
	F	0.19	0.16	0.10	0.15	0.23	0.18	0.23	0.22	0.00	0.16	0.03	0.13	0.20	0.16	0.03
	CL	0.00	0.00	0.01	0.01	0.06	0.00	0.05	0.01	0.03	0.00	0.02	0.00	0.04	0.01	0.05
	BR2O	0.00	0.00	0.00	0.00	0.13	0.00	0.00	0.00	0.18	0.28	0.00	0.00	0.03	0.09	0.00
	SRO	0.00	0.00	0.00	0.00	0.00	0.00	0.00	0.00	0.00	0.00	0.00	0.00	0.00	0.00	0.00
	BAO	0.20	0.00	0.12	0.00	0.02	0.00	0.04	0.00	0.04	0.00	0.12	0.00	0.22	0.32	0.10
	ZNO	0.00	0.00	0.02	0.00	0.03	0.18	0.15	0.00	0.05	0.05	0.04	0.03	0.03	0.01	0.07
	V2O3	0.02	0.06	0.01	0.06	0.02	0.00	0.09	0.02	0.07	0.06	0.08	0.08	0.14	0.06	0.09
	F2O5	0.00	0.00	0.00	0.02	0.06	0.00	0.00	0.00	0.13	0.01	0.09	0.00	0.15	0.00	0.02
	TOTAL	95.97	97.74	97.77	98.22	97.19	98.92	95.65	98.62	98.36	97.80	97.29	96.09	96.47	98.92	98.58
Feldspar	SAMPLE	* J121-F1*	* J121-F2*	* J121-F3*	* J121-F4*	* J734-F1*	* J734-F2*	* J734-F3*	*P857B-F1*	*P857B-F2*	*P857B-F3*	*P857B-F4*	* J133-F1*	* J339-F1*	* J339-F2*	* J339-F3*
	NA2O	6.73	6.71	5.16	5.60	5.71	5.77	6.01	6.09	1.39	1.87	1.66	4.64	4.52	4.87	5.33
	K2O	0.63	0.67	0.93	0.95	0.84	0.85	0.80	0.01	0.01	0.80	0.02	0.66	0.87	0.11	0.86
	FEO	0.08	0.11	0.16	0.11	0.07	0.16	0.13	0.12	0.03	0.07	0.05	0.16	0.14	0.16	0.18
	CAO	7.76	8.16	10.70	10.15	13.93	9.36	8.02	12.56	17.36	16.78	17.02	11.54	13.23	11.11	13.63
	SIO2	58.17	57.35	54.23	55.52	51.40	55.48	101.27	51.72	64.29	66.05	66.90	53.50	52.15	53.64	50.87
	AL2O3	25.74	26.02	28.25	27.50	30.27	27.20	0.03	30.04	21.60	19.90	19.50	28.88	28.10	28.48	30.76
	BAO	0.53	0.21	0.01	0.00	0.16	0.03	0.00	0.08	0.00	0.13	0.00	0.00	0.05	0.00	0.06
	TOTAL	98.84	98.81	98.46	98.54	99.10	98.21	101.46	98.63	98.95	99.10	99.63	99.78	98.03	98.36	99.11

Amphibole	SAMPLE	* J804-A1*	* J804-A2*	* J804-A3*	* J356-A1*	* J356-A2*	* J356-A3*	* J310-A1*	* J310-A2*	* J310-A3*
	NA2O	0.99	0.99	0.95	0.92	0.87	1.02	1.06	1.19	1.10
	K2O	0.36	0.29	0.29	0.76	0.75	0.80	0.51	0.42	0.36
	FEO	17.05	16.87	16.18	15.36	14.97	15.83	22.26	22.34	22.99
	MGO	10.43	10.50	10.50	12.10	11.87	11.22	6.55	6.21	6.26
	AL2O3	10.07	10.20	9.52	9.20	9.10	10.02	11.23	11.78	11.51
	SIO2	44.64	44.76	45.22	45.54	45.04	45.75	42.14	41.34	41.25
	CAO	11.46	11.56	11.88	12.26	12.62	11.96	12.00	11.93	11.64
	TIO2	0.90	0.77	0.75	0.68	0.78	1.01	0.76	0.61	0.70
	CR2O3	0.13	0.03	0.09	0.08	0.04	0.07	0.03	0.00	0.08
	MNO	0.19	0.24	0.23	0.23	0.34	0.36	0.29	0.32	0.31
	NIO	0.04	0.00	0.03	0.10	0.02	0.02	0.07	0.04	0.05
	F	0.19	0.08	0.13	0.29	0.17	0.16	0.27	0.15	0.13
	CL	0.00	0.03	0.04	0.01	0.00	0.00	0.01	0.04	0.03
	BR2O	0.06	0.00	0.03	0.00	0.02	0.06	0.06	0.05	0.06
	SRO	0.00	0.00	0.00	0.00	0.00	0.00	0.00	0.00	0.00
	BAO	0.00	0.00	0.29	0.55	0.00	0.35	0.00	0.08	0.00
	ZNO	0.07	0.07	0.06	0.02	0.00	0.13	0.16	0.06	0.13
	V2O3	0.08	0.01	0.14	0.02	0.10	0.10	0.08	0.11	0.02
	F2O5	0.02	0.00	0.00	0.07	0.00	0.16	0.13	0.00	0.09
	TOTAL	96.60	96.17	96.33	97.87	96.56	97.29	97.35	95.97	96.25
Feldspar	SAMPLE	* J804-F1*	* J804-F2*	* J804-F3*	* J356-F1*	* J356-F2*	* J356-F3*	* J310-F1*	* J310-F2*	* J310-F3*
	NA2O	6.90	6.26	7.44	6.27	5.89	6.66	8.17	8.95	8.92
	K2O	0.08	0.02	0.01	0.08	0.12	0.09	0.05	0.05	0.05
	FEO	0.12	0.08	0.08	0.06	0.14	0.16	0.12	0.09	0.09
	CAO	11.87	12.90	15.79	12.54	9.78	11.70	8.87	7.51	7.65
	SIO2	52.90	51.68	47.87	52.07	55.10	52.98	56.30	58.26	58.06
	AL2O3	28.91	29.57	32.44	29.36	27.27	29.14	26.37	25.17	25.36
	BAO	0.00	0.00	0.00	0.08	0.15	0.13	0.00	0.05	0.03
	TOTAL	99.27	99.11	98.61	98.67	98.54	99.78	97.78	98.52	97.95

Table 6-8: Results from hornblende-plagioclase thermometry.
Table b compares the average temperatures from various units, panels, and the Sturgeon greenstone belt

	TEMPERATURE (Celsius)	
SAMPLE	T1 (edenite-tremolite)	T2 (edenite-richterite)
"J804-A1"	723	564
"J804-A2"	717	584
"J804-A3"	745	588
"J510-A1"	760	630
"J510-A2"	741	611
"J510-A3"	771	647
"P857B-A1"	747	591
"P857B-A2"	950	739
"P857B-A3"	839	602
"P857B-A4"	917	716
"J121-A1"	811	622
"J121-A2"	780	570
"J121-A3"	856	744
"J121-A4"	759	652
"J734-A1"	775	643
"J734-A2"	754	658
"J734-A3"	741	512
"J339-A1"	788	685
"J339-A2"	836	736
"J339-A3"	907	775
"J356-A1"	761	597
"J356-A2"	744	656
"J356-A3"	783	677
"J135-A1"	774	606
"J135-A2"	855	591

Table b: T2 Edenite-richterite

Sample	**Assemblage**	Average T	Standard deviation
j804	Sturgeon	579	12
j510	Hilltop Lake	629	17
p857b	Mountairy Lake	662	76
j121	Brightsand River	647	72
j734	Rude Lake	604	80
j339	Scruffy Lake	732	45
j356	Stinson	643	41
j135	Northern	599	10
	Location (panel)		
-	Sturgeon belt	579	12
-	Southern panel	648	57
-	Central panel	660	80
-	Northern panel	626	38

Figure 6-11: Histogram of temperatures determined with T2 (Holland and Blundy. 1994). Thick horizontal bar denotes average temperature, shown with standard deviation.

Temperatures obtained from hornblende - plagioclase thermometry. Calculations follow method of Holland and Blundy, 1994.

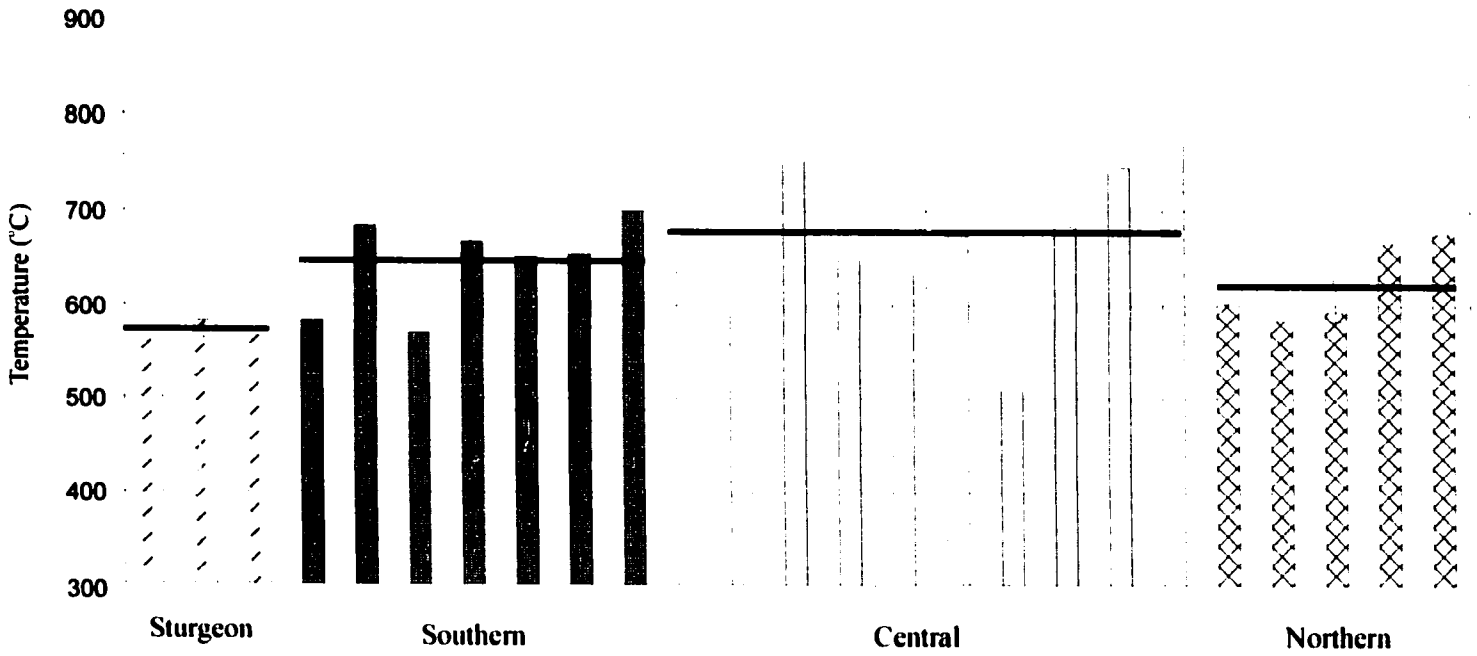

Thick horizontal line is the average temperature for a data set, with standard deviation.

Figure 6-12: Pressure-temperature-time path from ~2700 Ma to 2670 Ma. Dates referred to are in Ma, zm=metamorphic zircon, zi=igneous zircon, t=titanite. Following the deposition of sediment at 2701 Ma, the area was buried to a depth of 15 km and heated to ca. 650°C. Metamorphic zircon of 2697 Ma (Davis, 1990) in tonalite gneiss is the same age as 2697 Ma granodiorite that cross-cuts S3. Monazite grains (2687 – 2694 Ma) from sillimanite – pelite used to determine peak metamorphic conditions may indicate prolonged high temperature or circulation of hydrothermal fluids during cooling. Cooling between D3 and D4 is indicated by biotite overgrowths in D3a Hilltop Creek Fault; reheating occurred during D4 (M2). The 2688 Ma Wapikaimaski Lake pluton (V. McNicoll, unpublished result) is cut by D4a shear zones. Titanite ages shown (2685, 2670 Ma from Percival et al., 1999b) reflect cooling subsequent to deformation and metamorphism. Cooling ages for titanite taken from Heaman and Parrish, (1991)

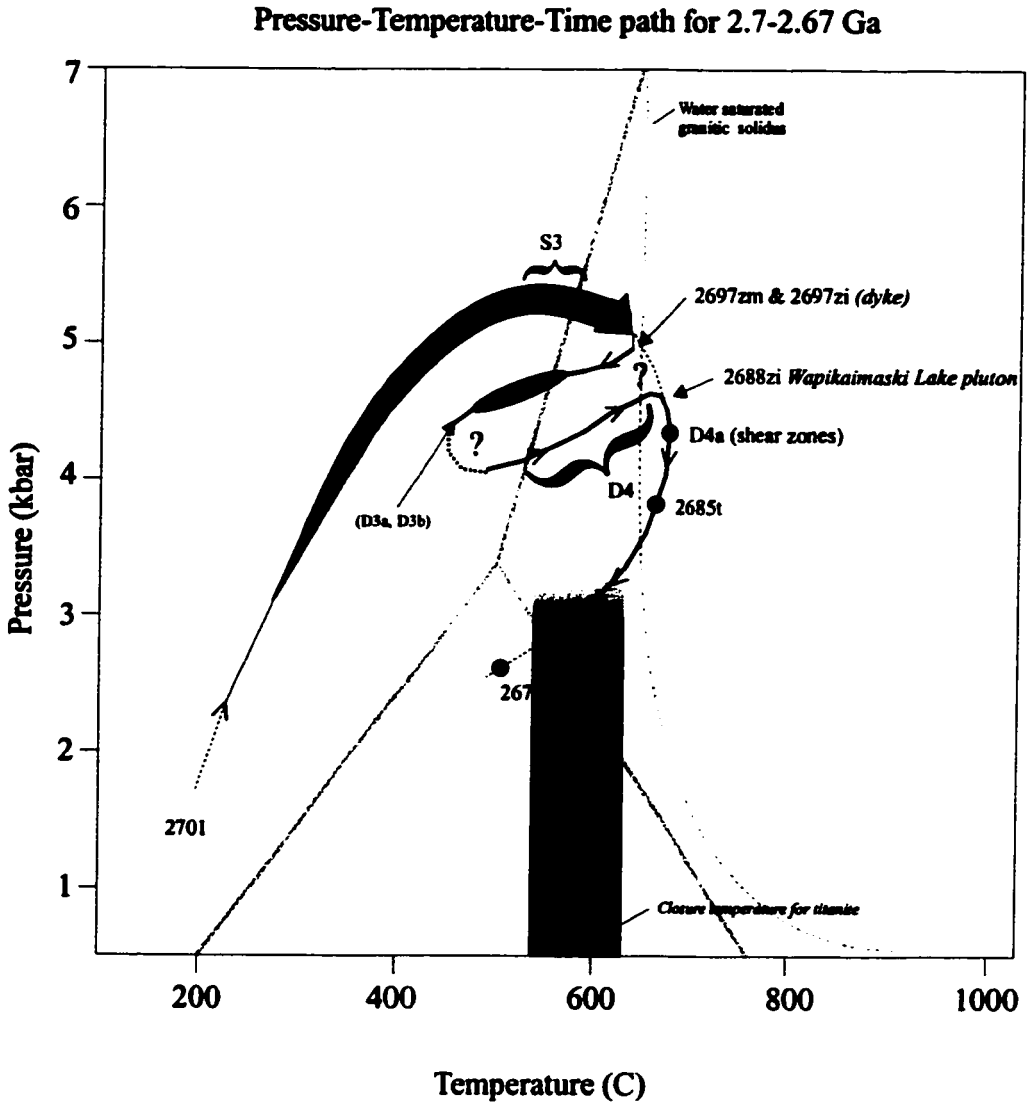
Pressure-Temperature-Time path for 2.7-2.67 Ga
Pressure (kbar)
Temperature (C)
7
6
5
4
3
2
1
200
400
600
800
1000
Water saturated granitic solidus
S3
2697zm & 2697zi (dyke)
2688zi Wapikaimaski Lake pluton
D4a (shear zones)
D4
2685t
(D3a, D3b)
?
?
267
2701
Closure temperature for titanite

CHAPTER 7: SUMMARY AND CONCLUSIONS

This chapter will integrate the results and interpretations of the preceding chapters, summarizing regional correlations and local constraints on deformation and metamorphism. A regional model, which includes those constraints defined for the evolution of the Brightsand Forest area, is proposed for Neoarchean tectonism from 2725 to 2670 Ma.

CORRELATION OF MAP UNITS: SUMMARY OF INTERPRETATIONS

Southern Panel

Amphibolite is continuous beneath sporadic glacial cover with lower grade massive and pillowed mafic volcanic rocks in the southeastern portion of the Sturgeon Lake greenstone belt. Southern panel amphibolites are correlated with the South Sturgeon and Central Sturgeon volcanic assemblages in the Sturgeon Lake greenstone belt on the basis of observed along-strike continuity and geochemical similarity, where data is available. Correlation of the Mountairy Lake amphibolite to volcanic rocks of the South Sturgeon assemblage is also possible. Fine-grained plagioclase-porphyritic gabbro dykes and sills are common within the South Sturgeon assemblage, representing part of the submarine caldera complex of Morton et al. (1991). Likewise, the southern panel amphibolites, most notably on Mountairy Lake, contain layer-parallel tectonized, intermediate rock units (likely andesitic in composition), similar to gabbros of the South Sturgeon assemblage. The Hilltop Lake amphibolite is correlated with the Central Sturgeon assemblage, interpreted as an intravolcanic rift sequence by Sanborn-Barrie and

Skulski (1999). High TiO_2 contents characterize some Central Sturgeon basalts, and are also recognized in the Hilltop Lake amphibolite (Chapter 3).

The southern and northern sedimentary groups of the southern panel are correlated on the basis of strike continuity with the < 2720 Ma Princess-Post and ca. 2720 Ma Quest Lake sedimentary groups respectively (Chapter 2).

Central Panel

Central panel rocks are more difficult to correlate with known units to the west owing to structural discontinuities and ambiguous geochemical affinities with the Sturgeon Lake greenstone belt. It is possible that some units, if not all, are equivalent to Jutten group continental margin volcanic rocks in the Sturgeon Lake-Savant Lake greenstone belt. In particular, the Rude Lake amphibolite package trace element signatures (Chapter 3) are indistinguishable from those of Jutten group volcanic rocks located to the northwest.

Quartz-rich metasedimentary rocks within the central panel were deposited after 2701 Ma. These rocks are similar in age to <2701 Ma quartz-rich arenites of the Princess-Post assemblage, <2704 Ma greywacke turbidites of the Savant sedimentary group, <2703 Ma greywackes of the Awkward Lake assemblage in the Obonga Lake greenstone belt, and <2706 Ma conglomeratic rocks of the Onaman-Tashota belt (Sanborn-Barrie et al., 2002; Sanborn-Barrie and Skulski, 1999; Tomlinson et al., 2002: Stott et al., 2002; and Percival et al., 2002). These data are plotted according to location on Fig. 7-1.

The fine-grained, 2707 Ma felsic sill west of Rude Lake exhibits similar trace element characteristics to proximal granodiorites of the central Wabigoon granitoid

corridor, dated at 2709 Ma 25 km to the north (Whalen et al., in press), and 2703 Ma dacite in the northern Obonga greenstone belt (Tomlinson et al., 2002). Two possibilities exist for the origin of this sill, within the context of models proposed for the generation of the Obonga dacite and central Wabigoon granodiorite. Tomlinson et al. (2002) suggested that the Obonga dacite could be the Archean equivalent of a Cenozoic adakite and that its genesis therefore involved a slab melt component. More likely, the felsic sill is a higher-level expression of granodioritic plutonism, interpreted by Whalen et al. (in press) to represent continental arc magmatism.

Northern Panel

Trace element geochemical profiles of amphibolite units in the northern panel are most similar to those of the Brightsand River and Scruffy Lake amphibolite units within the central panel (Chapter 3). Both the northern and central panel amphibolite units compare favourably with mafic units of the Jutten group. Hornblende-tonalite (Th) may represent an early phase of magmatism, as it carries D1 through D4 structures. It could correlate with similarly complex tonalite gneisses on Harmon Lake dated at ca. 2.89, 2.774, and 2.72 Ga (McNicoll, unpublished data 1999).

Significance of the Hilltop Creek fault zone

Cataclastic rocks in the Hilltop Creek fault zone are distinctive in that they preserve evidence of pre-D4 brittle deformation. Brittle D3 structures were overprinted by late D3 ductile features, and S4 foliation defined by M2 mineral growth. It is possible that this zone marks the transition from oceanic rocks in the southern panel to continental rocks within the central and northern panels. However, the Hilltop Creek fault is a late feature, and the collision between the west and central Wabigoon would pre-date the

development of this structure by >10-25 million years. Therefore, the Hilltop Creek fault is unlikely to be the surface expression of the enigmatic suture proposed by Sanborn-Barrie and Skulski (1999) to lie beneath the Savant sedimentary group within the Sturgeon-Savant belt, although it may lie along the same boundary.

REGIONAL CORRELATION OF DEFORMATION

Polyphase ductile deformation has been documented in several greenstone belts and gneissic domains in the Wabigoon subprovince, and is summarized in Fig. 7-1. Also included for comparison is the southern margin of the Winnipeg River subprovince, most notably in the Lake of the Woods area. Evidence for Mesoarchean deformation comes from gneisses in the Winnipeg River subprovince. Neoarchean (ca. 2715 Ma) deformation structures have been inferred within supracrustal and plutonic gneissic rocks in the western, central, and eastern Wabigoon subprovince. At ca. 2.7 Ga, deposition of metasedimentary rocks is related temporally to a subsequent, regionally penetrative ductile deformation (D3 of this study) that affected most rock types. D4 variably affected the rocks of the Wabigoon subprovince.

TECTONIC EVOLUTION OF THE BRIGHTSAND FOREST AREA

The Brightsand Forest area is located within the boundary region between the western and central Wabigoon subprovince. Large scale features of subprovince boundaries have parallels at many greenstone belt margins, and the study area is of two-fold significance in this respect. It is located at the margin of a greenstone belt, while also straddling the boundary between domains of broadly juvenile Neoarchean rocks to

the west, and granitoid rocks with Mesoarchean ancestry in the west. The implications of this study regarding the Neoarchean assembly of the western and central Wabigoon hinges on the history of deformation and metamorphism as constrained by field relationships and geochronology.

Observations from the Sturgeon Lake greenstone belt and Brightsand Forest area suggest that the central and western Wabigoon subprovince may have evolved as a common entity, at least since ca. 2725 Ma. In Chapter 5, early deformation (D1 and D2) in the map area was bracketed between 2725 and 2715 Ma. Constraints from the Pipestone Lake area, 225 km to the southwest, in the western Wabigoon subprovince (Fig. 7-1), indicate an early deformation event between 2727 and 2712 Ma (Edwards and Stauffer, 1999). In the Lake of the Woods area, thrusting of north-western Wabigoon greenstones onto the sialic Winnipeg River subprovince occurred by 2709 Ma (Davis and Smith, 1991). Further evidence that collision between western Wabigoon greenstones and older continental crust occurred prior to ca. 2710 Ma includes the presence of 3 Ga zircon in <2716 Ma sedimentary rocks of the Warclub group near the northern margin of the western Wabigoon (Davis, 1996), and the presence of 2802 Ma inherited zircon in 2708 Ma igneous rocks (Davis and Smith, 1991), in the northwestern Wabigoon subprovince (see Chapter 5).

The inference that collision between the western and central Wabigoon domains occurred prior to 2710 Ma brings into question the significance of sedimentary rocks deposited ca. 2.7 Ga throughout the Wabigoon subprovince (Fralick et al., 1992), including the Sturgeon Lake-Savant Lake belt, Obonga belt, Onaman-Tashota belt and Brightsand Forest area. Previous interpretations of these rocks as foredeep deposits

related to a ca. 2700 Ma ocean-continent collision (Sanborn-Barrie and Skulski, 1999) are seemingly not valid. However, < 2.701 Ga sedimentary rocks were rapidly buried to 15 km depths and heated by 2697 Ma, implying a close linkage between sedimentation and tectonic activity. Figure 7-2 illustrates convergence between the western and central Wabigoon with schematic sections at different time intervals. The main features of the tectonic evolution model include:

1) Initial collision of the western Wabigoon with the central Wabigoon subprovince occurred by ca. 2710 Ma (at the latest, Fig. 7-2i). This resulted in production of ductile D1 and D2 structures in central Wabigoon plutonic rocks and pre-D1 folds within the Sturgeon Lake belt. South of the Wabigoon subprovince, northward subduction (of a presumed oceanic plate) is inferred from 2745-2718 Ma arc and arc-rift volcanism in the Sturgeon Lake greenstone belt.
2) A subduction zone reversal at ca. 2700 Ma resulted in the obduction of the putative oceanic plate onto the Wabigoon subprovince. This was accompanied by the widespread deposition of foredeep sediments on hot arc crust; rapid burial, deformation (D3) and metamorphism (M1) (Fig 7-2ii,iii).
3) N-S compression after 2690 Ma generated open east-trending F4 folds, producing regional uplift of the central Wabigoon subprovince (Fig. 7-2iv)

There are few constraints on the orientation of ca. 2710 Ma convergence which produced early penetrative deformation structures in the map area. It is apparent from structural evidence in the Rude Lake tonalite gneiss (TgR) and hornblende tonalite (Th)

that there were two phases to this deformation: D1 and D2. Because they are inferred to be related to collision between the western and central Wabigoon subprovince, these structures might reflect a change in convergence (from oblique and(or) transpressive to direct or vice versa).

Widespread deposition of sedimentary rocks occurred throughout the Wabigoon subprovince between <2.706 and <2.701 Ma (Fralick and Davis, 1999; Stott et al., 2002, Sanborn-Barrie and Skulski, 1999, Tomlinson et al., 2002; Chapter 4). An unknown terrane, possibly made up of oceanic crust, may have been obducted onto the Wabigoon subprovince, providing a mechanism for rapid burial and metamorphism to amphibolite facies in areas where the underlying crust had been recently magmatically active. The upper plate invoked in this model may have been removed by erosion, or remnants could be preserved in fold keels.

North - south directed compression after 2.69 Ga produced open east-trending F4 folds and it is possible that fragments of the upper plate illustrated in Figure 7-2ii,iii could be preserved within synformal structures created during D4. The geometry of several small greenstone belts in the central Wabigoon subprovince supports this hypothesis: the Heaven Lake, Garden Lake, Lumby Lake, and Obonga Lake greenstone belts. In particular, the northern assemblage of the Obonga belt fulfills many of the criteria required to be considered part of the klippe of the overriding plate postulated in Figure 7-2. In addition to being fault bounded, the northern Obonga assemblage is constrained by geochronology to have erupted between 2724 and 2703 Ma, which is permitted by the timing prediction of the tectonic model (Fig. 7-2ii,iii). Also, perhaps most significantly, Nd isotope data (e.g. Fig. 3-4) indicate that these rocks were not

contaminated by continental crust. Therefore, the northern Obonga assemblage volcanic rocks are viable candidates to be part of an overriding, oceanic plate, that was thrust over the central Wabigoon (including the older, crustally contaminated southern Obonga assemblage volcanics) at ca. 2700 Ma. North-south D4 shortening allowed these rocks to be preserved in a synformal keel.

Late D3 thrusting along the Hilltop Creek fault elevated the central and northern panels. Subsequent E - W compression formed the Mountairy Lake fold and parasitic structures not shown on Figure 7-2. F4 folding led to regional uplift and cooling that is associated with the termination of D4 (Fig. 7-2iv). These events were followed by sinistral-normal oblique dip slip offset between the central and northern panel along the Robert Lake fault, and the regional Brightsand River and Wapikaimaski Lake shear zones that developed at this time.

CONCLUSIONS

1) Amphibolite units in the Brightsand Forest area are correlated with volcanic assemblages in the Sturgeon Lake greenstone belt using direct evidence from mapping, and indirect evidence from geochemistry.
2) U-Pb geochronology of major and minor rock types provides constraints on the absolute timing of four episodes of Neoarchean deformation.
3) The metamorphic history of the area consists of 2 separate thermal events. Peak metamorphism (M1; ca. 2700 Ma) was coincident with S3 fabric development, and was followed by a period of cooling. Subsequent reheating (M2; ca. 2688 Ma) was related to D4.
4) The main structural-metamorphic history of the study area followed the deposition of sedimentary rocks at ca. 2700 Ma: burial, M1 metamorphism during D3 deformation; minor cooling; D3a; D3b; M2 metamorphism during D4 deformation; and uplift and cooling to < 550°C by ca. 2670 Ma.
5) The model proposed for the western-central Wabigoon boundary zone unites the western and central domains through a D1 collision as early as 2725 Ma. Obduction of oceanic rocks from the south is the suggested mechanism to account for deposition and rapid burial of ca. 2700 Ma sediments and underlying composite terrane.

Figure 7-1: Correlation of deformation events in the Wabigoon subprovince. Deformation chronologies are linked by colour across the Wabigoon. Also shown, are sedimentary rocks deposited after 2706-2701 Ma.

1,2: *Lake of the Woods greenstone belt, Kenora gneisses; Corfu, 1988 and Melnyk et al., 2000*
3: *Pipestone Lake area; Edwards and Stauffer, 1999*
4: *Lac Seul, Miniss River area; Bethune et al., 2000*
5: *Onaman-Tashota greenstone belt; Stott et al., 2000*
6,7: *Warclub group, Savant sedimentary group; Davis 1996*


D1 <2725
D2 >2714
D3 <2701, >2697
50
0
50
100
km

Figure 7-2

i) Initial collision of the western Wabigoon with the central Wabigoon was accomplished by ca. 2710 Ma.
ii) Subduction reversal south of the Wabigoon. Oceanic rocks are obducted onto the Wabigoon subprovince.
iii) Rapid burial ensues, including over-ridden foredeep sediments.
iv) N-S compression generates open east-trending folds, driving uplift and exhumation.

i: ~ 2725 - 2710 Ma

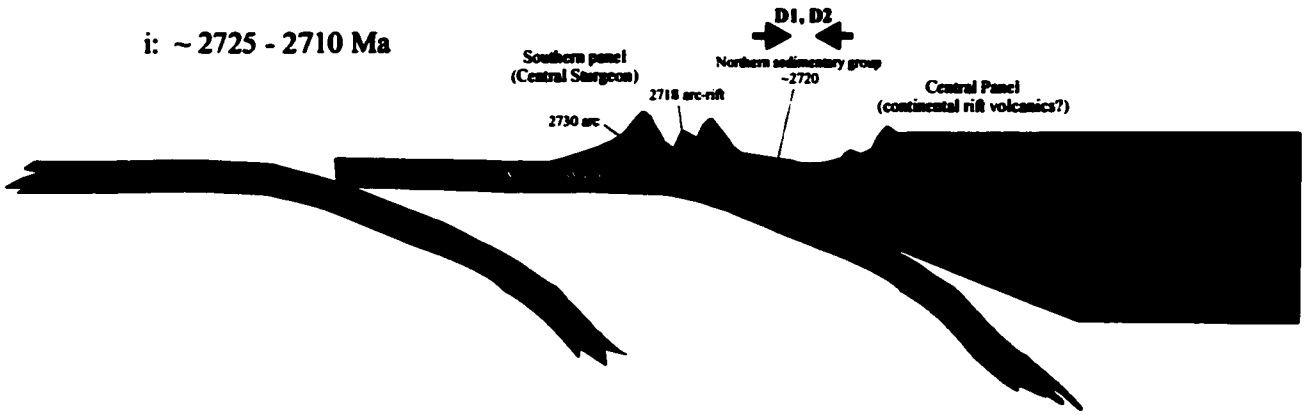

ii: 2710-2700 Ma

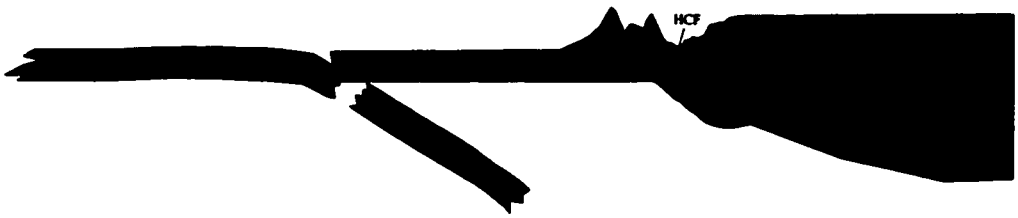

Subduction reversal

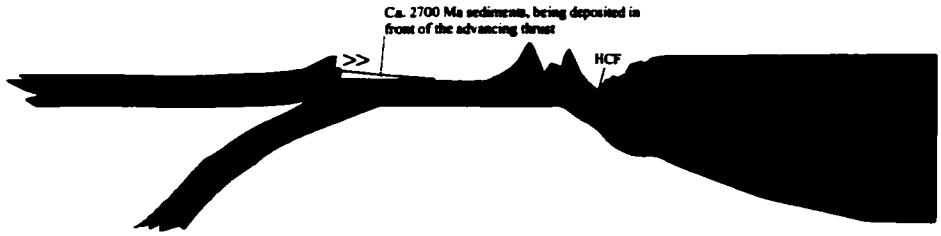

iii: ca. 2700 Ma

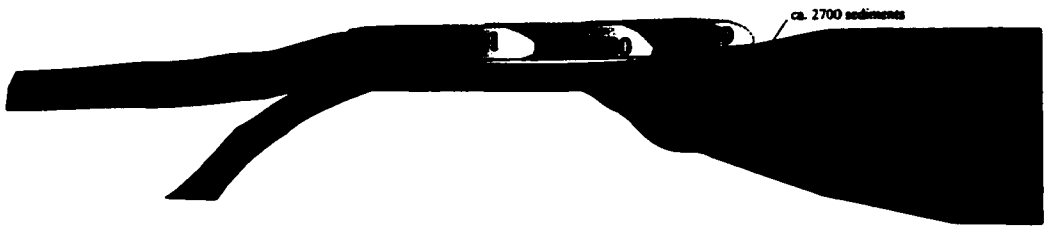

iv: <2697 Ma > 2685 Ma upright folding (F4) -schematic representation

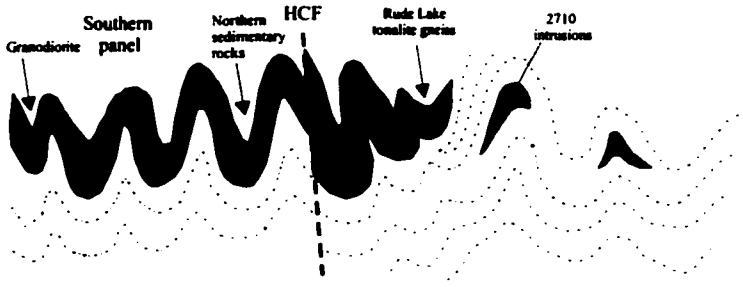

REFERENCES

Anhaeusser, C.R., Mason, R., Viljoen, M.J., and Viljoen, R.P., 1969. A reappraisal of some aspects of Precambrian Shield geology. Geological Society of America Bulletin 80: 2175 – 2200.

Arndt, N., Ginibre, C., Chauvel, C., Albarede, F., Cheadle, M., Herzberg, C., Jenner, G., and Lahaye, Y., 1998. Were komatiites wet? Geology, 26: 739-742.

Ayres, L.D., 1978. Metamorphism in the Superior Province of northwestern Ontario and its relationship to crustal development . *In:* Fraser, J.A. and Heywood, W.W. (Eds.), Metamorphism in the Canadian Shield, Geological Survey of Canada Paper, 78-10: 25-36.

Ayres, L.D. and Thurston P.C., 1985. Archean supracrustal sequences in the Canadian Shield – an overview. *In* Ayers, L.D., Thurston, P.C., Card, K.D., and Weber, W. (Eds.), Evolution of Archean supracrustal sequences, Geological Association of Canada Special Paper 28: 343-370.

Beakhouse, G.P., 1988. The Wabigoon – Winnipeg River subprovince boundary problem; *in* Summary of Field Work and Other Activities, Ontario Geological Survey Miscellaneous Paper 141, pp.108-115.

Berman, R.G., 1988. Internally-consistent thermodynamic data for minerals in the system Na_2O-K_2O-CaO-MgO-FeO-Fe_2O_3-Al_2O_3-SiO_2-TiO_2-H_2O-CO_2. Journal of Petrology, 29: 445-522.

_____, 1990. Mixing properties of Ca-Mg-Fe-Mn garnets. American Mineralogist, 75: 328-344.

_____, 1991. Thermobarometry using multi-equilibrium calculations: a new technique with petrological applications. Canadian Mineralogist, 29: 833-855.

Bethune, K.M., Helmstaedt, H., and McNicoll, V., 2000. U-Pb geochronology bearing on the timing and nature of deformation along the Miniss River fault. *In:* Harrap, R.M. and Helmstaedt, H. (Eds.), Western Superior Transect Sixth Annual Workshop, Lithoprobe Report # 77. Lithoprobe Secretariat, University of British Colombia, pp. 8-12.

Blackburn, C.E., Johns, G.W., Ayer, J.A., and Davis, D.W., 1991. Wabigoon subprovince. *In:* Geology of Ontario, Ontario Geological Survey Special Volume 4, Part 1, pp. 303-382.

Blundy, J.D. and Holland, T.J.B., 1990. Calcic amphibole equilibria and a new amphibole-plagioclase geothermometer. Contributions to Mineralogy and Petrology, 104: 208-224.

Brown, J.L., Percival, J.A., McNicoll, V., White, D., and Tomlinson, K.Y., 1999. Granite-greenstone relationships at the southeastern Sturgeon belt margin in the Brightsand Forest area, Ontario. *In:* Geological Survey of Canada Paper, 2000-C19, 10p. (CD-ROM).

Brown, J.L., Percival, J.A., White, D., and McNicoll, V., 2000. Structure and evolution of the western-central Wabigoon subprovince boundary zone at the southeastern Sturgeon belt margin, Brightsand Forest, Ont. *In:* R.M. and Helmstaedt, H. (Eds.), Western Superior Transect Sixth Annual Workshop, Lithoprobe Report # 77. Lithoprobe Secretariat, University of British Colombia, pp. 19-24.

Brown, J.L. and Percival, J.A., 2002. Geology, southeast Sturgeon Lake greenstone belt, Brightsand Forest area. Geological Survey of Canada, Open File Map 4286, scale 1: 25 000.

Calvert, A.J., Sawyer, E.W., Davis, W.J., and Ludden, J.N., 1995. Archean subduction inferred from seismic images of a mantle suture in the Superior Province. Nature 375: 670-674.

Campbell, M., 2000. Magnetics as a Mapping Tool. B.Sc. thesis, University of Ottawa.

Campbell, M., Roest, W.R., Brown, J.L, and Percival, J.A., 2000. Magnetic as a mapping tool. *In:* Harrap, R.M. and Helmstaedt, H. (Eds.), Western Superior Transect Sixth Annual Workshop, Lithoprobe Report # 77. Lithoprobe Secretariat, University of British Colombia, pp. 25-28.

Card, K.D., 1990. A review of the Superior Province of the Canadian Shield, a product of Archean accretion. Precambrian Research, 48: 99-156.

Card, K.D. and Ciesielski, A., 1986. Subdivisions of the Superior Province of the Canadian Shield. DNAG #1, Geoscience Canada, 13: 5-13.

Condie, K.C., 1984. Archean geotherms and supracrustal assemblages. Tectonophysics, 105: 29-41.

Condie, K.C., 1997. Plate tectonics and crustal evolution. Butterworth – Heinemann, 282p.

Condie, K.C., 1995. Episodic ages of greenstones: A key to mantle dynamics. Geophysical Research Letters, 22: 2215-2218.

Corfu, F., 1988. Differential response of U-Pb systems in coexisting accessory minerals, Winnipeg River Subprovince, Canadian Shield: Implications for Archean crustal growth and stabilization. Contributions to Mineralogy and Petrology, 98: 312-325.

Corfu, F., Stott, G.M., and Breaks, R., 1995. U-Pb geochronology and evolution of the English River Subprovince, an Archean low P-high T metasedimentary belt in the Superior Province. Tectonics, 14: 1220-1233.

Coryell, C.D., Chase, J.W., and Winchester, J.W., 1963. A procedure for geochemical interpretation of terrestrial rare-earth abundance patterns. Journal of Geophysical Research, 68; 2: 559-566.

Cruden, A.R., Ciceri, D., Robin, P.Y.F., 1997. Structural and Geochronological relationships between the Winnipeg River and Wabigoon subprovinces: Implications for the Terrane Accretion Model. *In:* Harrap, R.M. and Helmstaedt, H. (Eds.), Western Superior Transect Fourth Annual Workshop, Lithoprobe Report # 63. Lithoprobe Secretariat, University of British Colombia, pp.54-62.

Cruden, A.R., Davis, D.W., Melny, M., Robin, P.-Y.R., and Menard, T., 1998. Structural and geochronological observations at Kenora: Implications for the style and timing of deformation during the Kenoran orogeny, NW Ontario. *In:* Harrap, R.M. and Helmstaedt, H. (Eds.), Western Superior Transect Fifth Annual Workshop, Lithoprobe Report # 65. Lithoprobe Secretariat, University of British Columbia, pp. 54-62.

Davis, D.W., 1989. Precise U-Pb age constraints on the tectonic evolution of the western Wabigoon Subprovince, Superior Province, Ontario. Unpublished EMR Research Agreement no. 99, Final Report.

_____ 1990. Geological study of the Winnipeg River-Wabigoon Subprovince boundary. Unpublished EMR Research Agreement no. 45, Final Report.

_____ 1996. Provenance and depositional age constraints on sedimentation in the western Superior transect area from U-Pb ages of zircons. *In:* Harrap, R.M. and Helmstaedt, H. (Eds.), Western Superior Transect Third Annual Workshop, Lithoprobe Report # 53. Lithoprobe Secretariat, University of British Colombia, pp. 18-23.

Davis, D.W. and Edwards, G.R., 1982. Zircon U-Pb ages from the Kakagi Lake area, Wabigoon subprovince, northwest Ontario. Canadian Journal of Earth Science, 19:1235-1245.

Davis, D.W. and Trowell, N.F., 1982. U-Pb zircon ages from the eastern Savant Lake-Crow Lake metavolcanic-metasedimentary belt, northwest Ontario; Canadian Journal of Earth Science, 9: 868-877.

Davis, D.W., Krogh, T.E., Hinzer, J., and Nakamura, E., 1985. Zircon dating of polycyclic volcanism at Sturgeon Lake and implications for base metal mineralization. Economic Geology, 80: 1942-1952.

Davis, D.W., Poulsen, K.H, and Kamo, S.L., 1989. New insights into Archean crustal development from geochronology in the Rainy Lake area, Superior Province, Canada. Journal of Geology, 97: 379-398.

Davis, D.W. and Smith, P.M., 1991. Archean gold mineralization in the Wabigoon Subprovince, a product of crustal accretion: evidence from U-Pb geochronology in the Lake of the Woods area, Superior Province, Canada. Journal of Geology, 99: 337-353.

Davis, D.W. and Moore, M., 1991. Geochronology in the Western Superior Province, Jack Satterly Geochronology Laboratory, Royal Ontario Museum, unpublished Summary Report.

Davis, W., McNicoll, V., Bellerive, D.R., Santowski, K., and Scott, D.J., 1997. Modified chemical procedures for the extraction and purification of uranium from titanite, allanite, and rutile in the Geochronology Laboratory, Geological Survey of Canada. Geological Survey of Canada Paper,1997-F, pp. 33-35.

DePaolo, D.J. and Wasserburg, G.J., 1976. Nd isotopic variations and petrogenetic models. Geophysical Research Letters, 3: 249-252.

Devaney, J.R. and Williams, H.R., 1989. Evolution of an Archaean subprovince boundary: a sedimentological and structural study of part of the Wabigoon-Quetico boundary in northern Ontario. Canadian Journal of Earth Science, 26: 1013-1026.

de Wit, M.J., 1998. On Archean granites, greenstones, cratons and tectonics: does the evidence demand a verdict? Precambrian Research, 91: 181-226.

de Wit, M.J. and Hynes, A., 1995. The onset of interaction betweeen the hydrosphere and oceanic crust, and the origin of the first continental lithosphere. *In:* Coward, M.P., Reis, A.C. (Eds.), Early Precambrian Processes, Geological Society of London Special Publication, pp. 1-9.

Dickin, A.P., 1995. Radiogenic Isotope Geology. Cambridge University Press. 490p.

Edwards, G.R. and Sutcliffe, R.H., 1980. Archean granitoid terrains of the western Superior Province, Ontario; *in* Program with Abstracts, Geological Association of Canada – Mineralogical Association of Canada, v. 4, p.50.

Edwards, G.R. and Stauffer, M.R., 1999. Polyphase deformation and crustal evolution in the Pipestone Lake area of the Archean Wabigoon Subprovince, Superior Province, Canada. Canadian Journal of Earth Science, 36: 459-477.

Fralick, P. and Davis, D.W., 1999. The Seine-Coutchiching problem revisited; sedimentology, geochronology and geochemistry of sedimentary units in the Rainy Lake and Sioux Lookout areas. *In:* Harrap, R.M. and Helmstaedt, H. (Eds.), Western Superior Transect 1999 Annual Meeting, Lithoprobe Report # 70. Lithoprobe Secretariat, University of British Colombia, pp. 66-75.

Fralick, P., Wu, J., and Williams, H.R., 1992. Trench and slope basin deposits in an Achaean metasedimentary belt, Superior Province, Canadian Shield. Canadian Journal of Earth Science, 29: 2551-2557.

Furhman, M.L. and Lindsley, D.H., 1988. Ternary feldspar modeling and thermometry. American Mineralogist, 73: 210-215.

Fumerton, S.L., 1982. Redefinition of the Quetico Fault near Atikokan, Ontario. Canadian Journal of Earth Science, 19: 222-224.

Guiraud, M. and Powell, R., 1996. How well known are the thermodynamics of Fe-Mg-Ca garnet? Evidence from experimentally determined exchange equilibria. Journal of Metamorphic Geology, 14: 75-84.

Hamilton, W.B., 1998. Archean magmatism and deformation were not products of plate tectonics. Precambrian Research, 91: 143 – 179.

Heaman, L.M. and Parrish, R.R., 1991. U-Pb geochronology of accessory minerals. *In:* Applications of Radiogenic Isotope Systems to Problems in Geology, Mineralogical Association of Canada Short Course Handbook 19, pp. 59-102.

Helmstaedt, H. and Schulze, D.J., 1989. Southern African kimberlites and their mantle sample-implications for Archaean tectonics and lithosphere evolution. Geological Society of Australia Special Publication # 14, pp. 358-368.

Herzberg, C., 1992. Depth and degree of melting of komatiites. Journal of Geophysical Research, 97: 4521-4540.

Hoffman, P.F., 1989. Precambrian geology and tectonic history of North America. *In* Bally, A.W. and Palmer, A.R., (Eds.), The Geology of North America – An overview: Boulder, Colorado, Geological Society of America, The Geology of North America, v. A.

Holdaway, M.J., 1971. Stability of andalusite and the aluminum silicate phase diagram. American Journal of Science, 271: 97-131.

Holland, T.J.B. and Powell, R., 1992. Plagioclase feldspars; activity-composition relations based upon Darken's quadratic formalism and Landau theory. American Mineralogist, 77: 53-61.

Holland, T.J.B. and Blundy, J.D., 1994. Non-ideal interactions in calcic amphiboles and their bearing on amphibole-plagioclase thermometry. Contributions to Mineralogy and Petrology, 116: 433-447.

Cox, R.A. and Indares, A., 1999. Transformation of Fe-Ti gabbro to coronite, eclogite and amphibolite in the Baie du Nord Segment, Manicouagan imbricate zone, eastern Grenville Province. Journal of Metamorphic Geology, 17: 537-555.

Jensen, L.S., 1976. A new cation plot for classifying subalkalic volcanic rocks; Ontario Division of Mines, Miscellaneous Paper 66, 22p.

Jensen, L.S., 1985. Stratigraphy and petrogenesis of Archean metavolcanic sequences, southwestern Abitibi subprovince, Ontario. *In* Ayers, L.D., Thurston, P.C., Card, K.D., and Weber, W. (Eds.), Evolution of Archean Supracrustal Sequences, Geological Association of Canada Special Paper 28: 65-87.

Kretz, R., 1983. Symbols for rock-forming minerals. American Mineralogist, 68: 277-279.

Krogh, T.E., 1982. Improved accuracy of U-Pb ages by the creation of more concordant fractions using an air abrasion technique. Geochimica et Cosmochimica Acta, 46: 631-636.

Krogh, T.E. and Davis, D.W., 1971. Zircon U-Pb ages of Archean metavolcanic rocks in the Canadian Shield. Carnegie Institute of Washington Year Book, Volume 70, pp. 241-242.

Langford, F.F. and Morin, J.A., 1976. The development of the Superior Province of northwestern Ontario by merging island arcs. American Journal of Science, 276: 1023-1034.

Leake, B.E., 1978. Nomenclature of amphiboles. Canadian Mineralogist, 16: 501-520.

Lefebvre, J., Naert, K.A., and Gasparini, C.E., 1978. Coexistence of sillimanite, andalusite and kyanite in felsic to intermediate metavolcanics in the Savant Lake area, District of Thunder Bay, ON. Geological Association of Canada – Mineralogical Association of Canada, Abstracts with Programs, v.10, pp. 442-443.

Lucas, S.B. and St-Onge, M.R., 1995. Syn-tectonic magmatism and the development of compositional layering, Ungava Orogen (northern Quebec, Canada). Journal of Structural Geology, 17: 474-491.

Mader, U.K., Percival, J.A., and Berman, R.G., 1994. Thermobarometry of garnet-clinopyroxene-hornblende granulites from the Kapuskasing structural zone. Canadian Journal of Earth Science, 31: 1134-1145.

McMullin, D.W.A, Berman, R.G., and Greenwood. H.J., 1991. Calibration of the SGAM thermobarometer for pelitic rocks using data from phase-equilibrium experiments and natural assemblages. *In:* Gordon, T.M. and Martin, R.F. (Eds.), Quantitative methods in petrology; an issue in honor of Hugh J. Greenwood. Canadian Mineralogist, 29: 889-908.

Melnyk, M.J., Cruden, A.R., and Davis, D.W., 2000. Structural geometry and deformational chronology of the Kenoara gneisses. *In:* Harrap, R.M. and Helmstaedt, H. (Eds.), Western Superior Transect Sixth Annual Workshop, Lithoprobe Report # 77. Lithoprobe Secretariat, University of British Colombia, pp. 82-89.

Miall, A.D., 1990. Principles of sedimentary basin analysis. New York: Springer-Verlag. 668 p.

Miyashiro. A., Aki, K., and Sengör, A.M.C., 1982. Orogeny. Toronto: John Wiley and Sons. 242 p.

Morton, R.L., Walker, J.S., Hudak, G.J., and Franklin, J.M., 1991. The early development of an Archean submarin caldera complex with emphasis on the Mattabi ash-flow tuff and its relationship to the Mattabi massive sulphide deposit. Economic Geology, 86: 1002-1011.

Nisbet, E.G., Cheadle, M.J., Arndt, N.T., and Bickle, M.J., 1993. Constraining the potential temperature of the Archaean mantle – a review of the evidence from komatiites. Lithos, 30: 291-307.

Parrish, R.R. and Krogh, T.E., 1987. Synthesis and purification of ^{205}Pb for U-Pb geochronology. *In:* G. Faure (Ed.), New Developments and Applications in isotope Geoscience. Chemical Geology, 66:99-102.

Parrish, R.R., Roddick, J.C., Loveridge, W.D., and Sullivan, R.W., 1987. Uranium-lead analytical techniques at the Geochronology Laboratory, Geological Survey of Canada; Geological Survey of Canada Paper, 87: 3-7.

Percival, J.A., 1998. Structural transect of the central Wabigoon subprovince between the Sturgeon Lake and Obonga Lake greenstone belts, Ontario. *In:* Current Research 1998-C; Geological Survey of Canada, p.127-136.

Percival, J.A. and Skulski T., 2000. Tectonothermal evolution of the northern Minto Block, Superior Province, Quebec, Canada. Canadian Mineralogist, 38: 345-378.

Percival, J.A., Castonguay, S., Whalen, J.B., Brown, J.L., McNicoll, V., and Harris, J., 1999a. Geology of the central Wabigoon region in the Sturgeon Lake-Obonga Lake corridor, Ontario. *In:* Current Research 1999-C; Geological Survey of Canada, p. 197-208.

Percival, J.A., Castonguay, S., Whalen, J.B., Brown, J.L., McNicoll, V., and Harris, J., 1999b. Geology, Sturgeon Lake – Obonga Lake area, Ontario; Geological Survey of Canada, Open File 3738, scale 1: 100 000.

Percival, J.A. and Stott, G.M., 2000. Toward a revised stratigraphic and structural framework for the Obonga Lake greenstone belt, Ontario. *In:* Current Research 2000C-22; Geological Survey of Canada, 8 p. (CD-ROM).

Percival, J.A., Whalen, J.B., Tomlinson, K.Y., McNicoll, V., and Stott, G.M., 2002. Geology and tectonostratigraphic assemblages, North Central Wabigoon subprovince, Ontario: Geological Survey of Canada, Open File 4270; Ontario Geological Survey, Preliminary Map P3447, scale 1: 250 000.

Pollack, N.H., 1997. Thermal characteristics of the Archean. *In:* de Wit, M.J. and Ashwal, L.D., (Eds.) Greenstone Belts, Oxford University Press, Oxford, p. 223 – 232.

Pouchou, J.L. and Pichoir, F., 1985. "PAP" (phi-rho-Z) procedure for improved quantitative microanalysis. Microbeam Analysis, 20: 104-106.

Roddick, J.C., 1987. Generalized numerical error analysis with applications to geochronology and thermodynamics. Geochimica et Cosmochimica Acta, 51: 2129-2135.

Roddick, J.C. and Bevier, M.L., 1995. U-Pb dating of granites with inherited zircon; conventional and ion microprobe results from two Paleozoic plutons, Canadian Appalachians. Chemical Geology, 119: 307-329.

Rogers, D.P., 1964. Metionga Lake area; Ontario Department of Mines, Geological Report 24, 53 p.

Rollinson, H.R., 1993. Using Geochemical Data: Evaluation, Presentation, Interpretation. Geochemistry Series, Longman Group Ltd. 352p.

Sanborn-Barrie, M., 1989. Geology of the Savant Lake area. *In:* Summary of Field Work and Other Activities 1989; Ontario Geological Survey, Miscellaneous Paper 146, pp. 54-62.

Sanborn-Barrie, M., 1999. Geology, Geothermometry and Geochronology of the high-P granulite-facies Kramanituar complex, western Churchill Province. Unpublished Ph.D. thesis, Carleton University, Ottawa, On.

Sanborn-Barrie, M., Skulski, T., and Whalen, J.B., 1998. Tectonostratigraphy of central Sturgeon Lake, Ontario: deposition and deformation of submarine tholeiites and

emergent calc-alkaline volcano-sedimentary sequences. *In:* Current Research 1998-C; Geological Survey of Canada, p. 115-126.

Sanborn-Barrie, M. and Skulski, T., 1999. Tectonic assembly of continental margin and oceanic terranes at 2.7 Ga in the Savant Lake-Sturgeon Lake greenstone belt, Ontario. *In:* Current Research 1999-C; Geological Survey of Canada, p. 209-220.

Sanborn-Barrie, M., Skulski, T., Percival, J.A., Stott, G.M., Tomlinson, K.Y., and Davis, D.W., 1999. A suture zone within the Savant-Sturgeon greenstone belt and implications for a pan-Wabigoon superterrane boundary; Geological Association of Canada – Mineralogical Association of Canada, Program with Abstracts 24: 108.

Sanborn-Barrie, M., Skulski. T., Percival, J.A., Whalen, J.B., Brown, J., and McNicoll, V., 2002. Geology and tectonostratigraphic assemblages, western Wabigoon Subprovince, Ontario; Geological Survey of Canada Open File 4255, scale: 1:250 000.

Sandiford, M., 1989. Secular trends in the thermal evolution of metamorphic terrains. Earth and Planetary Science Letters, 95: 85-96.

Scott, D.J., Helmstaedt, H., and Bickle, M.J., 1992. Purtuniq ophiolite, Cape Smith belt, northern Quebec, Canada: A reconstructed section of Early Proterozoic oceanic crust. Geology, 20: 173-176.

Spear, F.S., 1990. Metamorphic Phase Equilibria and Pressure-Temperature-Time Paths. Mineralogical Society of America, Washington, D.C. 799p.

Stern, R.A., 1997. The GSC Sensitive High Resolution Ion Microprobe (SHRIMP): analytical techniques of zircon U-Th-Pb age determinations and performance evaluation. *In:* Geological Survey of Canada, Current Research 1997-F, Radiogenic Age and Isotopic Studies: Report 10, pp 1-31.

Stott, G.M. and Morrison, D., 1995. The geology and tectonic sequence of events in the south-central Onaman-Tashota greenstone belt, east Wabigoon subprovince. *In:* Summary of Field Work and Other Activities 1995, Ontario Geological Survey, Miscellaneous Paper 164, pp. 41-44.

Stott, G.M. and Parker, J.R., 1996. Geology of the Metcalfe Lake area, central Onaman-Tashota greenstone belt, east Wabigoon subprovince. *In:* Summary of Field Work and Other Activities 1996, Ontario Geological Survey, Miscellaneous Paper 166, pp. 46-54.

_____ 1997. Geology and Mineralization of the O'Sullivan Lake area, Onaman-Tashota greenstone belt, east Wabigoon subprovince. *In* Summary of Field Work

and Other Activities 1997, Ontario Geological Survey, Miscellaneous Paper 168, pp. 48-56

Stott, G.M. and Straub, K.H., 1999. The Marshall Lake volcano on the northern margin of the eastern Wabigoon subprovince, northwestern Ontario. *In* Summary of Field Work and Other Activities 1999, Ontario Geological Survey, Open File Report 6000, pp.23-1 – 23-13.

Stott, G. M., Davis, D.W., Parker, J.R., Straub, K.J., and Tomlinson, K.Y., 2002. Eastern Wabigoon Sheet, Contribution to the Western Superior NATMAP Project, Ontario Geological Survey Map, in press.

Stott, G.M., 1997. The Superior Province. *In:* de Wit, M.R. and Ashwal, L. (Eds.), Greestone Belts: Oxford University Press, Oxford, p. 480-507.

Sun, S.-S. and McDonough, W.F., 1989. Chemical and isotopic systematics of oceanic basalts; implications for mantle compositions and processes. *In:* Saunders, A.S. and Norry, M.J. (Eds.), Magmatism in the ocean basins. Geological Society of London, Special Publication 42, pp. 313-345.

Talbot, C.J., 1973. A plate tectonic model for the Archaean crust. Philosophical Transactions of the Royal Society of London, series A., 273: 413-427.

Thurston, P.C., 1968a. Kershaw Lake; Ontario Department of Mines, Map P-458, scale 1: 15 840.

Thurston, P.C., 1968b. Badour Lake; Ontario Department of Mines, Map P-459, scale 1: 15 840.

Thurston, P.C. and Davis, D.W., 1985. The Wabigoon diapiric axis as a basement complex. *In:* Summary of Field Work and Other Activities 1985; Ontario Geological Survey, Miscellaneous Paper 126, p. 138-141.

Thurston, P.C., Osmani, I.A., and Stone, D., 1991. Northwestern Superior Province: Review and Terrane Analysis. *In:* Geology of Ontario, OGS Special Volume 4, Part 1, pp. 81-142.

Tomlinson, K.Y., Davis, D.W., Thurston, P.C., Hughes, D.J., and Sasseville, C., 1999. Geochemistry, Nd isotopes and geochronology from the central Wabigoon subprovince and North Caribou terrane: regional correlations leading toward a Mesoarchean reconstruction. *In:* Harrap, R.M. and Helmstaedt, H. (Eds.), Western Superior Transect 1999 Annual Meeting, Lithoprobe Report # 70. Lithoprobe Secretariat, University of British Colombia, pp. 136-146.

Tomlinson, K.Y., 2000. Neodymium isotopic data from the central Wabigoon subprovince, Ontario: Implications for crustal recycling in 3.1 to 2.7 Ga

sequences. *In:* Geological Survey of Canada, Current Research 2000-F8; Radiogenic Age and Isotopic Studies: Report 13, 10p. (CD-ROM)

Tomlinson, K.Y. and Condie, K.C., 2001. Archean mantle plumes: Evidence from greenstone belt geochemistry. *In:* Ernst, R.E. and Buchan, K.L. (Eds.), Mantle Plumes: Their Identification Through Time. Geolocial Society of America, Special Paper 352, pp. 341-357.

Tomlinson, K.Y., Davis, D.W., Percival, J.A., Hughes, D.J., and Thurston, P.C., 2002. Mafic to felsic magmatism and crustal recycling in the Obonga Lake greenstone belt, western Superior Province: evidence from geochemistry, Nd isotopes and U-Pb geochronology. Precambrian Research, 114: 295-325.

Trowell, N.R., 1983. Geology of the Sturgeon Lake area; Ontario Geological Survey, Report 221, 97 p.

Tracy, R.J., 1982. Compositional zoning and inclusions in metamorphic minerals. *In*: Reviews in Mineralogy Volume 10, Mineralogical Society of America, pp. 355-397.

van Breemen, O., Henderson J.B., Loveridge, W.D., and Thompson., P.H., 1987. U-Pb zircon and monazite geochronology and zircon morphology of granulites and granite from the Thelon tectonic zone, Healey Lake and Artillery Lake map areas, N.W.T. *In:* Geological Survey of Canada Paper 87-1A, pp. 783-801.

Williams, H.R., 1990. Subprovince accretion tectonics in the south-central Superior Province. Canadian Journal of Earth Science, 27: 370-391.

Williams, H.R., Stott, H.M., Heather, K.B., Muir, T.L., and Sage, R.P., 1991. Wawa Subprovince. *In:* Geology of Ontario, Ontario Geological Survey Special Volume 4, Part 1, pp. 485-539.

Williams, H.R., Stott, G.M., Thurston, P.C., Sutcliffe, R.H., Bennett, G., Easton, R.M., and Armstrong, D.K., 1992. Tectonic Evolution of Ontario: Summary and Synthesis. *In*: Geology of Ontario, OGS Special Volume 4, Part 2, pp. 1255-1332.

Whalen, J.B., Percival, J.A. and McNicoll, V. 2002. A mainly crustal origin for tonalitic granitoid rocks, Superior Province, Canada: Implications for late Archean tectonomagmatic processes. Journal of Petrolgy, in press.

York, D., 1969. Least squares fitting of a straight line with correlated errors. Earth and Planetary Sciences, 5: 320-324.

Appendix 1: Geochemical Data

Major element data

Assemblage	Brightsand	Brightsand	Brightsand	Brightsand	Brightsand	Hilltop	Mountain	Mountain	Mountain	Mountain	Northern	Northern	Northern
Sample number	J-384	J-682	PBA98-J120	PBA98-J121	PBA98-P374	J-510	B-1	J-548	J-57	PBA98-857B	J-135	J-536	PBA98-J135
SIO2	47.40	46.70	47.90	49.30	53.30	48.80	53.90	55.60	56.50	50.40	48.60	48.60	49.60
TIO2	1.10	0.92	1.16	1.25	0.68	2.25	0.82	1.29	0.95	1.13	0.98	0.92	0.79
AL2O3	14.70	13.40	14.60	13.50	14.80	13.50	14.30	15.20	15.70	13.80	14.70	14.20	14.90
FE2O3T	13.60	13.00	13.70	15.90	10.70	17.30	12.30	10.60	9.80	13.30	13.60	12.80	12.50
MNO	0.21	0.22	0.21	0.21	0.18	0.23	0.20	0.25	0.10	0.20	0.23	0.22	0.22
MGO	8.13	9.10	5.37	6.52	6.39	4.32	5.26	3.97	4.74	6.62	6.89	8.43	6.55
CAO	11.61	12.91	13.22	10.02	9.94	10.70	11.23	9.27	8.03	11.22	11.39	11.53	12.43
NA2O	2.20	1.80	2.40	2.60	2.90	2.40	1.50	2.90	4.20	2.20	2.60	2.30	2.30
K2O	0.79	1.09	0.49	0.82	0.89	0.44	0.42	0.93	0.17	0.24	0.74	0.68	0.61
CO2T	0.10	-0.10	0.20	0.10	0.10	0.20	-0.10	-0.10	-0.10	0.20	-0.10	-0.10	0.20
P2O5	0.09	0.30	0.10	0.11	0.06	0.22	0.08	0.23	0.17	0.07	0.08	0.07	0.06
ST	0.02	0.08	0.10	0.03	0.05	0.19	0.04	-0.02	-0.02	-0.02	-0.02	-0.02	0.05

Assemblage	Rude	Rude	Rude	Rude	Rude	Rude	Rude felsic	Scruffy	Scruffy	Scruffy	Scruffy	Scruffy	Scruffy
Sample number	J-1000	J-339	J-734	J-772	PBA98-865B	PBA98-J142	J-737	J-316	PBA98-861	PBA98-906	PBA98-J095	PBA98-J115	PBA98-J141
SIO2	50.50	50.10	50.70	46.80	52.40	49.50	71.50	48.70	51.70	49.10	48.80	53.60	50.90
TIO2	1.04	1.10	1.13	0.73	0.82	1.02	0.34	0.65	0.66	0.82	0.77	1.10	0.43
AL2O3	14.90	15.50	13.00	13.40	15.80	15.20	15.10	14.10	14.20	15.30	15.00	17.00	14.30
FE2O3T	13.00	13.50	17.00	15.70	12.70	11.60	1.70	14.70	11.20	13.70	12.60	9.50	9.80
MNO	0.19	0.27	0.58	0.48	0.36	0.32	0.04	0.36	0.23	0.44	0.19	0.25	0.16
MGO	6.82	4.83	4.82	8.30	4.53	4.58	1.22	6.64	6.93	6.71	7.56	3.77	9.29
CAO	10.23	12.41	10.73	13.28	9.75	15.35	1.71	11.41	12.44	10.07	11.79	9.62	11.74
NA2O	2.60	1.80	1.80	1.10	3.00	2.30	5.10	2.20	2.00	2.30	2.50	4.40	2.30
K2O	0.41	0.50	0.47	0.51	0.75	0.48	1.94	0.93	0.45	0.59	0.53	0.61	0.54
CO2T	0.10	-0.10	0.10	-0.10	0.10	0.10	0.10	0.10	0.10	0.10	0.10	0.20	0.10
P2O5	0.09	0.09	0.08	0.07	0.06	0.08	0.07	0.04	0.05	0.06	0.06	0.08	0.04
ST	0.03	0.10	-0.02	-0.02	-0.02	-0.02	0.09	0.02	0.05	0.04	-0.02	-0.02	-0.02

Assemblage	Robert	Robert	Robert	Simson	Simson	Simson	Sturgeon	Sturgeon	Sturgeon
Sample number	J-446	P-780	PBA98-P872B	J-608	PBA98-J132	PBA98-P878	J-804	J-807	J-810
SIO2	49.20	51.20	48.00	55.50	45.40	48.80	50.20	49.00	52.70
TIO2	0.87	0.90	0.79	0.54	0.72	0.93	1.06	0.72	0.71
AL2O3	14.30	14.60	16.20	17.90	13.40	15.10	14.40	12.10	13.20
FE2O3T	12.50	11.20	11.90	7.30	13.30	13.20	13.40	9.20	8.70
MNO	0.22	0.20	0.17	0.11	0.23	0.23	0.19	0.21	0.14
MGO	7.50	6.57	7.84	5.15	9.19	5.74	7.46	11.02	10.33
CAO	13.33	12.77	12.94	8.34	15.33	12.94	11.33	11.33	10.54
NA2O	0.90	2.20	1.60	4.40	1.50	2.40	2.10	2.10	2.90
K2O	0.72	0.39	0.33	0.86	0.45	0.44	0.27	0.63	0.12
CO2T	-0.10	-0.10	0.10	-0.10	0.30	0.10	-0.10	2.20	-0.10
P2O5	0.04	0.07	0.06	0.07	0.05	0.07	0.09	0.27	0.28
ST	0.21	0.07	0.04	-0.02	0.08	0.03	0.07	-0.02	0.18

Trace element data

Assemblage	Brightsand	Brightsand	Brightsand	Brightsand	Brightsand	Hilltop	Mountain	Mountain	Mountain	Mountain	Northern	Northern	Northern
Sample number	J-384	J-682	PBA98-J120	PBA98-J121	PBA98-P374	J-510	B-1	J-548	J-57	PBA98-857B	J-135	J-536	PBA98-J135
AG	0.1	-0.1	0.2	-0.1	-0.1	0.1	-0.1	0.1	-0.1	0.2	-0.1	-0.1	-0.1
BA			88	75	160					70			54
BE	-0.5	0.5	0.5	-0.5	-0.5	0.6	-0.5	0.7	-0.5	-0.5	-0.5	-0.5	-0.5
BI	0.8	0.3	0.6	-0.5	0.5	0.4	0.3	0.6	0.3	-0.5	-0.2	0.3	-0.5
CD	-0.2	-0.2	-0.2	-0.2	-0.2	-0.2	-0.2	-0.2	-0.2	-0.2	-0.2	-0.2	-0.2
CL			117	174	-100					110			116
CO	51	54	62	63	57	51	48	32	33	56	61	53	63
CR	307	336	180	58	300	104	78	69	95	230	249	346	300
CS	0.68	0.88	0.48	0.69	1.80	0.39	1.20	11.00	0.23	0.63	0.29	0.18	0.51
CU	39	93	81	37	57	98	88	20	-10	71	48	35	89
F			533	395	541					180			744
GA	17.00	16.00	18.00	18.00	16.00	21.00	17.00	20.00	19.00	18.00	17.00	16.00	16.00
HF	1.60	2.10	2.00	2.10	1.40	3.00	1.60	3.40	3.00	1.50	1.50	1.30	1.50
IN	0.07	0.09	0.06	0.05	-0.05	0.12	0.07	0.07	0.09	0.07	0.07	0.05	-0.05
MO	0.4	0.3	0.7	0.3	1.7	0.6	0.6	1.0	0.7	0.3	0.7	2.4	0.7
NB	3.60	2.90	4.30	4.40	2.30	7.80	3.30	11.00	8.10	2.50	1.30	2.90	2.20
NI	138	137	95	43	68	50	52	53	60	62	163	157	150
PB	5	6	3	-2	4	2	3	3	1	-2	6	4	3
RB	12.00	14.00	5.50	19.00	26.00	20.00	7.60	74.00	1.10	5.90	8.40	8.60	13.00
SC	39.0	41.0	36.0	44.0	45.0	41.0	36.0	21.0	24.0	43.0	41.0	40.0	42.0
SN	0.7	0.9	0.9	-0.5	-0.5	1.5	0.8	2.6	2.3	0.6	0.8	0.6	-0.5
SR	120	470	160	110	220	170	170	180	260	94	260	100	130
TA	0.25	0.13	0.5	0.5	0.5	0.48	0.22	0.68	0.49	0.4	0.20	0.17	0.3
TH	0.63	4.90	0.90	0.49	0.82	0.81	1.30	1.90	1.40	0.33	0.53	0.54	0.55
TL	0.14	0.16	0.05	0.13	0.19	0.19	0.08	0.55	-0.02	0.05	0.10	0.10	0.09
U	0.46	0.76	0.46	0.17	0.41	0.21	0.49	0.53	0.46	0.08	0.41	0.58	0.34
V	285	282	290	340	260	395	243	166	196	310	289	272	260
ZN	92	104	84	85	63	133	80	79	30	37	111	99	87
ZR	54.0	83.0	72.0	73.0	48.0	120.0	61.0	150.0	130.0	54.0	54.0	46.0	56.0
CE	11.0	86.0	16.0	15.0	14.0	23.0	14.0	36.0	15.0	9.1	18.0	9.5	11.0
DY	4.10	4.30	4.20	4.50	2.60	7.10	3.10	4.60	3.60	3.80	3.80	3.60	3.10
ER	2.60	2.10	2.50	2.90	1.70	4.20	1.80	2.50	2.00	2.50	2.40	2.10	1.90
EU	0.98	2.20	1.10	1.10	0.70	1.79	0.82	1.40	1.30	0.93	1.10	0.87	0.74
GD	3.40	6.10	3.70	4.10	2.40	6.40	2.80	4.60	3.80	3.40	3.20	3.00	2.60
HO	0.87	0.79	0.90	1.00	0.58	1.50	0.65	0.94	0.71	0.89	0.81	0.78	0.65
LA	3.6	36.0	6.9	5.6	7.9	8.3	5.7	15.0	4.7	3.5	6.6	3.7	5.0
LU	0.42	0.31	0.43	0.46	0.28	0.70	0.29	0.40	0.32	0.41	0.39	0.36	0.32
ND	8.0	43.0	11.0	11.0	8.5	17.0	8.3	20.0	13.0	7.6	9.6	7.2	7.4
PR	1.60	11.00	2.20	2.30	2.00	3.50	1.90	4.70	2.40	1.50	2.20	1.40	1.50
SM	2.60	7.90	2.90	3.20	2.10	5.00	2.20	4.40	3.50	2.40	2.40	2.20	1.90
TB	0.61	0.77	0.65	0.74	0.43	1.10	0.48	0.73	0.58	0.65	0.56	0.52	0.48
TM	0.40	0.31	0.39	0.43	0.27	0.67	0.28	0.39	0.32	0.40	0.38	0.35	0.29
Y	26.00	23.00	25.00	27.00	16.00	44.00	19.00	28.00	22.00	25.00	25.00	22.00	18.00
YB	2.70	2.00	2.70	3.00	1.80	4.40	1.90	2.60	2.10	2.60	2.60	2.30	2.10

Trace element data (continued)

Assemblage	Robert	Robert	Robert	Rude	Rude	Rude	Rude	Rude	Rude	Rude felsic	Scruffy	Scruffy	Scruffy
Sample number	J-646	P-780	PBA98-P872B	J-1000	J-339	J-734	J-772	PBA98-865B	PBA98-J142	J-737	J-316	PBA98-861	PBA98-906
AG	-0.1	-0.1	-0.1	0.3	-0.1	0.3	-0.1	0.2	-0.1	-0.1	0.3	-0.1	-0.1
BA			73					150	170			120	790
BE	-0.5	-0.5	-0.5	-0.5	0.5	-0.5	-0.5	-0.5	0.6	0.8	-0.5	-0.5	-0.5
BI	0.5	0.5	0.5	-0.2	0.6	0.4	0.4	-0.5	-0.5	0.3	0.5	-0.5	-0.5
CD	-0.2	-0.2	-0.2	-0.2	-0.2	0.3	-0.2	-0.2	-0.2	-0.2	-0.2	-0.2	-0.2
CL			115					180	119			244	168
CO	52	54	58	52	58	46	46	70	59	-5	89	54	67
CR	268	145	270	294	247	118	351	270	300	30	1080	290	170
CS	3.60	0.87	1.80	0.28	0.27	1.10	1.90	3.00	1.80	1.30	1.10	1.20	2.70
CU	163	81	66	69	69	12	22	14	-10	10	11	43	41
F			359					410	480			503	370
GA	15.00	14.00	17.00	17.00	18.00	18.00	14.00	16.00	16.00	19.00	15.00	15.00	17.00
HF	1.20	1.30	1.30	1.80	1.60	1.70	1.10	1.20	1.70	3.10	1.20	1.30	1.40
IN	0.06	0.06	-0.05	0.08	0.06	0.08	0.05	0.07	-0.05	-0.05	0.05	-0.05	-0.05
MO	0.7	1.9	0.8	0.3	0.7	1.3	2.2	1.6	1.0	0.2	0.1	2.5	0.5
NB	2.30	2.90	3.50	3.20	3.60	3.60	2.20	2.20	2.80	2.00	2.20	2.10	2.30
NI	145	160	180	102	127	44	143	160	110	11	324	72	170
PB	3	4	-2	2	3	4	2	5	2	22	5	2	3
RB	39.00	9.20	9.60	5.10	5.50	14.00	10.00	29.00	15.00	75.00	22.00	7.10	33.00
SC	43.0	44.0	35.0	41.0	41.0	48.0	40.0	39.0	43.0	4.7	49.0	42.0	33.0
SN	0.7	0.7	-0.5	1.1	1.1	1.0	0.6	0.8	0.5	0.6	1.0	-0.5	-0.5
SR	170	120	100	120	120	120	78	150	140	400	180	110	120
TA	0.15	0.17	0.4	0.23	0.21	0.20	0.13	0.4	0.4	0.12	0.19	0.4	0.4
TH	0.30	0.61	0.29	0.45	0.27	0.25	0.37	0.36	0.30	1.90	0.43	0.65	0.25
TL	0.37	0.14	0.11	0.04	0.08	0.13	0.09	0.19	0.08	0.65	0.19	0.08	0.26
U	0.37	0.36	0.24	0.16	0.11	0.26	0.14	0.32	0.11	0.49	0.27	0.18	0.22
V	288	273	240	274	288	322	264	240	290	39	274	250	230
ZN	80	81	70	74	97	196	88	73	97	58	107	82	72
ZR	41.0	43.0	50.0	62.0	54.0	55.0	37.0	41.0	54.0	100.0	41.0	47.0	49.0
CE	7.9	8.9	7.5	8.5	9.9	10.0	7.1	7.5	9.0	18.0	9.2	9.7	7.7
DY	3.50	3.50	3.00	3.70	4.00	4.30	2.90	2.70	3.60	0.40	2.70	2.50	3.50
ER	2.20	2.20	1.90	2.20	2.40	2.80	1.90	1.80	2.20	0.21	1.80	1.60	2.00
EU	0.81	0.79	0.73	0.80	0.93	1.10	0.63	0.74	0.96	0.53	0.63	0.63	0.69
GD	2.80	2.80	2.50	3.20	3.30	3.60	2.40	2.50	3.10	0.75	2.10	2.10	2.80
HO	0.77	0.76	0.64	0.81	0.83	0.99	0.64	0.62	0.76	0.08	0.60	0.57	0.73
LA	3.0	3.5	2.9	2.9	3.8	4.0	2.8	2.9	3.4	9.5	4.0	4.4	3.0
LU	0.35	0.35	0.30	0.38	0.40	0.51	0.31	0.30	0.36	0.04	0.30	0.27	0.34
ND	6.2	6.6	6.0	6.9	7.8	8.1	5.3	6.1	7.7	7.0	5.2	6.1	6.4
PR	1.20	1.30	1.20	1.30	1.50	1.50	1.00	1.20	1.50	2.00	1.20	1.40	1.20
SM	2.10	2.10	1.80	2.20	2.50	2.60	1.70	1.80	2.30	1.10	1.50	1.70	1.80
TB	0.52	0.52	0.48	0.56	0.59	0.64	0.43	0.46	0.60	0.09	0.39	0.41	0.54
TM	0.33	0.35	0.28	0.37	0.37	0.48	0.30	0.28	0.34	0.03	0.29	0.24	0.32
Y	22.00	21.00	19.00	23.00	25.00	29.00	18.00	17.00	22.00	2.50	18.00	17.00	21.00
YB	2.30	2.30	2.00	2.40	2.40	3.20	2.00	1.90	2.30	0.24	2.00	1.70	2.20

Assemblage	Scruffy	Scruffy	Scruffy	Stinson	Stinson	Stinson	Sturgeon	Sturgeon	Sturgeon
Sample number	PBA98-J095	PBA98-J115	PBA98-J141	J-608	PBA98-J132	PBA98-P878	J-804	J-807	J-810
AG	-0.1	-0.1	0.2	-0.1	0.1	0.2	-0.1	-0.1	-0.1
BA	95	170	140		73	69			
BE	-0.5	0.8	-0.5	-0.5	-0.5	-0.5	-0.5	0.8	0.6
BI	-0.5	-0.5	-0.5	-0.2	-0.5	-0.5	0.4	-0.2	-0.2
CD	-0.2	-0.2	-0.2	-0.2	-0.2	-0.2	-0.2	-0.2	-0.2
CL	-100	116	-100		-100	116			
CO	54	70	49	28	69	62	50	56	41
CR	290	270	220	127	600	250	191	842	497
CS	0.27	0.45	1.10	4.60	1.90	0.81	0.28	0.91	0.12
CU	19	20	41	-10	110	56	77	40	51
F	334	634	368		366	555			
GA	15.00	19.00	12.00	16.00	17.00	18.00	17.00	15.00	17.00
HF	1.30	1.80	0.88	1.40	1.20	1.50	1.60	2.60	2.50
IN	-0.05	0.15	-0.05	-0.05	0.06	0.09	0.06	-0.05	0.06
MO	0.4	1.0	0.9	-0.2	0.3	1.1	0.2	0.5	-0.2
NB	2.10	3.80	1.30	4.10	1.70	3.00	1.30	4.50	4.10
NI	110	130	100	106	200	120	116	284	270
PB	-2	7	-2	4	2	-2	-1	5	8
RB	7.50	10.00	10.00	34.00	9.60	8.60	2.70	19.00	0.97
SC	40.0	44.0	42.0	18.0	46.0	18.0	40.0	31.0	21.0
SN	-0.5	1.1	-0.5	-0.5	2.1	1.6	0.7	1.0	2.1
SR	110	110	87	310	190	140	170	400	1000
TA	0.4	0.6	0.2	0.24	0.3	0.4	0.19	0.24	0.21
TH	0.32	0.67	0.22	0.35	0.33	0.28	0.47	5.29	5.80
TL	0.07	0.09	0.07	0.24	0.08	0.08	0.04	0.13	-0.02
U	0.36	0.46	0.09	0.13	0.28	0.15	0.12	1.10	1.20
V	250	290	200	102	280	270	301	196	176
ZN	68	85	45	50	82	84	86	68	71
ZR	45.0	62.0	30.0	56.0	38.0	52.0	0.0	100.0	100.0
CE	7.8	11.0	5.1	9.9	6.0	8.7	11.0	70.0	56.0
DY	3.00	4.00	1.70	2.00	3.00	3.50	4.00	3.50	2.50
ER	1.90	2.50	1.10	1.10	1.80	2.20	2.40	1.60	1.20
EU	0.72	1.10	0.41	0.66	0.68	0.86	0.91	1.70	1.50
GD	2.60	3.70	1.40	2.20	2.40	3.10	3.30	5.50	3.50
HO	0.69	0.87	0.38	0.41	0.64	0.79	0.84	0.60	0.44
LA	3.2	4.8	2.1	4.1	2.4	3.4	4.3	31.0	24.0
LU	0.33	0.41	0.19	0.20	0.28	0.37	0.42	0.21	0.17
ND	6.1	9.1	3.6	6.4	4.8	7.1	8.1	35.0	28.0
PR	1.20	1.80	0.74	1.40	0.90	1.40	1.70	8.60	7.10
SM	1.80	2.70	0.97	1.90	1.70	2.20	2.50	0.90	5.10
TB	0.48	0.66	0.26	0.35	0.46	0.59	0.58	0.68	0.45
TM	0.30	0.39	0.18	0.18	0.28	0.35	0.40	0.24	0.18
Y	19.00	25.00	10.00	12.00	18.00	22.00	25.00	19.00	13.00
YB	2.10	2.70	1.20	1.10	1.90	2.40	2.60	1.40	1.10

Normalized data used in spider diagrams

Assemblage	Brightwood	Brightwood	Brightwood	Brightwood	Brightwood	Hilltop	Monastery	Monastery	Monastery	Monastery	Northern	Northern	Northern
Sample number	J-384	J-682	PBA98-J120	PBA98-J121	PBA98-P374	J-510	B-1	J-548	J-57	PBA98-857B	J-135	J-536	PBA98-J135
Th	7.41	57.65	10.59	5.76	9.65	9.53	15.29	22.35	16.47	3.88	6.24	6.35	6.47
Nb	5.05	4.07	6.03	6.17	3.23	10.94	4.63	15.43	11.36	3.51	4.63	4.07	3.09
Ta	6.10	3.17	12.20	12.20	12.20	11.71	5.37	16.59	11.95	9.76	4.88	4.15	7.32
La	5.24	52.40	10.04	8.15	11.50	12.08	8.30	21.83	6.84	5.09	9.61	5.39	7.28
Ce	6.20	48.45	9.01	8.45	7.89	12.96	7.89	20.28	8.45	5.13	10.14	5.35	6.20
Pr	5.80	39.86	7.97	8.33	7.25	12.68	6.88	17.03	8.70	5.43	7.97	5.07	5.43
Nd	5.91	31.76	8.12	8.12	6.28	12.56	6.13	14.77	9.60	5.61	7.09	5.32	5.47
Zr	4.82	7.41	6.43	6.52	4.29	10.71	5.45	13.39	11.61	4.82	4.82	4.11	5.00
Hf	5.18	6.80	6.47	6.80	4.53	9.71	5.18	11.00	9.71	4.85	4.85	4.21	4.85
Sm	5.86	17.79	6.53	7.21	4.73	11.26	4.95	9.91	7.88	5.41	5.41	4.95	4.28
Eu	5.83	13.10	6.55	6.55	4.17	10.12	4.88	8.33	7.74	5.54	6.55	5.18	4.40
Ti	5.07	4.24	5.35	5.76	3.14	10.38	3.78	5.95	4.38	5.21	4.52	4.24	3.64
Gd	5.70	10.23	6.21	6.88	4.03	10.74	4.70	7.72	6.38	5.70	5.37	5.03	4.36
Tb	5.65	7.13	6.02	6.85	3.98	10.19	4.44	6.76	5.37	6.02	5.19	4.81	4.44
Dy	5.56	5.83	5.70	6.11	3.53	9.63	4.21	6.24	4.88	5.16	5.16	4.88	4.21
Ho	5.30	4.82	5.49	6.10	3.54	9.15	3.96	5.73	4.33	5.43	4.94	4.76	3.96
Y	5.71	5.05	5.49	5.93	3.52	9.67	4.18	6.15	4.84	5.49	5.49	4.84	3.96
Er	5.42	4.38	5.21	6.04	3.54	8.75	3.75	5.21	4.17	5.21	5.00	4.38	3.96
Tm	5.41	4.19	5.27	5.81	3.65	9.05	3.78	5.27	4.32	5.41	5.14	4.73	3.92
Yb	5.48	4.06	5.48	6.09	3.65	8.92	3.85	5.27	4.26	5.27	5.27	4.67	4.26
Lu	5.68	4.19	5.81	6.22	3.78	9.46	3.92	5.41	4.32	5.81	5.27	4.86	4.32

Assemblage	Robert	Robert	Robert	Rude	Rude	Rude	Rude	Rude	Rude	Rude felsic	Scruffy	Scruffy	Scruffy
Sample number	J-486	P-780	PBA98-P872B	J-1000	J-339	J-734	J-772	PBA98-865B	PBA98-J142	J-737	J-316	PBA98-861	PBA98-906
Th	3.53	7.18	3.41	5.29	3.18	2.94	4.35	4.24	3.53	22.35	5.06	7.65	2.94
Nb	3.23	4.07	4.91	4.49	5.05	5.05	3.09	3.09	3.93	2.81	3.09	2.95	3.23
Ta	3.66	4.15	9.76	5.61	5.12	4.88	3.17	9.76	9.76	2.93	4.63	9.76	9.76
La	4.37	5.09	4.22	4.22	5.53	5.82	4.08	4.22	4.95	13.83	5.82	6.40	4.37
Ce	4.45	5.01	4.23	4.79	5.58	5.63	4.00	4.23	5.07	10.14	5.18	5.46	4.34
Pr	4.35	4.71	4.35	4.71	5.43	5.43	3.62	4.35	5.43	7.25	4.35	5.07	4.35
Nd	4.58	4.87	4.43	5.10	5.76	5.98	3.91	4.51	5.69	5.17	3.84	4.51	4.73
Zr	3.66	3.84	4.46	5.54	4.82	4.91	3.30	3.66	4.82	8.93	3.66	4.20	4.38
Hf	3.88	4.21	4.21	5.83	5.18	5.50	3.56	3.88	5.50	10.03	3.88	4.21	4.53
Sm	4.73	4.73	4.05	4.95	5.63	5.86	3.83	4.05	5.18	2.48	3.38	3.83	4.05
Eu	4.82	4.70	4.35	4.76	5.54	6.55	3.75	4.40	5.71	3.15	3.75	3.75	4.11
Ti	4.01	4.15	3.64	4.80	5.07	5.21	3.37	3.78	4.70	1.57	3.00	3.04	3.78
Gd	4.70	4.70	4.19	5.37	5.54	6.04	4.03	4.19	5.20	1.26	3.52	3.52	4.70
Tb	4.81	4.81	4.44	5.19	5.46	5.93	3.98	4.26	5.56	0.83	3.61	3.80	5.00
Dy	4.75	4.75	4.07	5.02	5.43	5.83	3.93	3.66	4.88	0.54	3.66	3.39	4.75
Ho	4.70	4.63	3.90	4.94	5.06	6.04	3.90	3.78	4.63	0.49	3.66	3.48	4.45
Y	4.84	4.62	4.18	5.05	5.49	6.37	3.96	3.74	4.84	0.55	3.96	3.74	4.62
Er	4.58	4.58	3.96	4.58	5.00	5.83	3.96	3.75	4.58	0.44	3.75	3.33	4.17
Tm	4.46	4.73	3.78	5.00	5.00	6.49	4.05	3.78	4.59	0.41	3.92	3.24	4.32
Yb	4.67	4.67	4.06	4.87	4.87	6.49	4.06	3.85	4.67	0.49	4.06	3.45	4.46
Lu	4.73	4.73	4.05	5.14	5.41	6.89	4.19	4.05	4.86	0.54	4.05	3.65	4.59

Assemblage	Scruffy	Scruffy	Scruffy	Stinson	Stinson	Stinson	Sturgeon	Sturgeon	Sturgeon
Sample number	PBA98-J095	PBA98-J115	PBA98-J141	J-608	PBA98-J132	PBA98-P878	J-804	J-807	J-810
Th	3.76	7.88	2.59	4.12	3.88	3.29	5.53	61.18	68.24
Nb	2.95	5.33	1.82	5.75	2.38	4.21	4.63	6.31	5.75
Ta	9.76	14.63	4.88	5.85	7.32	9.76	4.63	5.85	5.12
La	4.66	6.99	3.06	5.97	3.49	4.95	6.26	45.12	34.93
Ce	4.39	6.20	2.87	5.58	3.38	4.90	6.20	19.44	31.55
Pr	4.35	6.52	2.68	5.07	3.26	5.07	6.16	11.16	25.72
Nd	4.51	6.72	2.66	4.73	3.55	5.24	5.98	25.85	20.68
Zr	4.02	5.54	2.68	5.00	3.39	4.64	-	8.93	8.93
Hf	4.21	5.83	2.85	4.53	3.88	4.85	5.18	8.41	8.09
Sm	4.05	6.08	2.18	4.28	3.83	4.95	5.63	15.54	11.49
Eu	4.29	6.55	2.44	3.93	4.05	5.12	5.42	10.12	8.93
Ti	3.55	5.07	1.98	2.49	3.32	4.29	4.89	3.32	3.27
Gd	4.36	6.21	2.35	3.69	4.03	5.20	5.54	9.23	5.87
Tb	4.44	6.11	2.41	3.24	4.26	5.46	5.37	6.30	6.17
Dy	4.07	5.43	2.31	2.71	4.07	4.75	5.43	4.75	3.39
Ho	4.21	5.30	2.32	2.50	3.90	4.82	5.12	3.66	2.68
Y	4.18	5.49	2.20	2.64	3.96	4.84	5.49	4.18	2.86
Er	3.96	5.21	2.29	2.29	3.75	4.58	5.00	3.33	2.50
Tm	4.05	5.27	2.43	2.43	3.78	4.73	5.41	3.24	2.43
Yb	4.26	5.48	2.43	2.23	3.85	4.87	5.27	2.84	2.23
Lu	4.46	5.54	2.57	2.70	3.78	5.00	5.68	2.84	2.30

Appendix 2: Mineral chemical data

Oxides

SAMPLE	"P857B-A1"	"P857B-A2"	"P857B-A3"	"P857B-A4"	"J135-A1"	"J121-A1"	"J121-A2"	"J121-A3"	"J121-A4"	"J734-A1"	"J734-A2"	"J734-A3"	"J339-A1"
SIO2	46 66	45.19	47 51	44 74	42.57	40 99	41.17	41 44	42.17	42.56	42.07	40 40	41 81
AL2O3	7.73	8.54	6 40	8 52	10.49	11 45	11.74	10.86	11.52	10 79	11.21	12.48	10 86
TIO2	0 78	0.59	0 37	0 45	0 93	1 98	1 97	1 76	1.50	0 73	0 71	0.83	0 58
CR2O3	0.00	0 00	0.00	0.10	0.07	0 04	0.00	0 00	0 00	0 07	0 00	0 09	0 13
FEO	17.29	18.37	16.28	18.50	17 96	18.06	17.61	18.23	17.46	21 26	21 98	20 74	20 75
MNO	0 22	0 36	0 30	0 25	0.38	0 27	0 43	0 42	0.39	0 78	0 62	0 50	0 29
MGO	10 69	9 54	11 62	9 35	9 46	8 93	9 06	9 06	9 14	7 16	6 55	6 45	7 67
CAO	11.99	12.21	11 93	11 99	11 76	11 72	11 31	11 87	11 56	11.74	11.68	11 53	11 78
NA2O	0 80	0.84	0 64	0 75	1 09	1 29	1.37	1 18	1 47	0 97	1 17	1 14	0 99
K2O	0.18	0.18	0.16	0 22	0.92	0 79	0 83	0 69	0 72	0 56	0 62	0 74	0 80
F	0.22	0 00	0 16	0 03	0.33	0 19	0 16	0 10	0 15	0 23	0 10	0 23	0 20
CL	0 03	0 03	0.00	0 02	0 00	0 00	0 00	0 01	0 03	0 06	0 00	0 05	0 04
TOTAL	96 60	95 85	95 36	94 92	95 97	95 71	95 65	95 61	96.12	96 91	96 71	95 17	95 91

SAMPLE	"J339-A2"	"J339-A3"	"J804-A1"	"J804-A2"	"J804-A3"	"J356-A1"	"J356-A2"	"J356-A3"	"J510-A1"	"J510-A2"	"J510-A3"	TEST
SIO2	41.27	41.01	44 64	44.76	45.22	45 54	45.04	43.75	42.14	41.24	41.25	43 27
AL2O3	10.96	11.12	10 07	10.20	9 52	9 00	9 18	10.02	11 23	11 78	11.51	9 26
TIO2	0.99	1.01	0.80	0 77	0 75	0 68	0 79	1 01	0 74	0 61	0 70	1.85
CR2O3	0.09	0 12	0 13	0.03	0.09	0 06	0 04	0.07	0 03	0 00	0 08	0.05
FEO	21.31	21.32	17 05	16.87	16.18	15 36	14 97	15 83	22.26	22.34	22.49	15 85
MNO	0 43	0.46	0 19	0 24	0.23	0 27	0 34	0.38	0 29	0.32	0 31	0 28
MGO	7.41	7.30	10.43	10 30	10.50	12.18	11 87	11.22	6 53	6 21	6 28	12.06
CAO	11.85	11.95	11 48	11.56	11 88	12.26	12.40	11.96	12.00	11 33	11 64	11.19
NA2O	1.03	1.21	0 99	0.96	0 95	0 92	0.87	1.02	1 06	1 19	1.10	1 40
K2O	1.00	0 71	0.38	0 29	0 29	0 76	0 75	0 90	0 35	0 42	0 38	1 30
F	0 14	0.03	0.19	0 06	0 13	0 29	0.17	0.16	0 27	0 15	0 13	0 14
CL	0 01	0.03	0.00	0 03	0.04	0 01	0 00	0.00	0 01	0 04	0 03	0 03
TOTAL	96.50	96.28	96.35	96.06	95 76	97 33	96 41	96.32	96.92	95 64	95 88	96 68

Molecular proportions

SAMPLE	"P857B-A1"	"P857B-A2"	"P857B-A3"	"P857B-A4"	"J135-A1"	"J121-A1"	"J121-A2"	"J121-A3"	"J121-A4"	"J734-A1"	"J734-A2"	"J734-A3"	"J339-A1"
SIO2	0.78	0 75	0 79	0 74	0 71	0 68	0 69	0.69	0 70	0 71	0 70	0 67	0 70
AL2O3	0 08	0 08	0.06	0 08	0 10	0 11	0 12	0 11	0 11	0 11	0 11	0 12	0 11
TIO2	0 01	0 01	0.00	0 01	0 01	0 02	0 02	0 02	0 02	0 01	0 01	0 01	0 01
CR2O3	0 00	0.00	0 00	0 00	0.00	0 00	0 00	0 00	0 00	0 00	0 00	0 00	0 00
FEO	0.24	0.26	0 23	0.26	0 25	0.25	0.25	0 25	0 24	0 30	0 31	0.29	0 29
MNO	0 00	0.01	0 00	0.00	0 01	0 00	0 01	0 01	0 01	0 01	0 01	0 01	0 00
MGO	0 27	0 24	0 29	0 23	0 23	0 22	0 22	0 22	0 23	0 18	0 16	0 16	0 19
CAO	0.21	0.22	0 21	0.21	0 21	0 21	0 20	0 21	0 21	0 21	0 21	0 21	0 21
NA2O	0 01	0.01	0 01	0 01	0 02	0 02	0 02	0 02	0 02	0 02	0 02	0 02	0 02
K2O	0 00	0 00	0 00	0 00	0 01	0 01	0 01	0 01	0 01	0 01	0 01	0 01	0 01
F	0.01	0 00	0 01	0 00	0 02	0 01	0 01	0.01	0 01	0 01	0 01	0 01	0 01
CL	0 00	0 00	0 00	0 00	0 00	0 00	0 00	0.00	0 00	0 00	0 00	0 00	0 00
TOTAL	1 61	1 57	1 61	1 56	1 57	1 54	1 54	1 55	1.56	1 55	1 54	1 51	1 54

SAMPLE	"J339-A2"	"J339-A3"	"J804-A1"	"J804-A2"	"J804-A3"	"J356-A1"	"J356-A2"	"J356-A3"	"J510-A1"	"J510-A2"	"J510-A3"	TEST
SIO2	0 69	0 68	0 74	0 74	0 75	0 76	0 75	0.73	0 70	0 69	0 69	0 72
AL2O3	0 11	0 11	0 10	0 10	0 09	0 09	0 09	0 10	0 11	0 12	0 11	0 09
TIO2	0 01	0 01	0 01	0 01	0 01	0 01	0 01	0 01	0 01	0 01	0 01	0 02
CR2O3	0.00	0.00	0 00	0 00	0 00	0 00	0 00	0 00	0 00	0 00	0 00	0 00
FEO	0.30	0.30	0 24	0 23	0 23	0 21	0 21	0 22	0 31	0 31	0 31	0 22
MNO	0 01	0 01	0 00	0 00	0.00	0 00	0 00	0 01	0 00	0 00	0 00	0 00
MGO	0 18	0 18	0 26	0 26	0 26	0 30	0 29	0 28	0 16	0 15	0 16	0 30
CAO	0 21	0 21	0 20	0 21	0 21	0 22	0 22	0 21	0 21	0 20	0 21	0 20
NA2O	0 02	0 02	0 02	0 02	0 02	0 01	0 01	0 02	0 02	0 02	0 02	0 02
K2O	0 01	0 01	0 00	0 00	0 00	0 01	0 01	0 01	0 00	0 00	0 00	0 01
F	0 01	0.00	0 01	0 00	0 01	0 02	0 01	0 01	0 01	0 01	0 01	0 01
CL	0 00	0 00	0 00	0.00	0.00	0 00	0 00	0 00	0 00	0 00	0 00	0 00
TOTAL	1 54	1 53	1 59	1.58	1 58	1 63	1.61	1 59	1 55	1 51	1 52	1 60

Atomic proportions of oxygen from each molecule

SAMPLE	"P857B-A1"	"P857B-A2"	"P857B-A3"	"P857B-A4"	"J135-A1"	"J121-A1"	"J121-A2"	"J121-A3"	"J121-A4"	"J734-A1"	"J734-A2"	"J734-A3"	"J339-A1"
SIO2	1.55	1.50	1.58	1.49	1.42	1.36	1.37	1.38	1.40	1.42	1.40	1.34	1.39
AL2O3	0.23	0.25	0.19	0.25	0.31	0.34	0.35	0.32	0.34	0.32	0.33	0.37	0.32
TIO2	0.02	0.01	0.01	0.01	0.02	0.05	0.05	0.04	0.04	0.02	0.02	0.02	0.01
CR2O3	0.00	0.00	0.00	0.00	0.00	0.00	0.00	0.00	0.00	0.00	0.00	0.00	0.00
FEO	0.24	0.26	0.23	0.26	0.25	0.25	0.25	0.25	0.24	0.30	0.31	0.29	0.29
MNO	0.00	0.01	0.00	0.00	0.01	0.00	0.01	0.01	0.01	0.01	0.01	0.01	0.00
MGO	0.27	0.24	0.29	0.23	0.23	0.22	0.22	0.22	0.23	0.18	0.16	0.16	0.19
CAO	0.21	0.22	0.21	0.21	0.21	0.21	0.20	0.21	0.21	0.21	0.21	0.21	0.21
NA2O	0.01	0.01	0.01	0.01	0.02	0.02	0.02	0.02	0.02	0.02	0.02	0.02	0.02
K2O	0.00	0.00	0.00	0.00	0.01	0.01	0.01	0.01	0.01	0.01	0.01	0.01	0.01
F	0.01	0.00	0.01	0.00	0.02	0.01	0.01	0.01	0.01	0.01	0.01	0.01	0.01
CL	0.00	0.00	0.00	0.00	0.00	0.00	0.00	0.00	0.00	0.00	0.00	0.00	0.00
TOTAL	2.55	2.50	2.53	2.48	2.49	2.48	2.48	2.47	2.50	2.48	2.46	2.44	2.46
	9.02	9.19	9.09	9.29	9.22	9.29	9.27	9.31	9.19	9.26	9.33	9.44	9.36

SAMPLE	"J339-A2"	"J339-A3"	"J804-A1"	"J804-A2"	"J804-A3"	"J356-A1"	"J356-A2"	"J356-A3"	"J510-A1"	"J510-A2"	"J510-A3"	TEST
SIO2	1.37	1.37	1.49	1.49	1.51	1.52	1.50	1.46	1.40	1.37	1.37	1.44
AL2O3	0.32	0.33	0.30	0.30	0.28	0.26	0.27	0.29	0.33	0.35	0.34	0.27
TIO2	0.02	0.03	0.02	0.02	0.02	0.02	0.02	0.03	0.02	0.02	0.02	0.05
CR2O3	0.00	0.00	0.00	0.00	0.00	0.00	0.00	0.00	0.00	0.00	0.00	0.00
FEO	0.30	0.30	0.24	0.23	0.23	0.21	0.21	0.22	0.31	0.31	0.31	0.22
MNO	0.01	0.01	0.00	0.00	0.00	0.00	0.00	0.01	0.00	0.00	0.00	0.00
MGO	0.18	0.18	0.26	0.26	0.26	0.30	0.29	0.28	0.16	0.15	0.16	0.30
CAO	0.21	0.21	0.20	0.21	0.21	0.22	0.22	0.21	0.21	0.20	0.21	0.20
NA2O	0.02	0.02	0.02	0.02	0.02	0.01	0.01	0.02	0.02	0.02	0.02	0.02
K2O	0.01	0.01	0.00	0.00	0.00	0.01	0.01	0.01	0.00	0.00	0.00	0.01
F	0.01	0.00	0.01	0.00	0.01	0.02	0.01	0.01	0.01	0.01	0.01	0.01
CL	0.00	0.00	0.00	0.00	0.00	0.00	0.00	0.00	0.00	0.00	0.00	0.00
TOTAL	2.46	2.45	2.54	2.53	2.53	2.58	2.55	2.53	2.48	2.44	2.44	2.53
	9.37	9.40	9.06	9.08	9.08	8.93	9.02	9.09	9.28	9.43	9.42	9.10

No. anions on basis of 23 oxygens.

SAMPLE	"P857B-A1"	"P857B-A2"	"P857B-A3"	"P857B-A4"	"J135-A1"	"J121-A1"	"J121-A2"	"J121-A3"	"J121-A4"	"J734-A1"	"J734-A2"	"J734-A3"	"J339-A1"
SIO2	14.01	13.83	14.37	13.83	13.06	12.67	12.70	12.84	12.90	13.12	13.07	12.70	13.02
AL2O3	2.05	2.31	1.71	2.33	2.85	3.13	3.20	2.98	3.12	2.94	3.08	3.47	2.99
TIO2	0.18	0.14	0.08	0.11	0.22	0.46	0.46	0.41	0.34	0.17	0.17	0.20	0.14
CR2O3	0.00	0.00	0.00	0.02	0.01	0.01	0.00	0.00	0.00	0.01	0.00	0.02	0.02
FEO	2.17	2.35	2.06	2.39	2.30	2.34	2.27	2.36	2.23	2.74	2.86	2.73	2.70
MNO	0.03	0.05	0.04	0.03	0.05	0.03	0.06	0.06	0.05	0.10	0.08	0.07	0.04
MGO	2.39	2.17	2.62	2.15	2.16	2.06	2.08	2.09	2.08	1.64	1.52	1.51	1.78
CAO	1.93	2.00	1.93	1.99	1.93	1.94	1.87	1.97	1.90	1.94	1.94	1.94	1.97
NA2O	0.12	0.12	0.09	0.11	0.16	0.19	0.20	0.18	0.22	0.14	0.18	0.17	0.15
K2O	0.02	0.02	0.02	0.02	0.09	0.08	0.08	0.07	0.07	0.06	0.06	0.07	0.08
F	0.10	0.00	0.08	0.01	0.16	0.09	0.08	0.05	0.07	0.11	0.05	0.11	0.10
CL	0.01	0.01	0.00	0.00	0.00	0.00	0.00	0.00	0.01	0.01	0.00	0.01	0.01

SAMPLE	"J339-A2"	"J339-A3"	"J804-A1"	"J804-A2"	"J804-A3"	"J356-A1"	"J356-A2"	"J356-A3"	"J510-A1"	"J510-A2"	"J510-A3"	TEST
SIO2	12.87	12.83	13.46	13.53	13.67	13.54	13.53	13.24	13.02	12.95	12.94	13.10
AL2O3	3.02	3.08	2.69	2.73	2.54	2.37	2.44	2.68	3.07	3.27	3.19	2.48
TIO2	0.23	0.24	0.18	0.17	0.17	0.15	0.18	0.23	0.17	0.14	0.16	0.42
CR2O3	0.02	0.02	0.02	0.01	0.02	0.01	0.01	0.01	0.00	0.00	0.01	0.01
FEO	2.78	2.79	2.15	2.13	2.05	1.91	1.88	2.00	2.88	2.93	2.95	2.01
MNO	0.06	0.06	0.02	0.03	0.03	0.03	0.04	0.05	0.04	0.04	0.04	0.04
MGO	1.72	1.70	2.34	2.32	2.37	2.70	2.66	2.53	1.50	1.45	1.47	2.72
CAO	1.98	2.00	1.85	1.87	1.92	1.95	1.99	1.94	1.99	1.91	1.96	1.82
NA2O	0.16	0.18	0.14	0.14	0.14	0.13	0.13	0.15	0.16	0.18	0.17	0.21
K2O	0.10	0.07	0.04	0.03	0.03	0.07	0.07	0.09	0.03	0.04	0.04	0.13
F	0.07	0.02	0.09	0.03	0.06	0.14	0.08	0.08	0.13	0.07	0.06	0.07
CL	0.00	0.01	0.00	0.01	0.01	0.00	0.00	0.00	0.00	0.01	0.01	0.01

No. of ions in formula

SAMPLE	"P857B-A1"	"P857B-A2"	"P857B-A3"	"P857B-A4"	" J135-A1"	" J121-A1"	" J121-A2"	" J121-A3"	" J121-A4"	" J734-A1"	" J734-A2"	" J734-A3"	" J339-A1"
Si	7.00	6.91	7.18	6.92	6.53	6.34	6.35	6.42	6.45	6.56	6.54	6.35	6.51
Al	1.37	1.54	1.14	1.55	1.90	2.09	2.13	1.98	2.08	1.96	2.05	2.31	1.99
Ti	0.09	0.07	0.04	0.05	0.11	0.23	0.23	0.20	0.17	0.08	0.08	0.10	0.07
Cr	0.00	0.00	0.00	0.01	0.01	0.01	0.00	0.00	0.00	0.01	0.00	0.01	0.02
Fe	2.17	2.35	2.06	2.39	2.30	2.34	2.27	2.36	2.23	2.74	2.86	2.73	2.70
Mn	0.03	0.05	0.04	0.03	0.05	0.03	0.06	0.06	0.05	0.10	0.08	0.07	0.04
Mg	2.39	2.17	2.62	2.15	2.16	2.06	2.08	2.09	2.08	1.64	1.52	1.51	1.78
Ca	1.93	2.00	1.93	1.99	1.93	1.94	1.87	1.97	1.90	1.94	1.94	1.94	1.97
Na	0.23	0.25	0.19	0.23	0.33	0.39	0.41	0.35	0.44	0.29	0.35	0.35	0.30
K	0.04	0.04	0.03	0.04	0.18	0.16	0.16	0.14	0.14	0.11	0.12	0.15	0.16
F	0.10	0.00	0.08	0.01	0.16	0.09	0.08	0.05	0.07	0.11	0.05	0.11	0.10
Cl	0.01	0.01	0.00	0.00	0.00	0.00	0.00	0.00	0.01	0.01	0.00	0.01	0.01

SAMPLE	" J339-A2"	" J339-A3"	" J804-A1"	" J804-A2"	" J804-A3"	" J356-A1"	" J356-A2"	" J356-A3"	" J510-A1"	" J510-A2"	" J510-A3"	TEST
Si	6.43	6.42	6.73	6.77	6.83	6.77	6.76	6.62	6.51	6.47	6.47	6.55
Al	2.01	2.05	1.79	1.82	1.70	1.58	1.62	1.79	2.05	2.18	2.13	1.65
Ti	0.12	0.12	0.09	0.09	0.09	0.08	0.09	0.11	0.09	0.07	0.08	0.21
Cr	0.01	0.02	0.01	0.00	0.01	0.01	0.00	0.01	0.00	0.00	0.01	0.01
Fe	2.78	2.79	2.15	2.13	2.05	1.91	1.88	2.00	2.88	2.93	2.95	2.01
Mn	0.06	0.06	0.02	0.03	0.03	0.03	0.04	0.05	0.04	0.04	0.04	0.04
Mg	1.72	1.70	2.34	2.32	2.37	2.70	2.66	2.53	1.50	1.45	1.47	2.72
Ca	1.98	2.00	1.85	1.87	1.92	1.95	1.99	1.94	1.99	1.91	1.96	1.82
Na	0.31	0.37	0.29	0.28	0.28	0.26	0.25	0.30	0.32	0.36	0.33	0.41
K	0.20	0.14	0.07	0.06	0.06	0.14	0.14	0.17	0.07	0.08	0.08	0.25
F	0.07	0.02	0.09	0.03	0.06	0.14	0.08	0.08	0.13	0.07	0.06	0.07
Cl	0.00	0.01	0.00	0.01	0.01	0.00	0.00	0.00	0.00	0.01	0.01	0.01

Edenite-richterite thermometer

SAMPLE	"P857B-A1"	"P857B-A2"	"P857B-A3"	"P857B-A4"	" J135-A1"	" J121-A1"	" J121-A2"	" J121-A3"	" J121-A4"	" J734-A1"	" J734-A2"	" J734-A3"	" J339-A1"
Xt1-Si	0.75	0.73	0.80	0.73	0.63	0.58	0.59	0.60	0.61	0.64	0.63	0.59	0.63
Xt1-Al	0.25	0.27	0.20	0.27	0.37	0.42	0.41	0.40	0.39	0.36	0.37	0.41	0.37
Xm2-Al	0.19	0.23	0.16	0.23	0.21	0.21	0.24	0.20	0.26	0.26	0.29	0.33	0.25
Xa K	0.04	0.04	0.03	0.04	0.18	0.16	0.16	0.14	0.14	0.11	0.12	0.15	0.16
Xa blank	0.75	0.62	0.76	0.65	0.51	0.44	0.44	0.42	0.46	0.56	0.46	0.50	0.48
Xa Na	0.21	0.21	0.18	0.19	0.31	0.38	0.40	0.31	0.40	0.27	0.32	0.35	0.27
Xm4 Na	0.01	0.05	0.01	0.04	0.01	0.01	0.00	0.04	0.02	0.02	0.03	0.00	0.03
Xm4 Ca	0.96	1.00	0.97	0.99	0.97	0.97	0.93	0.99	0.95	0.97	0.97	0.97	0.98
xAb	0.37	0.14	0.17	0.15	0.42	0.61	0.60	0.46	0.49	0.34	0.52	0.45	0.39
x An	0.63	0.86	0.83	0.85	0.58	0.39	0.40	0.53	0.51	0.66	0.48	0.55	0.61
numerator	92.65	90.86	90.09	90.52	101.45	106.01	104.45	103.02	100.84	97.63	96.25	99.27	98.62
den -num	0.08	0.14	0.03	0.12	0.05	0.09	0.04	0.33	0.14	0.10	0.30	0.02	0.20
den -den	5.69	2.47	2.12	2.58	9.53	15.74	14.70	11.56	11.49	7.52	11.87	11.55	9.11
ln term	-4.31	-2.90	-4.21	-3.04	-5.25	-5.12	-5.81	-3.55	-4.43	-4.30	-3.66	-6.55	-3.82
R*ln	-0.04	-0.02	-0.04	-0.03	-0.04	-0.04	-0.05	-0.03	-0.04	-0.04	-0.03	-0.05	-0.03
denominator	0.11	0.10	0.11	0.10	0.12	0.11	0.12	0.10	0.11	0.11	0.10	0.13	0.10
Temperature	858.15	944.48	841.03	929.55	876.24	924.77	867.33	1014.11	925.82	905.14	938.53	784.34	949.93
celsius	585.00	671.33	567.88	656.40	603.09	651.62	594.18	740.96	652.67	631.99	665.38	511.19	676.78

SAMPLE	" J339-A2"	" J339-A3"	" J804-A1"	" J804-A2"	" J804-A3"	" J356-A1"	" J356-A2"	" J356-A3"	" J510-A1"	" J510-A2"	" J510-A3"
Xt1-Si	0.61	0.60	0.68	0.69	0.71	0.69	0.69	0.66	0.63	0.62	0.62
Xt1-Al	0.39	0.40	0.32	0.31	0.29	0.31	0.31	0.34	0.37	0.38	0.38
Xm2-Al	0.22	0.23	0.26	0.29	0.27	0.17	0.19	0.20	0.28	0.33	0.30
Xa K	0.20	0.14	0.07	0.06	0.06	0.14	0.14	0.17	0.07	0.08	0.08
Xa blank	0.39	0.35	0.65	0.63	0.69	0.58	0.55	0.48	0.57	0.50	0.50
Xa Na	0.26	0.30	0.27	0.27	0.26	0.25	0.23	0.28	0.30	0.33	0.28
Xm4 Na	0.05	0.07	0.01	0.01	0.01	0.01	0.02	0.02	0.02	0.03	0.05
Xm4 Ca	0.99	1.00	0.93	0.94	0.96	0.98	1.00	0.97	0.99	0.95	0.98
xAb	0.44	0.32	0.41	0.38	0.22	0.38	0.51	0.41	0.56	0.62	0.63
x An	0.55	0.68	0.58	0.62	0.78	0.62	0.48	0.58	0.44	0.38	0.37
numerator	100.93	100.52	94.65	92.05	92.15	98.49	96.62	99.40	97.81	96.06	96.53
den -num	0.36	0.36	0.05	0.09	0.04	0.05	0.23	0.16	0.22	0.30	0.49
den -den	10.91	8.10	7.78	7.03	3.92	7.31	10.05	8.84	13.16	14.48	14.97
ln term	-3.41	-3.11	-4.96	-4.31	-4.52	-5.01	-3.77	-3.99	-4.11	-3.88	-3.42
R*ln	-0.03	-0.03	-0.04	-0.04	-0.04	-0.04	-0.03	-0.03	-0.03	-0.03	-0.03
denominator	0.10	0.10	0.11	0.11	0.11	0.11	0.10	0.11	0.11	0.10	0.10
Temperature	1004.91	1026.02	835.25	852.51	840.09	865.60	933.93	944.47	920.12	920.22	960.05
celsius	731.76	752.87	562.10	579.36	566.94	592.45	660.78	671.32	646.97	647.07	686.90

Natural Resources Canada | Ressources naturelles Canada

DESCRIPTIVE NOTES

INTRODUCTION

As a contribution to the Western Superior NATMAP project, detailed mapping of the southeastern margin of the Sturgeon Lake greenstone belt area was undertaken in order to further understand the relationship between rocks with Mesoarchean ancestry in the central Wabigoon subprovince and Neoarchean supracrustal rocks of the western Wabigoon subprovince (Fig. 1).

GEOLOGICAL SETTING

The Central Wabigoon subprovince was postulated to represent Mesoarchean basement (Thurston and Davis 1985) to supracrustal units of the western Wabigoon subprovince (Blackburn et al., 1991). Near the interface between these two distinct regions, the Sturgeon Lake – Savant Lake greenstone belt consists of several different volcanic assemblages, which together record a prolonged history, beginning with post ca. 2.9 Ga (Davis and Moore 1991) rifting and formation of the Jutten continental margin sequence. Subsequently, oceanic plateau (2.775 Ga), arc (2.745–2.733 Ga) and arc-rift (2.718 Ga) sequences formed outboard of the continental margin (Sanborn-Barrie and Skulski, 1999; Skulski et al., 1999). Collision between the continental margin sequence and composite oceanic terrane occurred by ca. 2.7 Ga; the interface is marked by the < 2.704 Ga Savant Lake sedimentary group, interpreted as a foredeep sequence (Sanborn-Barrie and Skulski 1999; Skulski et al. 1998). The Obonga Lake greenstone belt is located approximately 40 km east of the map area. It is divided into 3 parts. The southern assemblage is a northward-younging package of mafic and felsic (2.734–2.726 Ga) volcanic rocks (Tomlinson et al. 1999), separated from the northern assemblage by a core zone made up mainly of gabbroic rocks (Sage, 1998) dated at 2.733 Ga (Tomlinson et al. 1999). The northern assemblage consists largely of southward-younging mafic volcanic and metasedimentary units, as well as serpentinite and gabbroic intrusive bodies. Detrital zircon populations from sandstone units provide maximum depositional ages of 2.724 and 2.702 Ga (Tomlinson et al. 1999; Percival et al. 2000). Geochronology and stratigraphic discrepancies require a significant tectonic break between the northern and southern assemblages (Percival and Stott 2000).

Located at the southeastern margin of the Sturgeon Lake greenstone belt, the present map area straddles the interface between the western and central Wabigoon subprovince (Fig. 1). Rogers (1964) first mapped attenuated screens of supracrustal rock extending from the greenstone belt eastward into the map area.

LITHOTECTONIC MAP UNITS

The Hilltop Creek fault (HCF) and Robert Lake fault (RLF)(Fig. 2) divide the map area into lithologically distinct structural panels. From south to north, the grain size of amphibolites increases with the volume of pegmatitic intrusions, suggesting deeper structural levels, at least in the northernmost panel.

NEOARCHEAN SUPRACRUSTAL ROCKS:

SOUTHERN PANEL

Amphibolite of the southern panel (unit As) is fine- to medium-grained, with mineral assemblages containing 70–90% hornblende with subsidiary plagioclase, minor clinopyroxene and garnet, and accessory amounts of titanite, epidote and chlorite. The southern panel amphibolites are continuous along strike to the west with the Central Sturgeon sequence (2.718 Ga arc-rift sequence of Sanborn-Barrie and Skulski 1999). A small unit of relatively massive, coarse-grained gabbro (unit Gb) occurs in the hinge of the map-scale N–S fold centred on Mountairy Lake. This unit is mylonitic in southern Mountairy Lake. North of Mountairy Lake, the amphibolite screen is bound by sedimentary rocks to the south and north. To the south, sedimentary package (unit Sa) consists of sandstone and greywacke, whereas the northern (unit Sb) includes discontinuous units of granitoid clast conglomerate, slate, quartz-rich sandstone and greywacke. Oxide-facies iron formation occurs in proximity to the Hilltop Creek fault. The two sedimentary units can be correlated with the Post and Quest Lake sedimentary packages respectively, of the Sturgeon Lake greenstone belt (Trowell 1983, Skulski et al. 1998). West of the map area, graded bedding and scour features indicate younging to the north in both packages.

East of Mountairy Lake, the Hilltop Creek fault is a < 100m wide cataclastic zone (UNIT C) with fragments of granite, amphibolite, exhalative sedimentary rocks, and silicate-facies iron formation, set in a foliated, fine-grained matrix with abundant chlorite, epidote, hematite, metamorphic rutile, and finely disseminated sulphides.

CENTRAL PANEL

North of the HCF, amphibolite units (unit Ac) are medium-grained with mineral assemblages containing hornblende-plagioclase ± garnet ± clinopyroxene ± epidote ± titanite ± quartz. Plagioclase is variably altered to saussurite. A thick unit of amphibolite associated with quartz-rich sandstone (unit Sq) and conglomerate (unit Sc) is referred to as the Rude Lake package. Conglomerate at the southern edge of the package is in tectonic contact with amphibolite, possibly along a splay of the HCF. The narrow (< 10 m) unit of conglomerate consists of pebble-sized clasts of granodiorite and volcanic rock, and contains thin, quartz-rich, sandy beds. At the northern margin of this supracrustal package, metre-scale layers of quartz-rich, biotite-plagioclase-quartz sandstone (unit Sq) are interlayered with garnetiferous amphibolite. A quartz-rich rock yielded detrital zircon ages between 2.985 and 2.701 Ga (J. Brown and V. McNicoll, unpublished data, 2000, 2001). These rocks were deposited after 2.701 Ga, the age of the youngest grain, and may correlate with the Savant sedimentary group to the west and northern Obonga sediments to the east.

A 2 km thick pod of fine-grained felsic rock occurs within the Rude Lake package. The contacts of the homogeneous, plagioclase-quartz ± biotite ± muscovite ± pyrite rock are not exposed. The felsic unit is associated with muscovite schist, which exhibits N–S crenulations of schistose layers. Zircons from the felsic unit yielded a preliminary U/Pb age of 2707 ± 2 Ma, interpreted as its crystallization age (J. Brown and V. McNicoll, unpublished data, 2000) and provide a minimum age for the Rude Lake mafic package.

D3 deformation eve
Foliated, mediu
it appears to be late-

Granite (unit G):
Late, massive to w
plugs of pegmatite,
through cross-cuttin
(unit Gg).

DEFORMATIO
Within the southea
geochronology and
D1 and D2 struc
fabrics. D1 gneissc
folds. At and north
which is crenulated
Geochronologic
(Percival et al. 1999)
from west of Rude L
The D3 event
undeformed rocks a
migmatitic layering,
biotite-plagioclase-
central panel occu
amphibolite-facies
The Hilltop Cre
cataclastic fabric is
Creek fault represer
extrapolated eastwa
An open, map-s
the Hilltop Creek fa
crenulations. Base
this fold preserve L3
Biotite-muscovi
parallel to the trend
McNicoll, unpublish
D4 structures o
common. Broad hin
whereas limbs of F4
roughly parallel to th
The Wapikaima
structures characte
ductile feature char
style to the regional
U-Pb age of 2678 M
The Hilltop Cre
the regional Wapik
transcurrent movem
the third dimensio
differences in meta
both faults dip steep
a later, north-dippin
faults are probably o

Field assistance
geochronological g
Tomlinson and Joe
proprietary aeromag

Blackburn, C.E., J
1991: Wabigo
p.303–3
Campbell, M., Ros

aformation event (J. Brown and V. McNicoll, unpublished data, 2000).
Foliated, medium-grained diorite to quartz-diorite occurs as dykes and sills. In one locality, south of Scruffy Lake, pears to be late-comagmatic with fine-grained biotite-granite (< 10% biotite).

nite (unit G):

massive to weakly foliated leucocratic granitic rocks (< 5–10% biotite) occur commonly, as dykes, sills, and s of pegmatite, aplite, and medium-grained monzogranite. Several generations of late granites are evident gh cross-cutting relationships. Many of the pegmatites are garnet and muscovite bearing, rarely with tourmaline Gg).

FORMATION AND METAMORPHISM

In the southeastern Sturgeon belt area up to 4 phases of deformation are recognized and constrained by hronology and cross-cutting relationships.

D1 and D2 structures are rarely preserved in the map area owing in part to overprinting by penetrative planar D3 cs. D1 gneissosity, present in gneisses on Harmon Lake and west of Rude Lake, is folded into tight, upright, F2 . At and north of Robert Lake, hornblende-biotite tonalite and tonalite gneiss carry a penetrative S2 foliation h is crenulated into tight to close, locally chevron type F3 folds, in turn openly folded by F4.

Geochronological constraints on D1 and D2 come from a tonalite dyke in central Harmon Lake dated at 2714 Ma cival et al. 1999), which cuts S1 gneissosity and F2 folds, but carries an S3 foliation. The complex tonalite gneiss west of Rude Lake dated at 2723 Ma provides a maximum age for D1.

The D3 event affected most rock types, resulting in the development of a penetrative foliation in previously eformed rocks and folding of heterogeneous, layered rocks into F3 folds. In some areas, S3 foliation is defined by matitic layering, formed near the metamorphic peak. TWQ thermobarometry of garnet-sillimanite-cordierite - te-plagioclase-quartz mineral assemblages in metapelite near Robert Lake suggest peak metamorphism in the ral panel occurred at pressures between 4 and 5 kbar at temperatures of 650 ± 50oC, consistent with hibolite-facies metamorphic conditions.

The Hilltop Creek fault zone is curved at map-scale from NW- to N-trending, while at the outcrop scale, the clastic fabric is crenulated by small-scale, east-trending folds of probable D4 generation. Accordingly, the Hilltop k fault represents a zone of pre-D4 brittle deformation that was subsequently folded. The cataclastic zone can be polated eastward beneath cover to some extent.

An open, map-scale fold centered on Mountairy Lake plunges steeply north and affects bedding, S3 foliation and Hilltop Creek fault. Its trend is at a high angle to regional D4 structures and rocks on its eastern flank exhibit F4 ulations. Based on these observations, this unique fold is inferred to be late D3 in age. Amphibolite units east of old preserve L3 mineral lineations, and exhibit "S" folds that could be parasitic to the Mountairy Lake fold.

Biotite-muscovite granodiorite dykes throughout the central panel cut S3 foliation and layering, and intrude llel to the trend of F4 fold axes (060). Igneous zircon from this rock yielded an age of 2697 Ma (J. Brown and V. Nicoll, unpublished data, 2000), providing an upper limit for D3 deformation in the Brightsand Forest area.

D4 structures occur most commonly as gently ENE-plunging folds, and mesoscale F4 folds of S3 layering are mon. Broad hinge zones are accompanied by shallow-plunging quartz rodding and other mineral lineations (L4), reas limbs of F4 folds are generally steep. Within the central panel, the axial trace of a map-scale F4 synform is hly parallel to the trend of most map units.

The Wapikaimaski Lake and Brightsand River shear zones are east-northeast-trending sinistral ductile D4 ctures characterized by subhorizontal quartz stretching lineations (Percival et al. 1999). The Robert Lake fault is a le feature characterized by steeply- to moderately-dipping east-northeast-trending mineral lineations, similar in to the regional D4 shear zones. Post-tectonic titanite from the Brightsand River shear zone provided a minimum age of 2678 Ma for D4 deformation (J. Brown and V. McNicoll, unpublished data, 2000).

The Hilltop Creek and Robert Lake faults divide the study area into sigmoidal z-shaped panels as they deflect into regional Wapikaimaski Lake and Brightsand River shear zones, consistent with an overall sinistral sense of scurrent movement. Brown et al. (2000) used Lithoprobe seismic data to examine the attitudes of these faults in third dimension, in conjunction with hornblende-plagioclase thermometry of amphibolites to determine rences in metamorphic temperature across the faults and between panels. The resulting interpretation is that faults dip steeply north. The Hilltop Creek fault is a high angle reverse structure, whereas the Robert Lake fault is er, north-dipping feature with normal slip. Therefore the central panel has pop-up geometry, although its bounding s are probably of different generations.

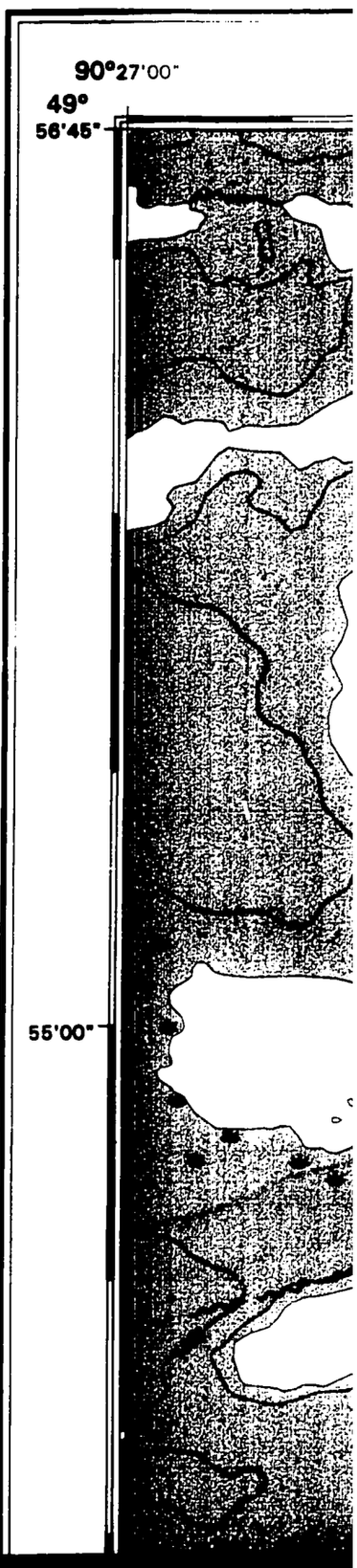

ACKNOWLEDGMENTS

d assistance by Miriam Campbell (1999) is gratefully acknowledged. Vicki McNicoll is thanked for chronological guidance and data. Discussions with Vicki McNicoll, Mary Sanborn-Barrie, Tom Skulski, Kirsty linson and Joe Whalen of the Western Superior NATMAP working group were helpful. Noranda provided prietary aeromagnetic data. The Ontario Ministry of Natural Resources granted access to closed roads.

REFERENCES

kburn, C.E., Johns, G.W., Ayer, J.W. and Davis, D.W.
Wabigoon Subprovince; *in* Geology of Ontario, Ontario Geological Survey, Special Volume 4, Part 1, p.303–381.

pbell, M., Peart, W.R., Brown, J.L. and Percival, J.A.

IP
AT
ce Mapping Program
ile géoscientifique du Canada

LEGEND

ARCHEAN
NEOARCHEAN

FAULT RELATED ROCKS

Cataclasite (Hilltop Creek fault): foliated cataclasite breccia containing angular fragments of granite, amphibolite, exhalative sedimentary rock oxide-facies iron formation, set in a granular, fine-grained matrix consi epidote, hematite, sulphides and metamorphic rutile

INTRUSIVE ROCKS

Granite: medium- to coarse-grained to pegmatitic or aplitic, massive to foliated, biotite ± magnetite granite; occurs as plutons and pegmatite d

Granite: leucocratic with biotite ± muscovite ± garnet granite; occurs as pegmatite dyke swarms

D

Diorite: medium-grained, foliated to migmatitic, hornblende-biotite diori gabbro, quartz diorite, quartz gabbro

Porphyritic granodiorite (ca. 2685 Ma): medium- to coarse-grained, K-f porphyritic or megacrystic, homogeneous, weakly foliated biotite ± horn granodiorite. Varies to monzodiorite, quartz monzodiorite, quartz diorit gabbro

Fs

Felsic sill (2707 Ma): fine-grained, plagioclase-quartz-biotite-pyrite toni with central panel amphibolites; includes some muscovite-biotite pyrite

Granodiorite (ca. 2709 Ma) medium- to coarse-grained, homogeneous, biotite-granodiorite; locally migmatitic with 5-10% leucocratic segregati

Mafic dyke-bearing zone: zone containing medium-grained amphibolit tonalite and tonalite gneiss (units Tg, Th); foliated and transposed adja Robert Lake fault

Gabbroic intrusions: medium- to coarse-grained, weakly to strongly foli mylonitic

Hornblende ± biotite tonalite: medium- to coarse-grained, strongly folia granodiorite; locally hornblende porphyritic

T

Tonalite (ca. 2722-2710 Ma): medium-grained, homogeneous, foliated hornblende tonalite; locally migmatitic (5-10% leucocratic segregations quartz diorite and trondhjemite; may include older homogeneous tonali Ma)

Tonalite orthogneiss: compositionally layered rocks consisting of medi biotite tonalite melanosome and 5-20% leucosome of medium-grained tonalite

USERID: jdohar METAFILE: /homeb/wrk/of4286_ps041402

Date : Wed Dec 4 2002
FType: post
Number of Copies: 1

Time : 14:11
Queue: 36in_check

Panel: Panel 1 of 1
Plotter: 36in_check

ı rounded and
ks, and
isting of chlorite,

o weakly
dyke swarms

ıs plutons and

rite; varies to

-feldspar
rnblende
ite and quartz

nalite associated
e schist

ıs, foliated
ıtions

ite dykes cutting
lacent to the

ɔliated to

iated tonalite to

ɔd biotite ±
ns); varies to
alite (2770-2930

dium-grained
ɔd leucocratic

preliminary U/Pb age of 2707 ± 2 Ma, interpreted as its crystallization age (J. Bi
data, 2000) and provide a minimum age for the Rude Lake mafic package.

Tonalite gneiss

These rocks are fine- to medium-grained biotite-plagioclase-quartz rocks with u
gneissosity is folded by isoclinal F2 folds and overprinted by regional D3 and D4 str

The single tonalite gneiss unit dated in the map area, at Rude Lake (unit T
However, similar rocks east of Harmon Lake (unit Th), 12 km northeast of the map
relationships and geochronology indicating that the gneisses have a protolith a
generation of zircon at ca. 2.883 Ga (V. McNicoll, unpublished data, 1998).

The northernmost amphibolite unit within the central panel is exposed in the
associated with thin units of muscovite-garnet-sillimanite-cordierite metapelite
formation (eif), which can be traced from Robert Lake westward for several kilo
northwest to Hilltop Lake on the basis of aeromagnetic data. In several locations
tectonic contact with granitoid units to the north. The fault zones are charac
extensive epidote alteration, and local brecciation. The Robert Lake fault (RLF) is
separating the northern and central panels. It is characterized by moderately
lineations.

NORTHERN PANEL

Amphibolite (unit An) in the northern panel is coarse-grained with mineral assem
plagioclase-actinolite-titanite-epidote-quartz ± clinopyroxene. Amphibolite units
generations of plutons, and in some areas can be traced only as enclave trains
occur locally. Intense retrograde alteration to chlorite-muscovite-saussurite is
plagioclase after garnet are common.

Ultramafic rocks (unit Um) occur as pods and layers of distinctive coarse-
crystals up to 10 cm in size, associated with gabbroic layers containing nodular plag

NEOARCHEAN INTRUSIVE ROCKS:

Tonalite gneiss (unit Tg):

These rocks are fine- to medium-grained biotite-plagioclase-quartz rocks, with up
mm- to cm-scale banding. Compositional layering is generally parallel to grain-sca
in complex units, or S3 in less complexly deformed bodies. A lens of tonalite gneiss
is the most structurally complex unit in the region, illustrating up to 11 phases o
intrusion (Percival 1998). The oldest phase of this unit yielded a preliminary U-Pb z
and V. McNicoll, unpublished data, 2000).

Homogeneous tonalite (T):

Based on cross-cutting relationships and existing geochronology, several genera
the map sheet. A tonalite body north of Robert Lake (unit Th) can be distinguished
structural complexity. The coarse- to medium-grained hornblende-biotite-plagiocl
or gneissosity, folded into tight F3 folds and overprinted by open F4 warps. A set
Robert Lake cut S2-foliated tonalite, but are cut by granodiorite and granite.

Elsewhere, tonalite has not been subdivided further, as there is insufficient
most part, tonalite bodies are medium-grained plagioclase-quartz-biotite ± hornl
one body east of Harmon Lake was dated at 2774 ± 2 Ma, with metamorphic grains

Medium- to coarse-grained, S3-foliated, homogeneous, biotite tonalite is
throughout the region. A tonalite dyke from Harmon Lake was dated at 2714 Ma (V.
The dyke cuts tonalite gneiss carrying D1 and D2 structures (Percival 1998, Fig. 6).

Granodiorite:

Foliated, medium-grained, homogenous, biotite granodiorite (unit Gd) occurs in t
sheet. It is progressively reworked within the Brightsand River shear zone, and
southern panel. Homogeneous biotite granodiorite from Seseganaga Lake 25 km
Pb age of 2709 Ma (Percival et al., 1999).

Small bodies of coarse-grained, K-feldspar porphyritic, biotite-hornblende gra
to larger plutons to the east of the map sheet (e.g., Wapikaimaski Lake, 2688 Ma; V.

West of Robert Lake, foliated biotite-muscovite granodiorite dykes cross
supracrustal rocks. The dykes intrude along the trend of regional F4 axial traces
S4 foliation. Igneous zircon from one such dyke yielded an age of 2697 Ma, yield

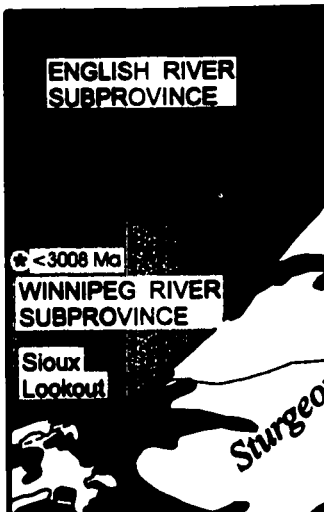

REFERENCES

Blackburn, C.E., Johns, G.W., Ayer, J.W. and Davis, D.W.

1991: Wabigoon Subprovince; *in* Geology of Ontario, Ontario Geological Survey, Special Volume 4, Part 1, p.303–381.

Campbell, M., Reed, W.R., Brown, J.L. and Percival, J.A.

2000: Magnetic as a Mapping Tool; *in* Harrap, R.M. and Helmstaedt, H.H. (eds.). 2000 Western Superior Transect Sixth Annual Workshop. Lithoprobe Report #77, Lithoprobe Secretariat, University of British Columbia, p. 19–24.

Davis, D.W.

1989. Precise U-Pb age constraints on the tectonic evolution of the western Wabigoon subprovince, Superior Province, Ontario. EMR Report No. 99, 30pp.

Davis, D.W. and Moore, M.

1991. Geochronology of the western Superior Province, OGS Summary Report, May 1991

Davis, D.W.

1996. Provenance and Depositional Age Constraints on Sedimentation in the Western Superior Transect Area from U-Pb Ages of Zircons. Lithoprobe Report # 53, p19–23.

Percival, J.A.

1998. Structural Transect of the central Wabigoon subprovince between the Sturgeon Lake and Obonga Lake greenstone belts; *in* Current Research 1998-C; Geological Survey of Canada, p. 127–136.

Percival, J.A., Castonguay, S., Whalen, J.B., McNicoll, V., Brown, J.L., and Harris, J.R.

1999. Geology of the central Wabigoon region in the Sturgeon Lake – Obonga Lake corridor, Ontario; *in* Current Research 1999-C; Geological Survey of Canada, p. 197–206.

Percival, J.A., McNicoll, V. and Stott, G.M.

2000. Revised stratigraphic and structural framework for the Obonga Lake greenstone belt; *in* Harrap, R.M. and Helmstaedt, H.H. (eds.). Western Superior Lithoprobe 2000 Annual Meeting, Lithoprobe Report # 77, Lithoprobe Secretariat, University of British Columbia, p. A1–A2.

Rogers, D.P.

1964. Metionga Lakes Area, Ontario Department of Mines, Geological Report # 24, 53pp.

Sage, R.P.

1996. Operation Ignace – Armstrong, Obonga Lake – Lac des Iles area. Geology of Area II Part 1 – Supracrustal rocks. Ontario Geological Survey Open File Report 5978.

Sanborn-Barrie, M. and Skulski, T.

1999. Tectonic assembly of continental margin and oceanic terranes at 2.7 Ga in the Savant Lake – Sturgeon Lake greenstone belt, Ontario; *in* Current Research 1999-C; Geological Survey of Canada, p. 209–220.

Skulski, T., Sanborn-Barrie, M. and Stern, R.

1998. Did the Sturgeon Lake supracrustal belt form near a continental margin? *in* Harrap, R.M. and Helmstaedt, H.H. (eds.). Western Superior Lithoprobe 1998 Annual Meeting, Lithoprobe Report # 65, Lithoprobe Secretariat, University of British Columbia, p. 87 – 98.

Thurston, P.C. and Davis, D.W.

1985. The Wabigoon diapiric axis as a basement complex; *in* Summary of Field Work and Other Activities 1985; Ontario Geological Survey, Miscellaneous Paper 126, p. 138 – 141.

Tomlinson, K.Y., Davis, D.W., Hughes, D.J., and Thurston, P.C.

1998. The central Wabigoon Subprovince: geochemistry, geochronology and tectonic reconstruction; *in* Harrap, R.M. and Helmstaedt, H.H. (eds.). Western Superior Lithoprobe 1998 Annual Meeting, Lithoprobe Report # 65, Lithoprobe Secretariat, University of British Columbia, p. 35 – 47.

Tomlinson, K.Y., Davis, D.W., Percival, J.A., Hughes, D.J., and Thurston, P.C.

1999. Neoarchean supracrustal development in the Central Wabigoon Subprovince: Nd isotope data and U-Pb geochronology; *in* Harrap, R.M. and Helmstaedt, H.H. (eds.). Western Superior Lithoprobe 1998 Annual Meeting, Lithoprobe Report # 65, Lithoprobe Secretariat, University of British Columbia, p. 147 – 152.

Trowell, N.F.

1983. Geology of the Squaw Lake – Sturgeon Lake area, District of Thunder Bay; Ontario Geological Survey Report #227, 114pp.

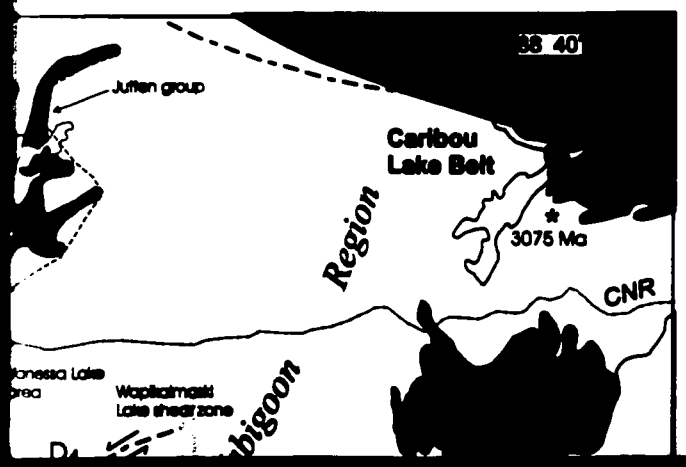

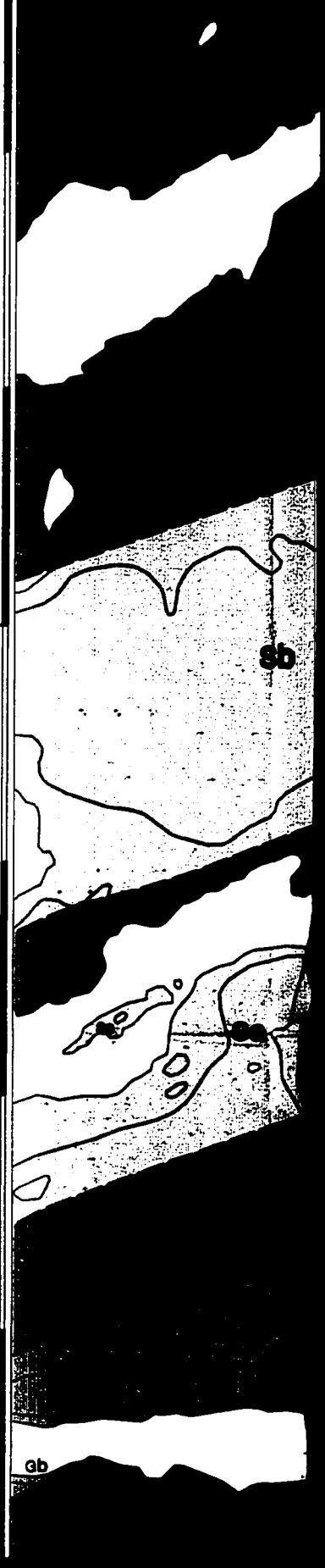


HILLTOP
HILLTOP
MOUNTAIRY

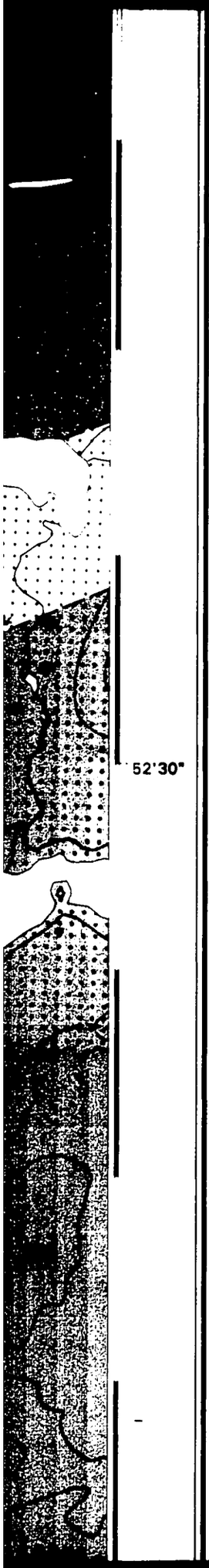

Ma)

Tonalite orthogneiss: compositionally layered rocks consisting
biotite tonalite melanosome and 5-20% leucosome of medium
tonalite

Tonalite orthogneiss ('Rude Lake'): Compositionally layered r
tonalite injected with several generations of leucocratic tonali
Distinguished from tonalite orthogneiss (unit Tg) by complex
including refolded folds

SUPRACRUSTAL ROCKS

SOUTHERN PANEL

Metasedimentary rocks: S, unsubdivided medium- to coarse-
plagioclase-biotite meta-psammite; Sa, fine- to medium-grain
quartz ± muscovite schist, mainly from wacke with minor argi
quartz-rich arenite horizons; Sb, includes granitoid-clast cong
greywacke, and oxide-facies (magnetite) iron formation

Amphibolite, southern panel: fine-, medium- or coarse-graine
plagioclase ± chlorite ± epidote ± garnet ± clinopyroxene schi
from massive and pillowed basalt and andesite; includes som
possible felsic volcanic (<2 m thick) layers

CENTRAL PANEL

Sp

Semipelite: coarse-grained garnet-cordierite-sillimanite schist
associated with oxide and silicate-facies (garnet-grunerite) iro

Conglomerate: clast-supported conglomerate consisting of pe
clasts in a fine-grained matrix varying from biotite- to quartz-,
interlayered with quartz-rich arenite layers. Highly attenuated
Hilltop Creek fault

Sq

Quartz-rich sandstone (<2701 Ma): quartz-plagioclase-biotite
preserved bedding

Amphibolite, central panel: medium- to coarse-grained, folia
plagioclase ± garnet ± quartz ± clinopyroxene ± epidote schis

NORTHERN PANEL

Mafic-ultramafic intrusions: medium-grained, plagioclase porp
includes some very coarse-grained pyroxenite (grain size to 1
northern panel amphibolite units

Amphibolite, northern panel: coarse- to medium-grained, foli
hornblende-plagioclase-quartz-biotite ± clinopyroxene schist
retrograde assemblages of actinolite-plagioclase-epidote an
saussurite

UNSUBDIVIDED UNITS

Amphibolite: medium- to fine-grained, foliated to gneissic hor
biotite schist

SYMBOLS

Geological boundary; compiled from existing sources or interpreted from aeromagnetic data (approximate) . . . . . .

Fault (approximate: 3rd, unknown generation) . . . . . .

Shear zone, D_4 (approximate; sinistral) . . . . . .

Deformation zone (D_4) . . . . . .

Fault zone of uncertain relative age . . . . . .

isting of medium-grained
idium-grained leucocratic

red melanocratic biotite-
onalite and granodiorite.
plex structural character

---

rse-grained quartz-
grained, biotite-plagioclase-
argillaceous beds, includes
conglomerate, breccia, slate,

ained, foliated, hornblende-
schist and gneiss derived
some gabbro, diorite and

chist and paragneiss
e) iron formation (SIF)

of pebble-sized plutonic
rtz-, feldspar-rich;
ated in proximity to the

otite schist with locally

oliated, hornblende-
chist and gneiss

porphyritic metagabbro;
to 10 cm); associated with

foliated to gneissic,
hist and gneiss; common
and fine-grained chlorite-

hornblende-plagioclase-

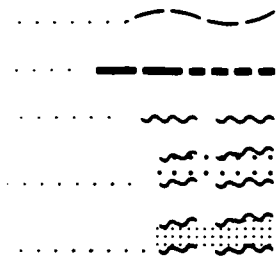

04140916.ps

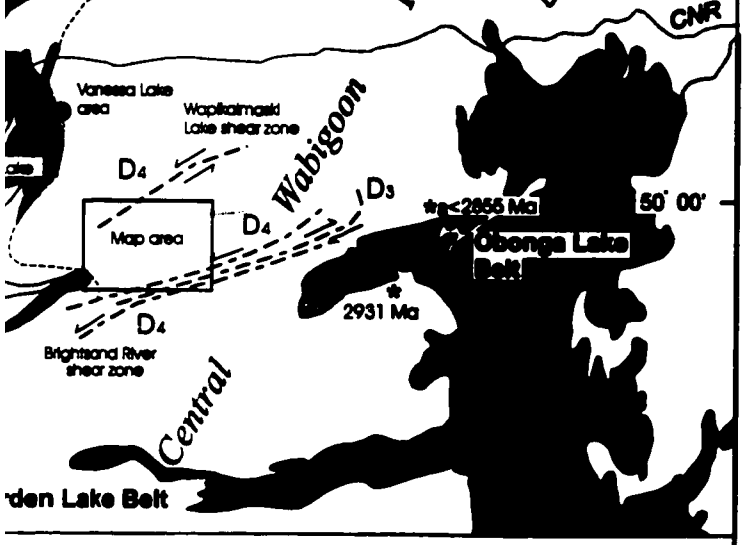

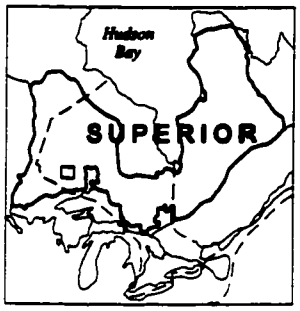

Location map of Figure 1 within Superior Province

cks
olcanic rocks
d gabbros
neissic rocks

boundary * dated locality

joon Region. The Savant Lake and Sturgeon Lake
ary with the Western Wabigoon Region.

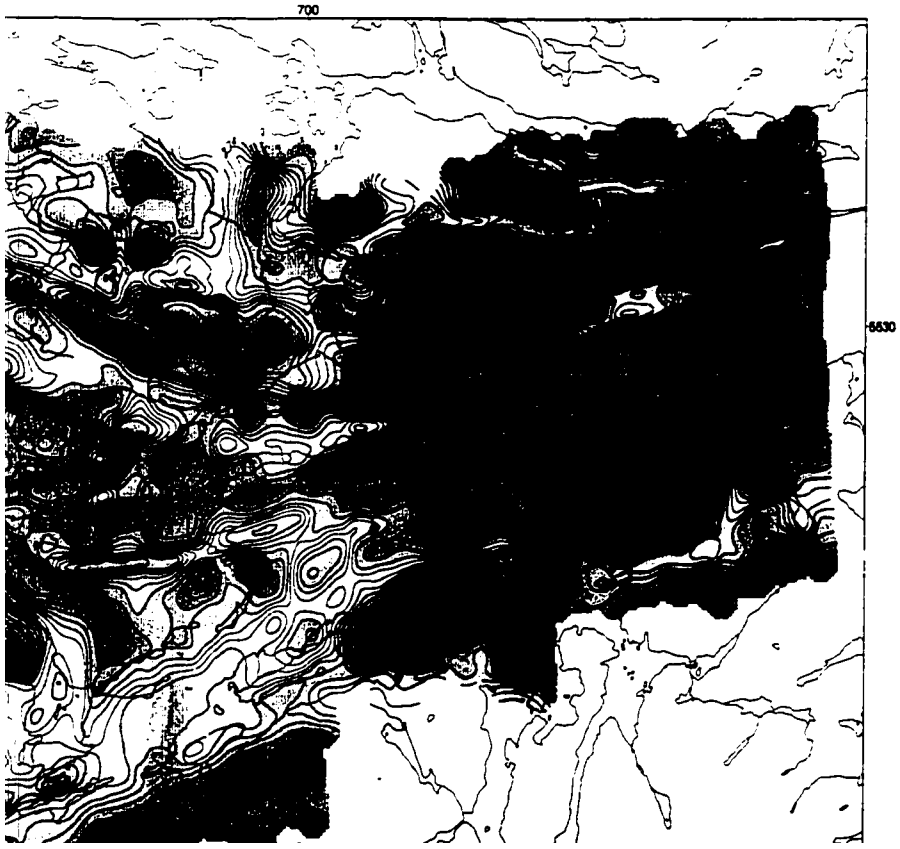

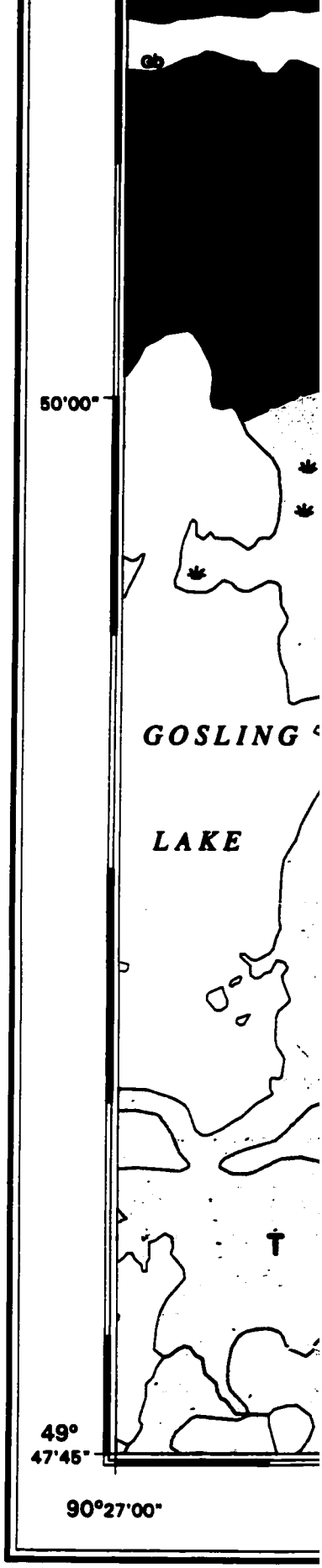

MOUNTAIRY

LAKE

SLING

KE

T

T

T

T

T

T

T

T

1000

25'00"

22'30"

Geology by J.L. Brown[1] and J.A. P

Scruffy

Lake

T

T

T

BRIGHT SAND

22'30"

20'00"

n[1] and J.A. Percival[2] 1998-1999

SOUTHEA

OPEN FILE 4286

GEOLOGY

THEASTERN STURGEON LAKE GREENSTONE BELT

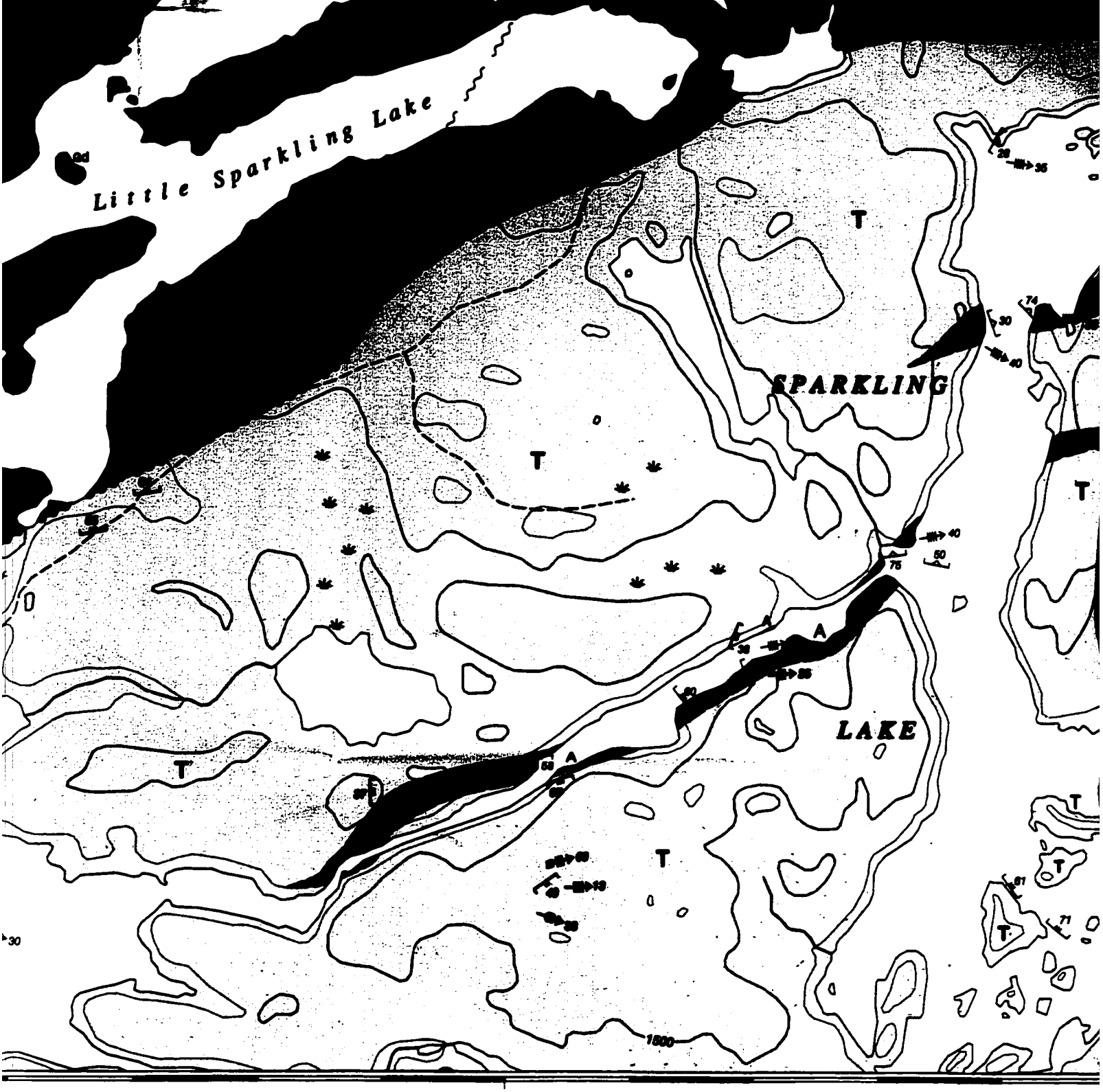

12'30"

Any revisions or additional geological information known to the user would be welcomed by the Geological Survey of Canada

Digital base map from data compiled by Geomatics Canada, modified by ESS Info

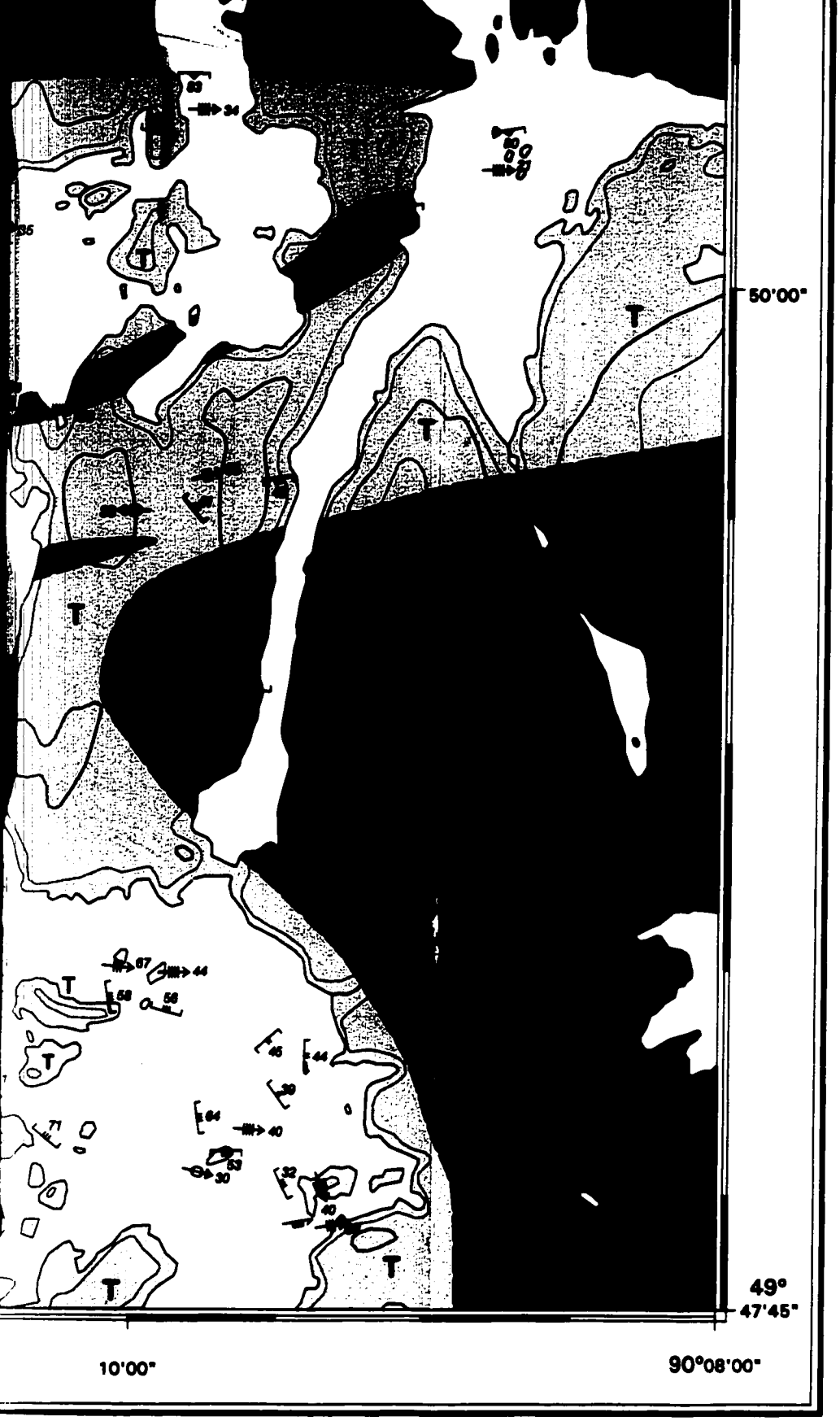

Fault zone of uncertain relative age . . . . .

F_4 fold (antiform) . . . . .

F_4 fold (synform) . . . . .

Slickenlines, generation unknown . . . . .

Intersection lineation (4th generation) . . . . .

Stretching lineation (4th, unknown generation; rodding)

U fold (2nd, 3rd, 4th, unknown generation) . . . . .

S fold (2nd, 3rd, 4th, unknown generation) . . . . .

Z fold (2nd, 3rd, 4th, unknown generation) . . . . .

Fold (2nd, 3rd, 4th generation) . . . . .

Dyke . . . . .

Vein . . . . .

Joint . . . . .

Macroscopic fault (dextral) . . . . .

Macroscopic shear zone (dextral, sinistral) . . . . .

Fold axial trace (2nd, 3rd, 4th, unknown generation) . .

Foliation, inclined (1st, 2nd, 3rd, 4th, unknown generatio

Bedding, inclined . . . . .

U-Pb age, Ma (z: zircon; t: titanite; m: monazite; i: igneous; d: detrital; m: metamorphic) . . . . .

Iron formation:

Oxide facies . . . . .

Silicate facies . . . . .

52J/2	52J/1	52-I/4
52G/15	52G/16	52H/13

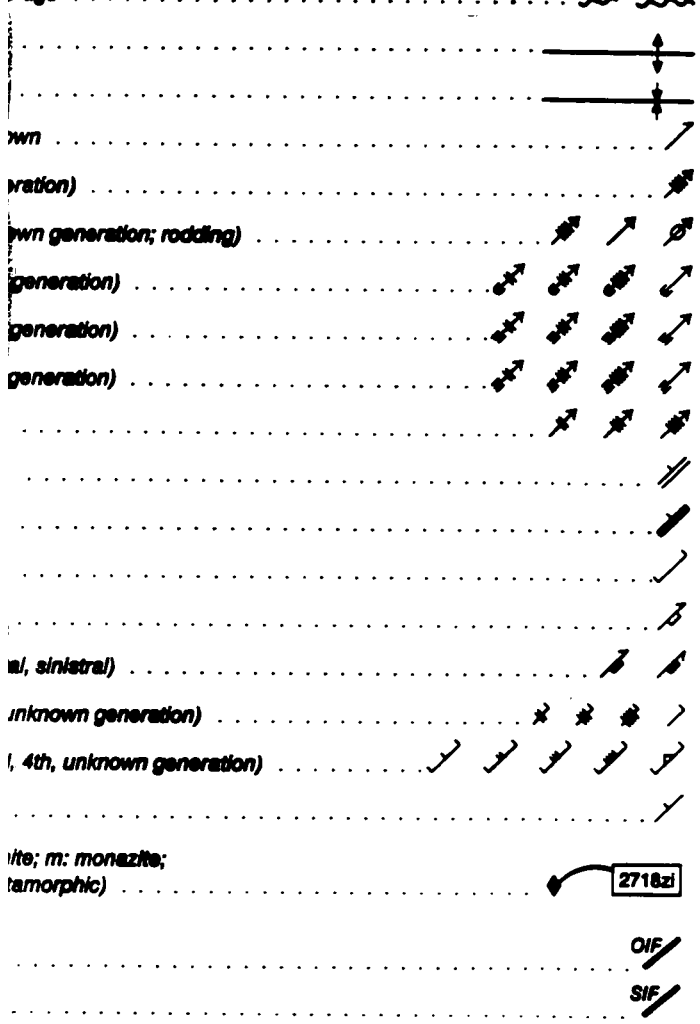

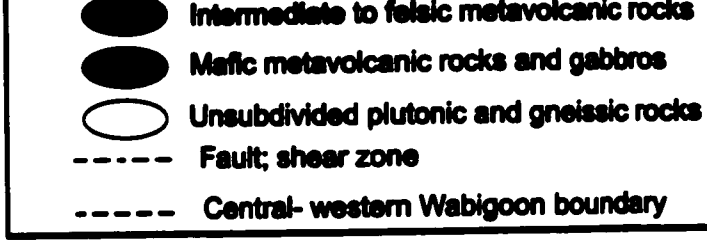

Figure 1: Location map of the Central Wabigoon Region. greenstone belts mark the boundary with the W

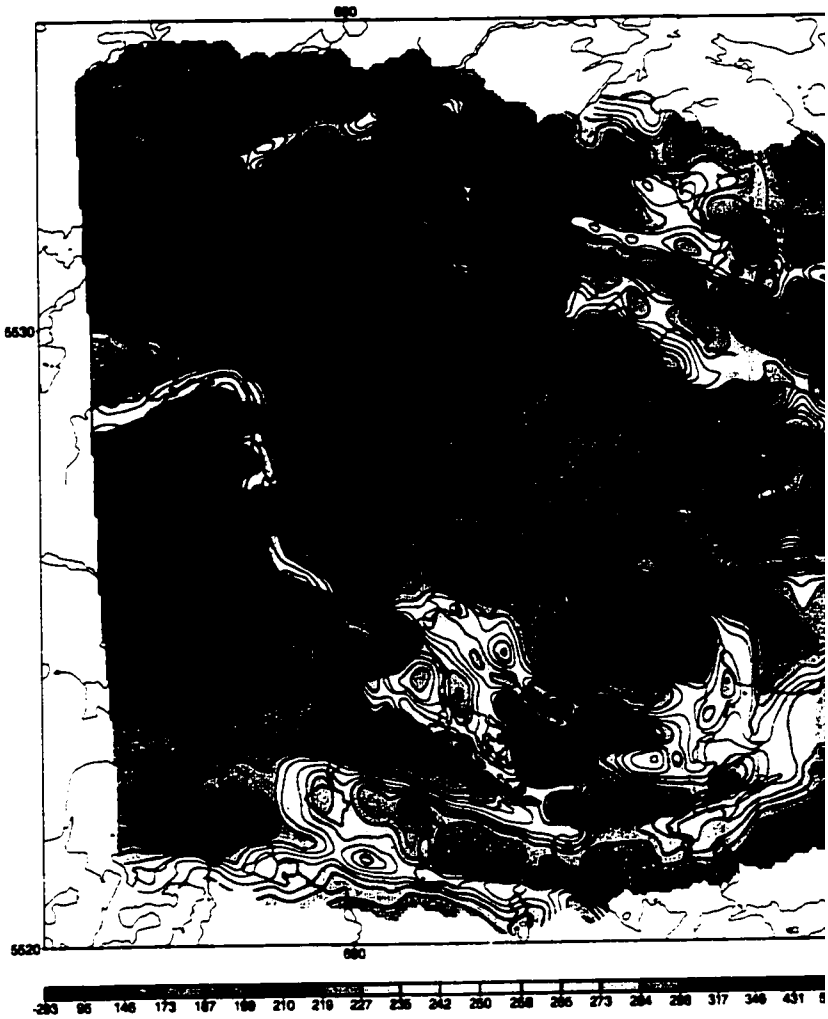

Figure 2. Aeromagnetic map of the southeastern Sturgeon Lake ar and processed by Campbell et al. (2000). Magnetic linea

Canada

ks and gabbros

and gneissic rocks

Location map of Figure 1 within Superior Province

goon boundary * dated locality

Wabigoon Region. The Savant Lake and Sturgeon Lake
oundary with the Western Wabigoon Region.

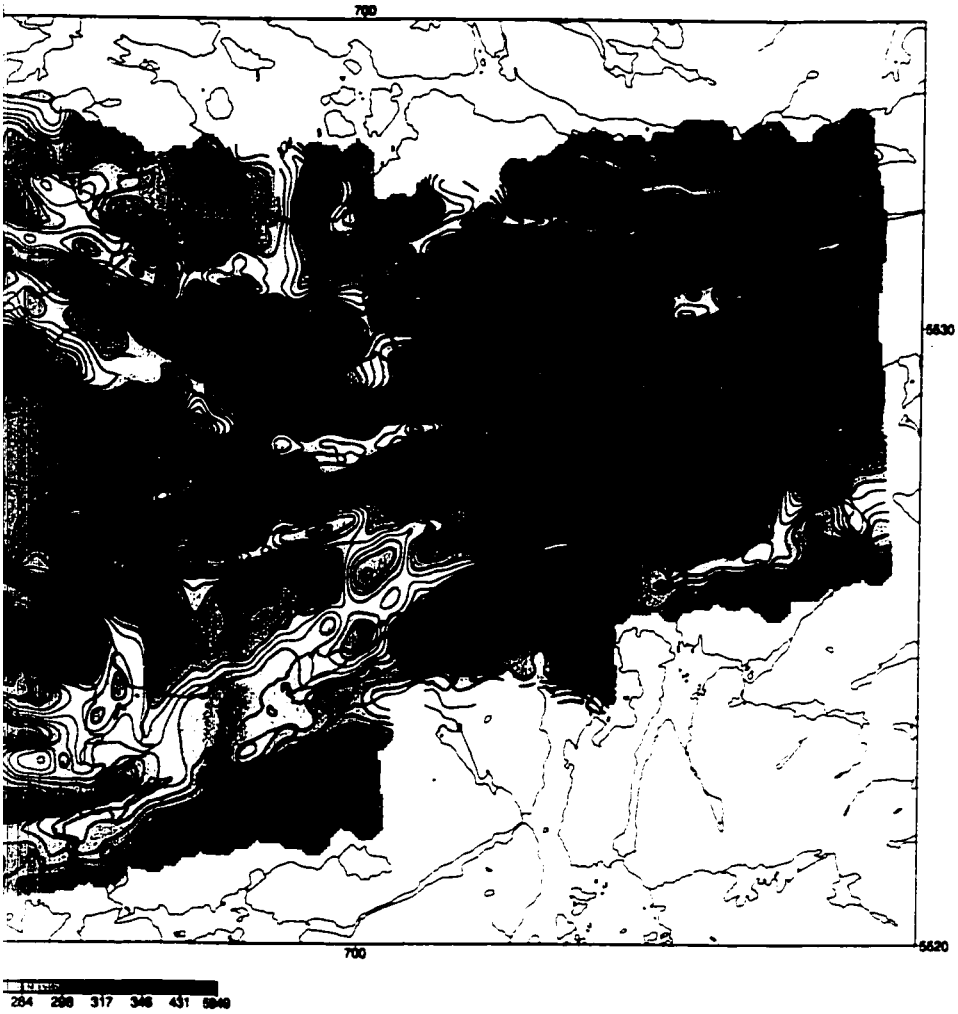

284 298 317 346 431 5849

Sturgeon Lake area based on proprietary data acquired from Noranda Ltd.
)). Magnetic lineaments reflect the trends of lithological units and faults.

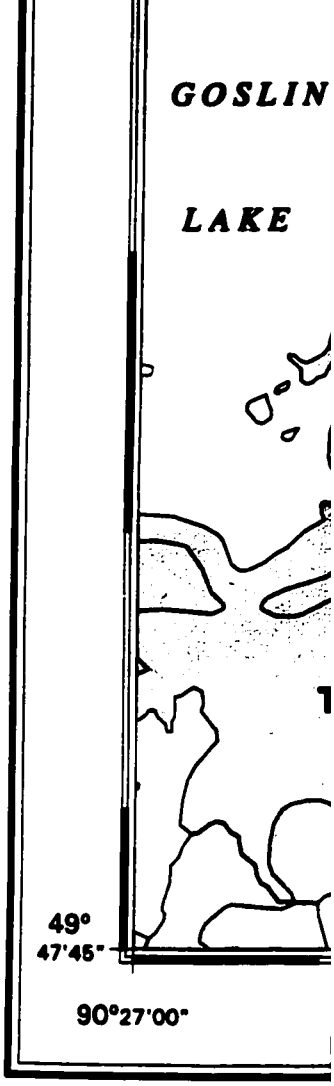

LOCATION MAP

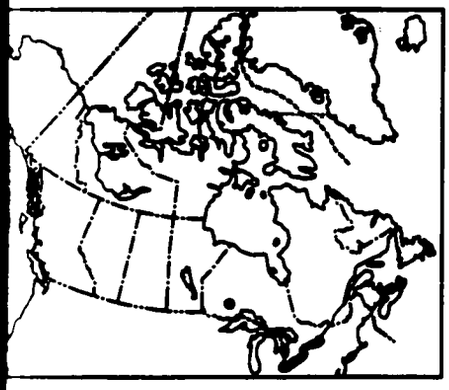

LOCATION MAP

Geology by J.L.

Coordinated through the e
[1]Department o
[2]Continental Geosci

Digi
Earth Sciences

This map was produced from pro
Section Quality Man
Quality Sy

22'30"

20'00"

SOUTH

J.L. Brown[1] and J.A. Percival[2] 1998-1999

he auspices of the Western Superior NATMAP project
ent of Earth Sciences, University of Ottawa
oscience Division, Geological Survey of Canada

Digital cartography by J. Doher,
nces Sector Information Division (ESS Info)

m processes in conformance with the Cartographic Services
Management System, Ottawa, registered to the
lity System ISO 9001: 1994 standards

metres 500

Universal Tr
North

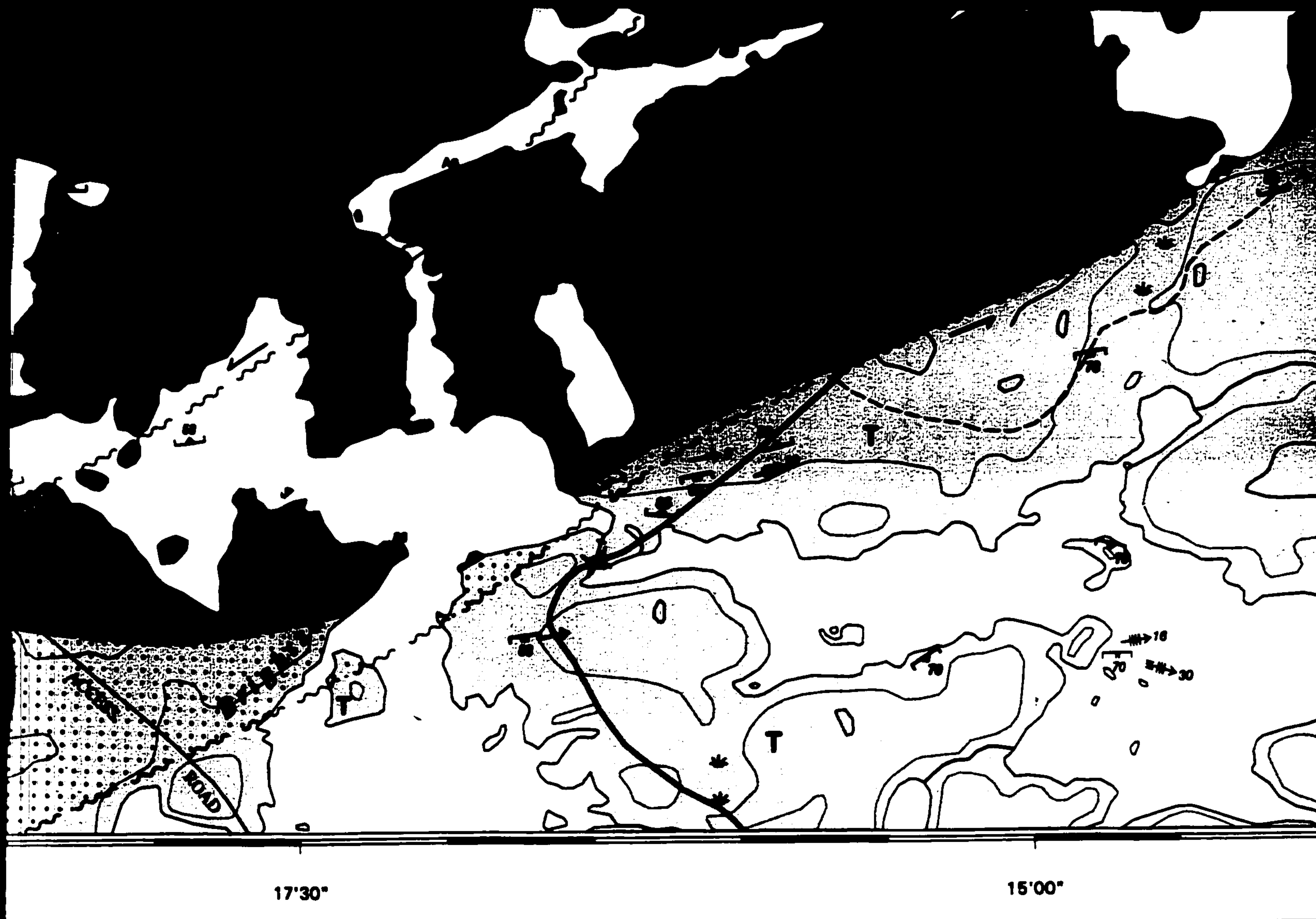

OPEN FILE 4286

GEOLOGY

HEASTERN STURGEON LAKE GREENSTONE BELT

ONTARIO

Scale 1:25 000/Échelle 1/25 000

0 | 0 | 500 | 1000 | 1500 | 2000 mètres

Transverse Mercator Projection
rth American Datum 1983

Projection transverse universelle de Mercator
Système de référence géodésique nord-américain, 1983

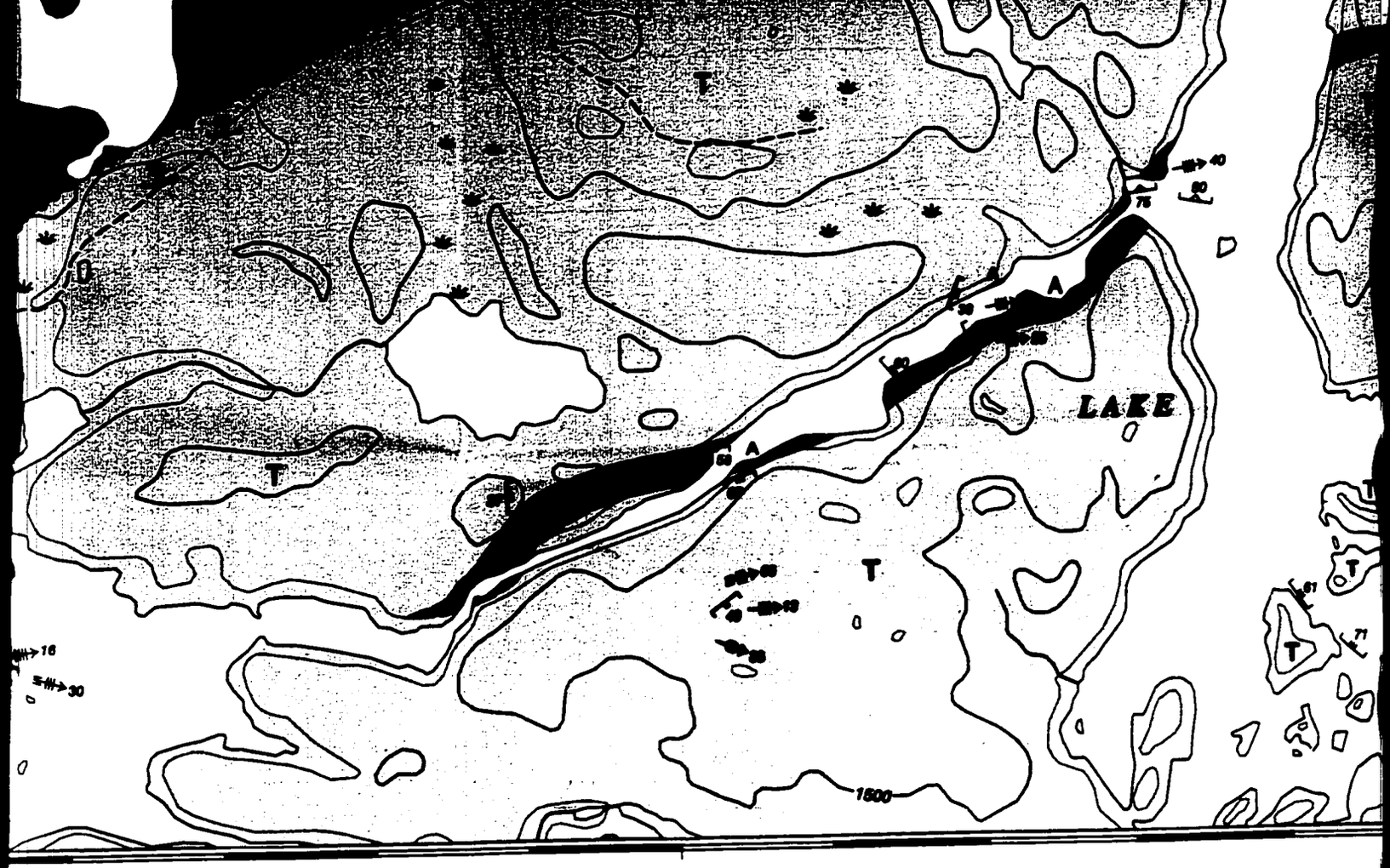

12'30"

Any revisions or additional geological information known to the user would be welcomed by the Geological Survey of Canada

Digital base map from data compiled by Geomatics Canada, modified by ESS Info

Magnetic declination 2001, 1°52'W, increasing 4.2' annually

Elevations in feet above mean sea level

Macroscopic fault (dextral) . . . . . .

Macroscopic shear zone (dextral, sinistral) . . . . . .

Fold axial trace (2nd, 3rd, 4th, unknown generation) .

Foliation, inclined (1st, 2nd, 3rd, 4th, unknown generat

Bedding, inclined . . . . . .

U-Pb age, Ma (z: zircon; t: titanite; m: monazite; i: igneous; d: detrital; m: metamorphic) . . . . . .

Iron formation:

Oxide facies . . . . . .

Silicate facies . . . . . .

52J/2	52J/1	52-I/4
52G/15	52G/16	52H/13
52G/10	52G/9	52H/12

NATIONAL TOPOGRAPHIC SYSTEM REFERENCE

OP
DOSS

GEOLOGICA
COMMISSION

DR

Recommended c
Brown, J.L. and
2001: Geology,
Geological

ic fault (dextral) . . . . . .

ic shear zone (dextral, sinistral) . . . . . .

trace (2nd, 3rd, 4th, unknown generation) . . . . . .

inclined (1st, 2nd, 3rd, 4th, unknown generation) . . . . . .

inclined . . . . . .

, Me (z: zircon; t: titanite; m: monazite;
us; d: detrital; m: metamorphic) 2718zi

tion:
facies . . . . . OIF

SIF

e facies . . . . . .

DRAFT COPY

Recommended citation:
Brown, J.L. and Percival, J.A.
2001: Geology, southeastern Sturgeon Lake greenstone belt, Ontario; Geological Survey of Canada, Open File 4286, scale 1:25 000.